AMMCS 2026
INTERNATIONAL CONFERENCE

AUGUST 17–21

WATERLOO, ONTARIO, CANADA

BOOK OF ABSTRACTS

General Chairs

Marc Kilgour
Roderick Melnik
Sunny Wang

Interdisciplinary AMMCS Conference Series

The AMMCS 2026 Conference

Book of Abstracts

Waterloo, Ontario, Canada

August 17–21, 2026

Disclaimer

Technical Designer: Roman N. Makarov

Publisher: AMMCS 2026

General Chairs

Marc Kilgour (Wilfrid Laurier University, Waterloo)

Roderick Melnik (Wilfrid Laurier University, Waterloo)

Sunny Wang (Wilfrid Laurier University, Waterloo)

Scientific Committee

Bjorn Birnir (University of California, Santa Barbara)

Carlos Garcia-Cevera (University of California, Santa Barbara)

Anatoli Ivanov (Penn State University)

Eduard Kirr (University of Illinois, Urbana-Champaign)

Shaofan Li (University of California, Berkeley)

Vakhtang Putkaradze (University of Alabama)

Enrico Scalas (Sapienza, University of Rome)

Chi-Wang Shu (Brown University)

Peter Kloeden (University of Tuebingen)

Organizing Committee

Herb Kunze (Conference Program Chair, University of Guelph)

Roman Makarov (Conference Treasurer, Wilfrid Laurier University, Waterloo)

Chester Weatherby (Student Prize Committee Chair, Wilfrid Laurier University, Waterloo)

Devan Becker (AMMCS Student Team Supervisor, Wilfrid Laurier University, Waterloo)

Monica Cojocaru (Global Organizing Committee University of Guelph)

Dong Liang Global (Organizing Committee York University)

Scott MacLachlan (Global Organizing Committee Memorial University of Newfoundland)

Zoran Miskovic (Global Organizing Committee University of Waterloo)

Nicolae Tarfulea (Global Organizing Committee Purdue University Northwest)

Technical Support Committee

Ama Ansah (Computer Support)

Ruveyda Nur Kizmaz (Web Coordinator)

Ruth MacNeil (Administrative Support)

Contents

Lectures

Plenary Lectures

Axioms and Impossibilities in the Theory of Voting

Wesley Holliday, University of California Berkeley, USA

Abstract: The axiomatic method familiar to mathematicians has inspired axiomatic approaches to other domains, including economic and political domains. I will discuss the axiomatic approach to the theory of voting, a topic that is both practically relevant for the design of elections and of interest to theorists in several fields. Although there are differences in how "axioms" are viewed across domains, there are also common types of questions. Given a set of axioms for geometry, set theory, etc., we may ask: does there exist a model that satisfies all of the axioms? Which axioms are independent of others? Can we find axioms that uniquely characterize a given model? Parallel questions arise in the theory of voting. After reviewing the classic axiomatic impossibility theorems of Arrow and Gibbard–Satterthwaite, I will discuss a new impossibility theorem for preferential voting, wherein voters submit rankings of the candidates. Roughly speaking, no voting rule satisfies the following four principles: a candidate who beats all other candidates in head-to-head majority comparisons must win the election; a candidate who loses to all others in head-to-head majority comparisons must lose; adding voters who rank a candidate first should not turn that candidate from a winner into a loser; and ties for winning can be broken by adding a bounded number of voters. Any three of these axioms is satisfied by some voting rule actually in use, whereas the classic impossibilities include axioms violated by almost all voting rules in use. Thus, the new theorem presents a genuine four-way fork in the road for choosing a voting rule. It exemplifies how axiomatic results can be useful in designing a voting rule for a particular application, by making salient the tradeoffs one must make.

Computing Attribution Scores for Classification in Explainable AI

Leopoldo Bertossi, Carleton University, Canada

Abstract: Attribution scores are used in XAI to quantitatively measure the strength of explanations for results from Machine Learning models. Several scores have been proposed and investigated. In addition to describing a few of them, including the popular SHAP-score, we will concentrate on the computational challenges they offer. Depending on the classifiers, some hardness and tractability results will be presented, so as an application with neural networks as classifiers.

Package Restructuring and the Pricing of Sovereign Debt

Pascal François, HEC Montréal, Canada

Abstract: Sovereign debt renegotiation agreements have generalized the practice of package restructuring – a form of debt relief combining rescheduling and write-off. The paper provides a contingent claims model with an expression for sovereign debt value and a bargaining game that rationalizes package restructurings as optimal renegotiation deals. It further shows how the parameters of the restructuring deal can be inferred from market information. A maximum likelihood inference from EMBI spread series is applied to four countries yielding realistic renegotiation outcomes. This is joint work with Amavi Hounlete, PhD student at HEC Montreal.

Recent Advances in Clustering Microbiome Data

Sanjeena Dang (Subedi), Carleton University, Canada

Abstract: The human microbiome plays a crucial role in health and disease. Advances in next-generation sequencing technologies have made it possible to quantify microbiome composition with high resolution. Clustering microbiome data can uncover meaningful patterns across samples, offering insights into biological variability and disease mechanisms. However, this task presents several challenges. Microbiome data are typically high-dimensional, over-dispersed, and compositional, the latter meaning they reflect relative, not absolute, abundances. As such, analyzing such compositional data presents many challenges because they are restricted to a simplex, which complicates standard statistical analysis. Various mixture model-based approaches have been proposed previously. These models assume that the population is a finite mixture of subpopulations (or clusters), each characterized by a probability distribution. My research team has focused on developing and refining such models to improve clustering accuracy and interpretability. We will present recent contributions from our group, emphasizing the strengths and limitations of different component-specific distributions used within mixture models. For example, Dirichlet-multinomial (DM) mixture models are computationally efficient but often fail to capture the complex correlation structures present in microbiome data. In contrast, models based on the logistic normal multinomial (LNM) distribution provide greater flexibility in capturing correlations but are computationally intensive. To overcome these limitations, we have developed a computationally efficient framework for parameter estimation in LNM-based models using variational Gaussian approximations. This approach significantly reduces the computational burden and enables application to large-scale datasets. Some other recent and ongoing developments using extensions of the LNM distribution and others to cluster microbiome data will be discussed.

Closing the gap between physical reality and the world of simulation

Nathan Kutz, University of Washington, USA

Abstract: Science and engineering is being revolutionized by computational advancements in machine learning and AI algorithms. Leveraging sensor measurements, often in combination with scientific computation proxies, such algorithms aim to learn effective models for a diversity of downstream tasks, including reconstruction, forecasting, design and control in challenging environments that include noisy measurements and or parametric variability. A grand challenge in the deployment of such algorithms is the fact that many physical systems are not amenable to full state measurements, but rather only discrete point sensor measurements at prescribed and limited locations. In fact, the only knowledge of the full state space is typically acquired by simulations of the approximating governing equations through a diversity of low- or high-fidelity models. This work aims to integrate scientific computing, data assimilation and physics informed AI in order to demonstrate tractable pathways forward for closing the SIM2REAL (simulation to reality) gap in science and engineering, thus enabling AI models that are accurate in reality, produce models that respect the fundamental laws nature, and are trustworthy in practice.

Semi-Plenary Lectures

Hard problems in post-quantum cryptography

Chloe Martindale, University of Bristol, UK

Abstract: Post-quantum cryptography is a rapidly growing area of cryptography which encompasses cryptographic algorithms that we can implement now, on current devices, but which are designed to be secure against future scalable quantum computers. In this talk, we will present some of the computational number theory problems that are at the core of post-quantum cryptography. This includes the ideal shortest vector problem, on finding small elements in ideals of orders in very high degree number fields, as well as the computational supersingular isogeny problem, on computing an isogeny between two given supersingular elliptic curves. We will also discuss some recent advances on these problems, including computational work interrogating the randomness of supersingular isogeny graphs.
This includes joint work with Ross Bowden and Felix Marsh.

Comparative Counterfactual Analysis of COVID-19 Policies and Vaccination

Marwa Tuffaha, York University, Canada

Abstract: Understanding how public health decisions shape epidemic outcomes is essential for future outbreak preparedness. In this study, we develop and apply an age-structured model of infection and immunity to investigate how different combinations of non-pharmaceutical measures and vaccination pathways influence COVID-19 dynamics across several regions. Using jurisdiction-specific calibration to observed epidemiological data, we construct hypothetical scenarios that modify intervention timing, policy intensity, primary vaccine rollout, and booster administration. The analysis reveals that epidemic severity is strongly shaped by the interplay between existing immunity levels and behavioural response to public health measures. In particular, non-school interventions have the biggest impact in reducing infections. Additionally, booster delivery has a pronounced effect on reducing hospitalizations and other severe outcomes, even when uptake is not universal. By enabling harmonized comparison across regions, this modelling approach provides a practical tool for evaluating alternative response strategies and informing future pandemic policy.

Robust Synchronization of Cascaded Pendulum Systems Under Markovian Switching

Mohamad S. Alwan, University of Saskatchewan, Canada

Abstract: This presentation outlines the systematic development of adaptive synchronization frameworks for leader-follower oscillator and pendulum systems, tracing a path from deterministic hybrid regimes to stochastic switching environments. We first establish a fundamental architecture for tracking under deterministic disruptions, including impulsive velocity resets and switched leader frequencies under a common external forcing environment. Using a first-order adaptive law to adjust the follower's natural frequency, we analyze the resulting cascaded error dynamics through composite Lyapunov methods. The analysis shows that unmatched hybrid events introduce structural mismatches that require an input-to-state stability (ISS) framework, while ideal matched resets may remove these mismatch effects and recover exact exponential synchronization. Extending this framework to stochastic switching environments, we focus on the realistic mismatched Markovian regime, where the leader's natural frequency undergoes random abrupt transitions modelled by a continuous-time Markov jump process. Since the follower cannot generally detect or implement these random frequency changes instantaneously, stochastic switching naturally leads to asynchronous operation, with a finite time lag between the leader's transition and the follower's response. During these asynchronous intervals, the frequency mismatch acts as a disturbance input and may temporarily increase the Lyapunov function. Thus, ISS provides the natural stability framework, yielding practical exponential synchronization with an ultimate bound determined by the magnitude, rate, and duration of the asynchronous mismatches. Numerical simulations validate the theoretical results and demonstrate the robustness of the proposed adaptive control strategy in application benchmarks such as robotic pendulums and computer-controlled oscillatory networks.

From the Blackboard to the Clinic: digital twinning, mathematical modeling, and artificial intelligence for personalized medicine

Giovanna Guidoboni, University of Maine, USA

Abstract: Digital twinning, mathematical modeling, and artificial intelligence combine mechanism-driven and data-driven models in a complementary and synergistic way to enable personalized medicine. Mechanism-driven models are based on the principles of physics and physiology and allow for identification of cause-to-effect relationships among interplaying factors in a complex system. While invaluable for causality, mechanism-driven models are often based on simplifying assumptions to make them tractable for analysis and simulation; however, this often brings into question their relevance beyond theoretical explorations. Data-driven models aim at extracting information and knowledge from data. These approaches are naturally interdisciplinary, as it bridges fundamental techniques of data analysis, typically developed by mathematicians, statisticians and computer scientists, with the needs of actionable insights that are specific to the particular application domain. The combination of mechanism-driven and data-driven models allows us to harness the advantages of both approaches, as mechanism-driven models excel at interpretability but suffer from a lack of scalability, while data-driven models are excellent at scale but suffer in terms of generalizability and insights for hypothesis generation. This combined, integrative approach represents the pillar of the interdisciplinary approach to data science that will be discussed in this talk, with applications spanning from glaucoma research to cardiovascular monitoring and physiology of the lower urinary tract (LUT).

Large Coherent Structures in Wave Equations via Computer Assisted Proofs

Eduard-Wilhelm Kirr, University of Illinois at Urbana-Champaign, USA

Abstract: While coherent structures play an essential role in the analysis and applications of wave equations it has been impossible (until now) to find all the nonlinear ones. This talk will focus on the Nonlinear Schrodinger Equations where coherent structures have the form e iEtf(x) with real frequency E and the profile f in the H1 Sobolev space over Rn. We show that all coherent structures must organize themselves in smooth branches accumulating to E equal infinity. In this limit they split into peaks and an algebraic equilibrium equation between peak-potential and peak-peak interaction emerges. The equation determines the possible limit points of the coherent structures as the frequency E approaches infinity. For small number of peaks or for peaks in a collinear configuration the limiting points can be obtained by hand. However, for large number of non-collinear peaks we employ computer assisted proofs. Once the limit points are determined we adapt techniques from local bifurcation theory to show existence of actual branches of coherent states emerging from the limit points and trace them from high frequency into the range of medium and small frequency.

AMMCS Prize-Winning Lecture

Kolmogorov–Wiener Prize for Young Researchers
Modelling Advancements in Bioheat Transfer

Manpreet Singh, BHSAI, USA

Abstract: In the realm of bioheat transfer, Dr. Singh's research on development of human physiology-based computationally predictive models of biological systems can assist in mitigating the risks associated with cold-related injuries (frostbite, hypothermia etc.) and increase Warfighter Readiness of soldiers in extreme cold-weather operations. Dr. Singh's anatomically detailed thermoregulatory model provides accurate thermal responses including temperature predictions of the body core temperature, mean skin temperature and as well as endurance times to cold injuries of the most susceptible body peripheral regions such as digits of hands and feet in the austere environmental conditions. Therefore, Dr. Singh's research assisted in the development of militarily relevant medical products that provide early alerts of a rise and fall in core body temperature to help reduce the risk of thermal injury in the field and during training and deployment at US installations. Although the human thermoregulatory system maintains core body temperature at 37°C, humans often fail to recognize early warning signs of an impending rise or fall in this temperature and hence fail to take appropriate mitigation strategies. Therefore, a temperature alerting system from Dr. Singh's mathematical algorithms can be used during rest, exercise in the heat, cold and extreme cold environmental conditions (−40°C) to inform the soldiers mitigate such injury risks. In this talk, Dr. Singh will also discuss key modifications to the Pennes bioheat equation, with particular emphasis on incorporating spatial heterogeneity in blood perfusion derived from medical imaging. Specifically, he integrates pixel-level blood perfusion data into the model, thereby relaxing the conventional assumption of uniform blood perfusion.

Presentations

Stability Analysis of a Multilayer Agent-Based SIWS Epidemic Model

Z. Abbasi[1], X. Liu[1]

[1] *University of Waterloo, Canada,*
zoya.abbasi@uwaterloo.ca, xzliu@uwaterloo.ca

This work presents a stability analysis of the Susceptible-Infected-Water-Susceptible (SIWS) epidemic model [1] formulated within a multi-agent systems (MAS) framework [2]. A multilayer, interconnected, heterogeneous agent-based SIWS model is proposed that explicitly incorporates population flow between cities, physical inter-city connectivity, and water-resource dynamics. Cities and water resources are modeled as autonomous agents operating across distinct layers (physical and resource), enabling a natural representation of distributed epidemic transmission pathways.

The disease-free solution (DFS) and endemic solution (ES) are explored. The basic reproduction number R_0 is computed via the next-generation matrix approach [3]. Local stability is established using the Jacobian matrix evaluated at the DFS: the DFS is locally asymptotically stable when $R_0 < 1$ and unstable when $R_0 > 1$. Global asymptotic stability of the DFS (for $R_0 < 1$) is proven by constructing a quadratic Lyapunov function that exploits the Metzler structure of the system Jacobian and the positive invariance of the meaningful domain. For $R_0 > 1$, the existence and uniqueness of ES is shown, and its global asymptotic stability is demonstrated through a coordinate-shifted quadratic Lyapunov function combined with the LaSalle invariance principle, using Perron-Frobenius properties of the associated irreducible Metzler matrix.

This stability analysis provides precise epidemic-threshold conditions and convergence guarantees essential for designing robust, distributed public-health interventions.

References

[1] P.E. Pare, A. Janson, S. Gracy, J. Liu, H. Sandberg and K.H. Johansson, *Multilayer SIS model with an infrastructure network*, IEEE Trans. Control Netw. Syst. **10**, 1, pp. 295–307 (2023).

[2] Z. Abbasi and X. Liu, “Observer-Based Adaptive Robust Control of Dual-Layer Multiagent Epidemic Model: Physical and Information Layers,” *IET Control Theory & Applications*, vol. 19, no. 1, e70052, 2025.

[3] P. van den Driessche and J. Watmough, *Reproduction numbers and sub-threshold endemic equilibria for compartmental models of disease transmission*, Math. Biosci. **180**, pp. 29–48 (2002).

On the Necessity of Effect Terms in Multi-Agent Systems

Z. Abbasi[1], X. Liu[1]

[1] *University of Waterloo, Canada,*
Zoya.abbasi@uwaterloo.ca, xzliu@uwaterloo.ca

In conventional formulations of the consensus problem for multi-agent systems (MAS), each agent's dynamics are assumed to evolve independently, with inter-agent coupling introduced solely through the communication graph and the designed control protocol. This modeling paradigm overlooks a fundamental reality observed across virtually all practical applications: the states of one agent continuously and structurally influence the states of its neighbors even before any control input is applied. To address this critical gap between theoretical models and real-world behavior, the present work discusses the Effect Term (ET) [1], which is directly embedded into the agent dynamics. The ET captures two distinct types of inter-agent influence: (i) an independent component (linear or nonlinear) representing the direct impact of neighboring agents' states on the current agent, and (ii) a dependent component that couples the current agent's own states with those of its neighbors. These terms are inherently state-dependent and activate only when agents are connected. Unlike external disturbances or noise, the ET vanishes when the connection is lost and is exclusive to interconnected MAS, thereby providing a structured, physically meaningful representation of mutual influence that is absent in standard MAS models. This paper focuses on demonstrating the necessity of incorporating ET in a wide spectrum of MAS applications beyond the classical epidemic modeling case. Specific domains where the ET proves indispensable include:

1. Biological and epidemiological systems: Cities or geographic regions are naturally modeled as autonomous agents in a multi-agent framework [2, 3]. During an infectious disease outbreak, the epidemiological state of one city directly and continuously augments the infection dynamics of neighboring cities through population movement and travel. This inter-city coupling is precisely captured by the ET, which adds structured terms to the local compartmental model representing the influx of infected (or susceptible) individuals from connected cities. Without the ET, standard compartmental models treat cities as isolated units, leading to unrealistic predictions of disease spread, underestimated transmission rates, inaccurate equilibrium analysis, and control policies that fail in practice.

2. Human behavior and social systems: Emotional, cognitive, and behavioral states propagate continuously and nonlinearly through social networks, altering the internal dynamics of neighboring individuals [4].

References

[1] A. H. Amiri Mehra, M. Shafieirad, and I. Zamani, "Leader-following consensus considering effects of agents on each other via impulsive control: A topology dependent average dwell time approach," *Journal of the Franklin Institute*, vol. 359, no. 16, pp. 8639–8668, 2022.

[2] A. H. Amiri Mehra, M. Shafieirad, and I. Zamani, "Leader-following consensus and qualitative analysis of a new multi-agent-based epidemic model," *IET Control Theory & Applications*, vol. 18, no. 4, pp. 408–421, 2024.

[3] Z. Abbasi and X. Liu, "Observer-Based Adaptive Robust Control of Dual-Layer Multiagent Epidemic Model: Physical and Information Layers," *IET Control Theory & Applications*, vol. 19, no. 1, e70052, 2025.

[4] C. Urban and B. Schmidt, "PECS–Agent-Based Modelling of Human Behaviour", in *Emotional and Intelligent–The Tangled Knot of Social Cognition*, AAAI Fall Symposium Series, North Falmouth, MA (2001).

Fractional-Order 5D Hyperchaotic Bi-Memristive System for Image Encryption with Compressed Sensing

O-M. Afolabi[1], J-C. Núñez-Pérez[2], V-A. Adeyemi[3], M-A. Estudillo-Valdez[4], , R-U. Almada Prieto[5]

[1] *Instituto Politechnico Nacional, Mexico, oafolabi@citedi.mx*
[2] *Instituto Politechnico Nacional, Mexico, nunez@citedi.mx*
[3] *Instituto Politechnico Nacional, Mexico, vademola@citedi.mx*
[4] *Instituto Politechnico Nacional, Mexico, mestudillo@citedi.mx*
[5] *Instituto Politechnico Nacional, Mexico, ramon_ulises@citedi.mx*

This paper proposes a five-dimensional (5D) chaotic system constructed by coupling two heterogeneous memristors including polynomial and sinusoidal memductance elements into a Lorenz-type oscillator topology. Unlike existing memristive chaotic systems that uses a single memristor with a polynomial memductance function, the proposed bi-memristive architecture introduces a structural asymmetry between the memductances, where one provides a monotone, single-equilibrium restoring characteristic and the other exhibits a non-monotone, infinite-extrema memductance landscape that alternates between energy-injecting and energy-dissipating regimes as the flux evolves. This co-evolutionary coupling mechanism is shown to be the principal source of the system's rich hyperchaotic behavior. We first establish a complete integer-order analysis of the system, including standalone characterization of both memristors via pinched hysteresis and lobe-count formulae, equilibrium analysis through Jacobian block-decoupling, Routh-Hurwitz stability conditions on the active 3×3 subsystem, computation of the full five-dimensional Lyapunov exponent spectrum via the QR-decomposition method, and bifurcation diagrams confirming the coexistence of periodic, chaotic, and hyperchaotic regimes. We then extend the analysis to the fractional-order domain using the Caputo derivative formulation, where the Matignon stability theorem replaces the classical Routh-Hurwitz criterion, and demonstrate that reducing the fractional order q introduces a continuous memory-depth parameter that further enriches the attractor structure and increases the Kaplan-Yorke dimension beyond that of the integer-order system. The resulting chaotic sequences are validated against NIST SP 800-22 statistical randomness tests across all five state variables. We then propose an image encryption and compression scheme in which the chaotic orbits simultaneously construct a restricted-isometry-property (RIP)-satisfying measurement matrix for compressive sensing and drive a permutation-diffusion encryption layer, yielding a compressed ciphertext whose reconstruction is computationally infeasible without precise knowledge of the system parameters, fractional order, and initial conditions. Security analysis confirms histogram uniformity, near-ideal pixel correlation suppression, information entropy exceeding 7.999, and differential attack resistance with NPCR > 99.6% and UACI ≈ 33.4%. The proposed scheme achieves a Kaplan-Yorke dimension and large key space comparable with the state-of-the-art fractional memristive systems, establishing it as a strong candidate for secure image transmission in resource-constrained environments.

Robust Synchronization of Cascaded Pendulum Systems Under Markovian Switching

M.S. Alwan

University of Saskatchewan, Canada, m.alwan@math.usask.ca

We investigate the synchronization problem between a controlled follower pendulum and a leader pendulum whose natural frequency undergoes random abrupt changes. The follower is equipped with an adaptive control law that adjusts its natural frequency to track the leader, resulting in a cascaded error dynamics structure. We first establish local exponential stability for the continuous-time system with constant leader frequency using composite Lyapunov arguments. The main contribution lies in extending this analysis to scenarios where the leader's frequency evolves as a continuous-time Markov jump process. Under a uniform interconnection growth condition, we construct a common quadratic Lyapunov function that guarantees mean-square exponential stability for the nonlinear Markov jump cascade, provided the damping ratio and frequency bounds satisfy a simple inequality. For comparison, we also present mode-dependent sufficient conditions in terms of linear matrix inequalities. Application examples illustrate the theoretical findings and demonstrate the robustness of the common Lyapunov approach to frequency variations.

The VII International AMMCS
Interdisciplinary Conference
Waterloo, Ontario, Canada

Modelling the Interplay between IUU Fishing, Wholesaler Fraud, and Consumer Awareness in the Seafood Supply Chain

R.C. Cui[1], M.P. Yodzis[2], J.D. Phillips[3]

[1] *University of Guelph, Canada, cuir@uoguelph.ca*
[2] *University of Guelph, Canada, myodzis@uoguelph.ca*
[3] *University of Guelph, Canada, jphill01@uoguelph.ca*

The overexploitation and depletion of global fish stocks is a serious challenge facing society today, compounded by the ever-increasing global demand for seafood. To meet this high demand, illegal, unreported, and unregulated (IUU) fishing is common in many fisheries. A further problem is that the opacity and complexity of the global seafood supply chain makes seafood quality control and labelling standards difficult to enforce, which enables fraud by opportunistic wholesalers. We focus on two mechanisms: when dishonest wholesalers mislabel and overprice low value seafood as high value; and when dishonest wholesalers support IUU fishing by providing a black market for IUU catch, while misrepresenting it to consumers as legally-caught. These activities negatively impact not only the economy, but also the health of humans and the sustainability of fish populations worldwide.

To better understand the dynamics of fraud in the seafood supply chain and its feedbacks to both society and the environment, we develop a four-dimensional discrete-time model that couples two components. The bioeconomic subsystem represents the dynamics of fish biomass and harvester effort, based on standard Ricker logistic growth and Gordon-Schaefer surplus production theory [**?**, **?**, **?**], but augmented to include heterogeneous fishing strategies [**?**] that are influenced by the prevalence of wholesaler fraud. The behavioural subsystem represents the decision of wholesalers about what level of fraud to engage in, and the ability of consumers to discover this fraud and respond by exiting the market. This builds on behavioural models of social learning, dynamic risk perception, and cycles of social and institutional change in a resource harvesting context [**?**, **?**].

Critically, when these systems are coupled, fraudulent wholesalers facilitate environmentally-damaging IUU activity by harvesters, while also taking advantage of consumer misperception to earn higher profit margins than honest wholesalers.Through detailed stability and bifurcation analyses, we identify conditions under which interesting qualitative dynamics emerge from the model, which can then be linked to real-world observations. The model has been implemented and visualized as a general software tool for the broader community-at-large using the Python programming language, and is expected to be calibrated by real-world empirical data where available.

References

[1] Bieg, C., McCann, K. S., and Fryxell, J. M. (2017). The dynamical implications of human behaviour on a social-ecological harvesting model. *Theoretical Ecology*, 10(3), 341–354. https://doi.org/10.1007/s12080-017-0334-3

[2] Fryxell, J. M., Hilborn, R., Bieg, C., Turgeon, K., Caskenette, A., and McCann, K. S. (2017). Supply and demand drive a critical transition to dysfunctional fisheries. *Proceedings of the National Academy of Sciences*, 114(46), 12333–12337. https://doi.org/10.1073/pnas.1705525114

[3] Bieg, C., Bartley, T. J., McCann, K. S., and Hanner, R. H. (2022). Replicating nature's fabric: High information markets and the sustainability of global seafood. *Food Webs*, 32, e00239. https://doi.org/10.1016/j.fooweb.2022.e00239

[4] Yodzis, M. (2024). Collective Action Problems in Fisheries and Banking. Thesis Ph.D. Mathematics. University of Guelph. https://hdl.handle.net/10214/28222

[5] Yodzis, M., Bauch, C. T., and Anand, M. (2016). Coupling fishery dynamics, human health and social learning in a model of fish-borne pollution exposure. *Sustainability Science* 11(2), 179–192. https://doi.org/10.1007/s11625-015-0317-5

Predefined-Time Control for Second-Order Neural networks

Yongfang Jin[1], Xinzhi Liu[2], Shouming Zhong[3]

[1] *School of Mathematical Sciences, Dalian University of Technology, Dalian, China, yongfangjindut@163.com*
[2] *Department of Applied Mathematics, University of Waterloo, Waterloo, ON, Canada, xzliu@uwaterloo.ca*
[3] *School of Mathematics Sciences,University of Electronic Science and Technology of China, Chengdu, China, zhongsm@uestc.edu.cn*

Neural networks have demonstrated remarkable effectiveness across diverse domains, ranging from financial prediction [1] to image encryption [2]. However, conventional neural networks models are predominantly governed by first-order differential equations. This representation is often insufficient for capturing the intrinsic dynamics of many biological and physical systems, where inertial effects (manifesting as second-order derivative terms) are ubiquitous. To bridge this gap, second-order neural networks (SONNs) were introduced by drawing inspiration from inductive elements in analog circuits [3]. Unlike their first-order counterparts, SONNs provide a more physically realistic framework for modeling neural dynamics.

Consider the following second-order neural networks model:

$$
\begin{aligned}
\frac{\mathrm{d}^2\omega_i(t)}{\mathrm{d}t^2} = & -a_i\frac{\mathrm{d}\omega_i(t)}{\mathrm{d}t} - b_i\omega_i(t) + \sum_{j=1}^{h} c_{ij}^{(1)}\mathscr{G}_j(z_j(t)) + \sum_{j=1}^{h} c_{ij}^{(2)}\mathscr{H}_j(z_j(t-d_j(t))) \\
& + \sum_{j=1}^{h} c_{ij}^{(3)}\int_{t-h_j(t)}^{t}\mathscr{F}_j(z_j(s))\,\mathrm{d}s + u_i(t), \quad \forall i\in\mathbb{I},
\end{aligned}
\tag{1}
$$

where $\omega_i(t)\in\mathbb{R}$ stands for the state of the i-th neuron. $u_i(t)\in\mathbb{R}$ represents the control input. a_i and $b_i\in\mathbb{R}_+\backslash\{0\}$ denote self-feedback coefficients. $c_{ij}^{(1)}$, $c_{ij}^{(2)}$, and $c_{ij}^{(3)}\in\mathbb{R}, i,j\in\mathbb{I}$, are connection weights. $d_j(t)\geq 0$ represents the unbounded discrete delay associated with the j-th neuron. $h_j(t)$ is the distributed delay fulfilling $0\leq h_j(t)\leq \bar{h}_j$. $\mathscr{G}_j(\cdot)$, $\mathscr{H}_j(\cdot)$, and $\mathscr{F}_j(\cdot)$ denote nonlinear activation functions.

This paper investigates the predefined-time control problem for SONNs with time-varying delays. Unlike existing works employing the reduced-order method to transform second-order dynamics into first-order forms, this work directly analyzes the original second-order system. The direct approach not only preserves the system's intrinsic structure but also simplifies the theoretical analysis and reduces computational complexity. By designing state feedback controllers, we derive algebraic criteria to ensure global predefined-time stability. These criteria are formulated as scalar inequalities with all parameters known, enabling direct stability verification without requiring numerical optimization solvers.

References

[1] C. Ju, Q. Shen, and X. Ni, "Leveraging lstm neural networks for stock price prediction and trading strategy optimization in financial markets," *Appl. Comput. Eng.*, **112**, pp. 47–53 (2024).
[2] Z. Li, X. Meng, C. Bi, and J. Cao, "Quasi-projective synchronization of fractional-order quaternion fuzzy cellular neural networks with applications to image encryption," *J. Appl. Math. Comput.*, **72**, 1, p. 31 (2026).
[3] K. Babcock and R. Westervelt, "Stability and dynamics of simple electronic neural networks with added inertia," *Physica D*, **23**, 1–3, pp. 464–469 (1986).

Recent approaches for analyzing convex relaxations of parametric ordinary differential equations

K. Khan[1]

[1] *McMaster University, Hamilton, Canada, kamilkhan@mcmaster.ca*

We consider the following optimization problem, representing a dynamic system from an engineering application:

$$\min_{\mathbf{p}\in P} g(\mathbf{p},\mathbf{x}(t_f,\mathbf{p})), \tag{1}$$

where $P \subset \mathbb{R}^{n_p}$ is a nonempty interval, and $\mathbf{x}$ is the well-defined unique parametric solution of the following ordinary differential equation:

$$\dot{\mathbf{x}} = \mathbf{f}(t,\mathbf{p},\mathbf{x}), \qquad \mathbf{x}(0,\mathbf{p}) = \mathbf{x}_0(\mathbf{p}). \tag{2}$$

The functions $\mathbf{x}_0$, $\mathbf{f}$, and g are presumed to be known finite compositions of functions from a library, such as the standard operations on a scientific calculator. In standard branch-and-bound approaches for solving (1) to global ε-optimality, lower bounds must be computed for the objective function of (1) on many subdomains, and these are typically ultimately supplied by minimizing convex relaxations, which in turn requires the capability to generate *state relaxations*: useful convex/concave relaxations of the solution $\mathbf{x}$ of (2) with respect to $\mathbf{p}$.

This presentation covers our recent approaches in analyzing state relaxations, to ultimately compare approaches for global dynamic optimization, and to supply subgradient information. By developing and applying new differential inequalities, we have proposed new *bound comparison* results under which one set of state relaxations is guaranteed to enclose a competing set, and we have also obtained the result that tighter convex relaxations of the ODE right-hand side function $\mathbf{f}$ will always translate into state relaxations that are no less tight [1]. We have also used these differential inequalities to develop what is essentially the first correct description of convex subgradients of state relaxations, analogous to classical ODE results governing the partial derivative $\frac{\partial \mathbf{x}}{\partial \mathbf{p}}$ [2, 3]. This description is compatible with adjoint-mode evaluation, which becomes computationally favorable when n_p is large. We illustrate these with numerical examples based on a fully-automated implementation of our subgradient construction procedure, written in the programming language Julia, which demonstrates the correct computational scaling in adjoint mode.

References

[1] Y. Song and K.A. Khan, *New inequalities for comparing ordinary differential equations arising in global dynamic optimization*, Syst. Control Lett. **196**, 106004 (2025).

[2] Y. Song and K.A. Khan, *Computing subgradients of convex relaxations for solutions of parametric ordinary differential equations*, Optim. Method Sofw. **39**, 6, pp. 1309-1351 (2024).

[3] Y. Zhang and K.A. Khan, *Evaluating subgradients for convex relaxations of dynamic process models by adapting current tools*, Comput. Chem. Eng., **180**, 108462 (2024).

Event-Triggered Game-Based Impulsive Control for Systems with Disturbances

Wenlu Liu[1], Xinzhi Liu[1]

[1] *Department of Applied Mathematics, University of Waterloo, Waterloo, Ontario N2L 3G1, Canada*
Email: w82liu@uwaterloo.ca, xzliu@uwaterloo.ca

Abstract: The stabilization and performance optimization of dynamic systems subject to exogenous disturbances remain critical challenges in modern control engineering. This paper proposes a novel game-based impulsive control framework for a class of disturbed systems, where the impulsive controller and the external disturbance are modeled as opposing players with conflicting objectives. Particularly, an ingenious Zeno-free event-triggered mechanism associated with Hamiltonian functions is developed to determine the optimal impulse frequency and improve control efficiency. Within this unified impulse game framework, sufficient conditions for achieving $\mathscr{L}_2$ stability are established by reformulating the disturbance attenuation problem as a two-player zero-sum differential game with impulsive control. Furthermore, the Nash equilibrium solution that consists of the optimal impulsive control strategy and the worst-case disturbance policy is explicitly derived via the event-triggered impulsive control technique. The stability of the system under the obtained equilibrium strategy pair is guaranteed simultaneously. The proposed framework bridges the connection between impulsive control and differential game theory and provides an effective scheme for both stability performance analysis and Nash equilibrium setting.

Keywords: Differential game; Event-triggered impulsive control; Zeno behavior; $\mathscr{L}_2$ stability; Nash equilibrium.

Bistability and Basin Geometry in a Nonlinear Macro-Financial Model

K. Wright[1], D. Robinson[2]

[1] *University of Waterloo, Canada, kirsten.wright@uwaterloo.ca*

[2] *Laurentian University, Canada, drdrrobinson@gmail.com*

Abstract: Hyman Minsky's Financial Instability Hypothesis holds that capitalist economies can endogenously generate crises. From a dynamical systems perspective, this most naturally corresponds not to equilibrium instability, but to the existence of multiple basins of attraction determining long-run outcomes. This reframes Minsky's hypothesis within the language of nonlinear dynamical systems, interpreting financial instability as a problem of basin selection rather than local equilibrium stability.

We analyze a three-dimensional nonlinear macro-financial system with state variables wage share ω, employment rate λ, and private debt ratio d, where d denotes private debt relative to output. The system evolves according to a coupled set of ordinary differential equations capturing feedbacks between income distribution, employment, and debt accumulation.

We identify conditions under which the system exhibits bistability, with two distinct long-run outcomes: a desirable equilibrium E^+ characterized by high employment and finite debt, and a crisis equilibrium E^- characterized by low wages and explosive leverage. These regimes are separated by a codimension-one boundary $\partial\mathcal{B}$, given by the stable manifold of an intermediate saddle equilibrium E^s.

This boundary partitions the state space into basins of attraction: initial conditions on one side converge to E^+, while those on the other converge to E^-. As a result, local stability of the good equilibrium is insufficient to ensure recovery once the system lies within the crisis basin.

We examine how the interest rate r acts as a control parameter that modifies the vector field and deforms the basin geometry. As r increases, the basin of attraction of E^+ shrinks. At a critical value r^*, the equilibria E^+ and E^s collide and disappear in a saddle-node bifurcation, eliminating the recovery regime.

Two classes of policy interventions follow from this geometry. A *parameter operation*, such as lowering the interest rate or increasing productivity, alters the vector field and reshapes basin boundaries. A *state operation*, such as a one-time debt reduction, shifts the system directly in state space:

$$(\omega, \lambda, d) \mapsto (\omega, \lambda, (1-\rho)d),$$

where $\rho \in (0,1)$ is the fraction of debt removed.

We characterize a minimal ρ^* required to cross the basin boundary and restore convergence to E^+. Numerical calibration suggests $\rho^* \approx 0.45$ for a representative over-indebted state. Near the bifurcation point r^*, where the recovery basin becomes vanishingly small, such state interventions become necessary for stabilization.

This perspective connects macro-financial instability to a broader class of nonlinear systems in which long-run outcomes depend on initial conditions and basin geometry rather than local stability alone.

References

[1] S. Keen, *J. Post Keynesian Econ.* **17**(4), 607–635 (1995).

[2] M.R. Grasselli & B. Costa Lima, *Math. Financ. Econ.* **6**(3), 191–210 (2012).

Structural Properties of Systems Controlled by Switching

I. O. Shevchenko[1], X. Liu[2]

[1] *University of Waterloo, Waterloo, Canada, i3shevch@uwaterloo.ca*
[2] *University of Waterloo, Waterloo, Canada, xzliu@uwaterloo.ca*

Switched systems are ubiquitous in scientific and engineering applications where multiple dynamical modes are necessary to model the system, as a result of rapidly changing parameters or environmental factors. In applications, it is often desirable to drive the state of the system to a particular position using some control input. In this work, we consider the case where there are no actuators in the physical system, and hence the only available control inputs to achieve this task are the switching signals. This particular setting is commonly found, for example, in models of DC-DC power converters [1].

In real-world systems, the exact parameter values governing system dynamics may be unknown or difficult to estimate. As such, it is important to determine how this uncertainty in the state-space model affects the controllability properties of the system. The concept of structural controllability, introduced in [2], directly addresses this issue. In particular, using the results of [2] and [3] for linear time-invariant systems, the problem of guaranteeing controllability of linear systems for a full-measure set of nonzero parameter values is reduced to proving controllability for a single choice of nonzero parameter values. Similar results have recently been established for switched systems with the control input coming from both the system actuators and the switching signals [4, 5], however the case of only having switching signals as the control input has not yet been treated. We will present some results towards bridging this gap in the literature.

References

[1] C. Albea, G. Garcia, and L. Zaccarian. *Hybrid dynamic modeling and control of switched affine systems: application to DC-DC converters*, in *54th IEEE Conference on Decision and Control* (CDC), Osaka, Japan, pp. 2264-2269 (2015).

[2] C. T. Lin, *Structural controllability*, IEEE Trans. Auto. Contr. 19(3), pp. 201-208 (1974).

[3] R. Shields and J. Pearson, *Structural controllability of multiinput linear systems*, IEEE Trans. Auto. Contr. 21(2), pp. 203-212 (1976).

[4] X. Liu, H. Lin, and B. M. Chen, *Structural controllability of switched linear systems*, Automatica 49, pp. 3531-3537 (2013).

[5] S. Pequito and G. J. Pappas, *Structural minimum controllability problem for switched linear continuous-time systems*, Automatica 78, pp. 216-222 (2017).

Sensitivity-Based Methods for Analyzing Nonsmooth Systems

P. Stechlinski[1], H. Abdelfattah[2], S.A. Eisa[2]

[1] *University of Maine, Orono, USA peter.stechlinski@maine.edu*
[2] *University of Cincinnati, Cincinnati, USA, {abdelfhm,eisash@mail.uc.edu}*

Nonsmooth systems, which are continuous but nondifferentiable and experience switches between modes, arise in a variety of applications in science and engineering. However, the presence of nonsmoothness invalidates standard theory from smooth dynamical systems, including analyzing the identifiability of a system using derivative-based information (to determine if the system parameters can be uniquely determined from system outputs). Identifiability is a key property of a system as it characterizes the ability to gain information about the system. Consider the following input-output system, with state variables x, inputs u, outputs y and parameters θ:

$$\dot{x} = f(x,u,\theta), \qquad y = h(x,u,\theta). \tag{1}$$

The system is said to be locally structurally identifiable if the system parameters θ can be uniquely determined from the outputs of the system, i.e., if for any admissible input u and time $t \in [t_0, t_f]$,

$$y(t;u,\theta_1) = y(t;u,\theta_2) \quad \Rightarrow \quad \theta_1 = \theta_2 \tag{2}$$

for all θ_1 and θ_2 near a reference parameter θ^* of interest. Local observability can be similarly characterized by setting $f_0(\theta) = \theta = x_0$, i.e., if the initial conditions can be uniquely determined from the outputs.

A variety of methods have been developed to tackle identifiability [1], including sensitivity-based methods such as the so-called sensitivity rank condition (SERC) approach. The SERC method is based on computing the the output sensitivity matrix $\frac{\partial y}{\partial \theta}$, with the idea being that if outputs are highly sensitivity to perturbations of a certain parameter, then it is likely identifiable. However, standard identifiability/observability methods crucially rely on the smoothness of the functions f and h. In order to extend sensitivity-based methods to the nonsmooth case, and hence directly treat nonsmooth systems, we use generalized derivatives theory.

In this work, we present a sensitivity-based method to determine identifiability of a nonsmooth system [2] using lexicographic directional derivatives [3], which are a type of generalized derivative that possess a strong theoretical and numerical toolkit. In order to do this, we develop a first-order Taylor-like approximation theory for nonsmooth functions. The resulting theory, called the lexicographic sensitivity rank condition (L-SERC), is applicable to both ODEs and differential-algebraic equations (DAEs), and it can be used for observability analysis and model reduction [4], among other things. Moreover, the new theory recovers the classical sensitivity rank condition (SERC) test for ODEs when participating functions are smooth, and establishes the SERC test for smooth DAEs. The new theory and methods are illustrated through examples and practical applications.

References

[1] H. Miao, X. Xia, A.S. Perelson and W. Hulin *On identifiability of nonlinear ODE models and applications in viral dynamics*, SIAM Review, **53**, pp. 3-39 (2011).

[2] P. Stechlinski, S.A. Eisa and H. Abdelfattah, *Identifiability and observability of nonsmooth systems via Taylor-like approximations*, IEEE TAC, **70**, pp. 4178-4185 (2025).

[3] K.A. Khan and P.I. Barton, *A vector forward mode of automatic differentiation for generalized derivative evaluation*, Optimization Methods and Software, **30**, pp. 1185-1212 (2015).

[4] P. Stechlinski, S.A. Eisa and H. Abdelfattah, *Parameter Identifiability and Reduction for Smooth and Nonsmooth Differential Algebraic Equation Systems*, IEEE L-CSS, **8**, pp. 3159-3164 (2024).

Maximum Likelihood Identification of Bistable Structural Nonlinear Systems via Analytical Fokker-Planck Solution

S. Takata[1]

[1] *National Institute of Technology, Tokyo College, Japan, takata@tokyo-ct.ac.jp*

Stochastic response of the noise-derived bistable nonlinear system is important for structural reliability analysis. In this paper, we report about the system identification problem based on maximum likelihood estimation (MLE) via analytical Fokker-Planck solutions using. Here, the system is Single-DOF system. The proposed method provides a methodology that does not depend on the features of the time series and the frequency spectrum, because the method is found on the response probability density. Even if the cases are unclear time series and frequency spectrum, the proposed method has the effectives that applicable.

Here, the target system is supposed the whitenoise-drived bistable nonlinear system [1], the Fokker-Planck solution is well known the analytical form [2]. Standard framework of MLE has already provided the well-known literature [3]. The likelihood function is formulated to Eq. (1), by combined with the Fokker-Planck solutions.

$$\mathcal{L}(x|\theta) = \prod_{i=1}^{N} \frac{\exp\left[\left(\frac{1}{2}kx_i^2 - \frac{1}{4}\mu x_i^4\right)/(D/c)\right]}{\sum_{x_n=-a}^{a} \Delta a \exp\left[\frac{1}{2}kx_n^2 - \frac{1}{4}\mu x_n^4\right]/(D/c)}. \tag{1}$$

Here, x represents the displacement of structure, k and μ are linear/nonlinear spring constant, c denotes damping constant, D is the diffusion coefficient and Δa is increment for the numerical integration.

A system response time series and identification results are shown in Fig. 1. The time series (Fig. 1(a)) shows the jump responses between two stable equilibrium points, also inset shows the restoring force characteristics of system. The identification results (Fig.1 (b)) represent the convergence of the estimation values (solid) to the true values (dotted) with increasing the number of samples for identification. The probability densities of the time series are good agreement with the reconstructed it is using the estimated parameters. Furthermore, we will discuss the collapse of the identification performance under the Non-Gaussian noise excitation in the conference.

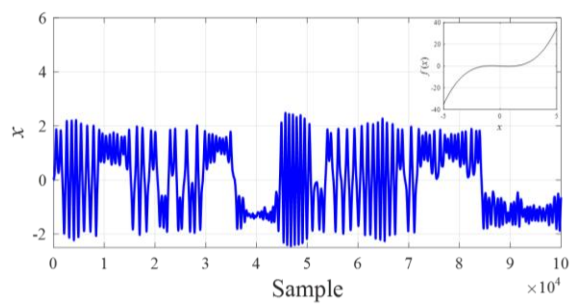

(a) Response time series

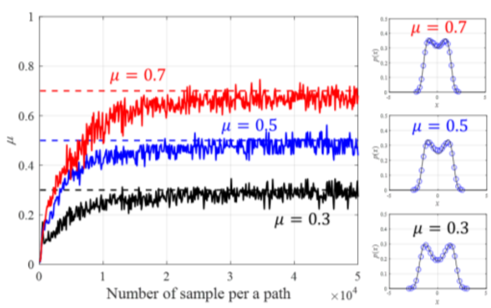

(b) Identification results

Figure 1: Bistable system response and identification results.

References

[1] J. B. Roberts and P. D. Spanos, *Random vibration and statistical linearization*, Dover Civil and Mechanical Engieering, (1990).
[2] T. K. Caughey, *Derivation and application of the Fokker-Planck equation to discrete nonlinear dynamic systems subjected to white noise wandom excitation*, J. Acoust. Soc. Am. **35**, 11, pp. 1683-1692 (1963).
[3] C. M. Bishop, *Pattern Recongnition and Mahcine Learning*, Springer, (2006).

Acknowledgements

This work was supported by JST Grant Number JPMJPF2115.

Adaptive vibration control of the Euler-Bernoulli beam system with an unknown payload

Yingying Wang[1], Xinzhi Liu[2]

[1] *Jiangnan University, Wuxi, China, wangyy_jiangnan@163.com*
[2] *University of Waterloo, Waterloo, Canada, xzliu@uwaterloo.ca*

The aim of this study is to provide an adaptive boundary controller for the Euler-Bernoulli beam's vibration control problem with an unknown payload. An adaptive law is designed to compensate for the nonlinearity caused by the uncertainty of system parameters. Partial differential equations involving time and space variables describe the dynamic features of the Euler-Bernoulli beam system. The operator semigroup under the adaptive boundary controller reveals that the system is well-posed. The asymptotic stability of the closed-loop system is obtained from the extended Krasovskii-LaSalle invariance principle. The proposed boundary control is verified using numerical simulations compared to previous findings.

Fiscal Policy as Basin Deformation: Critical Multipliers, Timing Thresholds, and Geometric Control of a Macroeconomic Attractor

K. Wright[1], D. Robinson[2]

[1] *University of Waterloo, Canada, kirsten.wright@uwaterloo.ca*

[2] *Laurentian University, Canada, drdrrobinson@gmail.com*

Abstract:

Macroeconomic policy is typically analyzed in terms of its effects on equilibrium output and stability conditions. From a dynamical systems perspective, we instead examine how fiscal intervention alters the geometry of macroeconomic trajectories.

We consider a three-dimensional macro-financial system with state variables representing economic activity, debt relative to output, and productivity. The system evolves according to $\dot{x} = f(x; G)$, where fiscal policy G enters as a control parameter. In particular, productivity evolves according to

$$\dot{\alpha} = -\mu_\alpha \alpha + \gamma G - \eta d,$$

capturing the competing effects of decay, policy support, and debt overhang, where d denotes debt relative to output.

We show how changes in fiscal intensity modify the underlying vector field and thereby deform basins of attraction, shifting separatrices that divide trajectories leading to recovery from those leading to persistent stagnation. If k denotes the effectiveness of fiscal expansion in raising productivity, the model yields a threshold of the form

$$k^* = \frac{\gamma}{\mu_\alpha + \eta d^*},$$

where d^* is the debt level at the basin boundary. Below this threshold, trajectories entering the high-debt region are unlikely to recover, while above it, the basin of recovery expands.

We further examine the timing of intervention near the basin boundary. Linearization implies that the latest effective intervention time satisfies

$$t^* \approx \frac{1}{\mu_u} \log\left(\frac{\varepsilon_0}{\varepsilon_{\min}(G_{\max})}\right),$$

where ε_0 is the initial distance to the boundary and $\varepsilon_{\min}(G_{\max})$ is the smallest recoverable perturbation under maximal feasible policy. Under the scaling observed in the model, increases in fiscal capacity yield diminishing extensions in intervention time.

These results suggest that fiscal policy operates not only by shifting equilibrium outcomes, but by reshaping the geometry of the system, altering which macroeconomic regimes are dynamically reachable.

References

[1] S. Keen, *J. Post Keynesian Econ.* **17**(4), 607–635 (1995).

[2] M.R. Grasselli & B. Costa Lima, *Math. Financ. Econ.* **6**(3), 191–210 (2012).

[3] O. Blanchard & D. Leigh, *Am. Econ. Rev. P&P* **103**(3), 117–120 (2013).

Near-Absorbing Boundaries in Macroeconomic Diffusions and the Mathematics of Institutional Floors

K. Wright[1], D. Robinson[2]

[1] *University of Waterloo, Canada, kirsten.wright@uwaterloo.ca*

[2] *Laurentian University, Canada, drdrrobinson@gmail.com*

Abstract: Many economic and social processes are constrained by non-negativity conditions, giving rise to boundary effects that fundamentally alter system dynamics. We study these effects in a stochastic setting by analyzing behavior near zero in diffusions with multiplicative noise.

We consider the geometric Brownian motion

$$\mathrm{d}X_t = \alpha X_t \,\mathrm{d}t + \beta X_t \,\mathrm{d}W_t,$$

and define the log-drift parameter $\gamma := \alpha - \frac{1}{2}\beta^2$, so that $\log X_t$ evolves as a Brownian motion with drift γ. In the regime $\gamma < 0$, trajectories exhibit a persistent tendency toward lower values. In this case, zero is a natural (non-attainable) boundary: it is not attained in finite time, but trajectories reach arbitrarily small values with probability one, and for any $\delta > 0$ the corresponding hitting time is finite almost surely.

Using standard diffusion theory, the expected time to reach a small threshold $\delta > 0$ from $X_0 = x_0 > \delta$ scales as

$$\mathbb{E}[\tau_\delta] \sim \frac{\log(x_0/\delta)}{|\gamma|}.$$

Thus, descent toward near-zero states is slow but persistent, leading to prolonged residence near boundary regions.

Near the boundary, both drift and diffusion coefficients vanish in level terms, but the process remains non-degenerate in relative terms, as

$$\frac{\mathrm{d}X_t}{X_t} = \alpha \,\mathrm{d}t + \beta \,\mathrm{d}W_t,$$

so that proportional fluctuations remain active even as absolute adjustments shrink.

From a dynamical systems perspective, these boundary regions act as effective dynamical traps: trajectories become increasingly sensitive to perturbations and exhibit persistent low-state behavior. In economic terms, these correspond to regimes in which income or liquidity constraints bind, causing price-based signals to become uninformative and shifting system dynamics from preference-driven to constraint-driven behavior. Ratios diverge, signal informativeness degrades, and standard equilibrium interpretations weaken.

We introduce a floor operator F_ε enforcing $X_t \geq \varepsilon$, implemented via Skorokhod reflection. This prevents entry into constraint-dominated regions and restores key structural properties, including stable relative dynamics and bounded inverse moments. The framework further suggests conditions under which an interior-optimal floor level ε^* may exist.

These results provide a unified perspective on instability near constraint boundaries, highlighting how maintaining positive floors can stabilize both individual trajectories and system-level dynamics.

References

[1] W. Feller, *Ann. Math.* **55**(3), 468–519 (1952).

[2] K. Itô & H.P. McKean, *Diffusion Processes and Their Sample Paths*, Springer (1974).

Event-Triggered Control of SIS Epidemic Models: Stability, Positivity, and Robustness to Delays

Kexue Zhang

Queen's University, Kingston, Canada, kexue.zhang@queensu.ca

In this talk, we study an event-triggered feedback control framework for a classical SIS epidemic model. The goal is to stabilize the disease-free equilibrium while preserving the natural positivity of the infected population proportion. Instead of using continuous-time control updates, the proposed method activates control actions only when a state-dependent error, defined as the difference between the current infection level and its value at the most recent triggering time, exceeds a given threshold.

We derive explicit triggering conditions that guarantee asymptotic stability of the disease-free equilibrium and show how the choice of the threshold affects the system behavior. Between triggering instants, the control input is kept constant over a finite interval, which leads to a hybrid closed-loop system with piecewise-constant feedback.

We also study the effect of execution delays and establish robustness of the proposed approach under delayed implementation. In particular, we prove that the controlled SIS system avoids Zeno behavior, which ensures practical implementation. These results provide a theoretically sound and resource-efficient approach for epidemic control based on event-triggered strategies.

This is joint work with Hilaire Nonhou-Zogo.

Air Pollution and Energy Innovation: A Spatial Optimal Control Approach

L. Bargna[1], D. La Torre[2], B. Montmartin[3], L. Nesta[4]

[1] *University of Insubria, Italy, lbargna1@uninsubria.it*
[2] *SKEMA Business School, Université Côte d'Azur, France, davide.latorre@skema.edu*
[3] *SKEMA Business School, Université Côte d'Azur (GREDEG), France, benjamin.montmartin@skema.edu*
[4] *GREDEG-CRNS, Université Côte d'Azur; OFCE, SciencesPo Paris; SKEMA Business School, France, lionel.nesta@univ-cotedazur.fr*

This talk revolves around the joint spatio–temporal dynamics of air pollution and climate–mitigation energy innovation, and proposes an optimal policy mix that steers their transition towards sustainable development. We introduce a coupled reaction–diffusion framework in which pollution and innovation interact through cross–effects and diffuse across regions for different reasons: pollution through physical transport and climate–mitigation energy innovation through knowledge spillovers. The framework is embedded in an optimal control problem in which a planner uses two instruments: emission abatement and innovation support. Using an innovative two–step panel estimator applied to European regional data on $PM_{2.5}$ and climate–mitigation energy patenting, we estimate the core parameters of the system. We find that pollution diffuses strongly across space while innovation remains localized, and that the two processes feed back on each other: a larger innovation stock lowers subsequent pollution, while higher pollution stimulates innovation. Simulations of the calibrated control problem show that innovation support is optimally positive and increasing throughout the time horizon, whereas the direction and timing of abatement depend on the welfare valuation of polluting activity and on terminal penalties. Because the two instruments operate over different horizons but affect coupled processes, environmental and innovation policies must be designed jointly.

Selective State-Space Model Prediction of Cancer Treatment Response

Y. Derbal[1]

[1] *Toronto Metropolitan University, {yderbal}@torontomu.ca*

Cancer is a complex adaptive system shaped by genetic, immunological, and eco-evolutionary determinants [1, 2, 3], with therapeutic resistance representing a major challenge to effective treatment. Adaptive therapy offers a plausible strategy to delay resistance but requires reliable monitoring and prediction of treatment response [4]. Although various mathematical models have shown clinical promise [5], they are difficult to parameterize and often apply only to narrow patient subsets. Large language models (LLMs), such as the Mamba selective state-space model (SSM) [6], may overcome these limitations by learning from extensive genetic, radiomic, and clinical data across large patient cohorts, capturing the multidimensional dynamics of cancer while reflecting patient diversity.

SSM learning of cancer nonlinear dynamics entails reconstructing these dynamics within the latent state-space of the SSM, where tumor clonal frequencies can plausibly serve as the state variables. The learned model can be used to predict treatment response to support adaptive therapy, or integrated into treatment decision-support systems used by oncologists to explore "$what-if$" treatment scenarios guided by LLM-based predictions of treatment response [7]. To explore this potential, a Mamba SSM is trained on a synthetic cohort of 1,000 prostate cancer patients. Their treatment response dynamics are simulated using an extension of a Lotka-Volterra (LV) evolutionary model [8], which incorporates testosterone production and clearance under an adaptive treatment regimen managed by a proportional-integral-derivative (PID) controller [4]. Individual patients are differentiated by their tumor clones' growth rates and competition coefficients.

The main investigation examines the accuracy of predicting treatment response at time $i+1$, given the observed response from time $i-N$ to i. Across all patients, the average mean square prediction error was $3x10^{-7}$, suggesting robust accuracy for one-step-ahead forecasting. This result provides a proof of concept for using SSMs to reconstruct the nonlinear dynamics of prostate cancer treatment response. However, clinical implementation would require fine-tuning and validation using real-world patient data. In this respect, a key objective for future research is to quantitatively characterize the model's prediction horizon, specifically, determining how far into the future it can reliably predict treatment response.

References

[1] Hanahan D. *Hallmarks of Cancer: New Dimensions*, Cancer Discov. **12**, 1, pp. 31-46 (2022)

[2] Greaves M. *Nothing in cancer makes sense except*, BMC Biol. **16**, 1, pp. 22 (2018)

[3] Derbal Y. *The Adaptive Complexity of Cancer*, Biomed Res Int. 2018, pp. 5837235 (2018

[4] Derbal Y. *Adaptive Control of Tumor Growth*, Cancer Control. **31**, pp. 10732748241230869 (2024)

[5] Phan T, Crook SM, Bryce AH, Maley CC, Kostelich EJ, Kuang Y. *Mathematical modeling of prostate cancer and clinical application*, Applied sciences. **10, 8**, pp. 2721 (2020)

[6] Gu A, Dao T. *Mamba: Linear-time sequence modeling with selective state spaces*. in *Proceedings of First conference on language modeling* (COLM), Philadelphia, United States.ed. pp. (2024).

[7] Derbal Y. *Generative AI - Assisted Adaptive Cancer Therapy*, Cancer Control. **32**, pp. 10732748251349919 (2025)

[8] Zhang J, Cunningham JJ, Brown JS, Gatenby RA. *Integrating evolutionary dynamics into treatment of metastatic castrate-resistant prostate cancer*, Nat Commun. **8**, 1, pp. 1816 (2017)

Robust Parametric Blind Deconvolution of Non-Linear Motion Blur via Spectral Analysis

Ali Elwazir[1,2], Oleg Michailovich[1]

[1] *Department of Electrical and Computer Engineering, University of Waterloo, Waterloo, ON, Canada*
[2] *Google, Hardware Engineering*

Motion blur in handheld photography is traditionally modeled as a linear integration of light along a straight path. However, real-world camera shake frequently exhibits rotational components during exposure, resulting in complex, nonlinear trajectories. This work addresses the challenging ill-posed problem of blind deconvolution for non-linear motion blur. Rather than estimating a dense 2D kernel, we parameterize the problem by modeling the blur trajectory as a "thin" quadratic curve defined by three precise geometric parameters: path length, orientation angle, and curvature. By analyzing the whitened Fourier spectrum of the blurred image, and leveraging the $1/f^{\alpha}$ power spectrum of natural images as a stochastic background, we demonstrate that these deterministic geometric parameters can be recovered directly from the frequency domain. Our framework isolates the kernel's spectral signature—specifically energy ridges and zero-crossing ripples. We introduce a robust estimation pipeline that resolves inherent structural ambiguities (such as the 90-degree angle ambiguity) via cost-based candidate selection, and improves length estimation accuracy by combining cepstral analysis with zero-crossing counting. Finally, a multi-start optimization process is employed to ensure consistent convergence on the global minimum for curvature and orientation. By reducing the complex 2D kernel estimation into a bounded, highly constrained parametric search, our approach achieves highly accurate trajectory reconstruction—yielding sub-pixel length and sub-degree orientation errors—while operating at a fraction of the computational cost of modern iterative optimization methods.

Topics: Artificial Intelligence, Inverse Problems, and Optimization

The VII International AMMCS
Interdisciplinary Conference
Waterloo, Ontario, Canada
April 26, 2026

Statistical Learning Approach for Tuning the Hyperparameter in the L-BFGS Optimization Algorithm

Y. Gao[1], N. Mudalige[2], T. Migot[3]

[1] *University of Toronto, Mississauga, Canada, felix.gao@mail.utoronto.ca*
[2] *University of Toronto, Mississauga, Canada, nishan.mudalige@utoronto.ca*
[3] *University of Toronto, Mississauga, Canada, tangi.migot@utoronto.ca*

We consider non-linear, non-convex, unconstrained, continuous optimization problems of the form

$$\min_{x \in \mathbb{R}^n} f(x) \tag{1}$$

where $f : \mathbb{R}^n \to \mathbb{R}$ is a continuously differentiable function. In this context, we aim at finding a local minimum.

The Limited-memory-Broyden-Fletcher-Goldfarb-Shanno algorithm (L-BFGS [1]) is a classical iterative method for such problems. It is a quasi-Newton method that uses only first order derivatives of the objective function to approximate the Hessian based on previous iterates. Its performance, however, depends strongly on the choice of the memory parameter `mem`, which controls the number of stored curvature pairs used to construct the inverse Hessian approximation. In this work, we investigate a statistical learning framework to systematically select the L-BFGS memory parameter that minimizes runtime based on problem-specific features. We use the collection of optimization test problems from OptimizationProblems.jl [2] package. This collection contains more than 350 constrained and unconstrained problems. We use the L-BFGS solver implemented in the JSOSolvers.jl [3].

The parameter `mem` introduces a critical tradeoff: larger values may improve the curvature approximation and reduce the total iteration count, but they also increase memory usage and per-iteration computational cost. Using analytical features and empirical data derived from initial objective and gradient evaluations, we trained and evaluated several machine learning predictive models. Among all the trained models, we pick the best one and compare it with two baseline models. Baseline1 uses the default configuration `mem`=5 as a lower bound, while Baseline2 utilizes `mem`=87, representing the global best mem across the entire dataset.

Table 1: Performance Ratio Quantiles (1.0 = Perfection). Bold values indicate the best performance in each row.

Quantile	**Best Trained Model**	**Baseline1**	**Baseline2**
0.50	1.175	1.234	**1.112**
0.75	**1.300**	1.783	1.476
0.95	**2.135**	5.279	2.266

The results reveal a clear progression in solver intelligence; notably, our approach closely approximates an oracle-level baseline on more difficult problems without requiring dataset-level knowledge.

References

[1] J. Nocedal and S. J. Wright, *Numerical Optimization*, 2nd ed., Springer, New York (2006).

[2] T. Migot, D. Orban, A. Soares Siqueira, and contributors, *OptimizationProblems.jl: A collection of optimization problems in Julia*, `https://github.com/JuliaSmoothOptimizers/OptimizationProblems.jl` (2023).

[3] T. Migot, D. Monnet, D. Orban, A. Soares Siqueira, JSOSolvers.jl: Unconstrained and bound-constrained optimization solvers. Journal of Open Source Software, 11(117), 9467 (2026). `https://github.com/JuliaSmoothOptimizers/JSOSolvers.jl` (2026)

The VII International AMMCS
Interdisciplinary Conference
Waterloo, Ontario, Canada

Orthogonality relations for derivatives of Discrete Fourier Transform and Discrete Cosine Transform basis functions

Amelia Kunze[1] and Edward R. Vrscay[2]

[1] *Universita degli studi dell'Insubria, Varese, Italia, akunze@uninsubria.it*
[2] *University of Waterloo, Waterloo, Canada, ervrscay@uwaterloo.ca*

The work reported here began as a tiny portion of an investigation [1] of the use of image gradients in image processing, primarily in (1) best approximation and (2) the Structural Similarity image quality measure (SSIM). Results obtained by incorporating image gradients into the SSIM were reported at AMMCS 2023 [2].

A motivation for considering gradients in best approximation schemes for images lies in the fact that the L^2 distances between image gradients are able to discern differences in visual quality better than the usual L^2-based mean square error (MSE). When a signal or image is expressed as the usual linear combination of basis functions ϕ_k (e.g., DFT, DCT), some simple best approximation schemes employing gradients will involve scalar products of the form $\langle D\phi_k, D\phi_l\rangle$, where "$D$" denotes the (discrete) derivative operator used to define the gradient [1]. In [1], it was shown that in the special case that D is the forward-difference operator, $Df[n] = f[n+1] - f[n]$, the nonzero derivatives of both DFT and DCT basis functions form orthogonal sets (in $\mathbb{C}^N$ and $\mathbb{R}^N$, respectively), leading to a significant simplification of the equations involved in these best approximation schemes.

Indeed, in the case of DFT basis functions, a rather simple application of the DFT Convolution Theorem yields that $D\phi_k = C_k\phi_k$, $0 \le k \le N-1$, for any derivative operator D (and, indeed, for any circular convolution with kernel g), where the C_k are constants determined by D (or kernel g). This implies that for any $n > 1$, the set of nonzero DFT derivative functions, $\{D^n\phi_k,\ 1 \le k \le N-1\}$, form an orthogonal set in $\mathbb{C}^N$. Admittedly, this is not an earth-shattering result but it does not appear to have ever been discussed in any research papers or books on signal/image processing, most probably since it has not been of any practical use – until now.

The investigation of derivatives of DCT basis functions $\{\phi_k\}$ is more complicated. For example, when $Df[n] = f[n+1] - f[n]$, each $D\phi_k$ is a linear combination of ϕ_k and ψ_k, the corresponding k-frequency discrete sine function. A very lengthy calculation (Appendix A of [1]) shows that the set of nonzero DCT derivatives $\{D\phi_k,\ 1 \le k \le N-1\}$ are orthogonal to each other. More recently, however, we have found that the nonzero second-order DCT derivatives, $\{D^2\phi_k, 1 \le k \le N-1\}$, do **not** form an orthogonal set. Although not to be found in usual textbook treatments of DCT, a method of "symmetric convolutions" does exist [3] and can be used to show that the (appropriate) convolution of DCT basis functions with kernels of odd or even symmetry produces orthogonal sets. For the symmetric difference operator, $D_S f[n] = \frac{1}{2}[f[n+1] - f[n-1]]$, we find that for any $n \ge 1$, the nonzero nth-order DCT derivatives, $\{D_S^n\phi_k, 1 \le k \le N-1\}$ form an orthogonal set in $\mathbb{R}^N$. The D_S operator may also be well suited to define the Laplacian in PDEs on lattices, e.g., discrete heat and wave equations, since both the DFT and DCT basis functions satisfy eigenfunction-eigenvalue equations of the form $D_S^2 u_k + \lambda_k u_k = 0$, where the λ_k are real and positive. As such, these basis functions could be useful in separation-of-variable-type solutions to these PDEs.

References

[1] A. Kunze, *An investigation of the use of gradients in imaging, including best approxmation and the Structural Similarity image quality measure*, M.Math. Thesis, Department of Applied Mathematics, University of Waterloo (2023).

[2] A. Kunze and E.R. Vrscay, *Exploring the use of gradients in the Structural Similarity quality measure* in The VI AMMCS International Conference, Waterloo, Canada, August 14-18, 2023, Springer Proceedings in Mathematics and Statistics (2023).

[3] S.A. Martucci, *Symmetric convolution and the discrete sine and cosine transforms*, IEEE Trans. Sig. Proc. **42** (5), 1038-1051 (1994).

Extended Cellular Automata on Spaces of Probability Measures

A. Kunze[1,2], D. La Torre[3], E. Formenti[1]

[1] *Université Côte d'Azur, CNRS, i3S, Nice, France*
[2] *Universitá degli Studi dell'Insubria, Dept. of Economics, Varese, Italy*
[3] *SKEMA Business School, Sophia Antipolis, France*

Cellular Automata (CA) are a powerful computational framework widely used to model complex systems driven by local interactions. Their simplicity lies in the use of a finite set of states and a space-invariant local rule, yet this simplicity leads to rich and diverse dynamical behaviors.

The classical CA approach assumes complete certainty in the state of each cell, which limits their ability to describe real-world systems with inherent uncertainty. To address this limitation, we have recently proposed an extended CA model, called "Cellular Automata on Probability Measures" (CAM), in which the classical state is replaced by a probability measure over the set of all possible states [1]. The probability measure may differ from cell to cell, allowing the framework to model heterogeneous and uncertain spatial systems. The local update rule then operates directly on configurations of probability measures, enabling the model to capture the full range of behaviors the system may exhibit. In this talk, we define the CAM model and develop many foundational results. We show that the CAM framework collapses to classical CA when Dirac probability measures are used. Unlike classical CA, we prove that every CAM has at least one fixed point. We also prove under what conditions a version of the well-known Curtis-Hedlund-Lyndon theorem holds for CAMs. Finally, we outline some applications for the CAM framework, including parameter estimation in dynamic modelling.

References

[1] E. Formenti, A. Kunze, D. La Torre (2026). *Cellular Automata on Spaces of Probability Measures*, Mathematics and Computers in Simulation, 250, 16-34.

IFSM with Grey-Level Maps on $L^p(0,1)$ for $0 < p < 1$: Theory, a Separating Example, and the Role of the Continuous Setting

H. Kunze[1], F. Mendivil[2], D. La Torre[3]

[1] *University of Guelph, Canada, hkunze@uoguelph.ca*
[2] *Acadia University, Canada franklin.mendivil@acadiau.ca*
[3] *SKEMA Business School, Université Côte d'Azur, France, davide.latorre@skema.edu*

We develop the theory of Iterated Function Systems with grey-level maps (IFSM) in the quasi-Banach metric spaces $(L^p(0,1),d_p)$ for $0 < p < 1$, where d_p is the natural p-th power metric $d_p(f,g) = \int_0^1 |f-g|^p\,dx$. We prove that a non-overlapping N-map affine IFSM with grey-level coefficients α_i, β_i acts as a strict contraction in $(L^p(0,1),d_p)$ if and only if $\sum_{i=1}^N |\alpha_i|^p < N$, and that the resulting Banach-type fixed-point theorem yields a well-posed inverse problem (collage minimisation) on the *enlarged* family of admissible targets that includes functions outside L^2 and even outside L^1.

We illustrate the theory on the one-parameter family of singular targets $h_r(x) = (1-x)^r$ for $r \in [-1,1]$ and $N = 4$. Because $h_r \in L^p(0,1)$ iff $pr > -1$, the parameter p must shrink as $r \downarrow -1$: for $r > -\frac{1}{2}$ the L^2 collage is appropriate, at $r = -\frac{1}{2}$ one must switch to L^1, and at $r = -1$ one must descend further to $L^{1/2}$. Throughout, the analysis takes place in the continuous setting: the collage functional is an honest integral of the singular function h_r, not a Riemann-sum surrogate. A dedicated section explains what changes when one discretises h_r first.

References

[1] S. Banach, *Sur les opérations dans les ensembles abstraits et leur application aux équations intégrales*, Fundamenta Mathematicae **3**, 133–181 (1922).

[2] J. E. Hutchinson, *Fractals and self-similarity*, Indiana University Mathematics Journal **30**, no. 5, 713–747 (1981).

[3] B. Forte and E. R. Vrscay, *Solving the inverse problem for measures using iterated function systems: a new approach*, Advances in Applied Probability **27**, 800–820 (1995).

[4] B. Forte and E. R. Vrscay, *Theory of generalized fractal transforms*, in *Fractal Image Encoding and Analysis* (Y. Fisher, ed.), NATO ASI Series F, vol. 159, Springer, Berlin, pp. 145–267 (1998).

[5] S. Rolewicz, *Metric Linear Spaces*, 2nd ed., Mathematics and its Applications (East European Series), vol. 20, D. Reidel, Dordrecht, and PWN, Warsaw (1985).

[6] M. F. Barnsley, *Fractals Everywhere*, 2nd ed., Academic Press, Boston (1993).

[7] K. Falconer, *Fractal Geometry: Mathematical Foundations and Applications*, 3rd ed., John Wiley & Sons, Chichester (2014).

[8] J. A. Nelder and R. Mead, *A simplex method for function minimization*, The Computer Journal **7**, no. 4, 308–313 (1965).

Recent Advances in Multi-Objective and Set-Valued Optimization with Applications

Davide La Torre[1]

[1] *SKEMA Business School, Université Côte d'Azur, France and University of Bologna, Italy. Email: davide.latorre@skema.edu*

Multi-objective and set-valued optimization provide powerful frameworks for decision-making problems involving multiple criteria, trade-offs, and uncertainty. In many modern applications, classical scalar optimization is insufficient to capture partial preferences, ambiguity, and conflicting objectives. This talk reviews key theoretical developments, including order structures induced by cones, Pareto-type minimality concepts, scalarization methods, and stability properties for vector and set-valued problems. Special attention is given to recent advances involving set-valued probabilities, which model distributional ambiguity and lead naturally to robust and ambiguity-aware optimization formulations. We then present applications in Artificial Intelligence and Machine Learning. We discuss multicriteria deep learning and federated learning, where performance, fairness, robustness, privacy, and communication costs must be jointly optimized. The talk illustrates how recent advances in set-valued and multi-objective optimization provide unified tools for handling trade-offs, uncertainty, and decentralized decision-making in complex systems.

References

[1] H. Kunze, D. La Torre, A. Riccoboni, and M. Ruiz Galán (eds.), *Engineering Mathematics and Artificial Intelligence: Foundations, Methods, and Applications*, CRC Press / Taylor & Francis, Boca Raton (2023). ISBN 978-1-032-25567-5.

[2] D. La Torre, F. Mendivil, and M. Rocca, *Generalized robust optimization using the notion of set-valued probability*, J. Optim. Theory Appl. **207**, art. 64 (2025). DOI: 10.1007/s10957-025-02790-6.

[3] D. La Torre, F. Mendivil, and M. Rocca, *Cone Ordering in Distributionally Robust Optimization with Set-Valued Probabilities*, J. Optim. Theory Appl. **209**, art. 52 (2026). DOI: 10.1007/s10957-026-02992-6

[4] D. La Torre and M. Rocca, *Distributionally robust multiobjective optimization with application to risk measure theory*, Ann. Oper. Res. (2024). DOI: 10.1007/s10479-024-06401-x.

[5] D. La Torre and F. Mendivil, *The Monge–Kantorovich metric on multimeasures and self-similar multimeasures*, Set-Valued Var. Anal. **23**, 2, pp. 319–331 (2015). DOI: 10.1007/s11228-014-0307-2.

[6] D. La Torre and F. Mendivil, *Iterated function systems on multifunctions and inverse problems*, J. Math. Anal. Appl. **340**, 2, pp. 1469–1479 (2008). DOI: 10.1016/j.jmaa.2007.09.057.

The obtainable limiting distributions for a Markov chain

F. Mendivil[1], K. Gingell[1]

[1] *Acadia University, Canada, franklin.mendivil@acadiau.ca*

It is common to try to approximate a given distribution by the limiting distribution of some dynamic process, often a Markov chain. An example of this is using an iterated function system with probabilities (IFSP) to approximate some given probability distribution.

A natural question in this case is "What distributions are possible to achieve by varying the probability weights for some given dynamic process?" For an IFSP, this could mean that we fix the geometric IFS maps but allow both place-dependent and time-varying probabilities in an attempt to exactly match the given target distribution. How wide a class of limiting distributions does this construct? How does the specific choice of the geometric IFS maps constrain the set of attainable limiting distributions? More broadly, for a Markov process driven by some dynamical system, how do the details of the dynamical system constrain the set of allowable limiting distributions?

In this talk we focus on the case of a finite state space discrete time Markov chain, which can be viewed as a random walk on a directed graph. We characterize the set of all possible limiting distributions for any possible choice of transition probabilities on a fixed set of allowable transitions.

References

[1] K. Gingell and F. Mendivil, *Random walks, directed cycles and Markov chains*, Amer. Math. Monthly **130**, 2, pp. 127-144 (2023).

In search of a collage theorem for iterated function systems on Riemannian manifolds

MD. Pham

[1] *University of Toronto, Canada, {martindopham}@gmail.com*

We present an application of iterated function systems (IFS) [2] with an application to modern computational neuroscience. IFS are defined as the collective action of contractive mappings on a metric space ($\mathscr{X}$, d). This action, the so-called Hutchinson operator $\mathscr{H}$, defines a discrete time non-local dynamical system with a unique fixed point $u^* \in (\mathscr{X}, d)$, i.e.

$$\mathscr{H}(u^*) = u^* \tag{1}$$

We recall the essential features of IFS, discuss modern v-variable extensions [1], and apply to an existing EEG source reconstruction dataset for brain activity signals [3]. We introduce an IFS for the space of symmetric positive definite matrices by taking random partial geodesics as the contractive mapping and present an inverse problem. We conclude by suggesting some possible solutions and preliminary results.

References

[1] BARNSLEY, M. F. *Superfractals*. Cambridge University Press, 2006.

[2] BARNSLEY, M. F. *Fractals everywhere*. Academic press, 2014.

[3] PABLE, H., PHAM, M. D., DEHNAVI, M. M., CHHABRA, R., AND DÂANGIULLI, A. Neural self-organization during episodic encoding: deep recurrent effective connectivity from source-localized eeg. *Frontiers in Psychology 17* (2026), 1766795.

The VII International AMMCS
Interdisciplinary Conference
Waterloo, Ontario, Canada

Sigmoidal Production Functions and Optimization Problems in Economics

R. G. Smirnov[1]

[1] *Dalhousie University, Canada, roman.smirnov@dal.ca*

This study investigates the structural origins of production functions, which are fundamental to constrained optimization and economic modelling. Our primary objective is to reconcile classical economic theory with data-driven dynamical systems to better understand how aggregate outputs like GDP emerge from exogenous inputs of capital, labour, and energy.

Utilizing a methodology grounded in data-driven dynamical systems identification, we derive production functions as time-independent invariants of these underlying dynamical systems. We demonstrate that sigmoidal production functions – increasingly prominent in recent economic and applied mathematical literature – emerge naturally from a generalized structural framework within this methodology.

Our results identify the canonical Cobb-Douglas specification not as a universal law, but as a restricted limiting case of this broader sigmoidal framework. Currently, our research status includes a completed theoretical derivation and a comparative analysis against historical economic data. The significance of this work lies in providing a more flexible, mathematically rigorous alternative to traditional models, allowing for a more accurate representation of growth patterns in modern economies.

Kolmogorov-Arnold Networks for Image Processing and Representation Learning

I. A. Urbaniak[1]

[1] ***Cracow University of Technology, Poland, {ilona.urbaniak*@pk.edu.pl**

Kolmogorov-Arnold Networks (KANs), inspired by the Kolmogorov-Arnold representation theorem and recently introduced as an alternative to conventional multilayer perceptrons (MLPs) through learnable edge-based functional mappings [1], have emerged as a promising framework for representation learning and inverse imaging problems. Building on our recent work on KAN-based autoencoder representation learning [2], KAN architectures have demonstrated potential across multiple image processing and medical imaging applications.

Our ongoing investigations have explored KAN-based architectures for medical image analysis, adaptive restoration, and image translation, including hybrid convolutional neural network (CNN)-FastKAN architectures for intelligent breast cancer detection under strict patient-level evaluation protocols for digital pathology systems. Additional studies examined KAN-driven restoration and compression artifact removal for medical images, where structured nonlinear modulation demonstrated improved robustness and cross-domain generalization under varying compression conditions compared to conventional CNN and MLP-based approaches. KAN-based modules were also investigated within Cycle Consistent Generative Adversarial Network (CycleGAN) image translation frameworks, highlighting the potential of structured nonlinear mappings for image translation tasks.

These findings suggest that KANs provide a flexible and interpretable framework for adaptive restoration, medical image analysis, image translation, and structured representation learning, with potential applications in medical imaging, scientific computing, and computer vision.

References

[1] Z. Liu, Y. Wang, S. Vaidya, F. Ruehle, J. Halverson, M. Soljačić, T. Y. Hou, and M. Tegmark, *KAN: Kolmogorov–Arnold Networks*, Proc. of the International Conference on Learning Representations (ICLR), (2025).

[2] I. A. Urbaniak, S. Wieczorek, and J. Kolodziej, *Autoencoder-Based Image Representation Learning with Kolmogorov–Arnold Networks*, Int. J. Appl. Math. Comput. Sci. **36**(2), (2026).

Using Linear Inverse Methods to Study Food Web Energy Flows and Whole Community Responses to Perturbation

M. Yodzis[1], K.S. McCann[2]

[1] *University of Guelph, Canada, myodzis@uoguelph.ca*
[2] *University of Guelph, Canada, ksmccann@uoguelph.ca*

Food webs are complex dynamical systems of interacting species that govern energy flow and ecological stability in natural environments that humans depend on for food and resources. These systems can be represented as networks, where topology describes species interactions and interaction strengths (IS) quantify the flow of energy between them. Generalized Lotka–Volterra (GLV) models are often used to formalize the dynamics of energy flow in food webs by linking interaction strengths to species-level growth, mortality, and biomass accumulation. Within this framework, feasibility requires that all species maintain non-negative equilibrium biomasses, while energetic constraints limit energy transfer efficiency to less than one [1].

Large-scale empirical implementations of GLV-type models, including Ecopath and Allometric Trophic Network approaches [2, 3], are widely used in ecological forecasting and resource management. In this setting, interaction strengths are critical for understanding food web stability and system-wide responses to perturbation, yet their empirical estimation remains difficult and highly uncertain across spatial and temporal scales [5]. Estimating interaction strengths from observations of biomass and vital rates constitutes an inverse problem with many feasible solutions, but empirical GLV models are typically parameterized to yield a single point estimate for each interaction strength, rather than characterizing a broad distribution of values consistent with biological constraints [4, 1].

Recent work by Gellner et al. introduces a variation of the Linear Inverse Method (LIM) using Markov Chain Monte Carlo (MCMC) sampling to estimate distributions of interaction strengths within feasibly and energetically constrained GLV models [1]. Building on this approach, we use LIM-based sampling in combination with press perturbations to quantify how uncertainty in interaction strengths propagates to whole-community responses under sustained environmental or anthropogenic change. This framework provides a probabilistic foundation for assessing ecosystem vulnerability and resilience, offering more robust guidance for ecological management under uncertainty. We present simulated examples motivated by policy-relevant questions in Great Lakes fisheries.

References

[1] Gellner, G., McCann, K., and Hastings, A. (2023). Stable diverse food webs become more common when interactions are more biologically constrained. *Proc. Natl. Acad. Sci. U.S.A.*, 120(31), e2212061120. https://www.pnas.org/doi/10.1073/pnas.2212061120

[2] Christensen, V., Pauly, D. (1992). ECOPATH II, A software for balancing steady-state ecosystem models and calculating network characteristics. *Ecol. Modell.*, 61(3–4), 169–185. https://doi.org/10.1016/0304-3800(92)90016-8

[3] Delmas, E., et al. (2017). Simulations of biomass dynamics in community food webs. *Methods in Ecology and Evolution*, 8(7), 881–886. https://doi.org/10.1111/2041-210X.12713

[4] van Oevelen et al. (2010). Quantifying Food Web Flows Using Linear Inverse Models. *Ecosystems*, 13, 32–45. https://doi.org/10.1007/s10021-009-9297-6

[5] Lawson et al. (2021). Bioenergetic Model Sensitivity to Diet Diversity Across Space, Time and Ontogeny. *Front. Mar. Sci.* 8, 1–13. https://doi.org/10.3389/fmars.2021.625855

Deep Learning Based on Train-Test Discrepancy Minimization

Kaixiang Zheng[1], En-Hui Yang[1]

[1] *University of Waterloo, Waterloo, Canada, {k56zheng,ehyang}@uwaterloo.ca*

Despite the vast applications and rapid development of deep learning (DL), understanding and improving the generalization ability of deep neural networks (DNNs) remains a fundamental challenge. To address this challenge, in this paper, we first define two new generalization quantities, dubbed train-test discrepancy (TTD) and conditional train-test discrepancy (CTTD), and establish a novel bias-variance decomposition framework to analyze them. Based on the decomposition result, we then present a new form of DL dubbed train-test discrepancy minimized (TTDM) DL by jointly minimizing the conventional optimization target and an analytical proxy for the CTTD. Extensive experimental results demonstrate that, in comparison with DNNs trained by the standard DL, TTDM DNNs have smaller train-test discrepancies and better generalization ability, thereby achieving improved prediction accuracy. Additionally, we show that TTDM DL can also be used to train DNNs with enhanced robustness against input perturbations, including FGSM adversarial attack and JPEG compression.

Isogeny graphs of abelian varieties and singular ideals in orders

S. Arpin[1], S. Marseglia[2], C. Springer[3]

[1] *Virginia Polytechnic Institute and State University, Blacksburg, VA, U.S., sarpin@vt.edu*
[2] *Laboratoire Jean Alexandre Dieudonné, Université Côte Azur, Nice, France, stefano.marseglia@univ-cotedazur.fr*
[3] *Center for Communications Research, Princeton, N.J., U.S., c.springer.math@gmail.com*

Isogeny graphs sit at the intersection of number theory, arithmetic geometry, and cryptography. In the setting of elliptic curves, these graphs have striking graph-theoretic structural properties: Kohel showed that ℓ-isogeny graphs of ordinary curves organize into *volcanoes*, a term coined by Fouquet and Mourain which invokes picture that has become a conceptual and algorithmic cornerstone of the field. For higher dimension abelian varieties, however, the setting becomes much more complicated – existing generalizations rely on strong hypotheses, such as maximal real multiplication, which leaves much of the landscape unexplored. In this work [1], we describe structure for isogeny graphs of higher-dimensional abelian varieties, in a very general setting. Working under the mild assumption that the endomorphism ring contains a fixed locally Bass order, our results apply in wide generality, including non-ordinary and non-simple isogeny classes. The guiding philosophy is to take an ideal-theoretic viewpoint, determining the graph-theoretic properties of isogeny graphs by using the arithmetic of orders in étale algebras.

Building up to this application, we prove a new structure theorem for the lattice of overorders of a Bass order at a prime $\mathfrak{l}$. These overorders arrange into a canonical chain, the $\mathfrak{l}$-*multiplicator ladder*, whose successive levels are determined by local properties of singular ideals. The underlying algebra of this $\mathfrak{l}$-multiplicator ladder dictates the shapes of the associated isogeny graphs. Given an $\mathfrak{l}$-multiplicator ladder, we define $(R,\mathfrak{l})$-isogeny graphs whose vertices correspond to abelian varieties with prescribed endomorphism rings and whose edges arise from $\mathfrak{l}$-isogenies, which are classes of isogenies we relate back to ideals. The main results show that each connected component admits a natural stratification into levels indexed by the $\mathfrak{l}$-multiplicator ladder, with explicitly computable edge behaviour between levels. The surface carries a transitive action of a class group, while deeper levels have prescribed ascending/descending edges, producing graphs that generalize classical volcanoes but still have cleanly described structure. We conclude with a precise characterization of when these graphs are genuine volcanoes, extending the classical picture to this broader setting. These results unify earlier work and also open the door to a systematic study of isogeny graphs in higher dimension, with potential implications for computing endomorphism rings of abelian varieties and isogeny-based cryptography.

References

[1] S. Arpin and S. Marseglia and C. Springer, *Isogeny graphs of abelian varieties and singular ideals in orders*, arXiv, `https://arxiv.org/abs/2508.03570` (2025).

A survey on exploring elliptic curves with machine learning

A. Babei[1]

[1] *Howard University, Washington, D.C., USA, angelica.babei@howard.edu*

The discovery of murmurations by He, Lee, Oliver and Pozdnyakov [6] has prompted the question of how machine learning can facilitate discovery in number theory, given the availability of data in databases such as the LMFDB. Elliptic curves present one such avenue of exploration.

Given an elliptic curve E over $\mathbf{Q}$, we can associate to E an L-function with Euler product

$$L(E,s) = \prod_p L_p(E,s). \tag{1}$$

If E has good reduction at p, the local factor is

$$L_p(E,s) = \frac{1}{1 - a_p(E)p^{-s} + p^{1-2s}}, \tag{2}$$

with

$$a_p(E) = p + 1 - |E(\mathbf{F}_p)|, \tag{3}$$

where $|E(\mathbf{F}_p)|$ is the number of solutions of E over the finite field $\mathbf{F}_p$.

Thus, the sequence $(a_p(E))$ encodes arithmetic information about the elliptic curve E, and is a natural starting point for using ML tools. We will showcase various methods used to study invariants of elliptic curves [5, 6, 7, 1, 2, 4, 3], highlighting what worked well and identifying current limitations.

References

[1] A. Babei, B.S. Banwait, A.J. Fong, X. Huang, and D. Singh, *Machine learning approaches to the Shafarevich-Tate group of elliptic curves*, Advances in Theoretical and Mathematical Physics **29**, 8, pp. 2353-2379, (2025).

[2] A. Babei, F. Charton, E. Costa, X. Huang, K.H. Lee, D. Lowry-Duda, A. Narayanan, and A. Pozdnyakov, *Learning Euler factors of elliptic curves*, Advances in Theoretical and Mathematical Physics **29**, 8, pp. 2327-2351, (2025).

[3] A. Babei, U. Shah, M. Kebe, *How Twist Class Redundancy Drives the Prediction of Traces of Frobenius of Elliptic Curves*, `https://arxiv.org/pdf/2605.14288`.

[4] Z. Bujanovic, M. Kazalicki, and D. Vlah, *Improving elliptic curve rank classification using multi-value and learned Mestre-Nagao sums*, International Journal of Data Science in the Mathematical Sciences **3**, 2, pp. 75-86, (2025).

[5] Y.H. He, K.H Lee, and T. Oliver, *Machine learning invariants of arithmetic curves*, Journal of Symbolic Computation **115**, pp. 478-491 (2023).

[6] Y.H. He, K.H Lee, T. Oliver, and A. Pozdnyakov, *Murmurations of elliptic curves*, Experimental Mathematics **34**, 3, pp. 528-540 (2025).

[7] M. Kazalicki and D. Vlah. *Ranks of elliptic curves and deep neural networks*, Research in Number Theory **9**, 53 (2023).

The Determination of norm-Euclidean cyclic cubic fields

G. K. Bagger[1], A. R. Booker[2], B. Kerr[3], K. J. McGown[4], V. Starichkova[5], T. Trudgian[6]

[1] *University of New South Wales Canberra, Australia, g.bagger@unsw.edu.au*
[2] *University of Bristol, England, andrew.booker@bristol.ac.uk*
[3] *University of New South Wales Canberra, Australia, bryce.kerr@unsw.edu.au*
[4] *California State University Chico, USA, kmcgown@csuchico.edu*
[5] *University of New South Wales Canberra, Australia, v.starichkova@unsw.edu.au*
[6] *University of New South Wales Canberra, Australia, timothy.trudgian@unsw.edu.au*

We show that there are precisely 13 cyclic cubic number fields that are norm-Euclidean. Let K be a number field. Let $\mathscr{O}_K$ denote the ring of integers and N denote the norm map. We say that K is norm-Euclidean if for all $\alpha \in K$ there exists $\beta \in \mathscr{O}_K$ such that $|N(\alpha - \beta)| < 1$. This is the classical generalization of the Euclidean algorithm to the number field setting (see [4, 3]). When K is quadratic it is known (see [2, 1]) that $K = \mathbb{Q}(\sqrt{d})$ with d square-free is norm-Euclidean precisely when

$$d = -1, \pm 2, \pm 3, \pm 7, \pm 11, 5, 6, 13, 17, 19, 21, 29, 33, 37, 41, 57, 73.$$

The case of cubic fields is still open and it remains a possibility that there are infinitely many totally real cubic fields which are norm-Euclidean. We restrict to the case of Galois cubic fields, which are necessarily cyclic. In this case, Heilbronn proved that only finitely many are norm-Euclidean (see [7]). By the conductor–discriminant formula, the discriminant of such a field takes the form $\Delta = f^2$, and by genus theory, it must be that either f is a prime with $f \equiv 1 \pmod 3$ or $f = 9$. We prove that a cyclic cubic field K is norm-Euclidean if and only if it has conductor

$$f \in \{7, 9, 13, 19, 31, 37, 43, 61, 67, 103, 109, 127, 157\}. \tag{1}$$

Previously, Godwin and Smith (see [5, 11, 6]) showed that the only cyclic cubic fields that are norm-Euclidean with $f \leq 10^4$ are the ones listed in (1). McGown proved (see [9, 10]) under the Generalised Riemann Hypothesis (GRH), that the list in (1) is complete, and unconditionally, that any exception must satisfy $f \in (10^{10}, 10^{70})$. This range was reduced to $(2 \times 10^{14}, 10^{50})$ by Lezowski and McGown (see [8]). We completely solve the problem.

References

[1] E. S. Barnes and H. P. F. Swinnerton-Dyer, *The inhomogeneous minima of binary quadratic forms. I*, Acta Math. **87**, (1952), 259–323.
[2] H. Chatland and H. Davenport, *Euclid's algorithm in real quadratic fields*, Canad. J. Math., **2**, (1950), 289–296.
[3] R. Dedekind, *Suppl. to L. Dirichlet, "Vorlesungen Über Zahlentheorie"*, Braunschweig, 1893.
[4] L. Dirichlet, *Recherches sur les forms quadratiques à coëfficients et à indeterminées complexes*, J. Reine Angew. Math. **24** (1842), 291–371.
[5] Godwin, H. J. *On the inhomogeneous minima of totally real cubic norm-forms*, J. London Math. Soc. **40** (1965), 623–627.
[6] H. J. Godwin and J. R. Smith, *On the Euclidean Nature of Four Cyclic Cubic Fields*, Math. Comp., **60**, no. 201, (1993), 421–423.
[7] H. Heilbronn, *On Euclid's algorithm in cubic self-conjugate fields*, Proc. Cambridge Philos. Soc., **46**, (1950), 377–382.
[8] P. Lezowski and K. J. McGown, *The Euclidean Algorithm in quintic and septic cyclic fields*, Math. Comp., **86** no. 307, (2017), 2535–2549.
[9] K. J. McGown, *Norm-Euclidean cyclic fields of prime degree*, Int. J. Number Theory, **8** no. 1, (2012), 227–254.
[10] K. J. McGown, *Norm-Euclidean Galois fields and the generalized Riemann hypothesis*, J. Théor. Nombres Bordeaux, **24** no. 2, (2012), 425–445.
[11] Smith, J. R. *On Euclid's algorithm in some cyclic cubic fields*, J. London Math. Soc. **44** (1969), 577–582.

Expansion, separation, and decomposition in the Markoff graph modulo p

C. Brown[1]

[1] *University of California, Davis, coabrown@ucdavis.edu*

Solutions to the Markoff equation

$$x^2 + y^2 + z^2 - xyz = 0 \tag{1}$$

can be enumerated via an iterative process forming the Markoff tree of solutions. When reduced modulo p, the solutions form a family of graphs which are almost 3-regular. It is conjectured that these graphs are not only connected but also form an expander family [1]. If the Markoff graphs form an expander family, then they are poorly decomposable as trees, and this will be evidenced by a lack of low order separations. In this talk, we outline recent advances in computational approaches to the Markoff graph modulo p related to expansion and tree decompositions.

References

[1] A. Baragar, *The Markoff equation and equations of Hurwitz*, dissertation, Brown University (1991).

Explicit Brauer-Manin obstructions on plane quartics

Nils Bruin[1], Brendan Creutz[2]

[1] *Department of Mathematics, Simon Fraser University, Burnaby BC*
[2] *School of Mathematics and Statistics, University of Canterbury, Christchurch, New Zealand*

We describe a method to show a plane quartic over a number field has no rational points. The method can be adapted to show that a curve does not have divisors of degree 1 or 2 and can be generalized to arbitrary smooth projective curves. Our approach significantly improves on the applicability over previous 2-cover descent methods by not requiring the computation of the full S-unit group of the étale algebras involved. We illustrate the practicality with several examples, including examples where we determine plane quartics to be of index 2 or 4 when the maximum local index is strictly smaller.

References

[1] Nils Bruin and Brendan Creutz, *Explicit Brauer-Manin obstructions on plane quartics*, ArXiv Preprint arXiv:2601.16975 (2026)

Computing isomorphisms between quaternion algebras with indefinite LLL

T. Chakroun[2], T. Morrison[1]

[1] *Virginia Tech, USA, {tmo}@vt.edu*
[2] *ENS Paris-Saclay, France, tommy.chakroun@ens-paris-saclay.fr*

We describe an algorithm for computing an isomorphism between two given definite quaternion algebras over the rational numbers. The algorithm uses Watkin's proposed method for computing isometries of isometric quadratic forms with Simon's algorithm for computing maximal isotropic subspaces of quadratic forms. When the quaternion algebras are ramified at precisely one rational prime p and we are given maximal orders in each algebra, the algorithm runs in polynomial time. That a polynomial time algorithm exists is a result of Csahók–Kutas–Montessionos–Zábrádi. The algorithm we describe, however, is practical, even on inputs of cryptographic size, and we give an implementation in Magma.

Solving the isogeny problem using orientations

Maria Corte Real Santos [1], Arthur Herledan Le Merdy[2], Joseph Macula[3], Travis Morrison[4], Eli Orvis[5], et. al

[1] *ENS Lyon, France, maria.corte_real_santos@ens-lyon.fr*
[2] *COSIC, KU Leuven, Belgium, arthur.herledanlemerdy@cosic.kuleuven.be*
[3] *Wake Forest University, North Carolina, USA, joseph.macula@colorado.edu*
[4] *The Virginia Polytechnic Institute, Virginia, USA, tmo@vt.edu*
[5] *University of Calgary, Canada, eli.orvis@colorado.edu*

Computing an isogeny between two supersingular elliptic curves is believed to be a hard computational problem, which lies at the heart of isogeny-based cryptography. In this talk, we will present an approach to solving this problem by extending the Delfs-Galbraith algorithm to oriented curves, which are supersingular curves with a specified embedding of a quadratic order in their endomorphism rings.

Statistical methodology for arithmetic statistics

A. Cowan[1]

[1] *University of Waterloo, Canada, alex.cowan@uwaterloo.ca*

We present statistical methodology tailored for comparing arithmetic data to random variables. Applying this methodology to a simple case of primes in arithmetic progressions discovers a certain arithmetic bias which appears to be largely unknown, and theoretically just out of reach.

Factoring Non-Negative Integer Matrices

L. Dever[1], E. Goedhart[2], G. Heilbrunn[3], W. Wong[4]

[1] *Millersville University, United States, Lindsay.Dever@millersville.edu*
[2] *Bryn Mawr College, United States, egoedhart@brynmawr.edu*
[3] *Independent Researcher, United States, gregoryheilbrunn@gmail.com*
[4] *Kutztown University of Pennsylvania, United States, wong@kutztown.edu*

Semigroups of matrices offer a setting where factorization is not necessarily unique. In this setting, we do not have prime elements in a traditional algebraic sense, therefore we study the *atoms*, or irreducibles, which do not factor without one factor being a unit. In 2022, Baeth et al. [1] applied many of the previously known techniques to the semigroup of nonnegative integer matrices with non-zero determinant, $M_n(\mathbb{N}_0)^\bullet$. While a complete classification of the atoms of $M_2(\mathbb{N}_0)^\bullet$ is unknown; Baeth et al. [1] found several classes of atoms in $M_2(\mathbb{N}_0)^\bullet$ and provided additional criteria for us to find other atoms of the semigroup.

After presenting some of the history and various definitions needed, we will examine the criteria for atoms and highlight some of the new classes of atoms that we have found, providing a sample of the techniques used in the proofs. The first new class of atoms we found by investigating determinants. In particular, a *doubly-balanced* matrix X with relatively prime adjacent entries is an atom when

$$|\det(X)| \in \{16, 32\} \cup \{p, 2p, 4p \mid p \text{ prime}\}.$$

An additional class of atoms uses bounds on the diagonal or off-diagonal entries. In particular, we show that for a *doubly-balanced*, factorable matrix $X = \begin{pmatrix} w & x \\ y & z \end{pmatrix}$ satisfying $\gcd(wz, xy) = 1$, then

$$x, y \leq 2(z-1)(w-1) \qquad \text{and} \qquad w, z \leq 2(x-1)(y-1).$$

This leads immediately to a new class of atoms where this bound is not satisfied.

We also specialize to a subset of bisymmetric matrices to find atoms which, being a divisor-closed subset, are then also atoms in the larger semigroup of $M_2(\mathbb{N}_0)^\bullet$. This subset is denoted by

$$\mathscr{B}^* = \left\{ \begin{pmatrix} x & y \\ y & x \end{pmatrix} \in M_2(\mathbb{N}_0)^\bullet : \gcd(x, y\} = 1 \right\}.$$

Since $\mathscr{B}^*$ contains a relatively small subset of possible factors when determining if a bisymmetric matrix is an atom, we use an algorithm to search potential factors and classify all bisymmetric atoms in $M_2(\mathbb{N}_0)^\bullet$ with minimum up to 500. Critically, the assumption that factors must be bisymmetric greatly simplifies the search for factors.

References

[1] Baeth, N. R. and Chen, H. and Heilbrunn, G. and Liu, R. and Young, M., *Semigroups of non-negative integer-valued matrices*, Comm. Algebra **50**, 3, pp. 1199-1219 (2022).

The VII International AMMCS
Interdisciplinary Conference
Waterloo, Ontario, Canada

Algorithmic Computation of Cohen–Lenstra-Type Measures for p-Class Tower

M. Fakhari[1]

[1] *University of Calgary, Canada, milad.fakhari@ucalgary.ca*

The classical Cohen–Lenstra heuristics predict the distribution of the p-parts of ideal class groups of number fields by assigning natural weights to finite abelian p-groups, typically involving the reciprocal of the size of their automorphism groups. Boston, Bush, and Hajir proposed a non-abelian analogue of this philosophy for p-class tower groups of imaginary and real quadratic fields (see [1] and [2]). Their approach is to define group-theoretic measures on suitable finite p-groups and to conjecture that these measures describe the distribution of p-class tower groups, or of their finite p-class quotients, as quadratic fields are ordered by discriminant.

In this setting, the main object is the pro-p Galois group

$$G_K = \mathrm{Gal}(K_\infty/K), \tag{1}$$

where K_∞ is the maximal unramified pro-p extension of K. Unlike the ordinary class group, which is abelian, the p-class tower group G_K is generally non-abelian, making its direct computation difficult. One therefore studies more accessible invariants obtained from its abelian quotients. By class field theory, the abelianization of G_K recovers the p-class group of K:

$$G_K^{\mathrm{ab}} = G_K/[G_K, G_K] \simeq \mathrm{Cl}_p(K). \tag{2}$$

Similarly, the abelianizations of the index-p subgroups of G_K correspond to the p-class groups of the unramified cyclic degree-p extensions of K. Following the framework of Boston–Bush–Hajir, this leads to the *index-p abelianization data* (IPAD), which records G_K^{ab} together with the abelianizations of the index-p subgroups of G_K.

This project develops an algorithmic framework for computing the predicted IPAD measures arising from the Boston–Bush–Hajir model. The approach organizes finite p-groups through descendant trees, identifies the branches relevant to a prescribed IPAD, and sums the corresponding group-theoretic measures to obtain the predicted IPAD measure. In this way, the IPAD framework of Boston–Bush–Hajir is turned into a systematic computational procedure, producing theoretical IPAD frequencies that can be compared with large-scale data from quadratic fields.

References

[1] N. Boston, M.R. Bush and F. Hajir, *Heuristics for p-class towers of imaginary quadratic fields*, Math. Ann. **368**, 1–2, pp. 633–669 (2017).

[2] N. Boston, M.R. Bush and F. Hajir, *Heuristics for p-class towers of real quadratic fields*, J. Inst. Math. Jussieu **20**, 4, pp. 1429–1452 (2021).

Efficient resolution of Thue–Mahler equations

A. Gherga[1], S. Siksek[2]

[1] *The Tutte Institute of Mathematics and Computing, Canada*
[2] *University of Warwick, United Kingdom*

Let F be a homogenous irreducible form of degree at least 3 with integer coefficients. A Thue-Mahler equation is a Diophantine equation of the form

$$F(X,Y) = a \cdot p_1^{z_1} \cdots p_v^{z_v},$$

where a is an integer and $p_1, \ldots, p_v$ are rational primes. To explicitly solve these equations when the degree and set of primes is small, there exists a practical method of Tzanakis-de Weger using linear forms in logarithms. We give new lattice sieving techniques and a refined algorithm capable of resolving Thue-Mahler equations with high-degree and large prime sets. In this talk, we describe our refined implementation of this method and discuss the key steps used in our algorithm.

The VII International AMMCS
Interdisciplinary Conference
Waterloo, Ontario, Canada

Apollonian Circle Packings and Rings of Integers

S. Haag[1]

[1] *University of Colorado Boulder, US, summer.haag@colorado.edu*

Apollonian circle packings (ACPs) are a fractal created by continual inversion through 4 mutually tangent circles or a quadruple. An integral ACP is when all the curvatures (1/radius) are integers. The study of integral ACPs has many connections to geometry, number theory, group theory, etc. and leads to very nice illustrations. But how much theory of integral ACPs still holds if we look at quadratic rings of integers as the curvatures? Some aspects still hold but we gain many more types of packings that are not covered by the integral case. We will go over reduction theory for quadruples, how that is equivalent to reduction of binary quadratic fields, and how using the parameter space of Apollonian circle packings can be used to discover more about these packings.

References

[1] R.L. Graham, J.C. Lagarias, C.L. Mallows, A.R. Wilks, and C.H. Yan, *Apollonian Circle Packings: Number Theory*, J. Number Theory **100**, 1, pp. 1-45 (2003).

[2] J.E. Holly, *What type of Apollonian circle packing will appear?*, Amer. Math. Monthly **128**, 7, pp. 611-629 (2021).

[3] J. Kocik, *Apollonian depth and the accidental fractal*, arXiv preprint arXiv:2002.04135 (2020).

[4] J. Rickards, *The Apollonian staircase*, Int. Math. Res. Not. **2024**, 2, pp. 1340-1372 (2024).

[5] K.E. Stange, *The Apollonian structure of Bianchi groups*, Trans. Amer. Math. Soc. **370**, 9, pp. 6169-6219 (2018).

[6] K.E. Stange, *Visualizing the arithmetic of imaginary quadratic fields*, Int. Math. Res. Not. **2018**, 12, pp. 3908-3938 (2018).

The Spine: A Supersingular Highway

T. Hedayat[1], R. Scheidler[2], S. Arpin[3]

[1] *University of Calgary, Canada, taha.hedayat@ucalgary.ca*
[2] *University of Calgary, Canada, rscheidl@ucalgary.ca*
[3] *Virginia Polytechnic Institute and State University, United States of America, sarpin@vt.edu*

Motivated by the post-quantum cryptographic applications of the Supersingular ℓ-isogeny graph over a finite field $\mathcal{G}_\ell(\overline{\mathbb{F}}_p)$ we study its spine: the subgraph made with vertices which have j-invariant in $\mathbb{F}_p$. When we are given ℓ and p, the works of [1], [2], and [3] accumulated to a deterministic description of the spine, $\mathcal{S}_\ell^p$, for $\ell = 2$ with $p \equiv 1 \pmod 4$, $p \equiv 3 \pmod 8$, or $p \not\equiv 71, 119 \pmod{120}$. In this presentation, we provide the approach, methodologies, and results of the analysis of $\mathcal{S}_\ell^p$ for $\ell = 2$ and $p \equiv 71, 119 \pmod{120}$.

Distinguishing between edge attachment and non-edge attachments is a crucial aspect of understanding the structure of $\mathcal{S}_2^p$. This is due to the increase in efficiency of the traversing $\mathcal{G}_2(\overline{\mathbb{F}}_p)$ using only isogenies defined over $\mathbb{F}_p$. We show how an edge attachment is guaranteed to increase the mean diameter of the spine, whereas a non-edge attachment may or may not decrease the diameter.

The understanding of the mean diameter of $\mathcal{S}_2^p$ enables us to distinguish between edge attachments and non-edge attachments. We are able to provide heuristics on the ratios of the number of spines which have edge attachment and those which do not by computing the spine for ten thousand values of p. We present the computational results and the heuristics provided thereof. In addition, we are able to determine the location of the new edge through the mean diameter.

Through our computations, we are able to conclude that the occurrence of edge attachment is random. However, the location of the new edge does not follow a uniform distribution.

References

[1] Christina Delfs and Steven D. Galbraith. “Computing isogenies between supersingular elliptic curves over Fp”. In: Des. Codes Cryptogr. 78.2 (2016), pp. 425-440. ISSN: 0925-1022,1573-7586. DOI: 10.1007/s10623-014-0010-1. URL: `https://doi.org/10.1007/s10623-014-0010-1`.

[2] Sarah Arpin et al. “Adventures in supersingularland”. In: Exp. Math. 32.2 (2023), pp. 241-268. ISSN: 1058-6458,1944-950X. DOI: 10.1080/10586458.2021.1926009. URL: `https://doi.org/10.1080/10586458.2021.1926009`.

[3] Taha Hedayat, Sarah Arpin, and Renate Scheidler. “The Spine of a Supersingular ℓ-Isogeny graph”. In: Contemporary Mathematics (2026). To appear. Link to arXiv version of paper pro- vided. URL: `https://arxiv.org/pdf/2502.03613`.

Post-critically finite polynomials in positive characteristic

P. Ingram

York University / Fields Institute, Canada
pingram@yorku.ca

A post-critically finite polynomial is one whose critical points all have finite forward orbit under iteration. These have been much-studied in the world of complex dynamics, but many of the results break down in positive characteristic. We will survey some recent results and computations around post-critically finite polynomials in characteristic smaller than the degree.

The VII International AMMCS
Interdisciplinary Conference
Waterloo, Ontario, Canada

Shape of Imaginary D_6 Sextic Log-Unit Lattices

J. Cruz[1], E. Holmes[2], F. Jalalvand[3], E. Nunez Lon-Wo[5], R. Scheidler[6], H. T. N. Tran[4]

[1] *University of Calgary, Calgary, Canada, jose.cruz@ucalgary.ca*
[2] *University of Toronto, Toronto, Canada, eholmes@math.toronto.edu*
[3] *University of Calgary, Calgary, Canada, fatemeh.jalalvand@ucalgary.ca*
[4] *University of Alberta, Edmonton, Canada, htran2@ualberta.ca*
[5] *University of Toronto, Toronto, Canada, enrique.nunezlon.wo@mail.utoronto.ca*
[6] *University of Calgary, Calgary, Canada, rscheidl@ucalgary.ca*

Let F be a number field and let $\mathscr{O}_F^\times$ denote the unit group of its ring of integers. After quotienting by torsion, the logarithmic Minkowski embedding realizes $\mathscr{O}_F^\times$ as a lattice, which we denote by Λ_F. We study this lattice up to scaling, rotation, and reflection, and call the resulting equivalence class its *unit shape*. For a rank n lattice Λ, the shape is represented by

$$[\Lambda] \in \mathscr{S}_n := \mathrm{GL}_n(\mathbb{Z})\backslash\mathrm{GL}_n(\mathbb{R})\big/\mathrm{GO}_n(\mathbb{R}). \tag{1}$$

where the matrix in $\mathrm{GL}_n(\mathbb{R})$ is the basis matrix of the lattice.

In rank two, this description is easier to visualize, since lattice shapes can be represented by points in a subspace of the complex upper half-plane. This talk is mainly concerned with the shapes of log-unit lattices arising from number fields F with Galois group D_6 and signature $(0,3)$. Figure 1 shows their corresponding points in the complex upper half-plane.

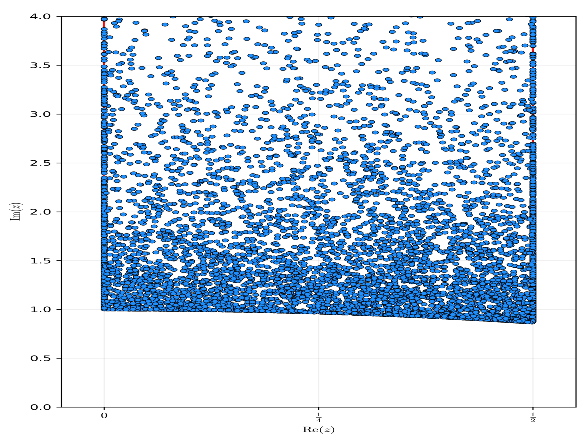

Figure 1: Unit shapes of D_6 sextics with signature $(0,3)$.

In this talk, we show that the unit shapes of number fields F in the family under consideration correspond to transcendental points in the interior of the above fundamental domain when F contains a totally real cubic subfield, and to transcendental points on the boundary otherwise. Although these points are transcendental, we prove that at least one algebraic point can arise as a limit point of such unit shapes. Time permitting, we will also discuss the non-CM case, in which two number fields F_1 and F_2 in this family are isomorphic if and only if their unit shapes are the same. Finally, for a fixed totally real number field K, we show that there exist only finitely many CM-extensions F/K such that $[\Lambda_K] \neq [\Lambda_F]$.

Eisenstein Circle Packings

J. Rickards[1], K.E. Stange[2]

[1] *Saint Mary's University, Halifax, Nova Scotia, Canada, james.rickards@smu.ca*
[2] *University of Colorado Boulder, Boulder, Colorado, USA, kstange@math.colorado.edu*

The Schmidt arrangement of an imaginary quadratic number field K is the orbit of the extended real line under $\mathrm{PSL}(2, \mathscr{O}_K)$ as Möbius transformations on the extended complex plane. If $K \neq \mathbb{Q}(\sqrt{-3})$, then the resulting set of circles can only intersect tangentially, leading to various classes of integral circle packings, including Apollonian circle packings. When $K = \mathbb{Q}(\sqrt{-3})$, circles can intersect at angles of $\frac{\pi}{3}$ and $\frac{2\pi}{3}$, making it unclear how to extract circle packings from the arrangement. In this talk, we will explain a modification of this arrangement, called the *Eisenpint Schmidt arrangement*, which leads to *Eisenstein circle packings*. We will explore the primitive integral Eisenstein circle packings, and demonstrate that as with the Apollonian case, reciprocity obstructions arise, sometimes preventing families such as n^2 from occurring as curvatures. Intriguingly, in some cases we find *alternating* obstructions, which produce such missing families in only half of the circles.

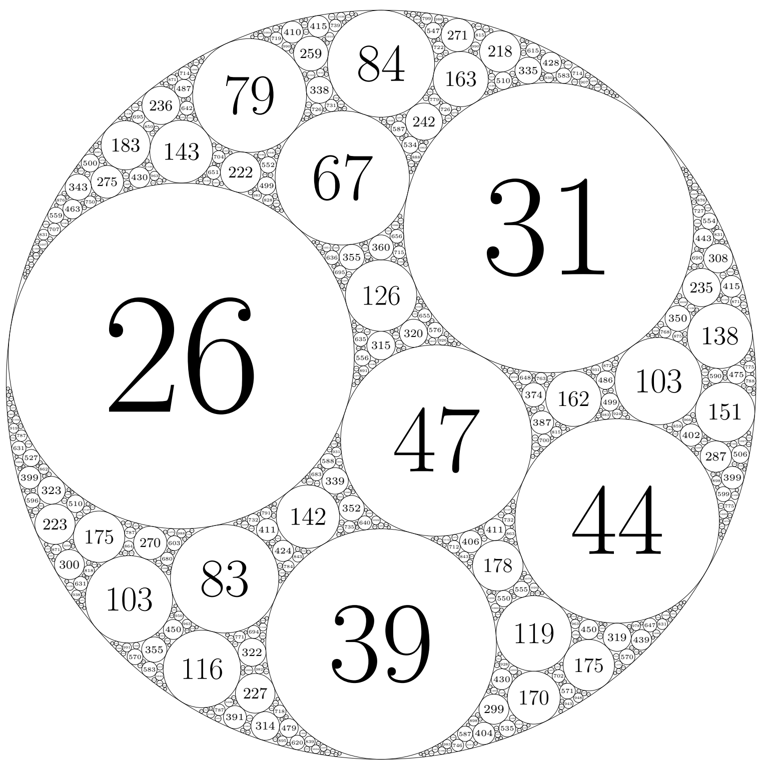

Figure 1: An Eisenstein circle packing with root quadruple $(-12, 26, 47, 31)$.

References

[1] J. Rickards and K.E. Stange, *Eisenstein circle packings and the Eisenpint Schmidt arrangement*, preprint.
[2] J. Rickards, *Eisenstein*. Version 1.0.0. 2026. DOI: 10.5281/zenodo.19827399. URL: `https://github.com/JamesRickards-Canada/Eisenstein`.

The VII International AMMCS
Interdisciplinary Conference
Waterloo, Ontario, Canada

Gleeful Numbers

J. Gross[1], S. Moore[2], C. O'Sullivan[3], D. Throop[1], A. Stahl[4], E. Waiss[5], J. Sorenson[1]

[1] *Butler University, Indianapolis IN, USA, {jgross2,dthroop,sorenson}@butler.edu*
[2] *University of Rochester, Rochester NY, USA, smoore55@u.rochester.edu*
[3] *AbbVie, North Chicago IL, USA, cbosulli@gmail.com*
[4] *Naval Surface Warfare Center, Bloomington IN, USA, arynstahl@gmail.com*
[5] *West Bend Insurance, West Bend WI, USA, waiss.eleanor@gmail.com*

A positive integer n is *k-gleeful* if it can be written as a sum of consecutive primes each raised to the kth power. For example, 74 is 2-gleeful since $74 = 5^2 + 7^2$. We write $f_k(n)$ for the number of k-gleeful representations of n. Also let $s_k(x)$ be the number of k-gleeful representations up to x, so that $s_k(x) = \sum_{n=1}^{x} f_k(n)$. In previous work, Moser [2] showed that $s_1(x) \sim x \log 2$. He also posed several open questions about $f_1(n)$. More recently, Tongsomporn, Wananiyakul, and Steuding gave an explicit upper bound for $s_2(x)$ [5].

We have the following new results:

- We present and analyze two algorithms to compute $f_1(n)$ for all $n \leq x$. Our implementations of these algorithms found $n = 84941668414584$, the smallest integer n with $f_1(n) = 14$ [4].
- We prove asymptotic and explicit upper and lower bounds on $s_k(x)$ for $k > 1$ [1, 3].
- We present and analyze efficient sequential [3] and parallel [1] algorithms for enumerating k-gleeful numbers and computing $s_k(x)$.
- We gathered data on *duplicates*, integers that have multiple gleeful representations, with the same or differing values of k. For example, $23939 = 23^2 + 29^2 + \cdot + 67^2 = 17^3 + 19^3 + 23^3$. Using this data, we state some conjectures on duplicates [1].
- Finally, we share some work-in-progress on when we allow the exponents to vary, based on some open questions given by Bob Silverman in 1997.

This work was supported by the Holcomb Awards Committee, the Butler Summer Institute, and the Mathematics Research Camp at Butler. Thanks to Frank Levinson for supporting research computing infrastructure at Butler. The first six authors were undergraduate students at Butler University when this work was done.

References

[1] Sara Moore and Jonathan P. Sorenson. Explicit bounds and parallel algorithms for counting multiply gleeful numbers, 2025. https://arxiv.org/abs/2507.09012, to appear in *Integers*.

[2] L. Moser. Notes on number theory. III. On the sum of consecutive primes. *Canad. Math. Bull.*, 6:159–161, 1963.

[3] Cathal O'Sullivan, Jonathan P. Sorenson, and Aryn Stahl. Algorithms and bounds on the sums of powers of consecutive primes. *Integers*, 24:Paper No. A4, 14, 2024.

[4] Jonathan P. Sorenson and Eleanor Waiss. Analysis of algorithms for Moser's problems on sums of consecutive primes, 2025. https://arxiv.org/abs/2509.00236.

[5] Janyarak Tongsomporn, Saeree Wananiyakul, and Jörn Steuding. Sums of consecutive prime squares. *Integers*, 22, 2022. A9.

Carmichael numbers up to 10^{24}

J. Webster[1]

[1] *Butler University, Indiana, USA, jewebste@butler.edu*

We present the results of a recent tabulation of all Carmichael numbers less than 10^{24}. We present an algorithm that is asymptotically faster than the previous tabulations algorithms and show that it is heuristically optimal. A central component of the algorithm relies on the ability to efficiently answer the query “Is n a Carmichael number?" We state an algorithm that is polynomial in time where the correctness is unconditional but the run-time argument depends on the ERH.

EOType: A Magma package for p-torsion group schemes

C. Weir[1]

[1] *Tutte Institute for Mathematics and Computing, Ottawa, Canada, Colin.Weir@cyber.gc.ca*

In this talk, we will present the latest updates to the magma package called EOType for computing with isomorphism types of p-torsion group schemes (called Ekedahl-Oort types or simply EO-types). The primary algorithm of EOType is to compute the EO-type of the Jacobian of a curve in characteristic p. However, the package also includes several auxiliary functions to compose, decompose, manipulate, and compute properties of EO-types. Together with Bryden Cais, some additional functionality has recently been added to produce Galois actions and more. In this talk, we will overview the full functionality now available.

The VII International AMMCS
Interdisciplinary Conference
Waterloo, Ontario, Canada

Fair-Division Auctions: Everybody Benefits

Steven J. Brams[1], D. Marc Kilgour[2], Christian Klamler[3]

[1] *New York University, New York, U.S.A., steven.brams@nyu.edu*
[2] *Wilfrid Laurier University, Waterloo, Canada, mkilgour@wlu.ca*
[3] *University of Graz, Graz, Austria, christian.klamler@uni-graz.at*

We analyze a Fair-Division Auction (FDA), wherein the high bidder, A, wins an indivisible item i with a bid of a. As in a Vickrey (1961) or second-price auction, A pays the second-highest bid, b, of B, but b does not go to a seller. Instead, it is distributed to all bidders in proportion to their bids. This not only gives A an incentive to bid truthfully (i.e., what it considers the true worth of i) but also all the lower bidders—who do not know other players' bids, or even where they stand in the bidding order—in order to achieve a maximin payoff. As an example of FDA, we discuss its application to the fair division of a family estate, in which the heirs may have different entitlements, different monetary assets, or different emotional or sentimental attachments to the items.

If there are multiple indivisible items, FDA can be repeated one item at a time. However, to avoid such repetition, we recommend that if there are two bidders, Adjusted Winner or AW (Brams and Taylor, 1996, 1999) be used first to allocate all items except a "pivotal item, p" (to be defined). Then, after the players have taken into account the possible synergies or asynergies that p has with the items that each player has already won under AW, FDA is used to award p to the high bidder, who pays b to all the bidders in proportion to their bids (A also gets $a - b$, the difference between the two highest bids, making FDA budget balanced).

The VII International AMMCS
Interdisciplinary Conference
Waterloo, Ontario, Canada

Mutual Preference Distance Visualizations Bring New Perspectives to Elections with Ranked Ballots

B. Brubach[1]

[1] *Wellesley College, Wellesley, MA, USA, bb100@wellesley.edu*

Analyzing real world elections reveals how often events such as axiom violations and strategic opportunities occur in practice under different voting systems. However, identifying the existence or frequency of these events does not tell the whole story. We also want to know whether seemingly undesirable events truly harm voters (or not) and better understand how they happen. To this end, we introduce mutual preference distance as a measure of similarity between candidates in elections with ranked ballots and mutual preference graphs as a way to visualize it. This allows us to represent relationships between candidates in two-dimensional space and gain new perspectives on both the effects of events and how they occurred. We demonstrate the usefulness of our distance measure and graph visualizations by exploring monotonicity anomalies [1], spoiler effects [2], and surprising strategies [3] identified in real world election data. In some cases, we show that seemingly undesirable events may actually be desirable. In others, we offer new explanations for unexpected or confusing events.

References

[1] D. McCune and A. Graham-Squire, *Monotonicity anomalies in Scottish local government elections*, in *Social Choice and Welfare*. 63, 1, pp. 69-101 (2024).

[2] D. McCune and J. Wilson, *Multiwinner elections and the spoiler effect*, *arXiv preprint arXiv:2403.03228*, (2024).

[3] S. Deshpande, N. Garg, and S. Jacobson, *Optimal Strategies in Ranked Choice Voting*, *arXiv preprint arXiv:2407.13661*, (2024).

Can we infer the single transferable vote winner set from bloc ballot data?

Jeanne Clelland[1], David McCune[2]

[1] *University of Colorado-Boulder, USA, jeanne.clelland@Colorado.edu*
[2] *William Jewell College, USA, mccuned@william.jewell.edu*

Under the method of plurality bloc voting (PBV), if there are k seats available then each voter submits an approval ballot with up to k candidates approved, and the k candidates with the most approvals are elected. Under the method of single transferable vote (STV), voters submit preference ballots with a (sometimes partial) ranking of the candidates, and the k winners are chosen using a sequential procedure of candidate eliminations and elections, where an elected candidate's surplus votes are transferred proportionally. While STV is designed to achieve proportional representation, PBV is not. For example, under PBV it is common for a slim majority coalition to win all k seats if the coalition's voters vote as a bloc, but such an outcome occurs under STV only in very extreme circumstances. Thus, the two voting methods can behave quite differently, and PBV generally should not be used if our goal is to achieve proportional representation.

The central question of this talk is: given the outcome of an election conducted under PBV, and assuming the same voters and candidates, can we determine whether the outcome would have been different if STV were used instead? In particular, can we decide if the STV and PBV winner sets coincide using just the bloc ballot data? We develop several algorithms to address both of these questions, often with mixed success. We validate the algorithms using 1,459 STV elections from Scotland and Australia where $k \in \{3,4\}$. Because these elections used preference ballots, we can convert the actual ballots to bloc ballots, allowing us to calculate the PBV and actual STV winners. We can then take the PBV ballot data and attempt to reconstruct the STV winner set from it.

Our general findings are that our best algorithms can accurately construct the STV winner set from bloc ballot data in approximately 70% of elections in our dataset. Furthermore, if the PVB and STV winner sets are different then our best algorithm predicts this difference in approximately 80% of such elections; if the PVB and winner sets are the same then our best algorithm predicts this agreement in 89% of such elections. Given the general difficulty of using approval ballots to predict the winner set under a method using preference ballots (among other issues), we suspect it will be difficult to improve on these success rates.

The VII International AMMCS
Interdisciplinary Conference
Waterloo, Ontario, Canada
May 27, 2026

Comparing Nash, Berge, and Kantian Equilibria in Strict Ordinal 2×2 Games

S. El-Badawy[1], D.M. Kilgour[2]

[1] *Wilfrid Laurier University, Waterloo, Canada, elba8270@mylaurier.ca*
[2] *Wilfrid Laurier University, Waterloo, Canada, mkligour@wlu.ca*

While the Nash equilibrium remains the dominant solution concept in game theory, its emphasis on self-interest fails to capture cooperative or altruistic tendencies often observed in real-world interactions. The Berge equilibrium, rooted in mutual support, and the Kantian equilibrium, based on self-regarding cooperation, offer alternative models for stable strategic choices. Utilizing the existing tabulation of all 144 strict ordinal 2×2 games, we locate, characterize, and compare all equilibria of these three types when choices are restricted to pure strategies, allowing us to identify when equilibria exist, coincide, diverge, or yield Pareto-inferior outcomes. The Nash and Berge frameworks are known to be dual, while the Kantian is distinctive. The properties of Nash and Berge equilibria include ordinal invariance, so they are unchanged when mixed strategies are allowed. But Kantian equilibria are not ordinally invariant, which may reduce their normative appeal. Our results offer descriptive insights into the topology of small games and its normative implications for models of cooperation, altruism, and Pareto efficiency.

The VII International AMMCS
Interdisciplinary Conference
Waterloo, Ontario, Canada

Non-Monotonicity in Fair Division of Graphs

Hadi Hosseini[1], Shraddha Pathak[2], Yu Zhou[3]

[1] *Penn State University, University Park, USA, hadi@psu.edu*
[2] *Penn State University, University Park, USA, ssp5547@psu.edu*
[3] *Beijing Normal University, Zhuhai, China, yu.zhou@bnu.edu.cn*

Fair division of indivisible items is a fundamental problem in multiagent systems and computational social choice [1]. Much of the existing literature assumes that agents have additive, or otherwise *monotonic* valuations. However, these assumptions often fail to capture more realistic scenarios where the value of an item is non-monotonic and may depend on the composition of the bundle it belongs to. In this work, we study non-monotonic *bundle-dependent* valuations, where the marginal value of an item may vary—potentially becoming negative—depending on the current bundle held by the agent.

We focus on a specific class of bundle-dependent preferences based on *cut-valuations* defined over undirected graphs. Here, items correspond to vertices of a graph $G = (V,E)$, and an agent's value for a bundle is determined by the number of edges that are cut, i.e. edges with exactly one endpoint in the bundle. Thus, the marginal value of an item is positive for bundle S if it has less neighbors inside S than outside S, otherwise it is zero or negative. This yields valuations that are inherently *non-monotonic*: adding an item can increase or decrease an agent's utility depending on the underlying structure of the bundle. This framework naturally captures applications such as team formation and committee design, where diversity and complementarity play a central role.

Our objective is to study the compatibility of standard fairness notions with economically meaningful efficiency guarantees under this non-monotonic setting. We consider envy-freeness up to one item (EF1) together with several efficiency notions, including social optimality (SO), Pareto optimality (PO), transfer stability (TS), and a relaxed version, weak transfer stability (wTS).

Our first set of results reveal an axiomatic non-monotonic relationship between existence guarantees for EF1+TS allocation and the number of agents n under cut-valuations: They exist for $n = 2$, may fail to exist for $n = 3$, but exist again for all $n \geq 4$. The $n = 3$ counter-example also shows the incompatibility of EF1 with PO and SO. This raises a natural question: *Is there an efficiency notion that is always compatible with* EF1*, regardless of n?* We show that a slight relaxation of TS (wTS) is the strongest efficiency notion which can always be guaranteed alongside EF1, irrespective of n. Moreover, such allocations can be computed in polynomial time. We also show that allocations that are $\frac{1}{2}$-EF1, a multiplicative approximation of EF1, can co-exist alongside PO.

Finally, we show that when the underlying graph is a forest (i.e. acyclic), EF1 and SO allocations always exist and can be computed in polynomial time. Interestingly, the standard techniques from the monotone settings—iteratively building toward an EF1 allocation where, on assigning each new item, EF1 is maintained as an invariant—do not apply. While our algorithm also iteratively builds towards an EF1 allocation, there are situations where we temporarily break intermediate EF1 guarantees, but ensure that such violations can be 'caught-up' through subsequent assignments. We note that the example showing the incompatibility of EF1+TS under general graphs is bipartite and has treewidth 2. This highlights that while strong existence and algorithmic guarantees hold for forests (bipartite graphs; treewidth 1), they break even for graphs that are only slightly different.

References

[1] G. Amanatidis, H. Aziz, G. Birmpas, A. Filos-Ratsikas, B. Li, H. Moulin, A. A. Voudouris, and X. Wu., *Fair division of indivisible goods: Recent progress and open questions.*, in *Artificial Intelligence*, 322, pp. 103965 (2023).

A Geometric Approach to Bias and Other Properties of Sequential Apportionment

Michael A. Jones[1], Jennifer Wilson[2]

[1] *Mathematical Reviews, American Mathematical Society, Ann Arbor, MI, USA; maj@ams.org*
[2] *Eugene Lang College of Liberal Arts, New School University, New York, NY, USA; wilsonj@newschool.edu*

Motivated by the sequential allocation of cabinet positions in Northern Ireland and Just-In-Time sequencing, we consider the sequences with which divisor methods allocate seats. It is well known that among divisor methods, the methods of Adams and Jefferson are the most biased in favor of small and large states, respectively. We extend bias to apportionment sequences based on the lexicographical ordering of the sequences. Using a geometric approach related to cutting sequences, we compare the asymptotic properties of parameterized families of divisor methods, such as stationary methods, power-mean methods, and power-apportionment methods, including a relationship between power-mean methods and Webster's method.

Two-Person Fallback Allocation of Indivisible Items

Fahimeh Ziaei[1], D. Marc Kilgour[2]

[1] *Wilfrid Laurier University, Waterloo, Canada, fziaei@wlu.ca*
[2] *Wilfrid Laurier University, Waterloo, Canada, mkilgour@wlu.ca*

Fallback Bargaining was originally proposed as a fair method for two or more players to choose one of many alternatives in a way that reflects each player's preferences. A Fallback outcome is Pareto-optimal and well-ranked by both players; it depends only on their ordinal (relative) preferences. We apply the Fallback procedure to find a balanced allocation of a set containing $2n$ indivisible items, utilizing sums of Borda scores to rank allocations. A Fallback allocation is then a Borda Max-Min allocation—it maximizes the minimum of the two players' sums of Borda scores. A good approximation to the Borda Max-Min (Fallback) allocation is the Bordasum allocation, which maximizes the sum of the players' Borda sums. The Bordasum allocation is easy to find but, unfortunately, must be further refined to find the Borda Max-Min allocation. We discuss how to identify situations in which no refinement is required or, if that does not apply, how to minimize the number of possibilities to be considered.

The VII International AMMCS
Interdisciplinary Conference
Waterloo, Ontario, Canada

The Uniform Core of an Approval-Based Committee Election

D. Peters[1], A. D. Taylor[2], W. S. Zwicker[3]

[1] *CNRS, LAMSADE, Université Paris Dauphine - PSL, France, mail@dominik-peters.de*
[2] *Union College, Schenectady, NY, USA, taylora@union.edu*
[3] *Union College, Schenectady, NY, USA, and Murat Sertel Center for Advanced Economic Studies, Istanbul, Turkey, zwickerw@union.edu*

In an *ABC election*, each voter approves a subset of the candidate set C, in order to elect a committee W – a parliament, perhaps – containing some pre-set number k of seats. Party list elections represent a special case, in which the meaning of proportional representation – aka *PR* – seems clear; if party X gets 30% of the vote, its candidates should fill 30% of W's k seats. But what should *PR* mean in the broader *ABC* setting, wherein approval ballots that overlap need not be identical?

One approach applies standard notions from *NTU cooperative games*. If a k-committee W is in the core of an *ABC* election, then each subgroup N' containing 30% of the voters weakly prefers W to any group containing $(.30)(k)$ candidates. It remains unknown whether every *ABC* election has a nonempty core, but G. Pierczyński and P. Skowron [1] proved that the *IR* domain restriction guarantees nonemptiness. Here, *IR* is the approval analogue of *single peaked preferences*: under some linear ordering of C, every approval ballot must be an interval.

In the party list context, those 30% who voted for party X can point to the 30% of W who serve as their delegation within W, representing their interests and views. The more general notion of core, however, provides no corresponding subset of W. Can we have our cake and also eat it . . . without any exogenous imposition of parties, can we achieve proportional representation of groups via delegations?

We introduce the *uniform core*, which does exactly this. Our main result is that under *IR* the uniform core is nonempty. However, when the approval profile fails badly to be *IR*, the uniform core can be empty. What types of overlap among approval sets can we tolerate while preserving proportional representation via delegations? Our results begin to outline some answers to this very basic question.

References

[1] Pierczński, G., and Skowron, P. *Core-Stable Committees Under Restricted Domains*. In: Hansen, K.A., Liu, T.X., Malekian, A. (eds) Web and Internet Economics. WINE 2022. Lecture Notes in Computer Science, vol 13778. Springer, Cham. (2022).

Borda Variants on Truncated Ballots

J. Wilson[1], M.A. Jones[2]

[1] *The New School, New York, New York, wilsonj@newschool.edu*
[2] *Mathematical Reviews, Ann Arbor, Michigan, maj@ams.org*

Several variants of the Borda score have been proposed for elections in which not all ballots include complete rankings of all the candidates. The Optimistic, Pessimistic, and Average variants award different point values to any candidates not included on the ballot. Emerson [1] suggests that Borda himself had yet another idea. At the same time, Cullinan et al. [2] and Jones and Wilson [3] propose two different generalizations of the Borda count when voters preferences are partially ordered. In this talk, we compare all of these variants when confined to the truncated setting, by assuming that a voter ranks all candidates on the ballot above all candidates omitted from the ballot and is indifferent between all candidates omitted from the ballot. We compare the properties of these different methods in this setting and discuss when they differ using both theoretical and empirical lenses and simulated data.

References

[1] P. Emerson, *The original Borda count and partial voting*, Soc. Choice & Welf. 40 (2), 353-358 (2013).
[2] J. Cullinan, S.K. Hsiao, and D. Polett, *A Borda count for partially ordered ballots*, Soc. Choice & Welf. 42 (4), 913-926, (2014).
[3] M.A. Jones and J. Wilson, *The Colley Matrix is an Extension of the Borda Count*, Mathematics Magazine, 97(2), 140-150. (2024).

The VII International AMMCS
Interdisciplinary Conference
Waterloo, Ontario, Canada

Borda Measures of Balanced Allocations of Indivisible Objects to Two Persons

Fahimeh Ziaei[1*], D. Marc Kilgour[2]

[1] *Wilfrid Laurier University, Waterloo, Canada, fziaei@wlu.ca*
[2] *Wilfrid Laurier University, Waterloo, Canada, mkilgour@wlu.ca*

A set of $2n$ distinct objects is to be allocated to two players, who are to receive n items each. Both players have a publicly known strict preference ranking over all $2n$ objects; all other preference information is private. A natural way to evaluate a possible allocation is based on players' Borda scores for objects received, or the sums of these scores. An individual's Borda score for an object is the number of items, among the original $2n$, that are less preferred than the focal object. A good allocation is one for which Borda scores tend to be high, but there are many ways to implement this idea. We study BordaSum allocations, that maximize the sum of both players' Borda sums, Borda Max-Min allocations, that maximize the minimum Borda sum, and Borda Max-Min Median allocations, that maximize the minimum of the two players' median Borda scores. BordaSum allocations are easy to find, whereas Borda Max-Min allocations can be computationally demanding. For the Borda Max-Min Median criterion, we develop a breakpoint-based algorithm that compares the players' top-ranked sets layer by layer and determines, or at least approximates, the desired allocation. These procedures enable an arbitrator, or an algorithm, to find good allocations when preference details are not available.

Conservation laws with flux discontinuous in the conserved quantity

F.Ancona [1], M.T. Chiri[2], B. Van Eeden[3]

[1] *University of Padova, Italy, ancona@math.unipd.it*
[2] *Queen's University, Kingston, Canada, maria.chiri@queensu.ca*
[3] *Queen's University, Kingston, Canada, 18bve@queensu.ca*

We explore a class of conservation laws with flux discontinuities in the conserved quantity, motivated by industrial applications such as conveyor belt systems and supply chains, as well as by traffic flow models exhibiting phase transitions. The flux under consideration is discontinuous at a critical density, corresponding for instance to the maximal density of processed parts or to transitions between different traffic regimes. This discontinuity leads naturally to solutions with multivalued fluxes, so that solutions are interpreted as pairs consisting of the conserved quantity and the associated flux. These models can be approximated by conservation laws with regularized fluxes exhibiting shocks with arbitrarily large slopes. As a consequence, the classical property of finite wave propagation is lost, and information propagates instantaneously. In this talk, we focus on the analysis of the associated boundary value problem. We introduce a suitable notion of entropy solution, whose formulation requires a trace operator describing the admissible phase transitions at the discontinuity. We then establish existence results via front-tracking techniques and prove Kruzhkov-type stability estimates.

Wedge problem and dispersive shock waves in the two-dimensional Toda lattice

M. Calabrese[1], G. Biondini[2], C. Chong[3], P. G. Kevrekidis[1]

[1] *Department of Mathematics and Statistics, University of Massachussetts, Amherst, MA*
[2] *Department of Mathematics, State University of New York at Buffalo, Buffalo, NY*
[3] *Department of Mathematics, Bowdoin College, Brunswick, M*

We study the formation and interaction of dispersive shock waves (DSWs) in the two-dimensional Toda lattice subject to wedge-type initial conditions. The initial jump across the wedge acts locally as a Riemann problem for the one-dimensional Toda lattice, producing two oblique DSWs whose leading-edge soliton amplitude is determined explicitly by the one-dimensional Whitham modulation theory. The two-dimensional nature of the problem manifests when these oblique DSWs meet along the symmetry axis. For type II wedge, we show that a critical slope q_{cr} separates two regimes: in the subcritical regime ($q < q_{cr}$) the interaction is resonant and it produces an expanding DSW whose amplitude, length and velocity are explicitly computed by using exact soliton solutions of the two-dimensional Toda lattice; in the supercritical regime ($q > q_{cr}$) the interaction is ordinary and produces a localized peak whose amplitude is determined analytically. For type I wedge the two regimes are also qualitatively described. All analytical predictions are confirmed by numerical simulations. The continuum limit of the result is shown to be consistent with the analogous theory for the Kadomtsev-Petviashvili equation, providing an independent validation of the analytical framework.

Scattering asymptotics for planar obstacles

K. Datchev[1]

[1] *Purdue University, West Lafayette, USA, kdatchev@purdue.edu*

The long time behavior of scattered waves is broadly governed by contributions from low and high frequencies. For obstacle scattering, geometric spectral invariants such as volume, perimeter, and capacity emerge in these asymptotic regimes. In this talk I will focus on two dimensional waves, which display particularly rich phenomena at low frequencies, with results from complex analysis contributing to their classification. This project is joint work with Tanya Christiansen, and parts are also joint with Colton Griffin, Pedro Morales, and Mengxuan Yang.

References

[1] T.J. Christiansen and K. Datchev, *Low energy scattering asymptotics for planar obstacles.* Pure and Applied Analysis, **5** 3 (2023), 767-794.

[2] T.J. Christiansen and K. Datchev, *Low energy resolvent expansions in dimension two*. Commun. Am. Math. Soc. **5** (2025), 48-80.

[3] T.J. Christiansen, K. Datchev and C. Griffin, *Persistence and disappearance of negative eigenvalues in dimension two*. To appear, Journal of Spectral Theory. Available at ArXiv 2401.04622.

[4] T.J. Christiansen, K. Datchev, P. Morales, and M. Yang. *Unconditional wave decay in dimension two.* Available at ArXiv 2507.03140.

[5] T.J. Christiansen, K. Datchev, and M. Yang. *From resolvent expansions at zero to long time wave expansions*. Communications in Partial Differential Equations, Vol. 50, No. 4, pp. 477–492, 2025.

[6] T.J. Christiansen, K. Datchev, and M. Yang. *Low energy resolvent asymptotics of the multipole AharonovâBohm Hamiltonian.* SIAM Journal on Mathematical Analysis, Vol. 57, No. 6, pp. 6282–6299, 2025.

Stability for Oscillatory Shocks of KdV–Burgers Equation

G. Chen[1], N. Eun[2], M.-J. Kang[3], Y. Shen[4]

[1] *University of Kansas, Lawrence, Kansas, USA, gengchen@ku.edu*
[2] *Korea Institute for Advanced Study (KIAS), Seoul, Republic of Korea, namhyuneun@kias.re.kr*
[3] *Korea Advanced Institute of Science and Technology (KAIST), Daejeon, Republic of Korea, moonjinkang@kaist.ac.kr*
[4] *University of Kansas, Lawrence, Kansas, USA, yshen@ku.edu*

The Korteweg–de Vries–Burgers (KdVB) equation

$$u_t + uu_x = \varepsilon u_{xx} - \delta u_{xxx}$$

is a fundamental model capturing the interplay of nonlinearity, viscosity (dissipation), and dispersion, with broad physical relevance. It is well known [1] that the KdVB equation admits traveling wave solutions, called viscous-dispersive shocks. In particular, for given states $u_- > u_+$, there exists a traveling wave solution $\tilde{u}(\xi := x - \sigma t)$:

$$-\sigma\tilde{u}' + \left(\frac{\tilde{u}^2}{2}\right)' = \varepsilon\tilde{u}'' - \delta\tilde{u}'''$$

and as $\xi \to \pm\infty$,

$$\tilde{u}(\xi) \to u_\pm, \qquad \tilde{u}'(\xi) \to 0,$$

where the traveling speed is given by Rankine–Hugoniot condition $\sigma = \frac{u_- + u_+}{2}$. These shock profiles are monotone in the viscosity-dominant regime, that is, when $\varepsilon^2 \geq 2\delta(u_- - u_+)$, whereas they exhibit infinitely many oscillations in the dispersion-dominated regime, i.e., $\varepsilon^2 < 2\delta(u_- - u_+)$.

In this talk, we discuss the stability of such viscous-dispersive shocks, focusing on an L^2-contraction property under arbitrarily large perturbations, up to a time-dependent shift. We begin with viscous shocks of the viscous Burgers equation (i.e., the KdVB equation with $\delta = 0$) in [2], then treat monotone viscous-dispersive shock [3]. Finally, we address the stability of oscillatory shocks [4]. More precisely, we establish the following L^2-contraction:

$$\int_{\mathbb{R}} (u(t,x) - \tilde{u}(x - \sigma t - X(t)))^2 dx \leq \int_{\mathbb{R}} (u_0(x) - \tilde{u}(x))^2 dx$$

where u_0 is the initial data satisfying $\|u_0 - \tilde{u}\|_{H^1(\mathbb{R})} < \infty$, and $X(t)$ is a Lipschitz continuous function. This further implies the following time-asymptotic stability:

$$\|u(t,\cdot) - \tilde{u}(\cdot - X(t))\|_{L^p(\mathbb{R})} \to 0, \qquad t \to \infty, \qquad \forall 2 < p \leq \infty.$$

Furthermore, we present detailed structural properties of the oscillatory shock profiles.

This is joint work with Geng Chen (University of Kansas), Moon-Jin Kang (KAIST), and Yannan Shen (University of Kansas).

References

[1] J. L. Bona and M. E. Schonbek, *Travelling-wave solutions to the Korteweg-de Vries-Burgers equation*, Proc. Roy. Soc. Edinburgh Sect. A **101**, pp. 207–226 (1985).

[2] M.-J. Kang and A. F. Vasseur, *L^2-contraction for shock waves of scalar viscous conservation laws*, Ann. Inst. H. Poincaré C Anal. Non Linéaire **34**, 1, pp. 139–156 (2017).

[3] G. Chen, N. Eun, M.-J. Kang and Y. Shen, *L^2-contraction of shock waves for the KdV–Burgers equation*, arXiv preprint arXiv:2603.09263 (2026).

[4] G. Chen, N. Eun, M.-J. Kang and Y. Shen, *Uniform stability of oscillatory shocks for the KdV–Burgers equation*, arXiv preprint arXiv:2602.22652 (2026).

Observability of Schrödinger Equations in Euclidean Space

W. Green[1], P. Kleinhenz[1]

[1] *Illinois State University, Normal, USA, {awgree1,pbklein}@ilstu.edu*

The Schrödinger equation is observable from a set if there is a uniform positive probability that a quantum particle will enter the set in finite time. On the flat torus, the Schrödinger equation is observable from any open set. These results have previously been extended to show periodic open sets can be used to observe the Schrödinger equation in Euclidean space. In this talk we prove observability from non-periodic sets in Euclidean space. The proof uses a propagation of singularities approach to replace the observation set by its average along a direction.

References

[1] W. Green and P. Kleinhenz, *Observability of Schrödinger equations in Euclidean space*, arXiv preprint arXiv:2604.11695 (2026).

Generalized Stress Models and Numerical Solvers for Blood Flow Problems

M.C. Haslam[1]

[1]*Department of Mathematics and Statistics, York University, Toronto, Canada, mchaslam@yorku.ca*

In this talk we discuss our recent investigations of generalized viscous stress models applicable to blood flow problems and our corresponding numerical implementations. A balance of momentum in an incompressible fluid continuum with velocity field $\mathbf{u}$, pressure p, and density ρ results in the classic formula

$$\frac{\partial \mathbf{u}}{\partial t} + (\mathbf{u}\cdot\nabla)\mathbf{u} = -\frac{1}{\rho}\nabla p + \frac{1}{\rho}\nabla\cdot\mathbf{S}, \tag{1}$$

where $\mathbf{S}$ denotes the stress tensor. Blood has complex mechanical properties that are not adequately described under the assumptions of a Newtonian fluid, particularly in small vessels [1]. Indeed, blood is well-known to exhibit not only viscoelastic properties but also a dependence on the local shear rates of the fluid [2].

Denoting λ_1 and λ_2 as the relaxation and retardation times, respectively, the Oldroyd-B stress model which accounts for the viscoelastic properties of the fluid and can be written as

$$\mathbf{S} + \lambda_1 \ddot{\mathbf{S}} = 2\mu\left(\mathbf{D} + \lambda_2 \ddot{\mathbf{D}}\right) \qquad \text{with} \qquad \mathbf{D} = \frac{1}{2}\left(\nabla\mathbf{u} + (\nabla\mathbf{u})^T\right). \tag{2}$$

The deformation rate tensor is denoted as $\mathbf{D}$ while $\ddot{\mathbf{D}}$ is the upper-convected time derivative of this quantity. In the Oldroyd-B model, the coefficient of viscosity μ is taken as a constant; extensions of the model, known as generalized Oldroyd-B models, which account for the dependence of viscosity on the local shear rates of the fluid, are the focus of our investigations.

In order to study the long-time behavior of generalized Oldroyd-B models in a simple physical setting, we greatly simplify the vessel geometry, representing it by a long straight rigid circular tube. Under the further assumption of an oscillating pressure gradient driving the flow, our models reduce to a system of three coupled partial differential equations to be solved for the stress and velocity fields. We outline a novel Chebyshev-tau spectral solver which we developed to compute numerical solutions of the problem. Our algorithm relies on a fourth order Runge-Kutta time stepping procedure with $O(N \log N)$ operations per time step enabled by the use of fast cosine transforms. The resulting code is spectrally accurate in the number of spatial discretization points N.

References

[1] N. Bessonov, A. Sequeira, S. Simakov, Yu. Vassilevskii and V. Volpert, *Methods of Blood Flow Modelling*, Math. Model. Nat. Phenom. **11**(1): 1–25, 2016.

[2] T. Bodnar, A. Sequeira and M. Prosi, *On the shear-thinning and viscoelastic effects of blood flow under various flow rates*. Applied Mathematics and Computation **217**: 5055-5067, 2011.

Large Coherent Structures in Wave Equations via Computer Assisted Proofs

E. Kirr[1]

[1] *University of Illinois at Urbana-Champaign, USA, ekirr@illinois.edu*

While coherent structures play an essential role in the analysis and applications of wave equations it has been impossible (until now) to find all the nonlinear ones. This talk will focus on the Nonlinear Schrödinger Equations where coherent structures have the form $\exp(iEt)f(x)$ with real frequency E and profile f in $H^1(\mathbf{R}^n)$ Sobolev space. We show that all coherent structures must organize themselves in smooth branches accumulating to $E = \infty$. In this limit they split into peaks and an algebraic equilibrium equation between peak-potential and peak-peak interaction emerges. The equation determines the possible limit points of the coherent structures as the frequency E approaches infinity. For small number of peaks or for peaks in a collinear configuration the limiting points can be obtained by hand. However, for large number of non-collinear peaks we employ computer assisted proofs. Once the limit points are determined we adapt techniques from local bifurcation theory to show existence of actual branches of coherent states emerging from the limit points and trace them from high frequency into the range of medium and small frequency.

`AMMCS2011-eps-converted-to.pdf`

Figure 1: The AMMCS Conference is organized in cooperation with SIAM and AIMS.

Sampling methods for solving electromagnetic inverse scattering problems associated with Maxwell's equation

T. Le[1], D.-L. Nguyen[2], T. Truong[3]

[1] *University of Wisconsin-Madison, USA, {tle38}@wisc.edu*
[2] *Kansas State University, USA*
[3] *Marshall Univeristy, USA*

We study an electromagnetic inverse scattering problem for time-harmonic Maxwell's equations, which aims to reconstruct the location and shape of an unknown object from boundary measurements of electric waves scattered by the object at a fixed frequency. This problem arises in applications such as nondestructive testing, radar, and medical imaging. In this talk, we develop the Orthogonality Sampling Method (OSM), together with a modified version, for this inverse problem in anisotropic and bianisotropic media. We discuss how the modified method accommodates a wider range of polarization vectors while remaining simple, fast, and stable. We provide theoretical justification through factorization analysis of the far-field operator. We also present 3D numerical results using both simulated and experimental data from the Fresnel Institute, and compare the performance of the OSM, the modified OSM, and a classical factorization method.

Minimum-Energy Control of a Wave Equation with Integral Action

L. Ma[1], R. Guglielmi[1]

[1] *Department of Applied Mathematics, University of Waterloo, ON, Canada*
ling.ma@uwaterloo.ca, roberto.guglielmi@uwaterloo.ca

This work studies the minimum-energy null controllability of a one-dimensional wave equation augmented with an integral action. Such an integral mechanism is known to improve regulation properties in infinite-dimensional systems, see [1, 2]. The resulting PDE–ODE cascade system is given by

$$\begin{cases} y_{tt}(x,t) = y_{xx}(x,t), & (x,t) \in (0,1)\times(0,T), \\ y(0,t) = 0, & t \in (0,T), \\ y_x(1,t) = u(t), & t \in (0,T), \\ y(x,0) = y^0(x), & x \in (0,1), \\ y_t(x,0) = y^1(x), & x \in (0,1), \\ \dot{z}(t) = y(1,t), & t \in (0,T), \\ z(0) = z_0. \end{cases} \tag{1}$$

This system extends classical boundary control settings for wave equations [3, 4]. In contrast with the classical wave equation, the presence of the integral state introduces a global coupling that destroys the modal decoupling structure and prevents the use of explicit constructions based on moment methods, such as those available for the classical wave equation [5]. To the best of our knowledge, such minimum-energy controllability problems for PDE systems with integral action have not been fully addressed in the literature.

To address this issue, we formulate a finite-time optimal control problem with an L^2-norm cost and derive the associated optimality system via a Lagrangian approach. The optimal control is characterized through the boundary trace of an adjoint system. A Hilbert Uniqueness Method (HUM)-based analysis [4, 6] is then carried out. By means of a spectral decomposition and an Ingham-type inequality, we establish a weak observability inequality for the cascaded adjoint dynamics. This estimate ensures the coercivity of the associated quadratic functional in a suitable weak energy space, which yields the existence and uniqueness of the minimum-energy control. Numerical simulations illustrate the effectiveness of the proposed approach and confirm the null controllability of the cascaded system.

References

[1] A. Terrand-Jeanne, V. Andrieu, V. Dos Santos Martins and C.-Z. Xu, *Adding integral action for open-loop exponentially stable semigroups and application to boundary control of PDE systems*, IEEE Trans. Automat. Control **65**, 11, pp. 4481–4492 (2019).

[2] L. Ma, V. Andrieu, D. Astolfi, M. Bajodek, C.-Z. Xu and X. Lou, *Integral action feedback design for conservative abstract systems in the presence of input nonlinearities*, IEEE Trans. Automat. Control **70**, 11, pp. 7580–7587 (2025).

[3] M. Krstic and A. Smyshlyaev, *Boundary Control of PDEs: A Course on Backstepping Designs*, SIAM, Philadelphia, 2008.

[4] M. Tucsnak and G. Weiss, *Observation and Control for Operator Semigroups*, Birkhäuser, Basel, 2009.

[5] M. Gugat, *Norm-minimal Neumann boundary control of the wave equation*, Arab. J. Math. **4**, 1, pp. 41–58 (2015).

[6] J.-L. Lions, *Exact controllability, stabilization and perturbations for distributed systems*, SIAM Rev. **30**, 1, pp. 1–68 (1988).

Magnetic Eigenfunctions, Landscapes, and Brownian Motion

H. Quan[1],

[1] *University of California Santa Cruz, hquan1@ucsc.edu*

In this talk we discuss exponential localization of Schrodinger eigenfunctions in the presence of both scalar and vector potentials (also known as electric and magnetic potentials). After recalling Agmon's celebrated method of obtaining exponential decay estimates away from the 'classically forbidden region', and certain approaches to practically determining localized regions via landscape functions, we discuss difficulties in this approach in the magnetic case, as well as recent work in the 2d case. Our results proceed by probabilistic methods, and will explain how such tools can sidestep difficulties posed by the magnetic field.

On the ergodic theory of some stochastic dispersive PDEs

C. Bechthold[1], N. Glatt-Holtz[2], V. Martinez[3], G. Richards[1]

[1] *University of Guelph, Guelph, Canada, grichards@uoguelph.ca*
[2] *Indiana University, Bloomington, USA*
[3] *Hunter College CUNY, New York, USA*

We will review recent progress and report on some preliminary results on the ergodic theory of stochastic perturbations of the Korteweg-de Vries equation (KdV), a widely studied canonical dispersive PDE. Roughly speaking, the subtlety of regularization inherent to nonlinear dispersive PDEs such as KdV motivates our generalization of the ergodic theory framework for stochastic PDEs to e.g., rely on probabilistic (rather than pathwise) control arguments [1], and to incorporate nonlinear estimates in function spaces better suited to dispersive equations [2]. This talk will discuss joint works with Cameron Bechthold (Guelph), Nathan Glatt-Holtz (Indiana), and Vincent Martinez (CUNY Hunter).

References

[1] N. Glatt-Holtz, V. Martinez, and G. Richards, *On the long-time statistical behavior of smooth solutions of the weakly damped, stochastically-driven KdV equation*, Trans. Amer. Math. Soc. **379**, 1, pp. 71-136 (2026).

[2] C. Bechthold and G. Richards, *On the well-posedness of a singular stochastic KdV-Burgers equation*, Work in progress, (2026).

The VII International AMMCS
Interdisciplinary Conference
Waterloo, Ontario, Canada

Exponential local energy decay of solutions to the wave equation with electric and magnetic potentials

A. Larraín -Hubach[1], J. Shapiro[2], G. Vodev[3]

[1] *University of Dayton, Dayton, Ohio, USA, alarrainhubach1@udayton.edu*
[2] *University of Dayton, Dayton, Ohio, USA, jshapiro1@udayton.edu*
[3] *University of Nantes, Nantes, France, georgi.vodev@univ-nantes.fr*

We prove sharp resolvent estimates for the magnetic Schrödinger operator in $\mathbb{R}^d$, $d \geq 3$, with L^∞ short-range electric and magnetic potentials. We also show that these resolvent estimates still hold for the Dirichlet self-adjoint realization of the Schrödinger operator in the exterior of a non-trapping obstacle in $\mathbb{R}^d$, $d \geq 2$, provided the magnetic potential is supposed identically zero. As an application of the resolvent estimates, we obtain an exponential decay of the local energy of solutions to the wave equation with L^∞ electric and magnetic potentials which decay exponentially at infinity, in all odd and even dimensions, provided the low frequencies are cut off in a suitable way. We also show that in odd dimensions there is no need to cut off the low frequencies in order to get an exponential local energy decay, provided zero is neither an eigenvalue nor a resonance.

Bloch-Floquet band gaps for water waves over a periodic bottom

Christophe Lacave[1], Matthieu Ménard[2], Catherine Sulem[3]

[1] *Université Paris-Cité, Paris, France, menard@imj-prg.fr*
[2] *Université Savoie Mont Blanc, Chambéry, France, christophe.lacave@univ-smb.fr*
[3] *University of Toronto, Canada, sulem@math.utoronto.ca*

A central object in the analysis of the water wave problem is the Dirichlet-Neumann operator. This study is devoted to its spectrum in the context of the water wave system linearized near equilibrium in a domain with a variable bottom, assumed to be a smooth periodic function. We use the analyticity of the Dirichlet-Neumann operator with respect to the bottom variation and combine it with general properties of elliptic systems and spectral theory for self-adjoint operators to develop a Bloch-Floquet theory and describe the structure of its spectrum. We find that under some conditions on the bottom variations, the spectrum is composed of bands separated by gaps, with explicit formulas for their sizes and locations.

Threshold-based wave propagation engineering: physics-based modeling and data-driven approach

Mohammad Reza Talebi Bidhendi [1]

[1] *University of Toronto, Toronto, Ontario, Canada*

Wave propagation management has been a canonical area of research over the past decades with diverse applications in energy devices, metamaterials, aerostructures, defense, and structural engineering. This talk provides insights for wave propagation engineering in nonlinear systems including a network of connected buckled beams and coupled nonlinear pendulums. Under certain exerted force thresholds, the occurrence of various nonlinear phenomena such as supratransmission, also known as an instability driven mechanism within band gap, and solitary wave propagation across the aforementioned physical nonlinear systems will be discussed. In particular, parametric excitation and time-periodic damping coefficient are highlighted as potential tuning parameters for threshold-based wave propagation engineering. Lastly and motivated by the growing surge in the use of artificial intelligence in computational modeling, various machine learning models such as neural network approach are also developed to further complement the analysis of the aforesaid nonlinear systems. The developed data-driven approaches can be beneficial for the possible parameter extraction in concert with response estimation for the considered nonlinear systems. Further, they might be utilized by the end-users with less experience in physics-based modeling of complex nonlinear structures for the pertinent engineering training purposes.

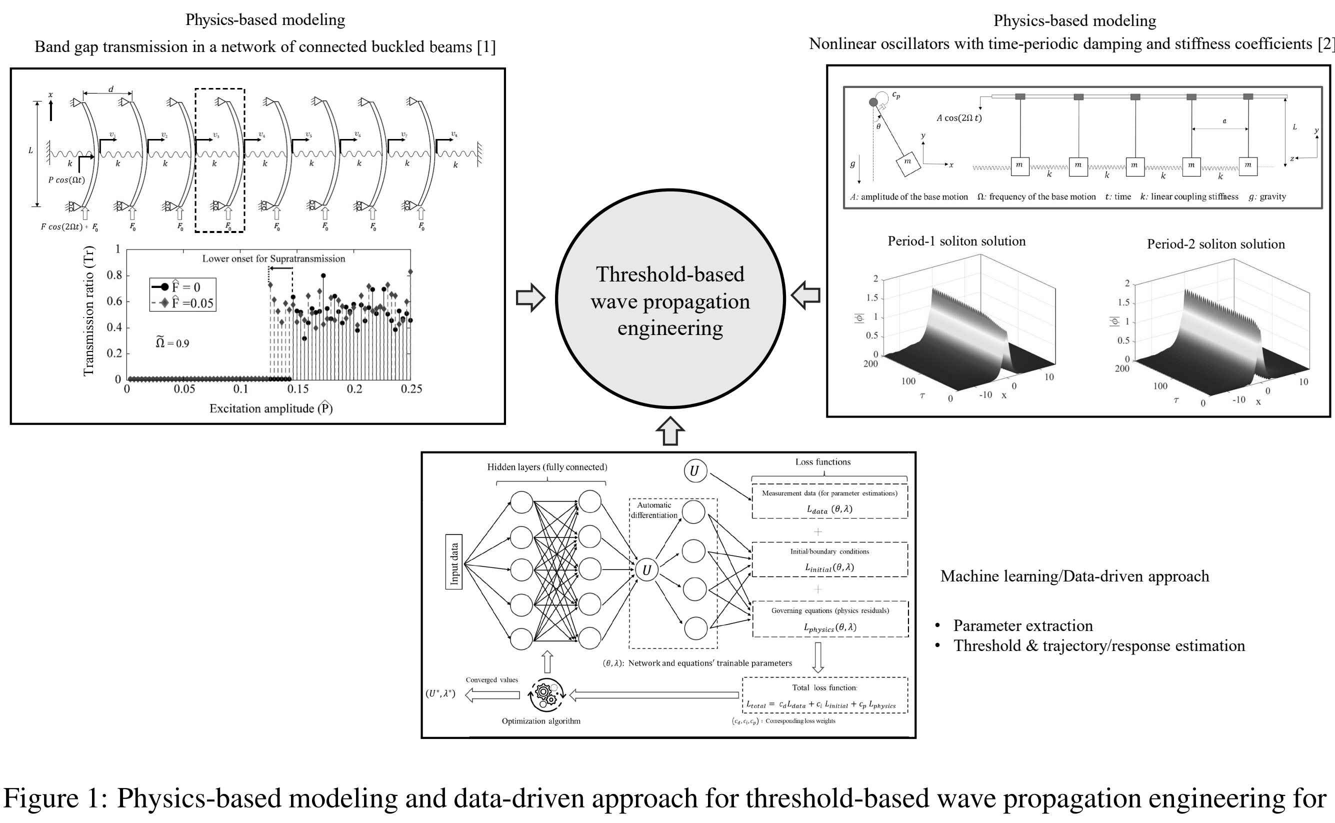

Figure 1: Physics-based modeling and data-driven approach for threshold-based wave propagation engineering for nonlinear systems including connected buckled beams and coupled nonlinear pendulums.

References

[1] Bidhendi, Band gap transmission in a network of coupled buckled beams. International journal of solids and structures, (2022).

[2] Bidhendi et al., Solitary waves in an array of nonlinear oscillators with time-periodic damping and stiffness coefficients. ASME International Mechanical Engineering Congress and Exposition, (2021).

[3] Hermann et al., Deep learning in computational mechanics: a review. Computational mechanics, (2024).

[1]mrt.bidhendi@gmail.com

The VII International AMMCS
Interdisciplinary Conference
Waterloo, Ontario, Canada

On Solving Constrained Hyperbolic Differential Equations Numerically

Nicolae Tarfulea[1]

[1] *Purdue University Northwest, USA, ntarfule@purdue.edu*

Hyperbolic differential equations with constraints arise in many physical applications (e.g., electromagnetism, magnetohydrodynamics, and general relativity). Frequently, the numerical solutions to such evolution problems are computed on artificial space cutoffs because of the necessary boundedness of computational domains. A challenging problem is choosing appropriate boundary conditions at the artificial boundaries.

The problem of finding the "correct" set(s) of boundary conditions, i.e., those that lead to a well-posed problem, is difficult in general from both theoretical and practical points of view. Nonetheless, well-posedness is crucial in that it guarantees the existence of a unique solution which depends continuously on the initial and boundary data. Furthermore, for a smooth solution to exist, the initial data must be compatible with the equations and boundary conditions at the boundary of the domain.

Both the analytical and numerical approaches become much more difficult if the solution to the initial-boundary-value problem (IBVP) must satisfy certain constraints. In this case, the boundary conditions have to be posed in such a way that the solution of the IBVP satisfies the constraints as well. Several methods for constructing constraint-preserving boundary conditions which make sure that the constraints propagate correctly in time once satisfied initially have been proposed, especially in the context of magnetohydrodynamics, electromagnetism, and general relativity. An informative review of results concerning continuum and discrete initial-boundary value problems arising from hyperbolic partial differential equations can be found in [1].

In this talk, I will present a few ideas and techniques for finding constraint preserving boundary conditions for a large class of constrained hyperbolic differential equations.

References

[1] O. Sarbach and M. Tiglio, *Continuum and Discrete Initial-Boundary Value Problems and Einstein's Field Equations*, Living Rev. Relativity **15**, (2012).

[2] N. Tarfulea, *Well-posed constraint-preserving boundary conditions for the AA formulation of Einstein's equations*, J. Math. Anal. Appl. **359**, pp. 711-721 (2009).

[3] N. Tarfulea, *On boundary conditions for first-order symmetric hyperbolic systems with constraints*, J. Hyperbolic Differ. Equ. **10**, pp. 725-734 (2013).

[4] N. Tarfulea, *Initial and initial-boundary value problems for first-order symmetric hyperbolic systems with constraints*, Mathematical and computational modeling, Pure Appl. Math. (Hoboken) John Wiley & Sons, Inc., Hoboken, NJ, pp. 222-253 (2015).

[5] N. Tarfulea, *Boundary conditions for constrained hyperbolic systems of partial differential equations*, Acta Math. Vietnam. **46**, pp. 675-688 (2021).

Local Energy Decay for Non-Stationary Damped Wave Operators

N. Arsenault[1], M. Tohaneanu[2]

[1] *University of Kentucky, Lexington, USA nick.arsenault@uky.edu*
[2] *University of Kentucky, Lexington, USA mihai.tohaneanu@uky.edu*

We establish integrated local energy decay (ILED) estimates for the damped wave equation on certain non-stationary asymptotically flat spacetimes. The main technical result is a high frequency estimate that holds in great generality, provided that null geodesics trapped in a compact region are sufficiently damped. This is joint work with Nick Arsenault.

On the ETH model for quantum measurement

Juerg Froehlich[1], Zhou Gang[2], Alessandro Pizzo[3],

[1] *ETH Zurich, Zurich, Switzerland juerg@phys.ethz.ch*
[2] *Binghamton University, Binghamton, NY, USA gangzhou@binghamton.edu*
[3] *University of Rome "Tor Vergata", Rome, Italy pizzo@axp.mat.uniroma2.it*

I will present our result on quantum measurement. Due to its mysterious nature and importance, determining what exactly happens during measurement is considered the last pillar of quantum mechanics. We solved this problem in the so-called ETH model. This is joint work with Juerg Froehlich and Alessandro Pizzo.

We look forward to welcoming you in Waterloo, Canada at the AMMCS Conference!

Figure 1: The AMMCS Conference is organized in cooperation with SIAM and AIMS.

References

[1] B. Keller and I. Reiten, *Cluster-titled algebras are Gorenstein and stably Calabi-Yau*, Adv. Math. **211**, 1, pp. 123-151 (2007).

[2] S. Washito and K. Karabashi, *Use This Template*, in *Proceedings of the 5th International Conference on Photon Interaction* (ICPI-2012), San Francisco, USA, ed. A. Chen, pp. 22-24 (2012).

[3] A.B. Smith, *Describing the style for the AMMCS-CAIMS-2015 book of abstracts*, in C.D. Science (ed.), General Book of Wisdom, 2nd ed., University of Queensland, pp. 23-42 (2011).

Global Behavior of Multispeed Klein-Gordon System

Xilu Zhu[1]

[1] *University of Michigan, Ann Arbor, USA, xiluzhu@umich.edu*

We explore the long-time behavior of multispeed Klein-Gordon systems in space dimension two, which look like

$$(\partial_t^2 - c_j^2\Delta + b_j^2)u_j = \mathscr{N}_j(u), \tag{1}$$

where $u = (u_1, \cdots, u_N)$ are unknown functions, and $\mathscr{N}_j$ are nonlinearities. Here in (1), the parameters c_j and b_j represent the *speeds* and *masses* of the wave component u_j. In terms of Klein-Gordon systems, the space dimension two is somehow considered as a *critical threshold* with possible transition form stability to instability. To illustrate this, we first prove a global wellposedness result when Klein-Gordon systems satisfy *Ionescu-Pausader* nondegeneracy conditions

$$\begin{cases} b_\sigma - b_\mu - b_\nu \neq 0 \\ (c_\mu - c_\nu)(c_\mu^2 b_\nu - c_\nu^2 b_\mu) \geq 0 \end{cases} \qquad \text{for any } \sigma, \mu, \nu \in \{1, \ldots, N\}. \tag{2}$$

and the nonlinearity is assumed to be semilinear. Second, on the other hand, we construct a specific Klein-Gordon system such that one of the nondegeneracy conditions (2) is violated and its solution has an infinite time blowup, which implies a type of illposedness.

References

[1] X.Zhu, *An Infinite Time Blowup Solution of Multispeed Klein-Gordon System in Space Dimension Two with Small Initial Data*, Preprint (https://arxiv.org/abs/2402.03727).

[2] X.Zhu, *Global Solutions of Multispeed Klein-Gordon System in Space Dimension Two with Small Initial Data*, J. Differential Equations. 437 (2025), 113279.

A Gutzwiller trace formula for singular potentials

J. Wunsch[1], M. Yang[2], Y. Zou[3]

[1] *Northwestern University, Evanston, IL, USA, jwunsch@math.northwestern.edu*
[2] *Princeton University, Princeton, NJ, USA, yangmx@princeton.edu*
[3] *Oakland University, Rochester, MI, USA yzou@oakland.edu*

We discuss extending the Gutzwiller trace formula, which relates the regularized trace of the solution operator for a semiclassical Schrödinger propagator to dynamical data of the corresponding Hamiltonian dynamics, from the case of smooth potentials to that of conormal potentials with derivative discontinuities across some hypersurface. We show, in addition to a main term as expected from classical dynamics, that there is a subleading contribution from dynamics associated to "branching" Hamiltonian trajectories that are allowed to reflect from the hypersurface of potential singularity. We discuss the computations behind the trace formula, some variational calculus needed to make sense of the dynamical quantities appearing in the formula, and an explicit 1-dimensional example whose eigenvalues have explicit asymptotics that demonstrate the contributions from the branching trajectories.

References

[1] J. Wunsch, M. Yang, and Y. Zou, *A Gutzwiller trace formula for singular potentials*, Preprint, arXiv:2509.05220 (2025).

[2] J. Wunsch, M. Yang, and Y. Zou, *The Morse index theorem for mechanical systems with reflections*, Nonlinearity, Vol. 37, no. 8 (2024).

[3] Y. Zou, *Asymptotic Expansion of the Eigenvalues of a Bathtub Potential with Quadratic Ends*, Communications in Mathematical Physics, Vol. 406, no. 220 (2025).

The VII International AMMCS
Interdisciplinary Conference
Waterloo, Ontario, Canada

Implied Volatility Expansions for VIX Options in Forward Variance Models

Y. Liao[1], A. Agarwal[2], F. Bourgey[3]

[1] *University of Glasgow, United Kingdom, ying.liao@glasgow.ac.uk*
[2] *Western University, London, Canada, aagarw93@uwo.ca*
[3] *New York University, New York, USA, fb2615@nyu.edu*

Accurate closed-form implied volatility expansions allow industry practitioners to efficiently calibrate their models to market data. This operation is crucial for computing risk sensitivities of derivative trading books based on current market conditions. In this work, we develop implied volatility expansions for options on the S&P 500 volatility index (VIX) within the class of forward variance models. Our implied volatility expansions are derived from VIX option price approximations developed by (1). Following (2), a natural way to model the joint dynamics of the S&P 500 spot price S_t and its implied volatility surface is to work directly with the term structure of implied variances of log-contracts, referred to as forward variances. As is well known, these forward variances are driftless under the risk-neutral measure and can be treated as additional state variables alongside S_t. The resulting models are referred to as *forward variance models*.

Our contributions are threefold. First, building on the weak VIX option price approximation of (1), we derive an explicit implied volatility expansion for the standard and rough Bergomi models. This gives a direct implied volatility formula, rather than requiring numerical inversion of the price expansion. Second, we extend the construction to mixed-kernel forward variance models by rewriting the mixed VIX option approximation by means of a Hermite expansion, and turning this representation into an implied volatility expansion. This complements existing Bergomi and rough-volatility asymptotic results for VIX futures, power payoffs, and volatility derivatives. Third, numerical tests and calibration studies show that the expansions allow rapid calibration across a wide range of parameters and that mixed specifications capture market VIX skews more effectively than single log-normal kernels, a phenomenon consistent with the limitations documented in (9). The accuracy of our formulas deteriorates in mixed-kernel models only in extreme parameter regimes, where the formulas still provide reliable initial guesses which can be used for standard root-finding procedures.

References

[1] F. Bourgey, S. De Marco, and E. Gobet, *Weak Approximations and VIX Option Price Expansions in Forward Variance Curve Models*, Quantitative Finance **23**(9), pp. 1259–1283 (2023).
[2] L. Bergomi, *Smile Dynamics I*, Risk (2004).
[3] L. Bergomi, *Smile Dynamics II*, Risk (2005).
[4] C. Bayer, P. Friz, and J. Gatheral, *Pricing under Rough Volatility*, Quantitative Finance **16**(6), pp. 887–904 (2016).
[5] A. Jacquier, C. Martini, and A. Muguruza, *On VIX Futures in the Rough Bergomi Model*, Quantitative Finance **18**(1), pp. 45–61 (2018).
[6] C. Lacombe, A. Muguruza, and H. Stone, *Asymptotics for Volatility Derivatives in Multi-Factor Rough Volatility Models*, Mathematics and Financial Economics **15**(3), pp. 545–577 (2021).
[7] J. Guyon, *The VIX Future in Bergomi Models: Fast Approximation Formulas and Joint Calibration with S&P 500 Skew*, SIAM Journal on Financial Mathematics **13**(4), pp. 1418–1485 (2022).
[8] E. Alòs, D. García-Lorite, and A. M. Gonzalez, *On Smile Properties of Volatility Derivatives: Understanding the VIX Skew*, SIAM Journal on Financial Mathematics **13**(1), pp. 32–69 (2022).
[9] B. Horvath, A. Jacquier, and P. Tankov, *Volatility Options in Rough Volatility Models*, SIAM Journal on Financial Mathematics **11**(2), pp. 437–469 (2020).

Option Pricing with Recurrent Variance Risk Aversion

Yaw Asante[†] Maciej Augustyniak[‡] Alexandru Badescu[§] Robert J. Elliott[¶]

Abstract

This paper develops an option pricing framework that jointly fits returns, realized volatility, and option prices, while capturing the regime- and maturity-dependent shape of the pricing kernel. The framework is built around a variance-dependent stochastic discount factor in which the variance risk aversion coefficient is modelled by a recurrent neural network (RNN). Using S&P 500 index options, we show that the RNN-based specification substantially improves the cross-sectional fit relative to benchmarks, with the largest gains for deep out-of-the-money and short-maturity contracts. The implied pricing kernel exhibits pronounced time variation, becoming U-shaped during periods of market stress and displaying a downward-sloping term structure consistent with stronger pricing of short-horizon volatility risk. Outside periods of elevated market stress, however, it is typically inverted U-shaped for all but the shortest maturities.

Keywords: Variance Risk Aversion; Recurrent Neural Networks; Variance-Dependent Pricing Kernels; Realized EGARCH; Option Pricing.

JEL Classification: C58, G12, G13.

[†]Department of Mathematics and Statistics, University of Calgary, 2500 University Drive NW, Calgary, AB, Canada, T2N 1N4; email: yaw.asomani@ucalgary.ca

[‡]Department of Mathematics and Statistics and Quantact Actuarial Financial Mathematics Laboratory, Université de Montréal, PO Box 6128, Station Centre-ville, Montréal, QC, Canada, H3C 3J7; email: maciej.augustyniak@umontreal.ca

[§]Corresponding author. Department of Mathematics and Statistics, University of Calgary, 2500 University Drive NW, Calgary, AB, Canada, T2N 1N4; email: abadescu@ucalgary.ca

[¶]Haskayne School of Business, Finance [FNCE], University of Calgary, 2500 University Drive NW, Calgary, AB, Canada, T2N 1N4; email: relliott@ucalgary.ca

Financial support from the Natural Sciences and Engineering Research Council of Canada (NSERC) is gratefully acknowledged by all authors.

The VII International AMMCS
Interdisciplinary Conference
Waterloo, Ontario, Canada

Beyond volatility of volatility: Decomposing the informational content of VVIX

É. Bacon[1], J.-F. Bégin[2], G. Gauthier[3]

[1] *HEC Montréal, Montréal, Canada, etienne.bacon@hec.ca*
[2] *Simon Fraser University, Burnaby, Canada, jbegin@sfu.ca*
[3] *HEC Montréal, Montréal, Canada, genevieve.gauthier@hec.ca*

This research studies the informational content of the VVIX index, commonly interpreted as a proxy for the volatility of volatility of the S&P 500. We show that this interpretation is incomplete: by construction, the VVIX reflects both volatility of volatility and long-run variance. Empirically, proxies for volatility of volatility explain only a small fraction of the variation in squared VVIX, while including measures of the variance level substantially improves explanatory power. We develop a tractable model linking VVIX to instantaneous variance, long-run variance, and volatility of volatility, and estimate these components using option-implied cumulants. The results show that long-run variance dominates VVIX dynamics in calm markets, whereas volatility of volatility drives VVIX during periods of financial stress.

The VII International AMMCS
Interdisciplinary Conference
Waterloo, Ontario, Canada

Optimal Timing of Imbalance Announcements in Closing Auctions

Jackson Baerg[1], Christoph Frei[1], Aari Vinayagasothy[1]

[1] *University of Alberta, Edmonton, Canada, {jbaerg,cfrei,avinayag}@ualberta.ca*

Closing prices in many equity markets are determined through auctions. Typically, the indicative order imbalance of the auction is announced before the close. Studies comparing the implications of different auction specifications include Bogousslavsky and Muravyev [1], Hu and Murphy [2], and Jegadeesh and Wu [3]. Motivated by the closing auction model of Jegadeesh and Wu [3], we study how the announcement time affects auction depth and price efficiency when informed traders arrive stochastically and the information environment changes after the imbalance is disclosed.

We consider a single risky asset with terminal value v and normally distributed prior. Informed traders have CARA preferences and receive noisy signals about v. Traders arriving before the imbalance announcement observe a signal with precision ψ_b, while traders arriving after the announcement observe a signal with precision $\psi_a > \psi_b$, capturing the richer information environment created by the closing auction dissemination process. Liquidity providers are uninformed and submit limit-on-close orders to absorb the imbalance. The numbers of informed traders arriving before and after the announcement time τ are modeled as independent Poisson random variables with intensities depending on τ.

The closing auction price p_τ is determined by market clearing. We derive the resulting price-impact coefficient and study the announcement time that minimizes the expected squared pricing error

$$\min_{0 \leq \tau \leq T} E\left[(v - p_\tau)^2\right].$$

Our numerical results show that the optimal announcement time can be interior. Announcing too late reduces the number of traders who can respond to the imbalance, while announcing too early may reduce the informational precision of participating traders. The optimal timing therefore balances participation, information precision, and liquidity provision. Comparative statics indicate that stronger post-announcement signals and higher post-announcement arrival rates can substantially reduce price error and shift the optimal announcement time. The model provides a tractable framework for studying closing-auction design and highlights how the timing of market-wide information disclosure can affect liquidity and price efficiency.

References

[1] V. Bogousslavsky and D. Muravyev, *Who trades at the close? Implications for price discovery and liquidity*, Journal of Financial Markets **66**, 100852 (2023).

[2] E. Hu and D. Murphy, *Vestigial tails? Floor brokers at the close in modern electronic markets*, Forthcoming in Management Science (2025)

[3] N. Jegadeesh and Y. Wu, *Closing auctions: Nasdaq versus NYSE*, Journal of Financial Economics **143**, pp. 1120–1139 (2022).

Habit Formation, Labor Supply, and the Dynamics of Retirement and Annuitization

Criscent Birungi[1], Cody Hyndman[1],

[1] *Department of Mathematics and Statistics, Concordia University, Montréal, Canada, {criscent.birungi,cody.hyndman}@concordia.ca*

We study the joint determination of consumption, labor supply, portfolio choice, and optimal annuitization when preferences exhibit internal habit formation and mortality follows a deterministic age-dependent (Gompertz) law. The problem is a combined stochastic control and optimal stopping problem, solved via dynamic programming and the associated Hamilton-Jacobi-Bellman variational inequality. We obtain semi-analytical optimal policies that reveal three distinct behavioural regimes. At low wealth relative to the habit stock, labor is supplied defensively to protect the accustomed standard of living. As wealth grows, the agent moves into a "work-to-retire" phase, supplying labor at the maximum rate in order to reach the annuitization threshold faster. At the point of annuitization, human capital vanishes, leading to an abrupt de-risking of the financial portfolio. The agent's subjective mortality beliefs are a key determinant of these dynamics: more pessimistic beliefs make annuities less attractive, rationally delaying annuitization. This framework provides a behaviour-based explanation for the low observed demand for annuities and highlights the interaction between consumption habits, labor flexibility, and the timing of retirement.

A Dynamic Equilibrium Model of Liquidity Risk

Agostino Capponi[1], Johannes Muhle-Karbe[2], Xiaofei Shi[3]

[1] *Columbia University, New York, New York, USA, ac3827@columbia.edu*
[2] *Imperial College London, London, UK, j.muhle-karbe@imperial.ac.uk*
[3] *University of Toronto, Toronto, ON, CA, xf.shi@utoronto.ca*

We present a framework for analyzing the equilibrium implications of liquidity risk dynamics on asset prices. Our model features two risk-averse agents who continuously trade a security to hedge nontraded risks, while facing stochastic transaction costs correlated with their trading needs. We derive explicit solutions for equilibrium prices and traded quantities under small transaction costs, showing that the illiquidity discount increases with the correlation between trading costs and trading needs. Calibrating the model using NYSE and AMEX data, we find that liquid portfolios recover faster from liquidity shocks and exhibit smaller fluctuations, whereas illiquid portfolios are highly sensitive to trading-cost dynamics. For the most illiquid portfolio, the illiquidity discount increases by 12% when transaction costs and high-frequency trading needs are fully correlated, compared to the uncorrelated case.

Equilibrium Exploratory Optimal Stopping under Non-Exponential Discounting

Y. Chen[1], B. Li[2], D. Saunders[3]

[1] *University of Waterloo, Waterloo, Canada, yuling.chen@uwaterloo.ca*
[2] *University of Waterloo, Waterloo, Canada, bin.li@uwaterloo.ca*
[3] *University of Waterloo, Waterloo, Canada, dsaunders@uwaterloo.ca*

We consider a continuous-time reinforcement learning approach to the problem of optimal stopping of a diffusion process with non-exponential discounting. We study an equilibrium approach to this time-inconsistent problem, and compare the solutions (stopping regions and stopping policies) derived from a time-consistent setting with exponential discounting and a time-inconsistent setting with non-exponential discounting. An algorithm to learn the optimal stopping policy is also presented, together with examples on the pricing of American options. This is joint work with Yuling Chen and Bin Li from the University of Waterloo.

Real Options for Naval Platform Design and Operations

Matt Davison[1], Ivailo Petrov[1]

[1] *Western University, London, Canada*

On 31 December 1942 British and German forces engaged in the Battle of the Barents Sea. During this battle British destroyer HMS Onslow repeatedly threatened a much heavier force of German Surface combatants by threatening, but never carrying out, torpedo attacks. These feints induced the German command decision to temporarily withdraw from the battle, with an excellent outcome for the Royal Navy. In financial math terms, Commander Sherbrooke of the Onslow deemed that the "hold" value of the torpedo option exceeded its "exercise" value.

This story motivates a consideration of considering the modelling of submarine combat decisions – and the platform design constraints which accommodate them – through a Real Options lens. We first consider a vessel which can fire a torpedo into various threat states, themselves imperfectly observed and governed by a Hidden Markov process. Torpedos are finite in number and can only be reloaded after a latency time.

We then expand the problem to a situation where a submarine can launch various types of vehicles into various threat states.

It turns out that the modelling of the latency in these problems is quite important. And that various interesting results can be drawn about the relative value of various design parameters. Come join me for a salty voyage in which we meet real options in an unusual setting

Infinite-Dimensional LQ Mean Field Games with Common Noise: Small and Arbitrary Finite Time Horizons

H. Liu[1], D. Firoozi[2]

[1] *HEC Montreal, Montreal, Canada, hanchao.liu@hec.ca*
[2] *Univeristy of Toronto, Toronto, Canada, dena.firoozi@utoronto.ca*

We extend the results of (Liu and Firoozi, 2025), which develops the theory of linear-quadratic (LQ) mean field games (MFGs) in Hilbert spaces, by incorporating a common noise. This common noise is modeled as an infinite-dimensional Wiener process affecting the dynamics of all agents. In the presence of common noise, the mean-field consistency condition is characterized by a system of coupled forward-backward stochastic evolution equations (FBSEEs) in Hilbert spaces, whereas, in its absence it is represented by coupled forward-backward deterministic evolution equations. We establish the existence and uniqueness of solutions to the coupled linear FBSEEs associated with the LQ MFG framework for small time horizons and prove the ε-Nash property of the resulting equilibrium strategy. Furthermore, we establish the well-posedness of these coupled linear FBSEEs for arbitrary finite time horizons. Beyond the specific context of MFGs, our analysis also yields a broader contribution by providing, to the best of our knowledge, the first well-posedness result for a class of infinite-dimensional linear FBSEEs, for which only mild solutions exist, over arbitrary finite time horizons.

The VII International AMMCS
Interdisciplinary Conference
Waterloo, Ontario, Canada

Lambda Value-at-Risk under ambiguity

P. Liu[1], A. Schied[2]

[1] *University of Essex, UK, peng.liu@essex.ac.uk*

[2] *University of Waterloo, Canada, aschied@uwaterloo.ca*

We investigate Lambda Value-at-Risk (ΛVar) under ambiguity, where the ambiguity is represented by a family of probability measures. We establish that for increasing Lambda functions, the robust (i.e., worst-case) ΛVar under such an ambiguity set is equivalent to ΛVar computed with respect to a capacity, a novel extension in the literature. This framework unifies and extends both traditional ΛVar, as introduced in [2], and the Choquet quantiles (Value-at-Risk under ambiguity) defined in [1]. We analyze the fundamental properties of this extended risk measure and establish a novel equivalent representation for ΛVar under capacities with monotone Lambda functions in terms of families of downsets. Moreover, explicit formulas are derived for robust ΛVar when ambiguity sets are characterized by ϕ-divergence or likelihood ratio constraints.

We further explore the applications in risk sharing among multiple agents. We demonstrate that the family of risk measures induced by families of downsets is closed under inf-convolution. In particular, we prove that the inf-convolution of ΛVar with capacities and monotone Lambda functions is another ΛVar under a capacity. The explicit forms of optimal allocations are also derived. Moreover, we obtain more explicit results for risk sharing under ambiguity sets characterized by ϕ-divergence and likelihood ratio constraints.

References

[1] Chambers, C. P. Ordinal aggregation and quantiles. *Journal of Economic Theory*, **137**(1), 416–431(2007).

[2] Frittelli, M., Maggis, M., and Peri, I. Risk Measures on $\mathscr{P}(R)$ and Value at Risk with Probability/Loss function. *Mathematical Finance*, **24**(3), 442–463 (2014).

[3] Liu, P., Schied, A. Lambda Value-at-Risk under ambiguity and risk sharing. Preprint arXiv:2511.00717.

Optimal Option Portfolios for Skew-Elliptical t Returns

K. Sung[1], T. A. Pirvu[2]

[1] *McMaster University, Hamilton Canada, sungk5@mcmaster.ca,*
[2] *McMaster University, Hamilton Canada, pirvut@mcmaster.ca*

This paper explores option portfolio optimization when the underlying returns are skew-elliptical t-distributed. We use the variance and value at risk (VaR) to measure portfolio risk. The novelty of our work is the departure from the traditional normal returns setting, allowing investors to capture both heavy-tailed and skewed market dynamics. We provide explicit portfolio weights for the variance and VaR approximation. Our second contribution is the numerical representation of portfolio weights, obtained from numerical optimization for better VaR approximations. The effect of skewness on the portfolio weights is quantified by comparing our optimal skew t weights with those generated in the Student t setting. We also find that, as expected, a better VaR approximation risk measure yields optimal portfolio weights which are more different than the variance optimal weights.

Please Insert the Title of Your Talk Here

B. E. Bartles[1], K. G. Stankova[2]

[1] *University of Western Ontario, London, Canada, bbartels@uwo.ca*
[2] *University of Western Ontario, London, Canada, kgstankova@stats.uwo.ca*

The influence of family income on longevity has been established by previous studies. In this research, we analyze the Longitudinal Administrative Database (LAD) to determine income's influence on longevity for single and married Canadians over the period of 1991 to 2020. The LAD being a 20% sample of the tax returns of Canadians, provides information that helps group individuals by marital status and income levels. We create three income classifications for the purposes of this study: low, medium and high, that are inflation-adjusted over time. Results indicate relationships and also produce life tables that incorporate marital status and income levels. Our findings are highly relevant to many industries such as insurance, healthcare and social welfare.

In Estimation, the Key Is the Volatility Index, Not the Returns

Marcos Escobar-Anel[1], Lars Stentoft[2], and Siming Tang[3]

[1] *Department of Statistical and Actuarial Sciences, University of Western Ontario, Canada, marcos.escobar@uwo.ca*
[2] *Department of Economics and Department of Statistical and Actuarial Sciences, University of Western Ontario, Canada, lars.stentoft@uwo.ca*
[3] *Department of Statistical and Actuarial Sciences, University of Western Ontario, Canada, stang378@uwo.ca*

This paper proposes a new methodology to estimate a subclass of square-root stochastic autoregressive volatility (SR-SARV) models using volatility index (vli) and returns data. The approach, denoted A-C-VIX-Ret, is based on fitting the vli via a M-estimator, while approximating returns; and it is shown to be vastly superior to the standard approach of fitting returns via likelihood with an approximation on the vli, denoted A-Ret-VIX. We focus on SR-SARV(1) models with a Chi-square, 1 df distribution for the conditional variance, as this accommodates most GARCH models in the literature. This type of models leads to infinite likelihood for infinitely many points, hence an ill-posed likelihood, a problem our approach overcomes while ensuring consistency. Our main focus is on the HN-GARCH of Heston & Nandi (2000), and the time series of S&P 500 Index returns and VIX data from CBOE. Our analyses demonstrate that the volatility index holds more information on the parameters than the returns, leading to A-C-VIX-Ret improving the quality of estimation compared to A-Ret-VIX, as seen by RMSE reductions of up to 90%. For robustness, we apply and compare the methodologies on two alternative choices of models, several volatility indexes, and stock data sets obtaining similar results.

The last passage time before ruin: Theory and applications in liquidation risk management

Zijia Wang[1], Jingyi Cao[2], Shu Li[3]

[1]*Department of Finance, The Chinese University of Hong Kong, Hong Kong SAR, zijiawang@cuhk.edu.hk*
[2]*Department of Mathematics and Statistics, York University, Canada, jingyic@yorku.ca*
[3]*Department of Statistical and Actuarial Sciences, Western University, Canada, shu.li@uwo.ca*

In response to challenges posed by emerging risks such as climate change, practitioners are increasingly aware of the need for a more forward-looking approach to insurance solvency risk management, which requires not only the identification of risks but also timely intervention. However, determining when to implement risk mitigation is often complex, as it involves balancing insolvency prevention against the potential costs and consequences of such actions. In this talk, we provide insights into the timing of risk mitigation before it is too late by studying the last time a Lévy insurance risk process is above a certain threshold before ruin. In the theoretical part, we first examine the joint Laplace transform of the last passage time and the remaining time until ruin. We then study an optimal prediction problem of approximating the last passage time before ruin with a stopping time under the L_1 distance, showing that the optimum occurs when the risk process first drops below a certain level. The stopping boundary is independent of the initial surplus level, and we provide an explicit characterization of this boundary. These theoretical results fill a gap in the literature, where last passage times are typically analyzed over an infinite time horizon or an independent exponential time horizon. By focusing on the dynamics of risk processes up to ruin, our findings offer interesting insights into liquidation risk management. These are discussed in the application part, where we develop a framework to endogenously determine financial distress and rehabilitation levels under contemporary regulations. We further analyze the liquidation time under Chapter 7 and Chapter 11 of the U.S. Bankruptcy Code. Numerical examples and an empirical study using real data are presented to illustrate the practical implications of our results.

References

[1] Wang, Z., Cao, J., Li, S. (2026). The last passage time before ruin: theory and applications in liquidation risk management. *Insurance: Mathematics and Economics* 126, 103173.

Optimal trading in day-ahead power markets with battery storage

Tony Ware[1]

[1] *University of Calgary, aware@ucalgary.ca*

Continuously-traded day-ahead power markets provide the opportunity to trade in hourly (or perhaps shorter) blocks. Owners of battery storage can take positions that capture intrinsic value from differences in those prices, with the battery guaranteeing that the positions can be fulfilled physically (i.e. are rateable). Moreover, they can adjust those positions when doing so would increase the net value of their position (while still being rateable). This is a rolling rated position, and if the intrinsic value is maximized at each point, it is called a rolling intrinsic value strategy. We propose a PMPP model (i.e. a Polynomial Map of a Polynomial Process) to capture the dynamics of the day-ahead price curve, and show how this can be used to determine a strategy that maximizes the expected revenue from a rolling rated position, providing a comparison with the expected revenue rolling intrinsic value strategy.

The VII International AMMCS
Interdisciplinary Conference
Waterloo, Ontario, Canada

Context-Aware Probabilistic Map Matching and LLM-Enabled Decision Support for Intelligent Transportation Systems

Kiran[1], Jaiteg Singh[2], Sukhjit Singh Sehra[3]

[1] *Department of Computer Science and Engineering, Chitkara University, India*
[2] *Department of Computer Applications, Chitkara University, India*
[3] *Department of Computer Science, Wilfrid Laurier University, Canada*

In populated urban areas, where GPS observations shows many possible route alternatives with comparable probabilities, road-network topologies, and complicated intersections are still major issues in transportation network system[1]. However, traditional map matching approach based on Hidden Markov Models (HMMs) showing inadequate results due to transition probabilities and geometric proximity[2]. Which leads to inaccurate trajectory inferences in urban areas. To resolve these issues, this paper proposes a multi-layered hybrid framework, combining the structural network indexing, semantic reasoning, and probabilistic error modeling. This work computes an index called Road Complexity Index (RCI) based on geometric and topology of road-network features using OpenStreetMap (OSM). It further embedded with HMM to adaptively update emission and transition probabilities, and Gaussian Mixture Models (GMMs) to find out where different GPS error patterns are seen in complex areas[3]. To improve trajectory estimation, an LLM-based reasoning layer is introduced as contextual filter, which analyses navigation context, road semantics, intersection characteristics, and movement patterns to resolve matching uncertainty and select the most possible trajectory. The experimental results validated with real-world GPS trajectories collected from Chandigarh, India. Results shows a step-by-step reduction in mean map-matching error from 18.6 m with nearest edge map matching method, to 8.4 m with RCI-HMM model and to 5.9 m with matching accuracy of 92.8% by RCI-GMM-HMM. Comparatively, proposed RCI-GMM-HMM-LLM pipeline outperforms with mean tracking error of 5.5 m and the route selection accuracy of 96%. The results shows that probabilistic trajectory inference coupled with LLM can work more effective to build interpretable, context-aware, and scalable Intelligent transportation system (ITS).

References

[1] N. Alexandrov, “Problem Complexity and LLM: H-M Team Reliability in Challenging Environments,” in *AIAA SCITECH 2025 Forum*, ser. AIAA SciTech Forum. American Institute of Aeronautics and Astronautics, Jan. 2025. [Online]. Available: https://arc.aiaa.org/doi/10.2514/6.2025-1914

[2] H. Gao, H. Chen, T. Qu, Y. Li, Y. Hu, and B. Gao, “Probabilistic Modeling of Human Driverâs Natural Behavior Distribution: An Ensemble Learning and GMM Framework for Car-Following Model,” *IEEE Transactions on Intelligent Transportation Systems*, pp. 1–17, 2026. [Online]. Available: https://ieeexplore.ieee.org/abstract/document/11523181

[3] X. Chen, Q. Qiu, and Z. Chen, “Enhanced Market Forecasting for Autonomous Vehicles Using a Hidden Mixture Gaussian Markov Model,” *INTERNATIONAL JOURNAL OF COMPUTERS COMMUNICATIONS & CONTROL*, vol. 20, no. 5, Sep. 2025. [Online]. Available: https://www.univagora.ro/jour/index.php/ijccc/article/view/6911

The VII International AMMCS
Interdisciplinary Conference
Waterloo, Ontario, Canada

Designing LLM Agents for Urban Mobility Planning and Operations: Optimizing the Agent-Simulator Interface

E. Jung[1], S. S. Sehra[2], J. Yeo[1]

[1] *Gachon University, Dept. of Smart City Convergence, Seongnam, Republic of Korea, jeunjoo1211@gachon.ac.kr, jihoyeo@gachon.ac.kr*
[2] *Wilfrid Laurier University, Dept. of Computer Science, Waterloo, Canada, ssehra@wlu.ca*

Recent LLM-based transportation systems, including ChatSUMO [1], AgentSUMO [2], and TrafficSimAgent [3], have demonstrated that natural-language interaction with simulators is possible. However, existing studies focus almost exclusively on the agent side and do not systematically compare alternative agent design choices, while the complementary question of how simulator outputs should be restructured to support agent reasoning remains largely unexplored. We frame this as an *agent–simulator co-design* problem and separate the design space into four layers: agent roles, workflow topology, per-node implementation, and the agent–simulator interface. Rather than applying a uniform level of information, reasoning, and control to every task, the framework follows a *task-specific design principle*: the required information structure, reasoning mechanism, and degree of simulator control are selected according to the characteristics of each task.

Following this design philosophy, we implement Agentic DTUMOS [4] as a six-agent LangGraph-based platform and validate it in three cities: Seongnam, Manhattan, and Seoul. Agentic DTUMOS is an AI Operator Layer in which six specialized agents—Orchestrator, Planner, Modeler, Simulator, Analyzer, and Interpreter—collaborate to enable users to operate the simulator through natural language. Moreover, the collaboration structure is switched dynamically according to the task characteristics: single-routing for simple queries, a sequential pipeline for first-round optimization, and a diagnostic feedback loop for iterative refinement.

Our experiments show that design choices have a stronger effect on system performance than the underlying model. For 39 evaluation questions, a 565-token structured summary achieved 79.5% accuracy, whereas a 50,005-token raw JSON (about 89 times larger) only reached 50.3%. The 29.2 percentage-point difference was also observed when six domain experts scored the outputs. By modifying around 50 lines of the simulator's output schema, we obtained 3-5 percentage-point improvements across all context levels without changing the LLM. Error analysis revealed that rule-based and LLM-driven diagnosis exhibit complementary strengths and weaknesses, so combining them through adaptive routing performs better than using either approach alone. These findings were consistently reproduced across seven LLMs provided by Google, Anthropic, and OpenAI, and the automated scores were cross-validated by six domain experts who manually graded the responses, with high inter-rater agreement (Fleiss' $\kappa = 0.81$). Variations in system architecture explained more than 50 percentage points of the observed accuracy variance, while model choice alone explained only about 18 percentage points, indicating that workflow and interface design contribute more to performance than the choice of foundation model itself.

Acknowledgment. This work was supported by the National Research Foundation of Korea (NRF) grant funded by the Korea government (MSIT) (No. RS-2026-25524099).

References

[1] S. Li, T. Azfar, and R. Ke, *ChatSUMO: Large Language Model for Automating Traffic Scenario Generation in Simulation of Urban Mobility*, IEEE Trans. Intell. Veh. **10**, 11, pp. 4962–4973 (2025).

[2] M. Jeong, J. Chang, and Y. Yoon, *AgentSUMO: An Agentic Framework for Interactive Simulation Scenario Generation in SUMO via Large Language Models*, arXiv:2511.06804 (2025).

[3] Y. Du, J. Zhang, J. Feng, Z. Liu, J. Yuan, and Y. Li, *TrafficSimAgent: A Hierarchical Agent Framework for Autonomous Traffic Simulation with MCP Control*, arXiv:2512.20996 (2025).

[4] H. Yeon, T. Eom, K. Jang, and J. Yeo, *DTUMOS, Digital Twin for Large-Scale Urban Mobility Operating System*, Sci. Rep. **13**, 5154 (2023).

The VII International AMMCS Interdisciplinary Conference Waterloo, Ontario, Canada

An Interpretable LLM-Assisted ABSA Framework for Validity-Weighted Attenuation of Affective Noise in Student Evaluations of Teaching

B. Obeidi[1], S. Fatahi[1], A. Asilian Bidgoli[1]

[1] *Wilfrid Laurier University, Ontario, Canada, {obei4210@mylaurier.ca, sfatahi@wlu.ca, aasilianbidgoli@wlu.ca}*

Student Evaluations of Teaching (SET) inform consequential institutional decisions on faculty performance, tenure, and promotion, yet their validity is systematically compromised by well-documented biases [1]. In particular, non-pedagogical content distorts numerical ratings in ways unrelated to instructional quality [2]. Informal platforms such as RateMyProfessors.com (RMP) exacerbate this through full anonymity and absence of modera-tion. Despite advances in computational SET analysis, existing work remains descriptive: sentiments are extracted but ratings are never intervened upon. This work addresses that gap with a five-stage interpretable Aspect-Based Sentiment Analysis (ABSA) framework that directly adjusts SET ratings to attenuate affective noise while pre-serving pedagogical signal and students' evaluative intent.

The framework is applied to N = 17,121 English-language RMP reviews. Clauses are extracted via spaCy and assigned to one of three pedagogical topics (Instructional Effectiveness, Fairness & Grading, Workload & Diffi-culty) or to a Miscellaneous category via zero-shot Sentence-BERT cosine similarity thresholding. A pedagogical density metric (Dmisc) captures the proportion of non-pedagogical content per review. Clause-level emotion vec-tors (27 non-neutral dimensions) are extracted via RoBERTa-GoEmotions and aggregated at the topic level. A CatBoost regressor trained on these features predicts ratings; adjusted scores are produced by recomputing predic-tions under proportionally attenuated Miscellaneous emotional inputs via attenuation factor $\zeta = 1 - (D_{\text{misc}})^s$ and computing

$$\hat{y}^{\text{adjusted}} = y^{\text{raw}} + \left(\hat{y}^{\text{attenuated}} - \hat{y}^{\text{baseline}}\right). \tag{1}$$

This prediction-based correction mechanism ensures adjustments remain attributable to specific review text and topic-level emotions, satisfying interpretability requirements for consequential decision-making [3].

The regressor achieves MAE = 0.637, Spearman ρ = 0.736, R^2 = 0.614 on a professor-level stratified hold-out set. Aspect-Term Categorization achieves an expert-validated accuracy of 0.77. SHAP-based internal validation confirms attenuation shifts model sensitivity away from *Miscellaneous* features (-10.7%) toward pedagogical categories (*Instructional Effectiveness*: +2.1%; *Fairness*: +2.7%; *Workload*: +2.6%), while maintaining or strengthening correlations with pedagogical features. External validation with a senior faculty expert yielded paired comparison accuracy of 88.9% under coarse conditions ($p < 0.001$) and 72.4% for fine-grained ($p < 0.012$).

To our knowledge, this is the first transparent computational mechanism to operationalize construct-irrelevant variance (CIV) mitigation directly into SET rating adjustment. The framework bridges Messick's unified validity theory [4] with classical reliability and robust estimation principles, yielding auditable corrections grounded in psychometric theory. The modular design also suggests applicability to other open-ended feedback domains where reviews are accompanied by numerical ratings.

References

[1] B. Keller and I. Reiten, *Cluster-titled algebras are Gorenstein and stably Calabi-Yau*, Adv. Math. **211**, 1, pp. 123-151 (2007).
[2] S. Washito and K. Karabashi, *Use This Template*, in *Proceedings of the 5th International Conference on Photon Interaction* (ICPI-2012), San Francisco, USA, ed. A. Chen, pp. 22-24 (2012).
[3] A.B. Smith, *Describing the style for the AMMCS-CAIMS-2015 book of abstracts*, in C.D. Science (ed.), General Book of Wisdom, 2nd ed., University of Queensland, pp. 23-42 (2014).
[4] S. Messick, Validity of psychological assessment, Amer. Psychologist 50(9), pp. 741–749 (1995).

The VII International AMMCS Interdisciplinary Conference
Waterloo, Ontario, Canada

An Empirical Study of Large Language Models for Grading and Feedback Generation of Programming Assignments

N. Shaffir[1], S. Fatahi[2]

[1] *Wilfrid Laurier University, Waterloo, Canada, { shaf3110}@mylaurier.ca*
[2] *Wilfrid Laurier University, Waterloo, Canada, sfatahi@wlu.ca*

Large Language Models (LLMs) are increasingly being explored as tools for supporting computer science education, particularly in automated grading and feedback generation for programming assignments. Traditional autograding systems provide scalable and timely assessment, but they often rely on predefined test cases and offer limited explanatory feedback. This study investigates whether fine-tuning an LLM improves its ability to assign grades and generate pedagogically useful feedback for student Java programming submissions.

The objective of this completed empirical study is to compare the grading accuracy and feedback quality of a base LLM and a fine-tuned LLM. We used 300 student submissions from the CSEDM Data Challenge CodeWorkout dataset, collected from an introductory Java programming course. The data were split into training and testing sets using a 75/25 split. The gpt-4o-mini model was evaluated in two settings: base and fine-tuned. In both settings, the model was prompted to grade student code using two styles: compassionate and strict. Model-generated grades were compared with human grades using Pearson correlation, Mean Absolute Error (MAE), and Root Mean Squared Error (RMSE). Feedback quality was evaluated using a rubric based on actionability, accuracy, and clarity.

The results show that fine-tuning substantially improved grading performance. The base model achieved Pearson correlations of approximately 0.75 under compassionate grading and 0.79 under strict grading. After fine-tuning, correlations increased to approximately 0.90 and 0.91, respectively. The fine-tuned strict model achieved the lowest grading error, with MAE $\approx$ 0.05 and RMSE $\approx$ 0.09. Feedback generated by both base and fine-tuned models was generally clear, accurate, and actionable. The fine-tuned strict model achieved the highest average feedback quality score, approximately 4.4 out of 5, comparable to human-written feedback.

These findings suggest that fine-tuned LLMs can closely approximate human grading while generating meaningful feedback for programming assignments. The study contributes empirical evidence on the value of fine-tuning for LLM-based programming assessment and highlights its potential to support scalable, timely, and educationally meaningful feedback in computer science education. Future work should examine larger and more diverse datasets, additional programming languages, multilingual feedback generation, and formal mechanisms for detecting hallucinations and grading inconsistencies.

References

[1] M. Jukiewicz, The future of grading programming assignments in education: The role of ChatGPT in automating the assessment and feedback process, *Thinking Skills and Creativity* 52, 101522 (2024).
[2] M. Akyash, K. Z. Azar and H. M. Kamali, StepGrade: Grading Programming Assignments with Context-Aware LLMs, arXiv:2503.20851 (2025).
[3] L. Korthals, H. Rosenbusch, R. Grasman and I. Visser, Grading University Students with LLMs: Performance and Acceptance of a Canvas-Based Automation, *Communications in Computer and Information Science*, pp. 36–43 (2025).

The VII International AMMCS
Interdisciplinary Conference
Waterloo, Ontario, Canada

Evaluating the Pedagogical Characteristics of LLM-Generated versus Human-Written Code Explanations

S. Talati[1], S. Fatahi[2]

[1] *Wilfrid Laurier University, Waterloo, Canada, tala4867@mylaurier.ca*
[2] *Wilfrid Laurier University, Waterloo, Canada, sfatahi@wlu.ca*

Large Language Models (LLMs) are increasingly used by students as informal tutoring tools in programming education. Although these systems can generate fluent and accessible code explanations, it remains unclear whether their explanations exhibit the pedagogical characteristics of high-quality human instruction. This study presents a reproducible computational framework for comparing LLM-generated code explanations with curated human-written explanations from high-scoring Stack Overflow answers.
The objective of this completed empirical study is to evaluate whether LLM-generated explanations differ from human-written explanations in terms of readability, structural characteristics, and semantic alignment. We constructed a dataset of 515 matched question–answer pairs from Stack Overflow, using human answers with community vote scores of at least 7 as expert explanation benchmarks. Matched LLM explanations were generated using GPT-4o-mini with a novice-directed prompt. Both human and LLM explanations were evaluated using three categories of metrics: Flesch Reading Ease for readability, word and sentence counts for structural complexity, and cosine similarity over Sentence-BERT embeddings for semantic alignment. Statistical analysis was conducted using Wilcoxon signed-rank tests, one-sample t-tests, and effect-size estimation.

The results show that LLM-generated explanations appear significantly more readable than human-written explanations in the raw dataset. However, this apparent readability advantage disappears after preprocessing removes code blocks, Markdown, HTML formatting, and other Stack Overflow-specific artefacts. In the raw data, LLM explanations achieved a higher mean Flesch Reading Ease score than human explanations, with a statistically significant difference. After cleaning, the difference was no longer significant, indicating that previously observed readability advantages may be partly caused by platform formatting rather than genuine linguistic accessibility. In contrast, verbosity remained a robust difference: LLM-generated explanations were substantially longer than human explanations, with median word counts of approximately 459 versus 96 words. Semantic similarity between matched human and LLM explanations was moderate, with a mean cosine similarity of approximately 0.603, suggesting that LLMs capture core conceptual content but differ from human experts in explanatory framing, specificity, and conciseness.

These findings suggest that LLM-generated code explanations can serve as accessible supplementary resources for novice programmers, but they should not be treated as direct replacements for expert human explanations. The study highlights the importance of preprocessing choices in evaluating AI-generated instructional text and demonstrates that readability, verbosity, and semantic similarity capture distinct pedagogical dimensions. Future work should incorporate learner studies, human evaluation, multi-model comparisons, and richer discourse-level metrics to better assess the educational value of LLM-generated explanations in programming education.

References

[1] J. Leinonen, P. Denny, S. MacNeil, S. Sarsa, S. Bernstein, J. Kim, A. Tran and A. Hellas, Comparing code explanations created by students and large language models, in *Proceedings of ITiCSE*, pp. 124–130 (2023).
[2] N. Reimers and I. Gurevych, Sentence-BERT: Sentence embeddings using Siamese BERT-networks, in *Proceedings of EMNLP*, pp. 3982–3992 (2019).
[3] S. Kabir, D. N. Udo-Imeh, B. Kou and T. Zhang, Is Stack Overflow obsolete? An empirical study of the characteristics of ChatGPT answers to Stack Overflow questions, arXiv:2308.02312 (2023).

Agent-Based Modeling of Epstein-Barr Virus Transmission Dynamics and Vaccine Impact

Bridgette Amoako[1], Zhongda Huang[2], Edward Thommes[1,3], Warren Hare[2], Monica Cojocaru[3]

[1] *University of Guelph*
[2] *University of British Columbia*
[3] *Global Medical Affairs, Sanofi Vaccines*

Epstein-Barr virus (EBV) is one of the most widespread human pathogens, with seroprevalence exceeding 90% in adults worldwide [1]. Primary infection usually occurs in childhood, where it is often asymptomatic, but acquisition during adolescence or early adulthood frequently results in infectious mononucleosis (IM). Following infection, EBV establishes latency within B cells and can periodically reactivate, leading to viral shedding and continued opportunities for transmission [1]. Beyond illness, EBV has been shown to result in several malignancies, including multiple sclerosis (MS), Hodgkin's lymphoma (HL), nasopharyngeal cancer and gastric cancer [4]. Despite its global burden, the transmission dynamics of EBV are not as thoroughly studied as those of other common viruses like influenza. The difficulty arises from asymptomatic infections, heterogeneous shedding, and the challenge of measuring interpersonal contacts relevant for transmission.

We present the first agent-based model (ABM) of EBV transmission, calibrated to age-specific seroprevalence data from the US National Health and Nutrition Examination Survey [3]. Two calibration strategies are compared: Approximate Bayesian Computation (ABC) and Bayesian Optimization with Expected Quantile Improvement (BO-EQI). ABC yields a posterior distribution over infection probability parameters, naturally capturing uncertainty and providing distributional inputs for downstream simulation; BO-EQI achieves comparable fit while requiring substantially fewer model evaluations and scaling efficiently to higher-dimensional parameterizations. Calibrated transmission rates reveal a biologically consistent U-shaped age pattern, reflecting saliva-exposure dynamics across the life course. Scenarios simulating a hypothetical EBV vaccine demonstrate that vaccine durability is at least as critical as efficacy, and that waning vaccines may paradoxically increase IM burden by deferring infection to higher-risk ages. These findings highlight the importance of vaccine target product profile design, including the potential value of dual efficacy against both EBV infection and IM progression.

References

[1] J. I. Cohen, *Epstein-Barr Virus Infection*, New England Journal of Medicine **343**, 7, pp. 481–492 (2000).

[2] S. K. Dunmire, K. A. Hogquist and H. H. Balfour, *Infectious Mononucleosis*, Current Topics in Microbiology and Immunology **390**, pp. 211–240 (2015).

[3] H. H. Balfour, F. Sifakis, J. A. Silman, J. A. Knight, D. O. Schmeling and W. Thomas, *Age-Specific Prevalence of Epstein-Barr Virus Infection among Individuals Ages 6-19 Years in the United States and Factors Affecting Its Acquisition*, The Journal of Infectious Diseases **208**, 8, pp. 1286–1293 (2013).

[4] T. R. Nielsen, K. Rostgaard, N. M. Nielsen, N. Koch-Henriksen, S. Haahr, P. S. Sorensen and H. Hjalgrim, *Multiple Sclerosis After Infectious Mononucleosis*, Archives of Neurology **64**, 1, pp. 72–75 (2007).

Individual and Population Level Uncertainty Interact to Determine the Performance of Outbreak Surveillance Systems

Callum R.K. Arnold[1], Alex C. Kong[2], Amy K. Winter[3], William J. Moss[4], Bryan N. Patenaude[5], Matthew J. Ferrari[6]

[1] *University of Toronto, Canada, contact@callumarnold.com*
[2] *Johns Hopkins Bloomberg School of Public Health, USA, akong4@jhu.edu*
[3] *University of Georgia, USA, awinter@uga.edu*
[4] *Johns Hopkins Bloomberg School of Public Health, USA, wmoss1@jhu.edu*
[5] *Johns Hopkins Bloomberg School of Public Health, USA, bpatena1@jhu.edu*
[6] *Pennsylvania State University, USA, mjf283@psu.edu*

Background

Outbreak detection frequently relies on imperfect individual-level case diagnosis. Both outbreaks and cases are discrete events that can be misclassified and uncertainty at the case level may impact the performance of outbreak alert and detection systems. Here, we describe how the performance of outbreak detection depends on individual-level diagnostic test characteristics and population-level epidemiology, and describe settings where imperfect individual-level tests can achieve consistent performance comparable to "perfect" diagnostic tests.

Methodology

We generated a stochastic SEIR model to simulate daily incidence of measles (i.e., true) and non-measles (i.e., noise) febrile rash illness. We modeled non-measles sources as either independent static (Poisson) noise, or dynamical noise consistent with an independent SEIR process (e.g., rubella). Defining outbreak alerts as the exceedance of a threshold by the 7-day rolling average of observed test positives, we optimized the threshold that maximized outbreak detection accuracy across sets of noise structures and magnitudes, diagnostic test accuracy (consistent with either a perfect test, or proposed rapid diagnostic tests), and testing rates.

Conclusions

The optimal threshold for each diagnostic test typically increased monotonically with testing rate. With static noise, outbreak detection with RDT-like and perfect tests achieved accuracies of 90%, with comparable delays to outbreak detection. With dynamical noise, the accuracy of perfect test scenarios was superior to those achieved with RDTs (≈ 90% vs. ≤ 80%). Outbreak detection accuracy declined as dynamical noise increased and leads to permanent alert status with RDT-like tests at very high noise. The performance of an outbreak detection system is highly sensitive to the structure and the magnitude of the background noise. Depending on the epidemiological context, outbreak detection using RDTs can perform as well as perfect tests.

The Effect of Time Delay on the Global Stability of Infectious Disease Models and Other Dynamical Systems

J.Christopher[1]

[1] *Wilfrid Laurier University, Waterloo, Canada*

When studying mathematical models of infectious disease, one characteristic of great interest is the long term persistence of the disease: given an initial infection rate, will it become endemic? or die out? Mathematically this is a question about the stability of an endemic equilibrium. Since the initial conditions of an outbreak are not under our control, local stability results are often insufficient: one would like to know whether the conditions present in a specific outbreak would lead the system to the endemic equilibrium, or to disease extinction. For this reason, global stability results play an important role in the analysis of epidemic models.

In this talk we examine the effect of delayed variables on the global stability of systems of ordinary differential equations. This problem arises naturally in mathematical models of infectious disease, where delays may represent vector-borne transmission, incubation periods, temporary immunity, or other biological processes that prevent instantaneous responses in the system. Our approach is based on Lyapunov's Direct Method. Specifically, we construct Lyapunov functionals for the delayed system by modifying the Lyapunov functions used for the corresponding ODE model. This approach allows us to extend stability results from the non-delayed system to the delayed system, and provides a framework for analyzing the effect of delays in a broad class of dynamic models.

Attractor and transient periodicities are invariant to seasonal transmission patterns in epidemic models

E. Coates[1], I. Papst[1,2], D.J.D. Earn[1]

[1] *Department of Mathematics & Statistics, McMaster University, Hamilton, Canada, {coatee4,earn}@mcmaster.ca*
[2] *Modelling Hub, Applied Public Health Sciences Directorate, Science and Policy Integration Branch, Public Health Agency of Canada, Toronto, Canada, irena.papst@phac-aspc.gc.ca*

Childhood diseases, such as measles and whooping cough, exhibit cyclical behaviour, and the frequencies of their recurrent epidemics change over decades or centuries [1,2,3]. A key mechanism that underlies these epidemic cycles is seasonal variation in contact rates stemming mainly from school terms (known as "term-time forcing") [2]. However, early mechanistic models represented seasonality with a simple sine wave for mathematical convenience [2], which leads to the question: to what extent do inferences about transitions in epidemic cycles stemming from mechanistic models depend on accurate representation of the seasonal forcing function's shape?

Papst and Earn [4] addressed this question by introducing a family of functions smoothly connecting sinusoidal and term-time forcing. They showed that the asymptotic epidemic dynamics predicted by these models can be made near-identical, which means that a single sinusoidal forcing function can be used when studying disease dynamics across historical periods with different seasonal patterns. Their method relies on adjusting the amplitude of forcing by following a period doubling bifurcation in the system. This key bifurcation exists for measles in a biologically-relevant parameter range, but not so for whooping cough, and so their method cannot be applied in the study of the latter disease.

Papst and Earn focused on asymptotic epidemic behaviour; here, we turn our attention to the *transient* dynamics in order to extend their method to diseases like whooping cough. We show that the transient periods of damped oscillations onto cyclical attractors can also be made invariant across different seasonal forcing schemes, and so invariance is a more general principle in these systems. This finding supports the ongoing search for a more general framework for understanding shifts in epidemic frequencies observed in childhood infectious diseases.

References

[1] R.M. Anderson and R.M. May, *Infectious Disease of Humans: Dynamics and Control*, Oxford University Press (1991).
[2] D.J.D. Earn, *Mathematical epidemiology of infectious diseases*, in Mathematical Biology, M. A. Lewis, M. A. J. Chaplain, J. P. Keener, and P. K. Maini, eds., **14** of IAS/Park City Mathematics Series, American Mathematical Society, pp. 151-186 (2009).
[3] W.O. Kermack and A.G. McKendrick, *Contributions to the mathematical theory of epidemics–I. 1927*, Bulletin of Mathematical Biology, **53**, pp. 33-35 (1991).
[4] I. Papst and D.J.D. Earn, *Invariant predictions of epidemic patterns from radically different forms of seasonal forcing*, Journal of The Royal Society, **16** (2019).

The VII International AMMCS
Interdisciplinary Conference
Waterloo, Ontario, Canada

Analysis of a General Vector Transmission Model for Infectious Disease Spread

K. Devries[1] C. McCluskey[2]

[1] *Wilfrid Laurier University, Waterloo, Canada, devr6090@mylaurier.ca*
[2] *Wilfrid Laurier University, Waterloo, Canada, cmccluskey@wlu.ca*

As an extension of the framework developed by Earn and McCluskey [1], we consider a very general vector transmission model for the spread of an infectious disease. The human and vector populations each contain a single susceptible class and an arbitrary number of post-infection compartments, allowing for general stage structure (e.g., exposed, infectious, treated or quarantined classes). **Key model assumptions:**

- no return from the infected classes to the susceptible classes in both populations
- each infected class can be reached from the respective susceptible class
- a mass action incidence function (with a criss-cross structure: infected vectors infect susceptible humans, and infected humans infect susceptible vectors)

For the resulting system of ordinary differential equations, we explicitly determine the disease-free and endemic equilibria and derive a closed-form expression for the basic reproduction number. Using techniques similar to those developed by McCluskey and Earn, we study the global stability of the disease-free equilibrium when $R_0 \leq 1$ and of the endemic equilibrium when $R_0 > 1$.

References

[1] D. Earn and C. McCluskey, *Global stability of epidemic models with uniform susceptibility*, PNAS. **Vol. 122**, No.49, pp. 1-12 (2025).

The VII International AMMCS
Interdisciplinary Conference
Waterloo, Ontario, Canada

A continuous-time stochastic model for mutation effects in microbial population

A. Maths[1], B. Sciences[2], C. Lemma[3], D. Technology[4]

[1] *University of Copenhagen, Denmark, {maths,social-sciences}@ku.dk*
[2] *Wilfrid Laurier University, Waterloo, Canada, natural-sciences@wlu.ca*
[3] *CSIRO, Canberra, Australia, lemma@csiro.au*
[4] *Massachusetts Institute of Technology, Cambridge, USA, technology@mit.edu*

Mutation accumulation (MA) experiments are crucial for understanding evolution. In microbial populations, these experiments typically involve periods of population growth, where a single individual forms a visible colony, followed by severe bottlenecks. Studies on the effects of positive and negative selection in MA experiments have shown that, even with as few as ten generations of growth between bottlenecks, beneficial mutations will be substantially over-represented [1]; this effect is known as "selection bias". In previous work, we developed a discrete-time model and demonstrated that when stochastic offspring distributions are considered, selection bias is even stronger than previously predicted [2]. Since bacterial division is unlikely to remain synchronized over 15 or more generations, this study extends the discrete-time model to a continuous-time framework. Since lineages that start reproducing early accrue a compounded advantage, a continuous-time model offers an even more accurate correction for selection in MA experiments. In addition, we develop techniques for estimating the selection bias when only colonies above a fixed threshold size (e.g. visible colonies) are selected at the bottleneck, an experimental protocol that further exacerbates selection bias. We develop and describe computationally efficient techniques for correcting experimental MA data whether all colonies or only visible colonies are considered.

References

[1] L. Wahl and A. Deepa, *Selection bias in mutation accumulation*, Evolution. **76**, 3, pp. 528-540 (2022).

[2] L. Wahl and M. Ezadian, *Stochastic offspring distributions amplify selection bias in mutation accumulation experiments*, Theoretical Population Biology. 161, pp. 25-33 (2025).

The VII International AMMCS
Interdisciplinary Conference
Waterloo, Ontario, Canada

Deep Learning for Early Warning Signals of Complex Dynamical Transitions in Epidemics

Ali Haghighatgooasiabar[1], Chris T. Bauch[2],

[1] *Department of Applied Mathematics, University of Waterloo, Waterloo, ON N2L 3G1, Canada; ali.haghighatgooasiabar@uwaterloo.ca*
[2] *Department of Applied Mathematics, University of Waterloo, Waterloo, ON N2L 3G1, Canada; cbauch@uwaterloo.ca*

Identifying tipping points, driven by subtle changes in system parameters, is essential for forecasting vaccine-preventable disease dynamics. Gradual Changes in vaccination or birth rates can induce quick transitions between epidemic cycles (e.g., annual to biennial), and detecting these shifts enables early intervention. We develop a deep learning-based early warning framework that combines Dynamic Mode Decomposition (DMD) with a ResNet architecture [1] to extract stability-related features from time series data and classify imminent transitions.

Synthetic training data are generated using a stochastic, seasonally forced SEIR model [2] with parameter variations to induce regime shifts. The model is evaluated on both synthetic and empirical datasets. In the first phase, it forecasts the system dynamics (see 1), while in the second phase it classifies impending transitions. The classification performance for real data achieves a precision of 0.91, recall of 0.76, and an F1-score of 0.83, indicating that bifurcation signatures are encoded in time series data and can be learned by neural networks.

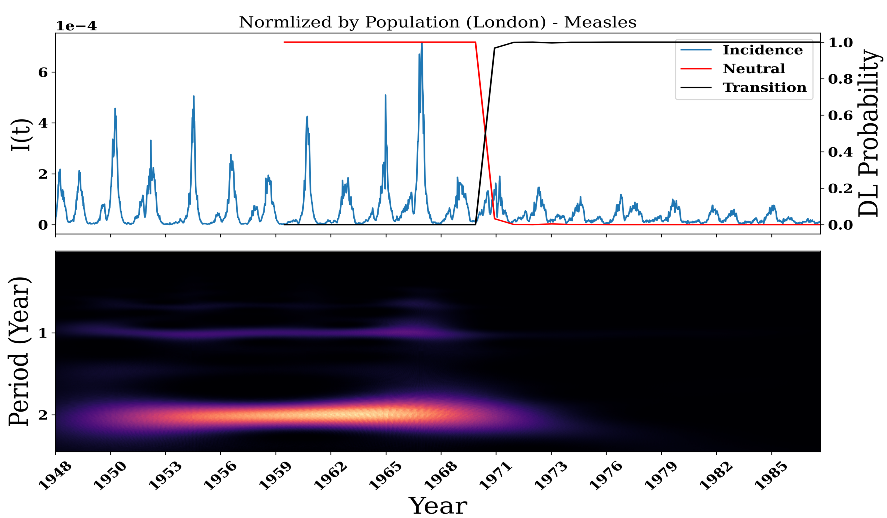

Figure 1: The lower panel shows a wavelet analysis of the number of cases normalized by the population of London. It shows that the dominant mode is biennial and recurrent, and it disappears around 1972; however, the transition probability exceeds 50% at approximately 1971.

References

[1] Z. He and C. T. Bauch, *Forecasting infectious disease outbreak risks from vaccine sentiments on social media: A data-driven dynamical systems approach*, in *Mathematical Biosciences and Engineering*, 22(10), pp. 2761–2779 (2025).

[2] D. J. Earn, P. Rohani, B. M. Bolker, and B. T. Grenfell, *A simple model for complex dynamical transitions in epidemics*, in *Science*, 287(5453), pp. 667–670 (2000).

The consequences of drug treatment for malaria parasite evolution, given pre-existing variation in sensitivity

Y. Jeong[1], N. Mideo[2]

[1] *University of Toronto, Toronto, Canada, youngseoclara.jeong@mail.utoronto.ca*
[2] *University of Toronto, Toronto, Canada, nicole.mideo@utoronto.ca*

For the past two decades, the main treatment for infections with the human malaria parasite Plasmodium falciparum has been artemisinin combination therapy, and resistance to artemisinin has been spreading, slowing parasite clearance in treated infections. At the same time, understanding of the genetic basis and the mechanisms of artemisinin resistance has been growing and their mechanism of action suggest a cost to within-host growth that may constrain resistance evolution [1]. Previous experimental study has revealed striking variation in susceptibility to artesunate (an artemisinin derivative) between strains of rodent malaria parasites (*Plasmodium chabaudi*), with the slowest clearing strains being quantitatively similar to what would be labelled “resistant” in the human malaria context [2]. In this system, transmission depends on the within-host dynamics, timing of which may impose evolutionary constraints for the parasite. Using experimental time series data of within-host infection dynamics and a previously published function-valued trait approach [3], we show how evolution of virulence and transmission at each infection age may be differently constrained in drug-treated vs. untreated populations, and whether different epidemiological scenarios change the evolutionary predictions.

References

[1] J. Birnbaum, S. Scharf, S. Schmidt, E. Jonscher, W.A.M. Hoeijmakers, S. Flemming, C.G. Toenhake, M. Schmitt, R. Sabitzki, B. Bergmann, U. Frohlke, P. Mesen-Ramirez, A.B. Soares, H. Herrmann, R. Bartfai, & T. Spielmann. *A Kelch13-defined endocytosis pathway mediates artemisinin resistance in malaria.* Science. **367**, 6473, pp. 51-59 (2020)

[2] L.C. Pollitt, D. Sim, R. Salathe, & A.F. Read. *Understanding the genetic variation in in vivo tolerance to artesunate: Implications for the treatment efficacy and resistance monitoring*. Evol. Appl. **8**, 3, pp. 296-304 (2015).

[3] N. Mideo, W.A. Nelson, S.E. Reece, A.S. Bell, A.F. Read, & T. Day, *Bridging scales in the evolution of infectious disease life histories: application.* Evolution. **65**, 1, pp. 3298-3310 (2011).

The VII International AMMCS
Interdisciplinary Conference
Waterloo, Ontario, Canada

AN AGE-AND-PHASE STRUCTURED MODEL OF THE MALARIA ASEXUAL ERYTHROCYTIC REPLICATION CYCLE

ZAHRA KHANZAD[1], MD AFSAR ALI[2], JANE M. HEFFERNAN[3], IAIN R. MOYLES[4]

[1] *Department of Mathematics & Statistics, York University, Toronto, Canada (zkhanzad@yorku.ca)*
[2] *Department of Mathematics & Computer Science, Alabama State University, Montgomery, United States*
[3] *Department of Mathematics & Statistics, York University, Toronto, Canada*
Centre for Disease Modelling, York University (jmheffer@yorku.ca)
[4] *Department of Mathematics & Statistics, York University, Toronto, Canada (imoyles@yorku.ca).*

We present a mathematical model of the asexual blood stage of a malaria infection from Plasmodium falciparum including time, maturation of infection, and phase of infection. The phases of infection include the merozoite phase, immature trophozoite phase, trophozoite phase, schizont phase, as well as the production of gametocytes. Our model shows oscillatory behaviour of the parasite between the phases with a period that strongly depends on the generation reproduction number of the parasite. We separate parasite evolution into different growth regimes classifying final sizes when the parasite population does not change and final proportions when it grows exponentially. Without fitting parameters, we compare our model to data for parasitized red blood cells showing excellent agreement. The phase structure of our model allows us to also gain insight into sequestered parasitized red blood cells which are unmeasured. We demonstrate how parameters within the phase structure can impact parasite growth and maturation with potential implications for antimalarial drugs and other therapies.

$$\frac{\partial P_i(t,a_i)}{\partial t} + \frac{\partial P_i(t,a_i)}{\partial a_i} = -R_i(a_i)P_i(t,a_i), \quad i \in \{M,I,T,S\}, \tag{1}$$

$$\frac{\mathrm{d}P_G(t)}{\mathrm{d}t} = (1-\alpha)\int_0^\infty R_I(a_I)P_I(t,a_I)\,\mathrm{d}a_I. \tag{2}$$

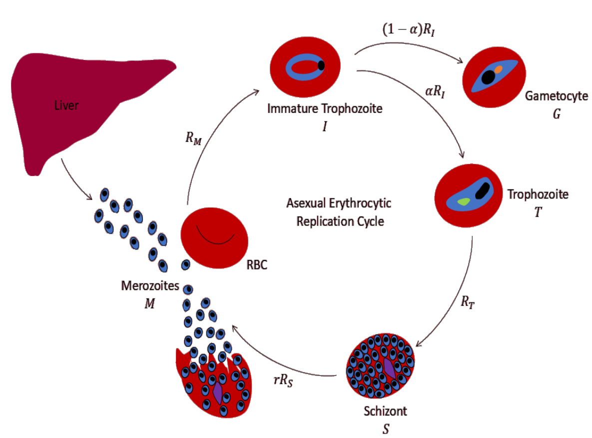

Figure 1: Illustration of the asexual malaria parasite life cycle within the human blood.

Analysis of a model of bacterial persister cells

C. Li[1], T. Meadows[2], T. Day[3]

[1] *Queen's University, Kingston, Canada, 20cl85@queensu.ca*
[2] *Queen's Univesity, Kingston, Canada, tyler.meadows@queensu.ca*
[3] *Queen's University, Kingston, Canada, day@queensu.ca*

Within many bacterial colonies, bacterial persister cells exist as a subpopulation that is seemingly immune to antibiotics, yet not genetically distinct from the rest of the colony. A recent paper [1] has suggested that epigenetic inheritance may be the mechanism that leads to the presence of persister cells. We analyze a non-local PDE model,

$$\partial_t n = \chi_\alpha[bR-d]n - \mu Rnb\chi_\alpha + \mu bR\int_0^1 n(y,t)\chi_\alpha(y)p(x;y)dy - \partial_x[v(x)n] + m\partial_{xx}n, \tag{1}$$

$$\partial_t R = \theta - \eta R - bR\int_0^1 \chi_\alpha n dx. \tag{2}$$

used to describe the epigenetic inheritance process and show that the model is biologically well posed. We find a parameter threshold delineating the extinction or persistence of the colony, which is independent of internal community structure. Numerical examples are used to show that the model can explain many of the key features of persister cells.

References

[1] T. Day, *Interpreting phenotypic antibiotic tolerance and persister cells as evolution via epigenetic inheritance*, Molecular Ecology **25**, (8), 1869–1882 (2016).

The VII International AMMCS
Interdisciplinary Conference
Waterloo, Ontario, Canada

Modelling Within-host HIV Dynamics Incorporating $CD31^+$ and $CD31^-$ Naive $CD4^+$ T Cell Subsets

J. Liu[1]

[1] *Western University, London, Canada, jliu2968@uwo.ca*

This paper investigates the role of T-cell homeostasis in HIV infection dynamics by incorporating the biological characteristics of the $CD31$ phenotypic marker. While standard models often treat $CD4^+$ T cells as a homogeneous population, we classify naive $CD4^+$ T cells into two distinct subsets: recent thymic emigrants ($CD4^+CD31^+$) and peripherally proliferated cells ($CD4^+CD31^-$). Building upon classical logistic growth frameworks, we develop a system of nonlinear differential equations that accounts for the unique proliferation and differentiation kinetics of these subsets. A central component of our study is the derivation of the basic reproduction number, $\mathscr{R}_0$, which serves as the fundamental threshold for viral persistence. The analytical focus lies in characterizing the existence, uniqueness, and stability of the model's equilibria. By analyzing special cases that isolate specific proliferative processes, this research identifies the presence of a backward bifurcation, providing a theoretical framework for understanding how the maintenance of the $CD4^+$ T-cell compartment influences both the clinical progression of HIV and the overall resilience of the immune system.

In-host modelling with immunity and virus loss term

Mahmuda Ruma[1] and Jane Heffernan[1]

[1] *Mathematics and Statistics, York University, Toronto, Ontario, Canada, mruma@york.ca*

We present a nonlinear model within the host of HIV infection that captures the interactions between target $CD4^+$ T cells, helper T cells, infected cells, and free virus particles. The important feature of the model is the addition of a virus loss mechanism during infection, which accounts for immune-mediated viral clearance and distinguishes it from classical models.

The purpose of this study is to investigate how the immune response and the dynamics of viral loss influence infection persistence and control. We derive the disease-free equilibrium and compute the basic reproduction number R_0, which characterizes the threshold for the establishment of infection. Stability analysis shows that disease-free equilibrium is locally asymptotically stable when $R_0 < 1$.

To better understand global dynamics, we perform a bifurcation analysis with respect to key immune related parameters. The results reveal that the system can exhibit both forward and backward bifurcation, indicating the presence of multiple stable equilibria when $R_0 < 1$. This implies that lowering R_0 below one may not be enough to eradicate the infection.

Numerical simulations are used to illustrate how immune activation and enhanced clearance of infected cells influence viral load dynamics and long-term outcomes. Specifically, parameters that regulate immunological destruction and viral loss substantially influence the presence of bistability and the magnitude of the basin of attraction of equilibria.

These findings highlight the essential role of immune response mechanisms in influencing within-host infection dynamics and offer insights into circumstances that may allow for viral persistence despite sub-threshold reproduction numbers. The model contributes to a better understanding of treatment and control strategies that target viral clearance and immune enhancement.

References

[1] X. Xie, J. Zou, and Y. Wang, *Backward bifurcation in within-host HIV models*, Journal of Mathematical Biology, **82**, 1-25 (2021).
[2] S.M. Ciupe and R.J. Heffernan, *In-host modeling*, Infectious Disease Modelling, **2**, 2, pp. 188-202 (2017).
[3] M.A. Nowak and R.M. May, *Virus dynamics: Mathematical principles of immunology and virology*, Oxford University Press (2000).
[4] A.S. Perelson and P.W. Nelson, *Mathematical analysis of HIV-1 dynamics in vivo*, SIAM Review, **41**, 1, pp. 3-44 (1999).

The VII International AMMCS
Interdisciplinary Conference
Waterloo, Ontario, Canada

Comparative Counterfactual Analysis of COVID-19 Policies and Vaccination

M. Z. Tuffaha[1], J. Heffernan[2], J. Li[3]

[1] *York University, Toronto, Canada, mtuffaha@yorku.ca*
[2] *York University, Toronto, Canada, jmheffer@yorku.ca*
[3] *California State University Northridge, Los Angeles, California, USA jing.li@csun.edu*

Understanding how public health decisions shape epidemic outcomes is essential for future outbreak preparedness. In this study, we develop and apply an age-structured model of infection and immunity to investigate how different combinations of non-pharmaceutical measures and vaccination pathways influence COVID-19 dynamics across several regions. Using jurisdiction-specific calibration to observed epidemiological data, we construct hypothetical scenarios that modify intervention timing, policy intensity, primary vaccine rollout, and booster administration. The analysis reveals that epidemic severity is strongly shaped by the interplay between existing immunity levels and behavioral response to public health measures. In particular, non-school interventions have the biggest impact in reducing infections. Additionally, booster delivery has a pronounced effect on reducing hospitalizations and other severe outcomes, even when uptake is not universal. By enabling harmonized comparison across regions, this modelling approach provides a practical tool for evaluating alternative response strategies and informing future pandemic policy.

Beyond Non-Linear Least Squares: Enhancing Epidemiological Inference with Chi-Square Fitting and Bayesian Informed Generalized Profiling

V. Tyuryaev[1], J. Heffernan[1], N. Jankowski[1]

[1] *York University, Toronto, Canada, {vadimtyu, jmheffer, hkj}@yorku.ca*

Nonlinear least squares (NLS) is the dominant parameter estimation paradigm in mathematical epidemiology, yet produces systematic forecasting bias when public health interventions render transmission dynamics non-stationary. We benchmark 250 SIR realizations across nine fitting windows, comparing NLS and Chi-Square objectives [3]—motivated by the Poisson variance structure of surveillance count data—each crossed with standard ODE integration and the Generalized Profiling (GP) framework [1, 2], with regularization tuned via Bayesian Optimization [4]. A Hybrid Projection step recovers the terminal transmission rate by substituting B-spline-fitted compartment values into $\dot{I} = \beta SI/N - \gamma I$ and solving for β,

$$\hat{\beta}_{\text{hybrid}} = \frac{\dot{I}_{\text{end}} + \hat{\gamma} I_{\text{end}}}{S_{\text{end}} \cdot (I_{\text{end}}/N)}, \tag{1}$$

where $\dot{I}_{\text{end}}$ is the B-spline derivative of the infectious compartment, S_{end} and I_{end} the fitted compartment values, $\hat{\gamma}$ the estimated recovery rate, and N the population size—all at the terminal observation point—thereby decoupling projections from historically averaged parameters. Chi-Square outperforms NLS under correct specification; GP with Hybrid Projection substantially reduces forecast error under intervention scenarios; and Bayesian Optimization matches exhaustive grid search at a fraction of the cost. No prior study has benchmarked these objectives across heterogeneous windows and policy regimes [5], and while nonparametric transmission rate reconstruction has been studied [6], the boundary-aligned Hybrid Projection constitutes a novel forecasting mechanism within a fully automated, reproducible pipeline.

References

[1] J.O. Ramsay et al., *Parameter estimation for differential equations: a generalized smoothing approach*, J. R. Stat. Soc. B **69**(5), 741–796 (2007).

[2] G. Hooker et al., *Parameterizing state-space models for infectious disease dynamics by generalized profiling*, J. R. Soc. Interface **8**(60), 961–974 (2011).

[3] G. Chowell, *Fitting dynamic models to epidemic outbreaks with quantified uncertainty*, Infect. Dis. Model. **2**(3), 379–398 (2017).

[4] J. Mockus, *Application of Bayesian approach to numerical methods of global and stochastic optimization*, J. Global Optim. **4**(4), 347–365 (1994).

[5] H. Karami et al., *Comparative study of Bayesian and frequentist methods for epidemic forecasting*, Stat. Methods Med. Res., advance online (2025).

[6] A. Smirnova, L. deCamp, G. Chowell, *Forecasting epidemics through nonparametric estimation of time-dependent transmission rates using the SEIR model*, Bull. Math. Biol. **79**(11), 2571–2589 (2017).

Noise-induced transitions in a coupled stochastic behavior-disease system

Qing Yang[1], Yanni Xiao[2], Xiaoe Ruan[3], Chris T. Bauch[4]

[1] *Xi'an Jiaotong University, Xi'an, Shaanxi, PR China, qyang@stu.xjtu.edu.cn*
[2] *Xi'an Jiaotong University, Xi'an, Shaanxi, PR China, yxiao@mail.xjtu.edu.cn*
[3] *Xi'an Jiaotong University, Xi'an, Shaanxi, PR China, wruanxe@mail.xjtu.edu.cn*
[4] *University of Waterloo, Waterloo, Canada, cbauch@uwaterloo.ca*

We develop a coupled stochastic behavior-disease model by incorporating noise to represent uncertainty in risk perception arising from external influences such as media reports and social information. Based on existing frameworks[1, 2], we derive a fully stochastic co-evolution system using the multidimensional Itô formula. We establish the existence and uniqueness of a global positive solution and derive conditions for stochastic asymptotic stability and strong persistence via Lyapunov methods. Numerical results show that the long-term dynamics are governed by protective efficacy. As noise intensity increases, the system undergoes transitions from the endemic equilibrium to either a boundary state or a disease-free state, depending on intervention effectiveness. In addition, increased behavioral sensitivity lowers the critical noise threshold by amplifying small fluctuations in perceived risk. We further introduce the entropy production rate (EPR) to quantify thermodynamic dissipation. Notably, the thermodynamic response precedes the dynamical transition, suggesting that EPR provides an effective signal for noise-induced regime shifts.

$$\begin{cases} dE = [(x+\eta(1-x))\beta(1-E-I)I-\delta E-\mu E]\,dt, \\ dI = [\delta E-\mu I-\gamma I]\,dt, \\ dx = \left[-\frac{(\mu+\gamma)xI}{1-I}+\phi x(1-x)(1-I)(k-I)\right]dt-\sigma xI(1-x)(1-I)\,dB(t). \end{cases} \tag{1}$$

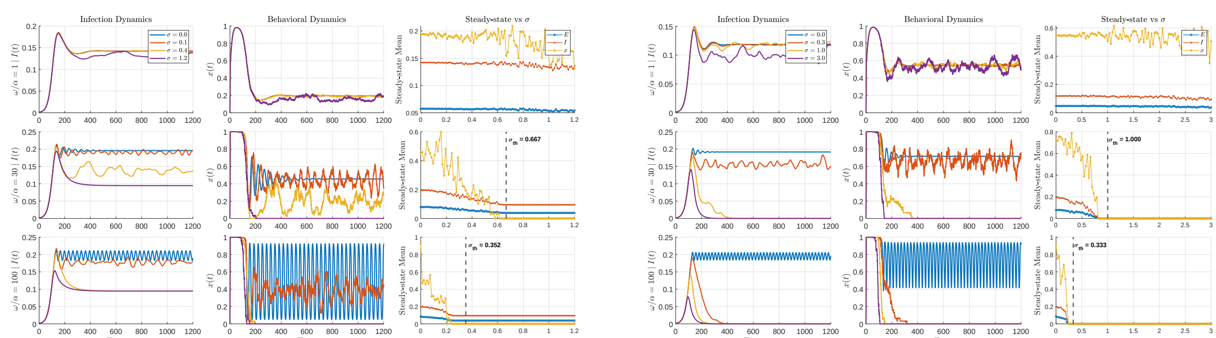

(a) $\eta = 0.7$ (b) $\eta = 0.4$

Figure 1: Comparison of noise-induced transitions under different intervention efficiencies. Rows correspond to $\omega/\alpha = 1, 30, 100$. Columns show time evolution of $I(t)$ and $x(t)$ and steady-state means versus σ. (a) $\eta = 0.7$: transition to the boundary state. (b) $\eta = 0.4$: transition to the disease-free state.

References

[1] T. Li, Y. Xiao and J. Heffernan, *Linking spontaneous behavioral changes to disease transmission dynamics: behavior change includes periodic oscillation*, Bull. Math. Biol. **86**, 6, 73 (2024).

[2] C. T. Bauch, *Imitation dynamics predict vaccinating behaviour*, Proc. R. Soc. B **272**, 1573, pp. 1669–1675 (2005).

Modelling of post-vaccination immunity for influenza with PapMV adjuvant trivalent vaccine

Z. Yu[1], J. Heffernan[2]

[1] *York University, Toronto, Canada, jecyyu@yorku.ca*
[2] *York University, Toronto, Canada, jmheffer@yorku.ca*

Introduction Influenza causes seasonal illness and pandemics, including well-known cases like avian flu (H5N1) [1]. Papaya mosaic virus (PapMV) is a promising, non-pathogenic adjuvant that, while shown to boost immune response to vaccines, haven't had conclusive explanations to its efficacy [2, 3]. This study aims to develop a mathematical model to identify the specific immune pathways affected by PapMV.

Methods We have developed a mathematical model of influenza vaccination that considers PapMV adjuvant as a continuous covariate. We employ mixed-effect modelling in Monolix to fit our mathematical model on trivalent, single-dose vaccination times-series data across 120 days. The model estimates immune system parameters from IFNγ, IL10, and Granzyme B measurements.

Results Sensitivity analysis of the model shows the decay parameter for helper T cells (γ_T) and IFNγ (γ_F) change the long-term directionality of the immune response. Preliminary fitting of the model with PapMV shows positive relations between PapMV dose and γ_T ($\beta_{\gamma_T} = 0.004$) and negative relationships with γ_F ($\beta_{\gamma_F} = -0.006$). Identifiability analysis shows that both decay terms are globally identifiable.

Conclusion These preliminary results establish a foundation for quantifying the biological impact of the PapMV adjuvant. IFNγ could be an important cytokine to indicate long-term immune response.

References

[1] F. Krammer, *The human antibody response to influenza A virus infection and vaccination*. Nat Rev Immunol **19**, 383–397 (2019).
[2] G. Rioux et al, *PapMV nanoparticles improve mucosal immune responses to the trivalent inactivated flu vaccine.* J Nanobiotechnology **12**, 19 (2014).
[3] J. Langley et al,*A Randomized Controlled Study to Evaluate the Safety and Reactogenicity of a Novel rVLP-Based Plant Virus Nanoparticle Adjuvant Combined with Seasonal Trivalent Influenza Vaccine Following Single Immunization in Healthy Adults 18-50 Years of Age*. Vaccines (Basel) **8**, 393 (2020).

Modelling the impact of vaccine failure mode on the evolution of escape variants

C. Yu[1], N. Mideo[2], A.L. Hill[3]

[1] *University of Toronto, Toronto, Canada, cindyy.yu@mail.utoronto.ca*
[2] *University of Toronto, Toronto, Canada, nicole.mideo@utoronto.ca*
[3] *University of Toronto, Toronto, Canada, alison.hill@utoronto.ca*

Vaccine escape variants, such as COVID-19's Omicron strain, are a topic of much concern as they circumvent the efficacy of one of our most effective methods of disease control. Many mathematical models seek to understand how vaccination may affect the emergence of a vaccine escape variant. In many of these studies, vaccinated individuals are still susceptible to disease to some extent, though these studies often neglect the mode of vaccine failure. Vaccine failure mode refers to the way in which a vaccine is not effective, that is, whether every vaccinated individual has imperfect protection (leaky) or some individuals have perfect protection while others have none (all-or-nothing). Past research has shown that vaccine failure mode has profound impacts on the epidemiological outcomes of mathematical models [1, 2, 3, 4]. This study explored the emergence and spread of vaccine escape variants under leaky and all-or-nothing vaccine failure modes. To investigate the impact of failure mode on escape variants, this study used a deterministic Susceptible-Infected-Recovered (SIR) model to track transmission. All-or-nothing vaccines consistently produced fewer cumulative infections than their leaky counterparts in the presence of escape variants, though this difference was smaller than in variant-free scenarios. Escape variants had greater impact under all-or-nothing regimes, especially at intermediate vaccine efficacies. Overall, findings suggest that modelling choices regarding vaccine failure mode should be disclosed and treated as a source of uncertainty in future studies.

References

[1] D.I. Lee, A. Nande, T.L. Anderson, M.Z. Levy and A.L. Hill, *Vaccine Failure Mode Determines Population-Level Impact of Vaccination Campaigns during Epidemics*, J. Roc. Soc. Interface. **22**, 223, 20240689 (2025).

[2] K.E. Langwig, A.R. Wargo, D.R. Jones, J.R. Viss, B.J. Rutan, N.A. Egan, P. Sá-Guimarães, M.S. Kim, G. Kurath, M.G.M. Gomes and M. Lipstich, *Vaccine Effects on Heterogeneity in Susceptibility and Implications for Population Health Management,* mBio. **8**, 6, (2017).

[3] R. Ragonnet, J.M. Trauer, J.T. Denholm, N.L. Geard, M. Hellard, E.S. McBryde, *Vaccination Programs for Endemic Infections: Modelling Real versus Apparent Impacts of Vaccine and Infection Characteristics*, Sci. Rep. **5**, 15468 (2015).

[4] F.M. Magpantay, M.A. Riolo, M.C. de Cellès, A.A. King and P. Rohani, *Epidemiological Consequences of Imperfect Vaccines for Immunizing Infections,* SIAM. J. Appl. Math. **74**, 6, pp. 1810-1830 (2014)

The VII International AMMCS
Interdisciplinary Conference
Waterloo, Ontario, Canada

Scarlet Fever Dynamics in 19th and 20th Century London

Kevin H. Zhao[1], David J. D. Earn[2]

[1] *McMaster University, Hamilton, Canada, zhaok22@mcmaster.ca*
[2] *McMaster University, Hamilton, Canada, earn@math.mcmaster.ca*

Weekly mortality records for London, UK, reveal that epidemics of scarlet fever (SF) occurred regularly from 1842 to 1930, as shown in Figure 1. Peak SF mortality occurred in the autumn until about 1900, after which no seasonal SF peak is evident in mortality records. A dramatic decline in the SF mortality rate began in the late 19th century, falling from approximately 2300 deaths annually in the early 1880s to about 80 deaths annually in the late 1920s. During this period of declining mortality—which preceded the antibiotic era—the typical inter-epidemic interval changed from one year to between four and seven years. We quantify temporal changes in the frequency

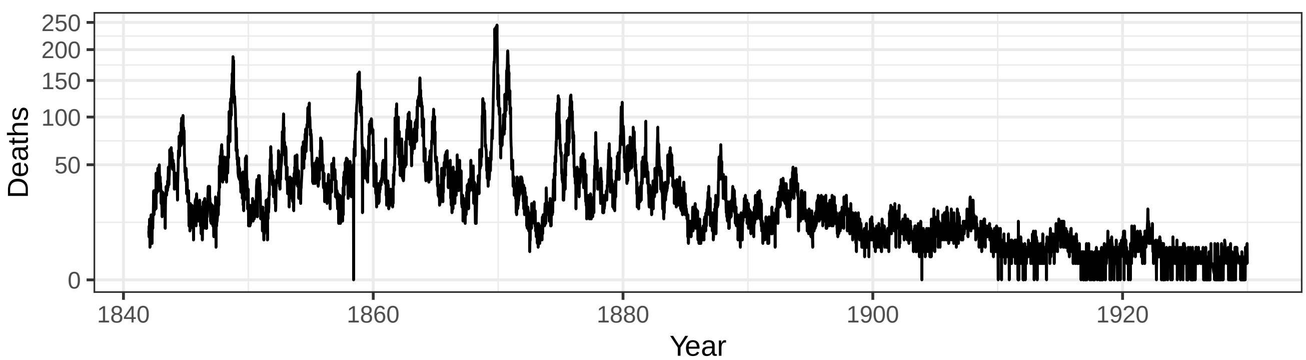

Figure 1: Weekly scarlet fever mortality series in London, with deaths on the square root scale. Data obtained from the Registrar General's Weekly Returns [1].

content of the mortality time series with a wavelet spectrum. Strong spectral peaks are evident from 1830 to 1892, one at period 1 year, and a second at a period in the range 4–7 years. A third spectral peak in the range 5–6 years is clear during 1850–1865, 1865–1870, and 1880–1892. In addition to describing these features of the mortality time series in detail, we attempt to explain why the frequency structure changed over time, using a mechanistic mathematical model of scarlet fever transmission dynamics (an extension of the seasonally forced susceptible-infected-removed (SIR) model). We estimate the values of the model parameters in part from the literature and in part from fitting the model to the observed time series. We use a mechanistic transition analysis [2]—considering both attractors and transients in model solutions—to relate the observed changes in frequency structure to our estimated changes in the effective reproduction number (which could have been induced by birth rate changes and/or pathogen evolution). We find that we can account for two of the three observed spectral peaks, but not the third. After 1899, the level of noise in the mortality data preclude reliable estimation of the temporally varying transmission rate, which is essential for our transition analyses.

References

[1] M. Cullen, *The Making of the Civil Registration Act of 1836*, J. Eccles. Hist., **25**, pp. 39-59 (1974).
[2] K. Hempel, D. J. D. Earn, *A Century of Transitions in New York City's Measles Dynamics*, J. Roy. Soc. Interface, **12**(106), 20150024 (2015).

Molecular Dynamics Investigation of Thermophysical and Viscoelastic Properties in Two-Stage Thermosets

Pratik Bipinchandra Laxmi Bhanuse[1], Colin Denniston[1]

[1] *Department of Physics and Astronomy, University of Western Ontario, London, Ontario, Canada {pbhanuse, cdennist}@uwo.ca*

Unsaturated polyester polyurethane hybrid (UPPH) thermosets exhibit complex curing behaviour arising from coupled urethane polyaddition and radical polymerisation reactions, resulting in heterogeneous cross-linked polymer structures with evolving thermomechanical properties. In this work, we investigate the curing dynamics and emergent thermophysical behaviour of two-stage thermoset systems using atomistic molecular dynamics simulations implemented in LAMMPS [1]. The curing process is modelled using probabilistic bond-formation algorithms based on distance criteria and Arrhenius-type reaction probabilities, allowing dynamic cross-link formation without intermediate minimisation steps.

Building upon previous molecular simulations of hybrid thermosets [2], we study the evolution of material properties during curing, including density, specific heat capacity, thermal conductivity, and viscoelastic response. In particular, we extend the computational framework through the incorporation of non-affine lattice dynamics (NALD) theory to compute frequency-dependent viscoelastic properties directly from atomistic configurations [3]. The non-affine formalism accounts for local structural disorder and non-centrosymmetric force balance, enabling prediction of storage modulus, loss modulus, and viscosity in disordered polymer systems.

The proposed methodology combines reactive molecular dynamics simulations with non-affine viscoelastic theory to provide a computational framework for studying curing-induced evolution of thermophysical and rheological properties in thermoset polymers. Preliminary results demonstrate strong sensitivity of thermal and viscoelastic behaviour to curing progression and cross-link formation. The framework provides a pathway toward predictive modelling of processing–structure–property relationships in advanced thermoset materials.

References

[1] S. Plimpton, *Fast Parallel Algorithms for Short-Range Molecular Dynamics*, Journal of Computational Physics, 117 (1995), pp. 1–19.

[2] F. K. Schwab and C. Denniston, *Reaction and Characterisation of a Two-Stage Thermoset Using Molecular Dynamics*, Polymer Chemistry, 10 (2019), pp. 4413–4427.

[3] A. Zaccone, A. M. Puosi, and M. Pica Ciamarra, *Viscosity of Polymer Melts Using Non-Affine Theory*, Journal of Chemical Physics, 162 (2025), 244504.

Familial Mutation-Aware Modelling of Amyloid-β Propagation in Alzheimer's Disease

Mohammad Alamgir Chowdhury[1], Hina Shaheen[2]

[1] *Department of Statistics, University of the Manitoba, Canada, chowdh62@myumanitoba.ca*
[2] *Department of Statistics, Faculty of Science, University of Manitoba, Canada, hina.shaheen@umanitoba.ca*

Alzheimer's disease (AD) constitutes about two-thirds of the total dementias in the world. AD can be both familial and non-familial [1]. Studies have established that familial mutations for AD are possible to be detected as early as a person is aged between 30 to 40, though the timing varies [2]. Even though the mutations are very rare, they are the cause of all familial AD. However, symptoms typically can be found around age 65, most often between 40 and 60. To mechanistically link molecular mutation effects to brain scale pathology, we developed a mutation-aware Smoluchowski aggregationâfragmentation-diffusion framework integrating mutation-specific nucleation propensities, network diffusion on the Budapest Reference Connectome, and stochastic biochemical fluctuations. Mutation-specific nucleation rates were derived from MoCHI-predicted free-energy barriers ($\Delta\Delta G^{+}_{+}$) and scaled to parameterize mutant kinetics [3]. Deterministic simulations reproduced the classic sigmoidal amyloid-β (Aβ) trajectories, lag, growth, and plateau while capturing mutation-dependent accelerations in oligomer buildup. Inclusion of diffusion transformed local aggregation into realistic brain-wide propagation patterns, consistent with PET and DIAN observations of early amyloid positivity $15-25$ years before symptom onset. The stochastic extension revealed noise-driven variability in early oligomer bursts, offering a plausible explanation for inter-individual heterogeneity in disease onset. Parameter sensitivity analysis identified clearance (δ) and fragmentation (k_{frag}) as key modulators of temporal dynamics. Using approximate Bayesian computation with ADNI biomarker data, we further calibrated posterior parameter distributions linking model outputs to CSF $A\beta$42, TAU, and PTAU. Our work is novel because it connects molecular, network, and clinical levels of AD within a single quantitative framework. We combine mutation-level nucleation data from the MoCHI model, which shows how amino acid changes alter the tendency of Aβ to start aggregating, with large-scale brain network diffusion using the Budapest Reference Connectome and with observed biomarker trends from ADNI. This integrated model explains how specific familial mutations, such as E22G, D23N, or A2V, lead to different speeds and patterns of toxic protein buildup across the brain. Unlike earlier studies that analyzed either molecular kinetics or network spread separately, our approach links them mechanistically through parameters like nucleation rate, diffusion, clearance, and stochastic noise. Together, these elements provide a unified and interpretable view of how small molecular differences can drive large-scale brain changes and clinical progression in AD, which constitutes the principal novelty framework on this study.

References

[1] H. Shaheen, S. Pal and R. Melnik, *Astrocytic clearance and fragmentation of toxic proteins in Alzheimerâs disease on large-scale brain networks*, Physica D: Nonlinear Phenomena **454**, p. 133839 (2023).

[2] A. Arutyunyan et al., *Massively parallel genetic perturbation suggests the energetic structure of an amyloid transition state*, Science Advances **11**(24), p.eadv1422 (2025).

[3] Y. Ding, L. Cai and Y. Kang, *Moment dynamics of oligomer formation in protein amyloid aggregation with secondary nucleation*, Advances in Continuous and Discrete Models **2024**(1), p. 25 (2024).

The VII International AMMCS
Interdisciplinary Conference
Waterloo, Ontario, Canada
28/05/2026

The Influence of Crowders on a Nanopore Fluid Flow Driven Polymer

C. Denniston[1], K. Grosvenor[2]

[1] *Western University, London, Canada, cdennist@uwo.ca*
[2] *Western University, London, Canada, kgrosven@uwo.ca*

There is considerable interest in the flow of multiple polymers in a fluid encountering a wall penetrated by a nanopore. For an efficient and inexpensive analysis of polymers, sensors could be attached along the nanopore channel; however, the actual viability is dependent on a well-developed understanding of the state of the polymer entering the nanopore [1, 2]. For example, if a polymer entered while folded over itself (hairpin), a sensor would gain invalid data across the section that contains two instances of the polymer. The success of scanning a polymer is also influenced by the time taken to cross through the nanopore (translocation time) - if it crossed too quickly, a sensor would not fully register the information before the next monomer entered the scanning area. A potential theoretical solution to these concerns was suggested using results from a simulated application of an opposing electric field, as it slowed the translocation time and decreased the likelihood of a hairpin forming [2].

Various elements of the polymer crowded by monomers have been explored, both in simulation and in theory; finding polymer length dependence, electric field influences, and monomer activity, density and size impacts on the success of translocation [3, 4, 5]. To begin exploring these predictions in an environment consisting of multiple polymers, it is necessary to start with a good base model that can be extended into a multiple polymer system. Thus, the chosen three-dimensional simulation was selected as its initial results were verified experimentally and its origin was in work completed by the research group which will allow ease of manipulation [1, 2, 6].

The base model will be extended by adding a varying volume of trimers, the simplest non-trivial polymer (a polymer with three monomers), into the initial box with the longer polymer. The simulation will then be run for different thermal noise random number generator seeds to mimic different starting conditions. Data will be collected about the motion, such as the amount of motion towards / away from the nanopore for that time step or an estimation of the trimers rate of interaction with the long polymer, as the long polymer approaches the nanopore to build a foundation. That foundation will be used to understand the results from the long polymer's translocation through the nanopore such as the rate of nanopore entry, the hairpin formation probability, or the rate of nanopore translocation. As well, from the foundation, the probability density function (PDF) of the long polymer's radial motion with respect to the nanopore will be determined allowing theoretical models of the potential of the trimers interaction with the long polymer to be constructed from the Smoluchowski differential equation relating the potential energy impacting an object to the PDF of its motion.

References

[1] Afrasiabian, Navid and Denniston, Colin, *The journey of a single polymer chain to a nanopore*, Soft Matter. **16**, 39, pp. 9101-9112 (2020).

[2] Afrasiabian, Navid and Wei, Matthew and Denniston, Colin, *Enhanced Pulley Effect for Translocation: The Interplay of Electrostatic and Hydrodynamic Forces*, Biomacromolecules. **24**, 9, pp. 4103-4112 (2023).

[3] Gopinathan, Ajay and Kim, Yong Woon, *Polymer Translocation in Crowded Environments*, Phys. Rev. Lett.. **99**, 22, 228106 pp. 1-4 (2007).

[4] Tan, Fei and Chen, Ying and Zhao, Nanrong, *Effects of active crowder size and activity-crowding coupling on polymer translocation*, Soft Matter. **17**, 7, pp. 1940-1954 (2021).

[5] Khalilian, Hamidreza and Sarabadani, Jalal and Ala-Nissila, Tapio, *Polymer translocation in an environment of active rods*, Phys. Rev. Res.. **5**, 2, 023107 pp. 1-10 (2023).

[6] Chen, Shulan and He, Wen and Li, Jun and Xu, Derong and Zhao, Rui and Zhu, Libo and Wu, Hongwen and Xu, Fei, *Pulley Effect in the Capture of DNA Translocation through Solid-State Nanopores*, Langmuir. **40**, 11, pp. 5799-5808 (2024).

The VII International AMMCS Interdisciplinary Conference
Waterloo, Ontario, Canada

Patient-Specific Multiphysics Modeling of Microwave Ablation in Breast Cancer: Effects of Tumor Geometry and Applicator Placement

M. Ellsworth-Reid[1], A. Chapman[2], W. Whelan[3], R. Melnik[4], S. Singh[5]

[1] *Faculty of Sustainable Design Engineering, University of Prince Edward Island, Charlottetown, Canada, mellsworth-reid@upei.ca*
[2] *Faculty of Sustainable Design Engineering, University of Prince Edward Island, Charlottetown, Canada, anchapman14546@upei.ca*
[3] *Department of Physics, University of Prince Edward Island, Charlottetown, Canada, wwhelan@upei.ca*
[4] *MS2Discovery Interdisciplinary Research Institute, Wilfrid Laurier University, Waterloo, Canada, rmelnik@wlu.ca*
[5] *Faculty of Sustainable Design Engineering, University of Prince Edward Island, Charlottetown, Canada, sunsingh@upei.ca*

Breast cancer remains the most frequently diagnosed cancer among women worldwide. In Canada, approximately 1 in 8 women are expected to develop breast cancer during their lifetime, and 1 in 36 will die from the disease [1]. Globally, the burden is projected to increase substantially, with incidence and mortality rates rising by approximately 38% and 68%, respectively, by 2050 [2]. Although surgical resection continues to be the gold standard for breast tumor removal, its applicability is often constrained by factors such as procedural morbidity, tumor accessibility, and proximity to critical vasculature. Consequently, alternative treatment modalities such as chemotherapy, radiation therapy, and thermal ablation are being increasingly explored to reduce hospital stays, minimize procedural invasiveness, and enhance cosmetic outcomes, with significant implications for patients' social, economic, and emotional well-being. Among minimally invasive thermal therapies, microwave ablation (MWA) has gained significant attention due to its ability to achieve highly localized heating, rapid energy deposition, and improved preservation of surrounding healthy tissue. However, existing MWA treatment protocols rely heavily on device-specific ablation charts derived from homogeneous ex vivo tissues and assume idealized (spherical or ellipsoidal) lesion formation [3]. Moreover, in clinical practice, particularly in breast tissue, tumor heterogeneity, irregular geometry, and practical constraints on applicator placement can lead to significant deviations from these idealized conditions, limiting their accuracy and generalizability to patient-specific treatment planning.

In this study, we investigate the impact of applicator placement within irregular, patient-derived breast tumor geometries using a coupled electromagnetic and bioheat transfer modeling framework. Thermal damage is quantified using the Arrhenius model, incorporating temperature-dependent tissue properties and damage-dependent blood perfusion rates to better capture physiological response during MWA ablation [4]. The results are compared against conventional spherical tumor assumptions to evaluate deviations in predicted thermal lesion formation. This work highlights the critical role of tissue heterogeneity, tumor geometry, and applicator positioning on MWA treatment outcomes. The findings support the need for more realistic, patient-specific modeling approaches and provide insights that may help refine applicator placement protocols, ultimately improving the precision and clinical effectiveness of MWA therapy in breast cancer treatment.

References

[1] Breast Cancer Statistics, Government of Canada: https://www.canada.ca/en/public-health/services/chronic-diseases/cancer/breast-cancer.html
[2] J. Kim, et al., *Global patterns and trends in breast cancer incidence and mortality across 185 countries*. Nature Medicine, 31, 4, pp. 1154-1162 (2025).
[3] A. Pfannenstiel, et al., *Shaping the future of microwave tumor ablation: a new direction in precision and control of device performance*, International Journal of Hyperthermia, 39, 1, pp. 664-674 (2022).
[4] S. Singh and R. Melnik, *Thermal ablation of biological tissues in disease treatment: A review of computational models and future directions*, Electromagnetic Biology and Medicine, 39, 2, pp. 49-88 (2020).

Designing Solar-Responsive Neighborhoods: Linking Neighborhood Morphology, Zoning, and Energy Performance

K.S. Gill, P. Singh, K.S. Grewal

[1] *Faculty of Sustainable Design Engineering (FSDE), University of Prince Edward Island, 550 University Ave, Charlottetown, PE C1A 4P3*

This study investigates the relationship between urban morphology and solar energy performance by integrating high-fidelity 3D reconstruction with large-scale urban simulation. The primary objective is to quantify how zoning-driven spatial configurations influence building-level and neighborhood-scale solar potential in Prince Edward Island (PE), Canada. The methodology employs a comprehensive library of building archetypes generated through a 3D Gaussian Splatting (3DGS) pipeline, which preserves detailed architectural characteristics such as roof geometry, façade articulation, and volumetric complexity. The archetype set includes a wide range of typologies, such as single-detached houses, semi-detached dwellings, townhouses, low-rise apartment buildings, schools, commercial retail units, restaurants, and supermarkets. These archetypes are systematically distributed across neighborhood samples extracted from municipal zoning maps, capturing diverse spatial arrangements representative of real urban conditions.

A parametric workflow converts 3DGS-derived radiance fields into watertight polysurface models suitable for physics-based simulation. These geometries are integrated with terrain meshes using a custom Rhinoceros–Grasshopper pipeline to ensure accurate topographic alignment and realistic boundary conditions. Solar performance is evaluated using EnergyPlus simulations, and three normalized indices are introduced: Heating Solar Index (HSI), Cooling Solar Index (CSI), and Active Solar Index (ASI), capturing internal heat gains, seasonal energy demand, cooling loads, and photovoltaic generation potential across building envelopes.

Building upon this simulation dataset, machine learning models are trained using the parametric neighborhood configurations as input features and the computed solar indices as target outputs. Morphological variables such as geometric characteristics, window-to-wall ratios, building types, orientation, etc., are used as predictors to learn nonlinear relationships between urban form and solar performance. Once trained, the models enable rapid prediction of solar energy potential across unseen neighborhood scenarios without requiring full EnergyPlus simulations.

Results demonstrate that zoning-driven variations in building orientation, density, and spacing significantly influence solar access and mutual shading. High-resolution 3DGS geometries improve prediction accuracy by capturing detailed roof and façade features. The study also reveals typology-dependent differences in solar performance, particularly between low-rise residential and large-scale commercial or institutional buildings.

The significance of this work lies in its scalable, data-driven framework that integrates simulation and machine learning. By enabling fast and reliable prediction of solar performance across diverse urban forms, the study supports evidence-based zoning decisions and climate-responsive design strategies in cold-climate regions. Further, the solar analysis framework supports net-zero energy goals by optimizing urban form to maximize passive solar gains and on-site photovoltaic generation across neighborhood scales.

Keywords: Neighborhood-Scale Analysis; Passive Solar Design; Photovoltaic Potential; Zoning-Based Analysis; Machine Learning; Climate-Responsive Design

References

[1] Z. Cai, J. Yang, T. Wang, H. Huang, and Y. Guo, 3D reconstruction of buildings based on 3D Gaussian splatting, *Int. Arch. Photogramm. Remote Sens. Spatial Inf. Sci.* 48, pp. 37–43 (2024).

[2] K.S. Grewal, C. Hachem-Vermette, and S. Yadav, Decision-making method to prioritize and implement solar strategies on neighborhood level, *Energy Reports*. 12, pp. 2062–2076 (2024).

A New Framework for Heterogeneity Measure in Numerical Health Data Using Heterogeneity Average Index

Lu Huang[1], Rosa Fallahpour[1], Pascal Tyrrell[1,2,3]

[1] *Department of Statistical Sciences, University of Toronto, Toronto, ON, M5S 1A1, Canada*
[2] *Department of Medical Imaging, University of Toronto, 263 McCaul Street, Toronto, M5T 1W7, ON, Canada,*
[3] *Institute of Medical Science, University of Toronto, Toronto, ON, Canada.*

Health datasets are inherently heterogeneous, with variability arising from complex interactions among demographic, behavioral, and clinical variables. Quantifying such multivariate heterogeneity is essential for understanding data complexity and its implications for machine learning performance. In this work, we adapt the HeTerogeneity Average (HTA) [1], originally developed for spatial data, to numerical health data.

The proposed approach defines regions in covariate space using Age and BMI, while heterogeneity within each region is quantified using joint trait combinations constructed from categorical variables such as Gender, Ethnicity, Education Level, and Smoking status. Local heterogeneity is measured using a normalized entropy-based index, the HeTerogeneity Index (HTI), defined as

$$\mathrm{HTI} = -\sum_{c=1}^{C} p_c \log_C(p_c), \tag{1}$$

where p_c denotes the proportion of observations belonging to trait combination c within a region.

The global heterogeneity score is computed as

$$\mathrm{HTA} = \sum_{r} \frac{n_r}{n} \mathrm{HTI}_r, \tag{2}$$

where n_r is the number of observations in region r and n is the total sample size.

The framework is evaluated on an Alzheimer's disease cohort and compared against a pseudo-homogeneous dataset to assess its ability to distinguish different levels of heterogeneity. Results show that the categorical trait-based numerical HTA captures meaningful within-region diversity and reflects expected differences between heterogeneous and homogeneous settings. A comparison with the alpha Simpson diversity index reveals closely aligned trends, suggesting that HTA primarily reflects within-region mixture diversity.

References

[1] R. Fallahpour, L. Sun, X. Shi, J. Stafford, P.N. Tyrrell, *An improved statistical framework for the HeTerogeneity Average (HTA) Index*, Spatial Statistics, 100985 (74) (2026).

Efficient Estimation of Second-Order Sensitivities in Stiff Stochastic Discrete Biochemical Networks

F. Jabeen[1], M.Suresh[2], S. Ilie [3]

Toronto Metropolitan University, Toronto, Canada,
[1]*fauzia.jabeen@torontomu.ca*
[3]*silvana@torontomu.ca*

In many biochemical networks, low molecular copy numbers and intrinsic noise make deterministic models inadequate, motivating the use of the Chemical Master Equation, a stochastic discrete model of well-stirred systems. We develop efficient methods for estimating second-order parameter sensitivities in stiff stochastic biochemical networks governed by the Chemical Master Equation, where multiscale reaction dynamics pose significant computational challenges. Our approach combines implicit simulation strategies and finite-difference techniques to construct accurate and efficient estimations of Hessian information. Numerical experiments on realistic networks demonstrate the advantages of the proposed method over existing approaches for still systems. This research was conducted in collaboration with Mareson Suresh and Silvana Ilie.

References

[1] Gillespie, D.T., *Exact Stochastic Simulation of Coupled Chemical Reactions*, J. Chem. Phys. , **81**, pp. 2340-2361 (1977).

[2] Gillespie, D.T., *Approximate Accelerated Stochastic Simulation of Chemically Reacting Systems*, J. Chem. Phys. , **115**, pp. 1716-1733 (2001).

[3] Varma, A., Morbidelli, M. and Wu, H. , *Parametric Sensitivity in Chemical Systems*, Cambridge University Press, Cambridge (1999).

[4] M. Morshed, B. Ingalls and S. Ilie, *An efficient finite-difference strategy for sensitivity analysis ofstochastic models of biochemical systems*, Bio. Systems, **151**, pp. 43-52 (2017).

[5] D.F. Anderson, *An Efficient Finite Difference Method for Parameter Sensitivities of Continuous Time Markov Chains*, SIAM. J.Numer. Anal. **50**, 5, pp. 2237-2258 (2012).

Recent Advances in Heat and Entropy Transfer in Multiphase Flows

G. F. Naterer [1]

[1] *University of Prince Edward Island, Charlottetown, Canada, gfnaterer@upei.ca*

Driven by an increasing need to improve energy efficiency and reduce emissions of greenhouse gases, researchers are striving to develop a better understanding of thermal engineering systems. This abstract provides a review of recent numerical and experimental studies of heat transfer in multiphase flows with droplets and particles. Recent advances are presented for convective heat transfer in icing of structures (aircraft, wind turbines), chemically reacting flows (applied to hydrogen production), two-phase flows (heat exchangers) and entropy-based design of thermal systems.

The 3rd Edition of the author's textbook, *Advanced Heat Transfer* [1], was published recently in 2022, with a 4th Edition scheduled for late 2026. It includes four chapters devoted to various modes of multiphase heat transfer, including predictive models of atmospheric icing of structures. Following impact by a droplet on a surface, conduction of heat into the substrate, convection, and the release of latent heat contribute to the heat balance on the surface. Impinging droplets on the icing surface lead to droplet spreading, freezing and either rime or glaze ice accretion, depending on environmental conditions. New methods of prediction and mitigation of icing of surfaces are presented in this work.

With respect to multiphase heat transfer with particles, the author has reported new understanding of thermal radiation in chemically reacting flows. Effects of absorption, scattering, chemical reactions, and the agglomeration of particles on participating solid–gas flow was reported for processes involving hydrolysis in a Cu–Cl cycle of hydrogen production. Further new insight into reaction pathways of gas–particle reactions was reported by the author and his team in pyrolysis of biomass and carbonization for hydrochar production.

The author also presents advances in transient responses in two-phase heat exchangers. Unlike traditional steady-state analysis, the method predicts transient responses under time-changing conditions, such as mass flow rate and/or temperature changes. Unlike past transient methods encountering challenges with instability, stiffness and lack of convergence, the current integral formulation provides a reliable alternative and efficient procedure for transient response within the heat exchanger.

Entropy based design is a systematic approach to improve energy system efficiency through the second law of thermodynamics, as detailed in the author's book published in 2008 [2]. Principles of the second law have identified and reduced thermodynamic irreversibilities by minimizing entropy generation in targeted regions of the flow field. Recent advances by the author and his team have applied entropy-based design to aircraft subsystems, hydrocarbon reservoirs, electrochemical ammonia production, unit operations of thermochemical hydrogen production, magnetic field effects on natural convection, and convection of nanofluids.

This design framework enables a novel treatment of numerical stability, error indicators and numerical convergence of numerical simulations based on physical analogies embodied by the second law. Entropy-based design provides a systematic formalism that ensures compliance with the second law by integrating specific entropy criteria into numerical models. For example, the author and his research team have reported entropy based artificial dissipation as a corrective mechanism for numerical stability using an apparent entropy production difference for numerical error characterization. These advances have provided robust alternatives to conventional approaches to nonlinear stability in computational heat and fluid flow.

References

[1] G. F. Naterer, *Advanced Heat Transfer*, 3rd Edition, CRC Press, Boca Raton, FL, 2022.
[2] G. F. Naterer, J. Camberos, *Entropy Based Design and Analysis of Fluids Engineering Systems,* CRC Press, Boca Raton, 2008.

Computational Field Intelligence for Precision Agriculture: AI-Driven Robotic Scouting for Disease Detection and Geospatial Crop Monitoring

Gurjit S. Randhawa[1], Aitazaz A. Farooque[2], Charanpreet Singh[2], Yuvraj S. Gill[1], Jacob Serafin[1]

[1] *University of Guelph, Ontario, Canada, randhawg@uoguelph.ca, gilly@uoguelph.ca, serafinj@uoguelph.ca*
[2] *University of Prince Edward Island, Charlottetown, Canada, afarooque@upei.ca, csingh15126@upei.ca*

Early and reliable crop disease detection is essential for improving yield, reducing unnecessary agrochemical use, and enabling more sustainable agricultural production. This talk presents AgriScout, an AI-powered autonomous field robot designed to convert field imagery into plant-level disease intelligence. The system integrates high-resolution RGB imaging, deep learning, RTK-based geolocation, and real-time mapping to support targeted scouting and precision crop management under real-world field conditions.

The first phase of this work focused on Potato Virus Y (PVY), one of the most damaging viral diseases in potato production. Field trials in Prince Edward Island were used to collect and label images of healthy and symptomatic potato plants across growth stages and environmental conditions. A YOLO-based detection pipeline processed captured images and generated geotagged infestation maps, allowing symptomatic plants to be located with high spatial precision. This work demonstrated the feasibility of robotic disease scouting as a scalable alternative to labour-intensive manual inspection and as a computational platform for data-driven decision-making in crop protection.

The current phase extends the same computational and robotic framework to soybean disease monitoring, with emphasis on white mould and under-canopy imaging. White mould presents a different sensing challenge because early symptoms and disease structures may occur within dense crop canopies, where conventional overhead scouting is limited. To address this, the platform is being refined with under-canopy imaging, improved lighting control, geotagged data collection, disease prediction models, and mapping workflows that can support future targeted fungicide application, mechanical weeding, and integrated pest management. Preliminary deployment has shown that ground-based robotic scouting can collect high-resolution, georeferenced field data and provide a practical foundation for disease prediction and spatial decision support.

By combining artificial intelligence, robotics, geospatial computation, and field-scale validation, this work contributes to the development of computational field intelligence systems for precision agriculture. The broader significance lies in moving plant disease detection from isolated image classification toward deployable, spatially aware robotic systems that can monitor crop health, quantify disease distribution, and guide more precise, sustainable interventions.

Keywords: precision agriculture; agricultural robotics; computer vision; plant disease detection; geospatial mapping; deep learning

References

[1] C. Singh, G.S. Randhawa, A.A. Farooque, Y.S. Gill, A. Fraser, L. Kumar K.M., R. Barrett and K. Al-Mughrabi, AgriScout: AI-powered robot for precise detection of PVY-infected potato plants, Computers and Electronics in Agriculture 238, 110781 (2025). https://doi.org/10.1016/j.compag.2025.110781

[2] T. Hein, PVY meets AI, Potatoes in Canada, May 12, 2026. https://www.potatoesincanada.com/pvy-meets-ai/

[3] G.S. Randhawa, Artificial Intelligence-Driven Robotic Systems for Scouting and Integrated Pest Management in Soybean Farming: Enhancing Crop Yield and Sustainability through Machine Learning and Precision Agriculture, OMAFRA Alliance - Tier I Annual Report UG-T1-2025-102863 (2026).

Generation of Model-Based Virtual Patient Cohorts with Neural Networks

S. Rezvani[1] and K.P. Wilkie[2]

[1] *Toronto Metropolitan University, Toronto, Canada, salim.rezvani@torontomu.ca*
[2] *Toronto Metropolitan University, Toronto, Canada, kpwilkie@torontomu.ca*

Virtual patient generation for in silico clinical trials retools experimental or clinical datasets to inform model parameterizations that can then be leveraged to explore new treatment protocols. Here we propose a new method of virtual patient generation that uses bootstrapping and neural networks to construct a population with the desired level of variability. We explore our framework with the addition of noise and denoising techniques, benchmark it against the standard Markov Chain Monte Carlo method, and apply it to a case-study of oncolytic viral therapy. Our results suggest that the new framework provides a scalable, computationally efficient method for virtual patient generation and the exploration of virtual clinical trials.

A Capital-Gains Tax Threshold for Housing Financialisation: A Bid-Function Analysis

K. Wright[1], D. Robinson[2]

[1] *University of Waterloo, Canada, kirsten.wright@uwaterloo.ca*

[2] *Laurentian University, Canada, drdrrobinson@gmail.com*

Abstract: Housing markets in many advanced economies have shifted from primarily allocating shelter to functioning as financial asset markets. We develop a tractable model that yields a closed-form condition for when investor demand dominates owner-occupier demand.

We model the market as a competition between a financial investor and an owner-occupier, each determining a willingness-to-pay (bid) based on net-present-value considerations. The investor's gross return Φ_{inv} aggregates rental income and expected capital gains. Applying an effective capital-gains tax rate $\tau_{\text{cg}} \in [0, 1]$ gives the investor bid

$$B_{\text{inv}}(\tau_{\text{cg}}) = (1 - \tau_{\text{cg}})\frac{\Phi_{\text{inv}}}{r_{\text{inv}}},$$

where $r_{\text{inv}} > 0$ is the investor's required rate of return. The owner-occupier's bid is given by

$$B_{\text{res}} = \frac{\Phi_{\text{res}}}{r_{\text{res}}},$$

where Φ_{res} denotes the flow value of housing services and $r_{\text{res}} > 0$ is the owner-occupier's discount rate. Unlike the investor bid, B_{res} is independent of τ_{cg}.

Under the condition that investors outbid owner-occupiers when gains are untaxed, the bids intersect at a unique point, defining a boundary in parameter space separating an investor-dominated (financialised) regime from an owner-occupier regime. Equating the bids yields the closed-form threshold

$$\tau^*_{\text{cg}} = 1 - \frac{\Phi_{\text{res}}\, r_{\text{inv}}}{\Phi_{\text{inv}}\, r_{\text{res}}},$$

with $\tau_{\text{cg}} < \tau^*_{\text{cg}}$ corresponding to the financialised regime and $\tau_{\text{cg}} > \tau^*_{\text{cg}}$ to the owner-occupier regime.

Comparative statics characterize how this boundary shifts with underlying parameters. The threshold increases with the investor's return Φ_{inv} and decreases with the owner-occupier's return Φ_{res} and the investor's discount rate r_{inv}. A key asymmetry arises from expected capital gains g, which enters Φ_{inv} directly but contributes less strongly to Φ_{res}. As a result, increases in g shift the boundary, raising τ^*_{cg} and making policy intervention more difficult during periods of rapid price appreciation.

A simple calibration using representative price–rent ratios and discount rates yields $\tau^*_{\text{cg}} \approx 0.28$, suggesting that capital-gains taxation acts as a structural parameter governing market access rather than merely a revenue instrument.

References

[1] K. Knoll, M. Schularick & T. Steger, *Am. Econ. Rev.* **107**(2), 331–353 (2017).

[2] O. Jordà et al., *Q. J. Econ.* **134**(3), 1225–1298 (2019).

[3] R.J. Shiller, *Irrational Exuberance*, 3rd ed., Princeton Univ. Press (2015).

Influence of Anisotropic Blood Perfusion on Magnetic Nanoparticle Migration in Cancer Treatment

M. Singh[1]

[1] *Department of Mechanical Engineering, University of Maryland Baltimore County, Baltimore, Maryland, USA, msingh6@umbc.edu*

Magnetic nanoparticle based thermal therapies [1-3] have emerged as promising approaches for targeted drug delivery, magnetic hyperthermia, and image-guided cancer treatment. The efficacy of these therapies strongly depends on the ability to control and predict nanoparticle transport within tumor tissues under the influence of externally applied magnetic fields. While previous studies have often assumed isotropic tissue perfusion, biological tissues exhibit highly heterogeneous and anisotropic vascular structures that can significantly alter blood flow patterns and the nanoparticle migration.

Anisotropic blood perfusion [4] is a critical characteristic of tumor vasculature that influences tumor growth, treatment response, and temperature distribution. We used the recently modified Pennes bioheat equation with heterogeneous blood perfusion term [4] to compute temperature distribution and associated changes in tumor porosity due to thermal damage induced by magnetic nanoparticles under alternating magnetic fields. Simulation results demonstrate that anisotropic perfusion substantially affects nanoparticle migration pathways, resulting in asymmetric accumulation patterns and localized variations in particle concentration. Increased perfusion anisotropy promotes preferential transport along dominant vascular directions, reducing magnetic nanoparticles deposition efficiency in certain tumor regions while enhancing accumulations in others. Furthermore, the interaction between magnetic forces and anisotropic blood flow creates complex transport dynamics that cannot be accurately predicted using isotropic perfusion assumptions.

References

[1] M. Singh, R. Ma, L. Zhu, *Quantitative evaluation of effects of coupled temperature elevation, thermal damage, and enlarged porosity on nanoparticle migration in tumors during magnetic nanoparticle hyperthermia*, Int. Commun. Heat Mass Transf. **126**, pp. 105393 (2021).

[2] M. Singh, *Incorporating vascular-stasis based blood perfusion to evaluate the thermal signatures of cell-death using modified Arrhenius equation with regeneration of living tissues during nanoparticle-assisted thermal therapy*, Int. Commun. Heat Mass Transf. **135,** pp. 106046 (2022).

[3] M. Singh, *Biological heat and mass transport mechanisms behind nanoparticles migration revealed under microCT image guidance*, Int. J. Therm. Sci. **184**, pp. 107996 (2023).

[4] M. Singh, *Modified Pennes bioheat equation with heterogeneous blood perfusion: A newer perspective*, Int. J. Heat Mass Transf. **218**, pp. 124698 (2024).

Toward Optimized Pulsed Field Ablation: A Coupled Multiphysics Model of Multi-Electrode Catheter

S. Subah[1], R. Gilmour[1], R. Melnik[2], S. Singh[1]

[1] *Faculty of Sustainable Design Engineering, University of Prince Edward Island, Charlottetown, Canada, sunsingh@upei.ca*
[2] *MS2Discovery Interdisciplinary Research Institute, Wilfrid Laurier University, Waterloo, Canada, rmelnik@wlu.ca*

Cardiac arrhythmia is one of the most common heart diseases, affecting millions of people worldwide. It occurs due to irregular heart rhythms caused by disrupted cardiac electrophysiological activity, which increases the risk of stroke, heart failure, and overall mortality. Antiarrhythmic drugs are typically the first-line treatment. However, they fail in many cases, with reported failure rates ranging from 30–60% depending on the drug and patient population [1]. Consequently, catheter ablation has become a well-established treatment for patients with persistent or recurrent arrhythmias. Traditional catheter ablation approaches rely on thermal energy, such as heating or cryogenic cooling, to disrupt the arrhythmic conduction pathway by heating or freezing the diseased tissue. More recently, pulsed field ablation (PFA), a non-thermal technique based on irreversible electroporation, has gained considerable attention for the treatment of atrial and ventricular fibrillation, supported by the growing body of clinical trial data [2-4]. Unlike thermal methods, the non-thermal mechanism of PFA offers enhanced tissue selectivity, enabling precise ablation of targeted myocardial tissue while minimizing damage to adjacent critical structures, including the esophagus, phrenic nerve, and healthy myocardium.

As a relatively new and emerging technology, the efficacy of PFA is influenced by several factors, including electrode type, pulse parameters, and lethal electric field thresholds, which are not fully understood to date. In the present study, a coupled multiphysics computational framework is developed to investigate the performance of multi-electrode catheter systems. The model integrates Maxwell's equations to resolve electric field distributions, the Pennes bioheat equation to capture thermal responses, and the Navier–Stokes equations to account for blood flow dynamics. The study focuses on two types of multi-electrode catheters, linear and circular, and systematically investigates the effects of electrode discharge modes, pulse parameters (interphase delay, pulse width, and waveform type), pulse amplitude, and electrode-tissue contact depth on PFA treatment outcomes [3-4]. The impact of these parameters is evaluated in terms of the irreversible electroporation volume of the target tissue, the maximum tissue temperature, and the peak blood temperature post PFA. The results aim to provide deeper insight into the interplay between device design and treatment parameters in PFA, contributing to the optimization of catheter-based therapies and helping bridge the gap between computational modeling and clinical applications.

References

[1] E. J. Jacobs IV, P. P. Santos, and R. V. Davalos, *Comprehensive characterization of waveform-dependent cardiac tissue electroporation for pulsed field ablation*, Biosensors and Bioelectronics, 289, pp. 117890 (2025).
[2] E. Nabuurs, et al., *Optimizing pulsed field ablation for cardiac arrhythmias integrating Taguchi method, machine learning and genetic algorithms*, Results in Engineering, 29, pp. 108978 (2026).
[3] X. Ji, et al., *Multi-electrode catheter PFA: Computational modeling and in vivo validation of lesion dynamics under energy-dose variants*, Computer Methods and Programs in Biomedicine, 271, pp. 109025 (2025).
[4] X. Ji, H. Zhang, L. Zang, S. Yan, and X. Wu, *The effect of discharge mode on the distribution of myocardial pulsed electric field—A simulation study for pulsed field ablation of atrial fibrillation*, Journal of Cardiovascular Development and Disease, 9, 4, pp. 95 (2022).

Sinc Collocation Methods for Nonlinear PDEs

Muhammad Usman

University of Dayton, Dayton, OH, USA,
musman1@udayton.edu

In this work, we present a numerical investigation of the eventual periodicity of solutions to an initial-boundary value problem for a Korteweg-de Vries (KdV)-type equation. The study aims to verify previously established theoretical results for the problem posed on a bounded domain:

$$\begin{cases} u_t + u_x + uu_x + u_{xxx} = 0, \quad 0 < x < 1, t > 0 \\ u(x,0) = \phi(x), \\ u(0,t) = h(t),\, u(1,t) = 0,\, u_x(1,t) = 0, \end{cases} \tag{1}$$

A numerical scheme combining finite difference discretization in time with sinc collocation in space is employed to approximate the solution and demonstrate its eventual periodic behavior [1]. Furthermore, the results are compared with recent approximations obtained using artificial neural networks [2], highlighting the accuracy and effectiveness of the proposed method.

References

[1] K. Al-Khaled, N. Haynes, W. Schiesser and M. Usman, Eventual periodicity of the forced oscillations for a Korteweg-de Vries type equation on a bounded domain using a sinc training method. *Journal of Computational and Applied Mathematics* Volume 330, 1 March 2018, Pages 417-428

[2] San Desgupta, Ju Shen, Kyle Helfrich, and Muhammad Usman, *Work in Progress*.

Double Dressing, Quasienergy-Resolved Dissipation, and Floquet-Liouville Spectroscopy in Strongly Driven Quantum Systems

K. Akbari and S. Hughes

Department of Physics, Engineering Physics and Astronomy, Queen's University, Kingston ON K7L 3N6, Canada, kamran.akbari@queensu.ca

Strong periodic driving can fundamentally alter the dynamics of quantum systems by inducing transitions beyond those available in static settings [1]. When such driving acts on an already strongly interacting quantum system, two distinct "dressing" mechanisms coexist: interaction-induced dressing arising from internal couplings and drive-induced dressing arising from the external periodic field [2]. Treating these effects simultaneously leads to a regime of *double dressing*, where the relevant physical states are neither the bare states nor the static dressed states, but Floquet quasienergy states of the fully driven and strongly interacting system [2].

In this talk, we present a unified theoretical framework for strongly driven quantum systems that combines Floquet theory [3], generalized master equations [5], and Floquet-Liouville spectral analysis [6]. Starting from ultrastrong-coupling cavity quantum electrodynamics, We show how periodic modulation of the light-matter interaction can Floquet engineer the quantum Rabi model, producing nonperturbative quasienergy structures, higher-order hybridization processes, and the generation of real photons from the quantum vacuum [2]. The periodic drive thus dresses an already dressed light-matter system, creating a hierarchy of nonequilibrium quantum states.

We then extend this concept to open quantum systems by formulating a nonsecular Floquet generalized master equation in which dissipation is spectrally resolved directly in the quasienergy basis. The resulting theory treats internal and external dressing on equal footing and reveals that environmental relaxation proceeds through drive-assisted quasienergy channels rather than static energy transitions. Using Floquet-Liouville spectroscopy, observable resonances can be decomposed into microscopic quasienergy channels, decay pathways, and collective dissipative modes.

Finally, we apply this framework to strongly driven open cavity-QED systems in the ultrastrong-coupling regime. The analysis demonstrates that dissipation is intrinsically quasienergy resolved and that conventional time-independent dissipative descriptions can fail even for weak dissipation and spectrally flat reservoirs. More broadly, the framework provides a systematic route toward quantum-state control, Floquet engineering, reservoir engineering, and the exploration of nonequilibrium quantum phenomena in strongly driven interacting systems.

References

[1] J. H. Shirley, *Solution of the Schrödinger Equation with a Hamiltonian Periodic in Time*, Phys. Rev. **138**, 4B, pp. B979–B987 (1965).

[2] K. Akbari, F. Nori and S. Hughes, *Floquet Engineering the Quantum Rabi Model in the Ultrastrong Coupling Regime*, Phys. Rev. Lett. **134**, 6, pp. 063602 (2025).

[3] M. Grifoni and P. Hänggi, *Driven quantum tunneling*, Phys. Rep. **304**, 5, pp. 229–354 (1998).

[4] S. I. Chu and D. A. Telnov, *Beyond the Floquet theorem: generalized Floquet formalisms and quasienergy methods for atomic and molecular multiphoton processes in intense laser fields*, Phys. Rep. **390**, 1, pp. 1–131 (2004).

[5] W. Salmon *et al.*, *Gauge-independent emission spectra and quantum correlations in the ultrastrong coupling regime of open system cavity-QED*, Nanophotonics **11**, 8, pp. 1573–1590 (2022).

[6] S. I. Chu and D. A. Telnov, *Beyond the Floquet theorem: generalized Floquet formalisms and quasienergy methods for atomic and molecular multiphoton processes in intense laser fields*, Phys. Rep. **390**, 1, pp. 1–131 (2004).

Anisotropic Charge Transport in Phosphorene: Effects of Screening, Impurities, and Dielectric Environment

A. Chalechale[1]

[1] *University of Waterloo, Waterloo, Canada, achalehc@uwaterloo.ca*

Monolayer black phosphorus (phosphorene) is a particularly appealing two-dimensional material since its strongly anisotropic band structure leads to markedly different transport behavior along its principal crystal directions, making it a suitable platform for exploring how microscopic scattering processes, dielectric screening, and device geometry shape transport properties.

We present a brief review of our theoretical studies of charge transport in phosphorene, emphasizing the mathematical modeling of anisotropic mobility in a nanoscale environment. Using an analytical energy loss method, we develop a analytical description of impurity-limited transport in dielectric-encapsulated phosphorene and use it to examine the effects of impurity location, temperature, dielectric environment, impurity correlation, and channel misalignment. Across these regimes, the theory reveals how the mobility tensor and current response emerge from the interplay between intrinsic anisotropy and external dielectric environment.

The results show that nearby charged impurities can amplify transport anisotropy, finite temperature generally suppresses it through enhanced screening, high-κ dielectrics increase mobility while reducing its temperature dependence, and impurity-correlation effects are strongest in the low-temperature regime. The emphasis of the talk will be on the physical interpretation of the model, supported by illustrative figures and an overview of our recent results, rather than on technical derivations. In this way, we highlight how the analytical mathematical approach can efficiently capture complex transport phenomena in anisotropic quantum materials and provide useful insight for the interpretation and design of phosphorene-based nanoelectronic and optoelectronic systems.

The VII International AMMCS
Interdisciplinary Conference
Waterloo, Ontario, Canada
August 2026

A Quantum Field-Theoretic Approach to the Quantization of Electromagnetic Fields in a Superconducting Condensate

A. Dhillon[1], and A. H. Majedi[2]

[1] *University of Waterloo, Canada, a33dhillon@uwaterloo.ca*
[2] *University of Waterloo, Canada, ahmajedi@uwaterloo.ca*

In this work, we develop a field-theoretic framework for superconducting systems in regimes where spatial structure, vacuum fluctuations, and strong light-matter coupling necessitate a description of the fundamental interplay between a condensate and its electromagnetic environment beyond lumped-element approximations.

We model the condensate as a complex scalar field, minimally coupled to a quantized electromagnetic field, treating both as an interacting bipartite quantum system. By constructing the dressed eigenmodes of the interacting Hamiltonian, we show that the resulting spectrum exhibits photon-number-dependent spectral shifts that remain finite in the zero-photon limit due to vacuum fluctuations. This leads to a modified ground state characterized by fluctuation-induced dressing, analogous to renormalization mechanisms in quantum electrodynamics.

We further compute the back-action of the condensate on the quantized electromagnetic field and show that the dressed ground state modifies field correlation functions, resulting in a suppression of electric-field fluctuations within the condensate relative to free space. This effect arises directly from the operator structure of the coupled field theory, yielding behaviour consistent with quantum fields in dielectric media.

These results establish a unified quantum-optical field-theoretical framework for superconducting condensates in quantized electromagnetic environments, providing a formal basis for light-matter hybridization phenomena in superconducting platforms and more broadly in quantum many-body systems and nanoscale quantum devices.

References

[1] A. Dhillon and A. H. Majedi, *Microwave Dressed States and Vacuum Fluctuations in a Superconducting Condensate*, Phys. Scr. **101**, 085902 (2026).

Self-consistent two-scale formulation of the macroscopic electromagnetic boundary conditions in the presence of a polarizable sheet

A. Hansen

University of Waterloo, Canada, ON, amghanse@uwaterloo.ca

Existing polarization-sheet, generalized sheet transition condition, and 2D-material electrodynamics literature widely use infinitesimal-sheet boundary conditions and near universally evaluate the interfacial field using the arithmetic mean of the limiting field values on either side [1-8]. However, this field prescription is most often presented as a choice or justified by notions eliminating singular and discontinuous contributions. As a consequence, the limits of validity of the arithmetic mean as the appropriate interfacial field have not been established further than the generally accepted notion of validity when $k_0 l \ll 1$, where k_0 is the wavenumber and l is the material width.

Taking $k_0 l \ll 1$ as the scale separation condition, we apply a self-consistent two-scale formulation to derive the boundary conditions for a finite-width, generally nonlocal susceptibility kernel, in vacuum. We show that, in general, the arithmetic mean prescription appears naturally as the leading-order interfacial field. The leading-order truncation of the multiscale expansion gives this result an explicit error $O(k_0 l)$. We further show that out-of-plane asymmetry does not induce a change in the field prescription; rather, it renormalizes the effective surface susceptibility through in-plane/out-of-plane coupling terms. For symmetric susceptibility kernels, the coupling terms vanish, yielding the conventional infinitesimal-sheet boundary conditions with the arithmetic mean field prescription to leading order. This multi-scale formulation further opens a convenient path to including finite-size effects through the higher-order components of the expansion.

References

[1] Tassin, P., Koschny, T., Soukoulis, C.M.: Effective material parameter retrieval for thin sheets: Theory and application to graphene, thin silver films, and single-layer metamaterials. Physica B: Condensed Matter 407(20), 4062–4065 (2012)
[2] Cheng, J., Sipe, J., Vermeulen, N., Guo, C.: Nonlinear optics of graphene and other 2d materials in layered structures. Journal of Physics: Photonics 1(1), 015002 (2018)
[3] Majérus, B., Dremetsika, E., Lobet, M., Henrard, L., Kockaert, P.: Electrodynamics of two-dimensional materials: Role of anisotropy. Physical Review B 98(12), 125419 (2018)
[4] Xu, Z., Ferraro, D., Zaltron, A., Galvanetto, N., Martucci, A., Sun, L., Yang, P., Zhang, Y., Wang, Y., Liu, Z., et al.: Optical detection of the susceptibility tensor in two-dimensional crystals. Communications Physics 4(1), 215 (2021)
[5] Dremetsika, E., Kockaert, P.: Enhanced optical kerr effect method for a detailed characterization of the third-order nonlinearity of two-dimensional materials applied to graphene. Physical Review B 96(23), 235422 (2017)
[6] Mansuripur, M.: Radiation pressure and the linear momentum of the electromagnetic field. Optics Express 12(22), 5375–5401 (2004)
[7] Volokitin, A.I., Persson, B.N.J.: Electric field effect in heat transfer in 2d devices. Journal of Physics: Condensed Matter 32(25), 255301 (2020
[8] Kuester, E.F., Mohamed, M.A., Piket-May, M., Holloway, C.L.: Averaged transition conditions for electromagnetic fields at a metafilm. IEEE Transactions on Antennas and Propagation 51(10), 2641–2651 (2003)

Dirac Fermions, Excitons, and Trions in TMDCs and Bilayer Graphene Quantum Dots

M. Korkusinski[1,2], K. Sadecka[3], Y. Saleem[4], D. Miravet[2], P. Hawrylak[2]

[1] *Quantum and Nanotechnologies, National Research Council,Ottawa, Canada Marek.Korkusinski@nrc-cnrc.gc.ca*
[2] *Physics Department, University of Ottawa, Ottawa, Canada,*
[3] *Department of Physics, Wroclaw University of Science and Technology, Wroclaw, Poland*
[4] *Institute for Theoretical Physics and Astrophysics, Julius-Maximilans-Universitat Wurzburg, Germany*

There is currently interest in semiconductor quantum dots (QDs) as building blocks of electronic quantum circuits and nanophotonic devices based on Dirac Fermions in 2D materials, bilayer graphene (BLG) [1-4] and transition metal dichalcogenides (TMDCs). BLG is unique in that it allows for lateral gate confinement of both electrons and holes due to applied electric field opening an energy gap. This gap can be tuned from the terahertz (THz) to far infrared (FIR) range [2, 4]. In this talk we describe electronic and multi-exciton (X, X- and XX) complexes in BLG and TMDC quantum dots (QD). We start with massive Dirac Fermions laterally confined in gated BG quantum dots [2,4,5]. The single particle spectra are computed using atomistic tight-binding approach, followed by the microscopic calculation of Coulomb and dipole matrix elements. This allows us to formulate a Hamiltonian of interacting quasiparticles accounting for the BLG valleys, trigonal warping, and details of the electrostatic potentials on equal footing. The electronic properties are computed using exact diagonalization approach to configuration interaction Hamiltonian. We predict ground and excited states of Dirac Fermions as a function of filling of electronic shells. Next, we use the generalized Bethe-Salpeter equation to predict the emission spectra of strongly interacting X, XX, and X- complexes. We find their energies to be tunable by voltage from the terahertz to FIR range. The conservation of spin, valley, and orbital angular momentum results in an X, XX, and X- fine structure with a band of dark low-energy states, making this system a promising candidate for constructing nanodevices for storage, emission and detection of photons.

In TMDC monolayers we predict a new set of states associated with additional Q valleys and with valley-resolved Landau levels in high magnetic fields. We predict the evolution of the optical absorption spectrum of such a system as a function of the carrier density using exact diagonalization tools, and identify the optical signatures of the exciton, the trion X-, and the exciton interacting with the filled lowest LL of the gated MoS_2 TMDC [8].

References

[1] D. Guclu, P. Potasz, M. Korkusinski, and P. Hawrylak, "Graphene Quantum Dots", Springer-Verlag (2014).
[2] Y. Saleem, K. Sadecka, M. Korkusinski, et al., *Nano Lett.* **23**, 2998 (2023).
[3] D. Miravet, L. Szulakowska, M. Bieniek, et al., Phys. Rev. B 110, 235404 (2024).
[4] M. Albert, Y Saleem, K Sadecka, et al., *Phys. Rev. B 110, 155421 (2024).*
[5] K. Sadecka, Y. Saleem, D. Miravet, et al., *Phys. Rev. B* **109**, 085434 (2024).
[6] J. Klein, A. Hötger, M. Florian, et al., *Phys. Rev. Research 3, L022009 (2021).*
[7] K. Oreszczuk, A. Rodek, M. Goryca, et al., 2D Materials 10, 045019 (2023).
[8] K. Sadecka, M. Korkusinski, L. Szulakowska, and P. Hawrylak, arxiv:2601.11993 (2025).

Classification of metals

Sung-Sik Lee[1,2]

[1] *McMaster University, Hamilton, Canada, slee@mcmaster.ca*
[2] *Perimeter Institute for Theoretical Physics, Waterloo, Canada*

Phases of matter are usually classified by scale-invariant fixed points of the renormalization group flow. In metals, however, the finite scale set by the particle density prevents their low-energy effective theories from flowing to such fixed points. In this talk, I will introduce a generalized notion of fixed points and present a classification of strongly interacting metals that often arise near quantum phase transitions.

References

[1] S. Kukreja, D.M. Willerton, S.-S. Lee, Classification of non-Fermi liquids and universal superconducting fluctuations, arXiv:2601.21047

What Can Quantum Entanglement Tell Us About Quantum Materials ?

Erik S. Sørensen[1]

[1] *McMaster University, Canada, sorensen@mcmaster.ca*

Entanglement is what separates quantum mechanics from classical physics. Aside from its fundamental applications in quantum technologies, it is also increasingly being recognized as a powerful tool for understanding the properties of quantum materials. It can be used to characterize and detect quantum phase transitions and determine entire phase diagrams of quantum many-body systems [1]. Unfortunately, it is computationally very difficult to access and even more difficult to measure in experiments. Many insights into the entanglement structure and so-called entanglement spectrum of quantum materials have been obtained by using the computational approach of Matrix Product States (MPS), known as tensor trains in the mathematics community. This approach has been generalized to higher dimensions through the development of tensor networks, which have been used to study the entanglement structure of two-dimensional quantum materials. In combination with Baxter's corner transfer matrix renormalization group method from mathematical physics, it is now possible to use tensor networks to obtain high-precision numerical characterization of two-dimensional quantum materials directly in the thermodynamic limit, for cases where the sign problem prevents the use of quantum Monte Carlo methods. On the experimental side, recent results have shown that the quantum Fisher information, a generalization of the usual Fisher information used in statistics, can be used to experimentally measure multipartite entanglement in quantum materials, even at finite temperatures [3]. Of particular interest is the multipartite entanglement structure of quantum materials, where recent results indicate that so-called quantum spin liquids, a class of exotic quantum states that exhibit long-range entanglement and fractionalized excitations, have a very intricate multipartite entanglement structure [2]. In this talk I will try to illustrate some of these recent developments, from the fundamental bipartite entanglement structure of quantum materials to the use of the quantum Fisher information to estimate the multipartite entanglement in quantum materials, and finally to the intricate loop-like multipartite entanglement structure of quantum spin liquids.

References

[1] E. S. Sørensen, A. Catuneanu, J. Gordon, H.-Y. Kee, *Heart of Entanglement: Chiral, Nematic, and Incommensurate Phases in the Kitaev-Gamma Ladder in a Field*, PRX **11**, 011013 (2023).

[2] L. Lyu, D. Chandorkar, S. Kapoor, S. Takei, E. S. Sørensen, W. Witczak-Krempa, *Multiparty entanglement in quantum spin liquids*, Nature Communications, to appear (2026).

[3] J. Lambert and E. S. Sørensen, *From classical to quantum information geometry: a guide for physicists*, New Journal of Physics **25**, 08121 (2023).

New frontiers in artificial intelligence for large-eddy simulation of atmospheric turbulence

J. Alam[1]

[1] *Memorial University of Newfoundland, St John's, Canada, alamj@mun.ca*

Large-eddy simulation (LES) is a numerical framework of solving the Navier-Stokes system for turbulent flows at high Reynolds number $\mathscr{R}e$. While LES is uniquely suited for capturing the complex turbulence occurring in marine atmospheric boundary layers and floating offshore wind farms, its computational cost scales as $\mathscr{R}e^{1.8}$ to resolve the necessary range of flow scales. Central to this challenge is ensuring the relative orientation of vorticity vector ($\boldsymbol{\omega}$), the eigenvectors of strain-rate tensor ($\mathscr{S}_{ij}$), and the subgrid-scale stress tensor (τ_{ij}) within the subgrid-scale modelling scheme [1].

This research investigates the integration of Artificial Intelligence (AI) in LES, specifically evaluating whether a data-driven representation of tensorial alignment can accurately preserve the energy cascade across the cutoff length scale [2]. We propose a novel encoder-decoder architecture that integrates a wavelet decomposition framework within a U-Net-based topology [3]. This structure is specifically designed to capture the tensorial alignment of subgrid scale turbulence. We also assess whether AI-based approaches offer enhanced predictive capabilities in simulating subgrid scale turbulence in LES of floating offshore wind farms.

Preliminary numerical experiments for floating offshore wind farms demonstrate that the proposed AI-based LES framework produces different subgrid-scale energy distributions compared with a conventional LES closure. Using the classical LES accuracy index that compares resolved energy (k_{res}) and subgrid-scale energy (k_{sgs}) via the distribution of $k_{\text{sgs}}/(k_{\text{sgs}}+k_{\text{res}})$, we observe that AI-based LES exhibits stronger subgrid-scale activity only in localized regions.

These findings also demonstrate that AI-based LES maintains accuracy even if the grid is coarsened; in contrast, classical LES requires grid refinement to achieve comparable improvement in accuracy. This study highlights the potential for AI-augmented solvers to provide a stable, computationally efficient pathway for the multi-scale modelling of offshore renewable energy systems, significantly reducing the reliance on massive high-performance computing resources.

References

[1] J. Singh and J. Alam, *Characterization of atmospheric and wind farm turbulence*, Computers and Fluids, **289**, pp. 106537, (2025).

[2] A. Beck and D. Flad and C. Munz, *Deep neural networks for data-driven turbulence models*, Journal of Computational Physics, **398**, pp. 609-630, (2019).

[3] A. Marefat and J. Alam and K. Pope, *An adaptive subgrid-scale model using wavelet-assisted encoder-decoder for turbulent flow past a sphere*, Engineering with Computers, **in-press**, (2026).

Progress in Surface Reconstruction from Signed Distance Data

Christopher Batty[1]

[1] *University of Waterloo, Canada, christopher.batty@uwaterloo.ca*

Signed distance functions (SDF) are a powerful implicit surface representation that finds applications ranging from the level set method in applied mathematics to shape modeling in computer graphics to multiview surface reconstruction in computer vision, among others. To describe a shape, a signed distance function returns a value whose magnitude gives the distance from a query point in space to the closest point on the shape's surface and whose sign indicates whether the query point is in the interior (negative) or exterior (positive). The prevalence of SDFs makes recovering from them an explicit (triangle) mesh surface a critical computational task.

In recent work, my collaborators and I have explored how to improve the quality of mesh reconstruction from a set of discrete SDF samples on a uniform grid. Classical techniques, such as the well-known *marching cubes* algorithm, treat the SDF as a generic scalar field and consider only strictly local information in the meshing process, such as the values at eight nodes of each grid cell. Our approach instead accounts for the distance property of the data and exploits useful information contained in grid points further from the surface. Our central geometric insight is that each SDF sample corresponds to a sphere that the (unknown) surface must touch (at least) once, but may not penetrate into. Any valid surface reconstruction from the data must therefore satisfy these conditions for every SDF sample point.

Leveraging this new perspective, we have approached the problem from several directions, which I will discuss. In our initial "shrinkwrap" approach, an initial enclosing mesh is evolved inward under a gradient flow to minimize an energy that measures the degree to which the SDF conditions above are satisfied [1]. This approach is remarkably effective, but struggles to handle objects with complex topology due to the mesh becoming entangled. By instead iteratively optimizing for an oriented point cloud that conforms to the SDF data and performing standard point cloud reconstruction, we overcome this limitation to handle shapes of arbitrary topology [2]. Most recently, to handle SDF possessing distinct sharp features (as is common for shapes in Computer-Aided Design), we have proposed a new approach that combines a classical dual contouring technique with our sphere-based optimization approach [3]. The resulting meshes much more faithfully recover the salient shape features implicit in the SDF data.

References

[1] S. Sellán, Y. Ren, C. Batty, and O. Stein. *Reach for the Spheres: Tangency-aware Surface Reconstruction of SDFs*, ACM SIGGRAPH Asia 2023.

[2] S. Sellán, Y. Ren, C. Batty, and O. Stein. *Reach for the Arcs: Reconstructing Surfaces from SDFs via Tangent Points*, ACM SIGGRAPH (North America) 2024.

[3] X. Carrera, N. Wang, C. Batty, O. Stein, and S. Sellán. *Dual Contouring of Signed Distance Data*, in ACM SIGGRAPH SIGGRAPH (North America) 2026.

The VII International AMMCS
Interdisciplinary Conference
Waterloo, Ontario, Canada

A Stabilized Mixed Finite Element Method Glacier Drainage System Model

N. Betancourt[1], R. Gracie[2]

[1] *University of Waterloo, Waterloo, Canada, knbetanc@uwaterloo.ca*
[2] *University of Waterloo, Waterloo, Canada, rgracie@uwaterloo.ca*

The Glacier Drainage System (GlaDS) models are used widely in subglacial hydrology [1,2]. The flow system is divided into a two-dimensional distributed film (slow system) and a network of one-dimensional channels (fast system), each of which grow and shrink over time with seasonal loading and glacier dynamics. This work presents a new reduced-dimension formulation (xGlaDS) that more realistically models mass exchange mechanism between channels and the film. In addition, the model introducing inertial forces through transient and advective terms based on methodologies from lubrication and hydraulic fracture models [3,4]. The nonlinear and transient governing system of equations (mass and momentum) are solved using a fully coupled stabilized mixed finite element method, in which pressure and flux are independent variables. An advantage of the extended formulation, is that film flux approximations improve significantly from piece-wise constant to quadratic. The convergence and accuracy of xGlaDS is demonstrated. Examples show that the mass exchange mechanism converges to the original GlaDS formulation, under specific conditions, and that inertial effects are important in regions of high flow, such as around channelized regions or injection sources like moulins.

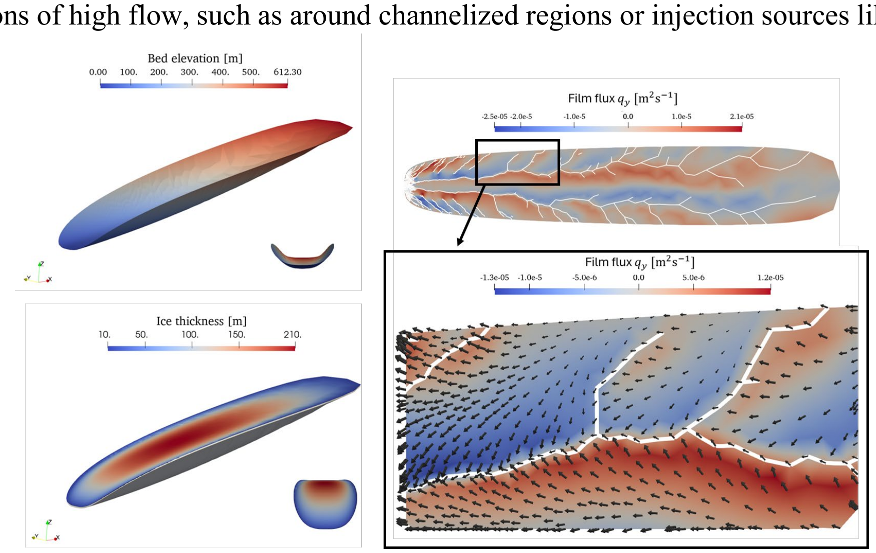

Left: bed elevation and ice thickness. Right: Film flux converging towards channels (white lines).

References

[1] M. A. Werder, I. J. Hewitt, C. G. Schoof, and G. E. Flowers, *Modeling channelized and distributed subglacial drainage in two dimensions*, J. Geophys. Res.: Earth Surface 118, 4, pp. 2140-2158 (2013).
[2] C. Ehrenfeucht, K. Dow, K. McArthur, M. Morlighem, and F. S. McCormack, *Antarctic-wide subglacial hydrology modeling*, Geophys. Res. Lett. 52, 1, e2024GL111386 (2025).
[3] V. N. Constantinescu, *Laminar Viscous Flow*, 1st ed., Mechanical Engineering Series, Springer, New York, NY, USA (1995).
[4] B. Gee and R. Gracie, *Beyond Poiseuille flow: A transient energy-conserving model for flow through fractures of varying aperture*, Adv. Water Resour. 164, 104192 (2022).

Big Data, Small Footprint: Compressing Linear Algebra for the Modern Era

Kazem Cheshmi[1]

[1] *McMaster University, Canada, cheshmi@mcmaster.ca*

Linear algebra is fundamental to numerous applications, including graph analytics, machine learning, and scientific simulation. The ever-increasing scale of data, however, poses significant challenges to sustainability and cost. Data often contains substantial redundancy, frequently introduced for programming convenience, such as when using simple data structures. At the SwiftWare lab, we address these challenges by introducing novel compression techniques designed to reduce the cost of both memory access and computation. These techniques focus on compressing computation patterns to minimize metadata overhead associated with compressed data structures. Critically, these methods are integrated with new automation techniques to alleviate the programmer's burden and facilitate ease of use. This presentation specifically demonstrates how the methods employed in the SwiftWare pipeline enhance the performance of modern machine learning and scientific simulations across a wide range of architectures.

The VII International AMMCS
Interdisciplinary Conference
Waterloo, Ontario, Canada

Exascale Direct Numerical Simulation of Stratified Turbulence

M.M.P. Couchman[1], A. Lefauve[2], M. Gopalakrishnan Meena[3], S.M. de Bruyn Kops[4]

[1] *York University, Toronto, Canada, mmpc@yorku.ca*
[2] *Imperial College London, London, UK, a.lefauve@imperial.ac.uk*
[3] *Oak Ridge National Laboratory, Oak Ridge, USA, gopalakrishm@ornl.gov*
[4] *University of Massachusetts Amherst, Amherst, USA, debk@umass.edu*

Understanding the dynamics of turbulence in the presence of a background density gradient, referred to as stratified turbulence, is a central problem in industrial and environmental fluid dynamics. Stratified turbulence is fundamentally different and more complex than unstratified turbulence due to the presence of a restoring buoyancy force that leads to flow anisotropy, strong spatiotemporal intermittency, and new exchange pathways between kinetic and gravitational potential energies. We here present recent efforts to generate and analyze massive-scale direct numerical simulations (DNS) of stratified turbulence, based on the Boussinesq approximation of the Navier-Stokes equations. Using the Frontier supercomputer (Oak Ridge National Laboratory), we have generated 3D DNS containing over 6 trillion grid points, allowing for the exploration of previously inaccessible regions of parameter space spanned by the buoyancy-Reynolds, Froude, Prandtl, and Richardson numbers. Particular focus is given to recent DNS of stratified turbulence driven by vertical shear, as is relevant to the modelling of estuarine flows where salt water intrusions may contaminate the fresh water supplies of coastal communities. We conclude by discussing the nascent STRATA database [1], a growing public repository containing almost a petabyte of our DNS data and associated analysis tools.

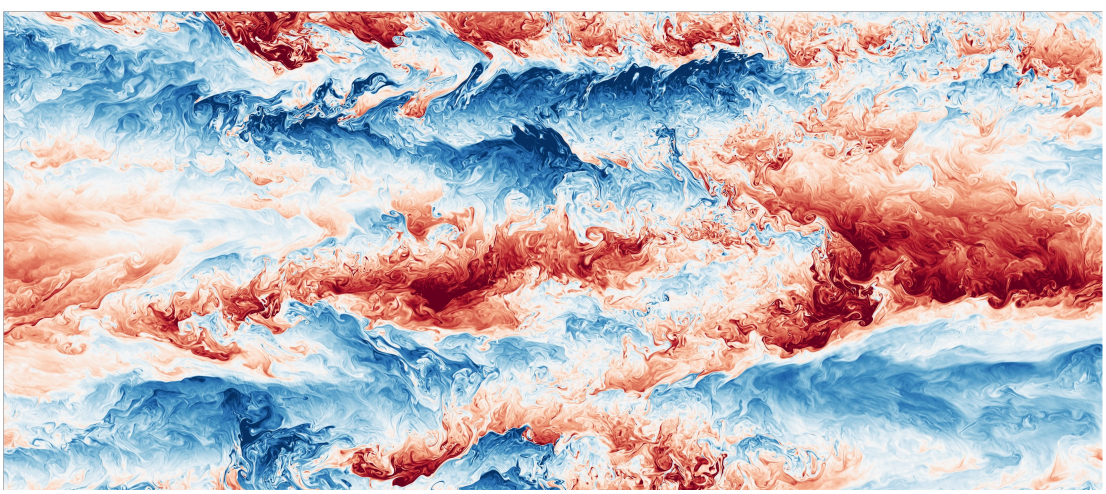

Figure 1: A vertical slice of the turbulent density field within one of our direct numerical simulations (see visualization video [2])

References

[1] *STRATA Stratified Turbulence Database*, `https://stratified-turbulence.github.io/web/`.

[2] M.M.P. Couchman, M. Gopalakrishnan Meena and S.M. de Bruyn Kops, *Stratified Turbulence: A Journey Across Scales*, `https://youtu.be/uRvasupvYDU?si=qDlvdgpHYtauWB-q` (2025).

The VII International AMMCS
Interdisciplinary Conference
Waterloo, Ontario, Canada

A Single-Distribution Higher-Moment Lattice Boltzmann Scheme for Thermal and Complex-Fluid Flows

Brian Duong[1], Colin Denniston[1]

[1] *University of Western Ontario, London, Canada*

The lattice Boltzmann method has become a powerful numerical framework for simulating hydrodynamics in complex fluids, porous media, and other multiscale systems [1]. Its efficiency comes from the locality of the collision-streaming algorithm and the direct parallelization of discrete particle populations. However, standard low-order lattice Boltzmann schemes are primarily designed to recover isothermal Navier-Stokes dynamics [2]. Extending these schemes to thermal flows is nontrivial because the discrete velocity set must reproduce sufficiently high-order moments of the Maxwell-Boltzmann distribution while maintaining lattice symmetry. This limitation is especially relevant for complex fluids, where heat transport can couple to internal degrees of freedom such as concentration, orientation, or order-parameter fields. A compact thermal lattice Boltzmann method is therefore useful not only for heat transport, but also for non-isothermal complex-fluid simulations.

Existing thermal lattice Boltzmann approaches typically introduce either additional distribution functions or enlarged velocity stencils [3, 4, 5]. Multi-distribution methods separate the evolution of momentum and energy, while higher-order velocity sets improve moment isotropy by coupling to further lattice neighbours. Both approaches are effective, but they also increase algorithmic complexity, and computational cost.

Here we introduce a higher-moment lattice Boltzmann discretization that retains a single distribution function and a nearest-neighbour velocity stencil. The method replaces standard point-supported discrete populations with compactly supported bump functions. By retaining internal cumulants of these bump functions, the scheme introduces additional local degrees of freedom without enlarging the velocity set. Previous work showed that retaining the variance is consistent with standard lattice Boltzmann discretizations [6].

In this work, we extend the construction by incorporating an additional skewness degree of freedom. This allows the equilibrium populations to satisfy the higher-order moment constraints required in the Chapman-Enskog recovery of thermal hydrodynamics. We construct the corresponding equilibrium distributions, analyze their moment structure, and show that the resulting scheme recovers the Navier-Stokes-Fourier equations using a single distribution function on a nearest-neighbour lattice. The method therefore provides a compact and local route to non-isothermal complex-fluid simulations in which heat transport, hydrodynamic flow, and internal microstructure evolve simultaneously.

References

[1] S. Chen and G. D. Doolen, *Lattice Boltzmann method for fluid flows*, Annu. Rev. Fluid Mech. **30**, pp. 329–364 (1998).

[2] X. He and L.-S. Luo, *Theory of the lattice Boltzmann method: From the Boltzmann equation to the lattice Boltzmann equation*, Phys. Rev. E **56**, pp. 6811–6817 (1997).

[3] X. He, S. Chen, and G. D. Doolen, *A novel thermal model for the lattice Boltzmann method in incompressible limit*, J. Comput. Phys. **146**, pp. 282–300 (1998).

[4] Q. Li, K. H. Luo, Y. L. He, Y. J. Gao, and W. Q. Tao, *Coupling lattice Boltzmann model for simulation of thermal flows on standard lattices*, Phys. Rev. E **85**, 016710 (2012).

[5] S. Busuioc, V. E. Ambrus, T. Biciusca, and V. Sofonea, *Two-dimensional off-lattice Boltzmann model for van der Waals fluids with variable temperature*, Comput. Math. Appl. **79**, pp. 111–140 (2020)

[6] N. Afrasiabian and C. Denniston, *A novel velocity discretization for lattice Boltzmann method: Application to compressible flow*, Phys. Fluids **37**, 036128 (2025).

The VII International AMMCS
Interdisciplinary Conference
Waterloo, Ontario, Canada

Finite Data Error Bounds for Approximating the Koopman Operator

D. Fassler[1], R. Morris[2], J. Bramburger[3], S. Brugiapaglia[4]

[1] *Concordia University, Montreal, Canada, daniel.fassler@mail.concordia.ca*
[2] *Concordia University, Montreal, Canada, rachel.morris@mail.concordia.ca*
[3] *Concordia University, Montreal, Canada, jason.bramburger@concordia.ca*
[4] *Concordia University, Montreal, Canada, simone.brugiapaglia@concordia.ca*

Nonlinear dynamical systems arise throughout science and engineering. Recent advances in sensing and computation have led to an unprecedented availability of data, placing data-driven methods at the forefront of dynamical systems analysis. The goal of modern data-driven methods is to interpolate data, learn governing equations, forecast beyond observed data, and infer hidden structure. The Koopman operator provides a framework that can achieve all these tasks by lifting nonlinear dynamics to a linear (infinite-dimensional) function space. The operator is defined as $\mathscr{K}^{\tau}\varphi(x) := \mathbb{E}\left[\varphi(x_{t+\tau}) \mid x_t = x\right]$, and describes the evolution of scalar observable functions along trajectories $\{\mathbf{x}_t\}_{t\geq 0}$, shifting the focus from state-space dynamics to the evolution of observables.

Here, we approximate $\mathscr{K}^{\tau}$ using Extended Dynamic Mode Decomposition (EDMD), which computes a finite-dimensional approximation $K^{\tau}_{m,n}$ of $\mathscr{K}^{\tau}$ as a Galerkin projection on a collection of user-specified observables acting as a basis for a finite-dimensional approximation subspace. EDMD converges asymptotically to a finite dimensional projection of the Koopman operator in the limit of infinite data [1]. In practice, however, we only have finite data, and there is a need for error bounds to answer the fundamental question underlying this approach: when do we have enough data to reliably approximate dynamics?

In this work, we provide a unified finite-data perspective on Koopman operator approximation, with applications to system identification, reduced-order modeling, and data-driven forecasting. In this particular, we derive finite-sample error bounds for $K^{\tau}_{m,n}$ (n is our number of samples and m the dictionary size) in both over- and under-sampled regimes. In the over-sampled regime $n > m$, we connect EDMD with least-squares approximation [2, Ch. 5], and prove the well-observed Monte Carlo convergence rate $\mathscr{O}(n^{-1/2})$ under minimal assumptions. We analyze the effects of different sampling measures, dictionaries of observables and in particular the impact of Christoffel sampling in this setting through numerical experiments. Building on recent advances in least-squares approximation [3], we further show that for smooth dynamics, convergence rates faster than any algebraic rate can be achieved under appropriate scaling between sample size and dimension of the approximation subspace. In the under-sampled regime $n < m$, we reformulate EDMD within a compressed sensing framework [4], leading to sparsity-promoting estimators based on LASSO and quadratically constrained basis pursuit. Under suitable sparsity assumptions on the Koopman operator, we establish recovery guarantees for these modified algorithms. These results are proven theoretically and verified numerically.

References

[1] J. J. Bramburger and G. Fantuzzi, *Auxiliary Functions as Koopman Observables: Data-Driven Analysis of Dynamical Systems via Polynomial Optimization*, J. Nonlinear Sci. **34**, 1, p. 8 (2023).
[2] B. Adcock, S. Brugiapaglia, and C. G. Webster, *Sparse Polynomial Approximation of High-Dimensional Functions*, SIAM, Philadelphia (2022).
[3] B. Adcock and S. Brugiapaglia, *Monte Carlo is a good sampling strategy for polynomial approximation in high dimensions*, arXiv preprint arXiv:2208.09045 (2023).
[4] H. Schaeffer, G. Tran, and R. Ward, *Extracting Sparse High-Dimensional Dynamics from Limited Data*, SIAM J. Appl. Math. **78**, 6, pp. 3279–3295 (2018).

Parameter-robust preconditioning for hybridizable discretizations

E. Henríquez[1], J. J. Lee[2], S. Rhebergen[3]

[1] *University of Waterloo, Waterloo, ON, Canada, ehenriquez@uwaterloo.ca*
[2] *Baylor University, Waco, TX, USA, jeonghun_lee@baylor.edu*
[3] *University of Waterloo, Waterloo, ON, Canada, srheberg@uwaterloo.ca*

When solving discretized partial differential equations (PDEs) numerically, it is crucial - especially with an eye toward applications in multiscale/multiphysics problems - to develop solution methods that show consistently good performance independent of the values of problem parameters. The seminal review paper by Mardal and Winther [1] introduced a general framework to develop parameter-robust preconditioners. Since then, parameter-robust preconditioners have been designed for a wide variety of problems.

Meanwhile, static condensation and hybridization techniques are widely employed in many modern finite element methods as a means of reducing the size of the linear systems resulting from the discretization of a PDE. In this talk, we present an example demonstrating that a naively derived preconditioner for the statically condensed system, obtained from a parameter-robust preconditioner for the original discretized problem, does not necessarily inherit parameter robustness. Furthermore, we identify necessary and sufficient conditions under which a parameter-robust preconditioner for the original problem induces a parameter-robust preconditioner for the statically condensed system.

References

[1] Mardal K.-A., Winther R., *Preconditioning discretizations of systems of partial differential equations*, Numer. Linear Algebra Appl. **18**, pp. 1-40 (2011).

Random Feature Bayesian Lasso Takens Model for time series forecasting

Thu Nguyen[1], Lam Ho[1,2]

[1] *Department of Mathematics and Statistics, Dalhousie University, Canada*
[2] *Lam.Ho@dal.ca*

Predicting the future is difficult because we usually only observe the history of a single variable, leaving the rest of the complex system hidden. While traditional models are too rigid and machine learning often lacks reliable uncertainty measures, I introduce the Random Feature Bayesian Lasso Takens model to bridge this gap. By leveraging Takens' Theorem, our method mathematically reconstructs the entire unobserved system using only that one available variable. Integrated into a Bayesian framework, the model captures complex nonlinear patterns while providing a clear "range of certainty" for its predictions. I demonstrate that by combining dynamical systems with modern statistics, we can create forecasting tools that are accurate and transparent, even when we can only monitor one part of a larger system.

Automatic Hexahedral Meshing via Reinforcement Learning for Block Decomposition

S. Holtshousen[1], T. Gargano[2], N. Tomes[2], D.C. Del Rey Fernández[1]

[1] *University of Waterloo, Waterloo, Canada {s2holtshousen,ddelreyfernandez}@uwaterloo.ca*
[2] *Pratt & Whitney Canada, Mississauga, Canada*

High-fidelity numerical simulations of partial differential equations rely critically on the quality of the underlying spatial discretization (mesh). While meshes composed of hexahedral elements are often required in domains such as aerospace and structural engineering due to their superior numerical accuracy and computational efficiency, generating them for complex geometries remains a significant challenge. Currently, this process requires extensive manual intervention to decompose computer-aided design (CAD) models into sub-domains (blocks) that support the automatic generation of conformal hexahedral meshes. Block decomposition can consume up to months of engineering time, severely limiting rapid prototyping and design optimization. Consequently, automating this task is an essential prerequisite for achieving fully automated hexahedral mesh generation.

To address this bottleneck, we build upon an existing reinforcement learning (RL) approach [1], introducing a refined sequential decision-making framework to automate 3D CAD decomposition. Unlike traditional heuristic approaches, the RL agent is trained to autonomously explore and execute decomposition actions that facilitate valid, conformal meshing. A critical component of this framework is the decomposition action space; we use Coreform Cubit's webcutting functionality to enable the agent to act with similar freedom to human experts, theoretically enabling expert-level block decompositions. By training the agent to learn an optimal decomposition policy through autonomous interaction with the CAD environment, this approach provides a data-driven pathway to greatly accelerate numerical simulation workflows.

References

[1] S. Zhang, Z. Guan, X. Wang, P. Tan, and H. Jiang, *Reinforcement learning based automatic block decomposition of solid models for hexahedral meshing*, in *Computer-Aided Design* Vol. 182, 103850 (2025).

The VII International AMMCS
Interdisciplinary Conference
Waterloo, Ontario, Canada

A Transformer-Based Optimization Framework for Clustering and Feature Selection

A. Singh[1], P. Jeganathan [2]

[1] *School of Compuatational Science and Engineering, Department of Mathematics and Statistics, Hamilton, Canada, {singa429}@mcmaster.ca*
[1] *School of Compuatational Science and Engineering, Department of Mathematics and Statistics, Hamilton, Canada, {jeganp1}@mcmaster.ca*

Many clustering algorithms can be formulated as optimization problems that seek a partition of observations while maximizing a criterion measuring cluster separation [1]. Let $\boldsymbol{X} \in \mathbb{R}^p$ be a p-dimensional random vector, $\boldsymbol{x}_1, \ldots, \boldsymbol{x}_n \in \mathbb{R}^p$ denote n observations, $\boldsymbol{w} \in \mathbb{R}^p_+$ denote a feature-weight vector, and $\Theta = \{C_1, \ldots, C_K\}$ denote a partition of the n observations into K disjoint clusters. A general clustering formulation can be written as

$$\underset{\Theta, \boldsymbol{w}}{\text{maximize}} \quad \sum_{j=1}^{p} w_j f_j(X_j, \Theta) \quad \text{subject to} \quad \|w\|_2 \leq 1 \quad w_j \geq 0 \quad \forall j. \tag{1}$$

Several clustering methods incorporate feature selection by introducing an additional L_1-type constraint, $\|w\|_1 \leq s$, which shrinks the feature weights toward zero. However, these approaches typically estimate a single set of feature weights shared across all clusters, implicitly assuming that the same features are equally relevant for identifying every cluster.

In this talk, I will first review clustering algorithms from an optimization perspective and discuss how feature selection can be incorporated. I will then introduce a Transformer-based optimization framework for clustering and feature selection that addresses the limitation of global feature weights. The proposed approach leverages attention mechanisms to learn adaptive similarities between observations and feed-forward network gates to perform feature selection. These components are integrated within a unified optimization framework that jointly learns prototype representations and feature relevance.

To estimate the model, I propose a stage-wise optimization procedure that separates prototype learning and feature selection. This framework enables the identification of features that characterize specific clusters while maintaining interpretable cluster representations. I will conclude by presenting simulation studies demonstrating that the proposed approach successfully recovers cluster-specific features in settings where different clusters are driven by distinct subsets of variables.

References

[1] D. M. Witten and R. Tibshirani, *A framework for feature selection in clustering*, *Journal of the American Statistical Association* **105**, 490, pp. 713–726 (2010).

Efficient Parallel Method for Contamination Convection-Diffusion Problems in Porous Media

D. Liang[1]

[1] *York University, Toronto, Canada, dliang@yorku.ca*

The time-dependent convection diffusion equations have been widely used to describe the transport of solutes in groundwater modelling, the displacement of oil in petroleum reservoirs, the atmospheric aerosol transport, and many other applications. Due to advective stirring in the convection-dominated diffusion problems, the classical numerical methods encounter serious problems of non-physical oscillations and excessive numerical dispersions at steep fronts. The Eulerian Lagrangian methods have been efficient and attractive in solving convection-dominated diffusion equations. While the computational complexity and the large scale and long-term prediction require efficient parallel computing, it is significantly important and challenging to develop efficient parallel computing for solving simulation of contamination flows in porous media.

In this talk, we would like to present our development of an efficient parallel Eulerian Lagrangian method for the contamination convection-diffusion problems in porous media. Meanwhile, we will also present our study of an optimization approach for contamination flows in porous media. Numerical experiments demonstrate the performance of the developed parallel methods. Numerical simulations in more realistic shaped aquifers validate the control approach's efficiency.

RAS: A Riccati-Schur Active-Set QP Solver for Resource-Constrained Model Predictive Control

D. Ma[1], K. Cheshmi[1]

[1] *Department of Electrical and Computer Engineering, McMaster University, Hamilton, Canada*

Embedded Model Predictive Control (MPC) on bare-metal microcontrollers requires solving Quadratic Programs (QPs) under strict real-time and memory constraints. Existing sparse solvers either lose tracking accuracy or require online Karush-Kuhn-Tucker (KKT) factorization that exceeds available static RAM. To overcome this, we propose RAS, an active-set solver achieving exact constraint satisfaction without forming or factorizing the working-set KKT matrix online. RAS splits the solution: the equality-constrained core is solved via a horizon-linear Riccati sweep using precomputed factors, while active inequalities are resolved through a reduced Schur-complement system ($S_W \lambda_W = r_W$). Rather than assembling the Schur matrix S_W, RAS solves this implicitly via conjugate gradients, where each operator application is a single Riccati sweep. This formulation ensures the workspace is sized strictly at compile time, avoiding dynamic allocation. On a Cortex-M7 microcontroller, RAS successfully matches the fixed memory profile of embedded first-order methods like OSQP [1] and TinyMPC [2].

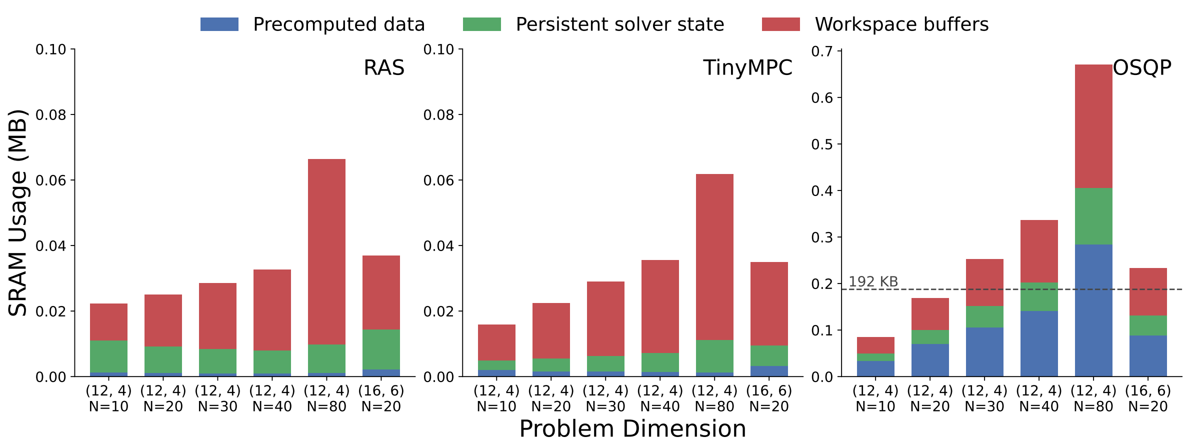

Figure 1: Runtime SRAM usage of RAS, TinyMPC, and OSQP across benchmark problem dimensions. The bars decompose the total runtime memory into precomputed data, persistent solver state, and workspace buffers. The dashed line in the OSQP panel marks the 192 KB SRAM budget of the target microcontroller.

References

[1] B. Stellato, G. Banjac, P. Goulart, A. Bemporad, and S. Boyd, *OSQP: an operator splitting solver for quadratic programs*, Mathematical Programming Computation **12**, 4, pp. 637-672 (2020).

[2] K. Nguyen, S. Schoedel, A. Alavilli, B. Plancher, and Z. Manchester, *TinyMPC: Model-predictive control on resource-constrained microcontrollers*, in *IEEE International Conference on Robotics and Automation* (ICRA), (2024).

The VII International AMMCS
Interdisciplinary Conference
Waterloo, Ontario, Canada

Mathematical Models for Medical Image Registration

Mia Carmela Mojica[1], Mehran Ebrahimi[2]

[1] *Krembil Brain Institute, Toronto Western Hospital, University Health Network, Toronto, Ontario, Canada, mia.mojica@uhn.ca*
[2] *Faculty of Science, Ontario Tech University, Oshawa, Ontario, Canada, mehran.ebrahimi@ontariotechu.ca*

Medical image registration is a core component of many biomedical imaging pipelines. It enables the alignment of images acquired from different modalities, time points, or subjects. Accurate registration supports tasks such as multimodal image fusion, population-based analysis, motion correction, and longitudinal assessment. However, registration remains challenging due to anatomical variability, subject motion, and the difficulty of obtaining reliable anatomical correspondences. This work presents a set of strategies to improve robustness and accuracy across a range of common imaging tasks.

In these applications, registration is formulated using models capable of adapting to different sources of variation. In pairwise alignment, this facilitates alignment between images of the same subject acquired under different conditions or at different time points. Extending this formulation, groupwise registration is used to construct population templates and atlases, which provide a shared coordinate system that captures both average structure and meaningful inter-subject anatomical variability.

The framework is further adapted to image sequences, where motion introduces inconsistencies that can obscure subtle but clinically relevant temporal changes. By explicitly accounting for temporal variation, the proposed methods reduce motion-related misalignment and improve the reliability of downstream analysis.

To address limitations associated with relying on a single source of information, the registration process is augmented with additional structural cues. Automated landmark detection methods are introduced to identify anatomically meaningful correspondences without manual intervention. These landmarks are integrated with intensity-based similarity models, allowing global intensity information and local structural features to jointly guide alignment. This combination improves robustness in challenging cases where either source alone may be insufficient.

Overall, this work demonstrates how a flexible registration framework can be adapted to a range of imaging tasks, including multimodal alignment, atlas construction, motion correction, and anatomically informed registration. The results highlight the value of integrating complementary imaging features to achieve accurate and reliable medical image registration.

References

[1] J. Modersitzki, *Numerical Methods for Image Registration*, Oxford University Press, Oxford, UK (2004).

[2] J.B.A. Maintz and M.A. Viergever, *A survey of medical image registration*, Medical Image Analysis, **2**, 1, pp. 1–36 (1998).

[3] D.L.G. Hill, P.G. Batchelor, M. Holden, and D.J. Hawkes, *Medical image registration*, Physics in Medicine and Biology, **46**, 3, pp. R1–R45 (2001).

An application of equivariant machine learning in contact detection

S. Morin[1]

[1] *Polytechnique Montréal, Canada, sophie-4.morin@polymtl.ca*

This study concerns the problem of computing the signed distance between two ellipses in the plane, which is an important and surprisingly subtle test case for an approach to contact detection and contact force evaluation for more general shapes in 2D and 3D, primarily for application in Discrete Element Method (DEM) simulations.

We parametrize an ellipse in the plane by the semi-major and semi-minor axis lengths $a \geq b > 0$, the coordinates (c_x, c_y) of the centre, and the orientation angle $\theta \in [0, \pi)$, measured counterclockwise from the positive x-direction to the major axis. The ellipse $\mathscr{E}$ with parameters (a, b, θ, c_x, c_y) is then the zero set of a potential function $f(x,y)$ given by

$$f(x,y) = \left\| D(a,b)^{-1} R_\theta^{-1} (x - c_x, y - c_y)^T \right\|_2^2 - 1 \tag{1}$$

where $D(a,b)$ is the diagonal matrix with diagonal entries a, b and R_θ is the matrix of rotation by θ. Given two ellipses $\mathscr{E}_i, \mathscr{E}_j$ with parameters $(a_i, b_i, \theta_i, c_{x,i}, c_{y,i}), (a_j, b_j, \theta_j, c_{x,j}, c_{y,j})$ and potential functions f_i, f_j respectively, we seek the *minimum-potential pair*

$$(x_i^*, y_i^*) = \operatorname{argmin}_{(x,y)\in\mathscr{E}_i} \quad f_j(x,y), \qquad (x_j^*, y_j^*) = \operatorname{argmin}_{(x,y)\in\mathscr{E}_j} \quad f_i(x,y). \tag{2}$$

Note that $f_j(x_i^*, y_i^*) \leq 0$, equivalently $f_i(x_j^*, y_j^*) \leq 0$, if and only if $\mathscr{E}_i, \mathscr{E}_j$ intersect, with equality only when the intersection is tangential, so the sign of the value $f_j(x_i^*, y_i^*) \leq 0$ decides the binary contact detection question for $\mathscr{E}_i, \mathscr{E}_j$, and the value

$$\varepsilon(\mathscr{E}_i, \mathscr{E}_j) = \operatorname{sign}(f_j(x_i^*, y_i^*)) \sqrt{(x_j^* - x_i^*)^2 + (y_j^* - y_i^*)^2} \tag{3}$$

gives a reasonable notion of signed distance between $\mathscr{E}_i, \mathscr{E}_j$, which is used to compute the contact forces between $\mathscr{E}_i, \mathscr{E}_j$ when contact is detected. The (decoupled) minimization problem (2) was analyzed in [1], leading to an implementation by Banna of an algorithm described in [2] for generating datasets of pairs of ellipses with prescribed distributions of parameters, together with their minimum-potential points in (2) and the signed distance (3).

In the present study, we fit the data generated by Banna's code using features that are exactly equivariant with respect to all of the inherent geometric symmetries of the problem (translation, rotation, dilation, and reflection). We compare the performance of ridge regression, LASSO, and neural networks in fitting these features to the generated minimum-potential pair data. We also show that the problem of computing the signed distance (3) directly from the 10 parameters defining the ellipses $\mathscr{E}_i, \mathscr{E}_j$ is ill-conditioned, and we illustrate the consequences of this ill-conditioning with numerical experiments. We close by indicating how we are extending this approach to contact detection for more general shapes in 2D and 3D.

References

[1] E. Kheradmand, M. Laforest, and S. Prudhomme. *A mathematical framework for the analysis and comparison of contact detection methods for ellipses and ellipsoids*, Comp. Part. Mech. **9**, pp. 1153–1203 (2022).

[2] G. Banna, M. Laforest, and S. Prudhomme. *Generation of pairs of ellipses and ellipsoids from distributions in parameter space*, Comp. Part. Mech. **12**, pp. 2775–2785 (2025).

Stable Mesh-Free Variational Radial Basis Function Approximation for Elliptic PDEs and Obstacle Problems

T.P.D. Le[1], G. Tran[1], , H.De Sterck[1]

[1] *University of Waterloo, Canada, {pdle, giang.tran, hans.desterck}@uwaterloo.ca*

We present a comprehensive study of radial basis function (RBF) approximations for elliptic and obstacle-type boundary value problems under a variational formulation. Our focus is on practical accuracy, robustness and efficiency. To address ill-conditioning in dense systems, we apply truncated singular value decomposition and investigate its effect on stability and accuracy trade-offs. Numerical experiments report benchmarks on accuracy and show fast error decay. We investigate the trade-off between approximation and truncation errors for practical settings for the number of basis functions, the oversampling ratio and the truncation threshold. In comparison with other methods, RBF variational solvers deliver high accuracy at similar or lower cost for boundary value problems.

References

[1] T.P.D. Le, G. Tran, and H. De Sterck, *Stable Mesh-Free Variational Radial Basis Function Approximation for Elliptic PDEs and Obstacle Problems*, https://arxiv.org/abs/2604.19882 (2026)

Methods for Solving Three-Dimensional Nonlinear Flexural-Gravity Wave Problems

C. Tugulan[1], O. Trichtchenko[2], D. Technology[2]

[1] *The University of Western Ontario, Canada*
[2] *The University of Western Ontario, Canada otrichtc@uwo.ca*
[3] *The University of East Anglia, UK*

Three-dimensional flexural-gravity waves beneath ice are studied using the fully nonlinear Euler equations. Building on recent work examining waves generated by moving loads on ice-covered surfaces [1], the governing equations are reformulated as boundary integral equations within a unified framework that accommodates a variety of physical geometries and forcing configurations [2]. Efficient numerical solutions are obtained using iterative methods together with novel preconditioning techniques developed for nonlinear hydroelastic wave problems [3]. These methods make possible the computation of fully nonlinear three-dimensional wave patterns and their extension to increasingly realistic settings, including variable bottom topography [4]. The resulting solutions reveal a rich variety of wave behaviours that depend on disturbance speed, bottom geometry, forcing configuration, and the mechanical properties of the ice. The talk will provide an overview of these developments and discuss current challenges in the numerical simulation of waves beneath ice [5].

References

[1] C. C. Tugulan, O. Trichtchenko, E. I. Părău, and A. Stevenson, *Flexural-gravity waves generated by different load sizes and configurations on varying ice cover*, Water Waves, **6**, 127–142 (2024).

[2] E. I. Părău, C. C. Tugulan, O. Trichtchenko, and A. Alberello, *Flexural-Gravity Waves Under Ice Plates and Related Flows*, in *Nonlinear Dispersive Waves*, Advances in Mathematical Fluid Mechanics, Birkhäuser, Cham (2024).

[3] C. C. Tugulan, O. Trichtchenko, and E. I. Părău, *Three-dimensional waves under ice computed with novel preconditioning methods*, Journal of Computational Physics, **459**, 111129 (2022).

[4] C. C. Tugulan, O. Trichtchenko, and E. I. Părău, *Three-dimensional steady nonlinear flexural–gravity waves over bottom topography*, submitted.

[5] E. I. Părău, C. C. Tugulan, and O. Trichtchenko, *Hydroelastic waves on floating ice plates*, Proceedings of the 40th International Symposium on the Okhotsk Sea & Polar Oceans, Monbetsu, Hokkaido, Japan (2026).

Stochastic Resonance Enhances Forecastability in a Noisy Predator–Prey System

N. Yu

Toronto Metropolitan University, nayu@torontomu.ca

We study the effect of stochastic resonance on forecasting performance in a noisy predator–prey system near a Hopf bifurcation. A stochastic Lotka–Volterra model is simulated using a stochastic Runge–Kutta method, while reservoir computing is used to predict the stochastic dynamics. Oscillatory coherence and forecasting performance are quantified using CV, SNR, RMSE, and predictability horizon. Results show that intermediate noise levels enhance both oscillatory coherence and forecasting accuracy, leading to extended predictability horizons. The study reveals a quantitative connection between stochastic resonance and machine-learning predictability in stochastic ecological systems.

Dynamics of Cell Cycle Models with Quiescence and Time Delay Due to Interphase

S. Alsibaai[1], T. Day[1], F. Magpantay[1]

[1] *Department of Mathematics and Statistics, Queen's University, Kingston, ON, Canada K7L 3N6*

The cell cycle is a tightly regulated biological process governing cell growth and division. In this talk, I will discuss two mathematical models of cell cycle dynamics introduced in [1, 2]. Previous analytical studies focused either on a reduced constant-delay model without a quiescent phase or on the full model with zero interphase duration ($\tau = 0$), which neglects the time required for interphase. We analyze the full model incorporating both cell quiescence and the delay associated with interphase. We consider both a constant-delay model, in which the interphase duration is fixed, and a state-dependent delay model, in which the interphase duration increases with the number of mitotic cells due to competition for limited resources.

For the constant-delay model, we show that when the death rate of mitotic cells exceeds twice their proliferation rate ($\mu_1 > 2b_1$), the trivial equilibrium is the unique biologically feasible steady state and is asymptotically stable. In contrast, when $\mu_1 < 2b_1$, a critical interphase duration τ^* emerges. In this regime, the trivial equilibrium remains the only biologically feasible equilibrium for all $\tau \neq \tau^*$ and is asymptotically stable for $\tau > \tau^*$ and unstable for $\tau < \tau^*$, corresponding to extinction and unbounded growth, respectively. At the critical value $\tau = \tau^*$, the system admits a one-parameter family of equilibria. Numerical bifurcation analysis using DDE Biftool [3] in MATLAB [4] confirms these analytical results. We then investigate the state-dependent delay model in which the interphase duration depends on the total number of mitotic cells, $\tau = \tau(U)$. Numerical simulations and bifurcation analysis indicate that, for a range of parameter values, the system admits a positive bounded equilibrium that is absent in the constant-delay case, demonstrating that state dependence fundamentally alters the system dynamics. Establishing the non-negativity of solutions for the state-dependent model presents additional analytical challenges. I will discuss the current results and the remaining open problems.

References

[1] MV. Barbarossa, C. Kuttler, J. Zinsl, *Delay equations modeling the effects of phase-specific drugs and immunotherapy on proliferating tumor cells*, Math. Biosci. Eng., 9(2), pp. 241-257 (2012).

[2] Barbarossa MV, *On a class of neutral equations with state-dependent delay in population dynamics*, PhD thesis (2013).

[3] Engelborghs K, Luzyanina T, Roose D, *Numerical bifurcation analysis of delay differential equations using dde-biftool*, ACM Trans. Math. Softw., 28(1), pp. 1-21 (2002).

[4] The MathWorks, Inc (2024) MATLAB, version 24.1. The MathWorks, Inc., Natick, Massachusetts, United States.

The VII International AMMCS
Interdisciplinary Conference
Waterloo, Ontario, Canada
April 25, 2026

Event-Triggered Pinning Impulsive Control with Actuation Delays

Ethan Astri[1], Hamza Saleem[2], Kexue Zhang[3]

[1] *Queen's University, Kingston, Canada, 22kc41@queensu.ca*
[2] *Queen's University, Kingston, Canada, 24sm13@queensu.ca*
[3] *Queen's University, Kingston, Canada, kexue.zhang@queensu.ca*

Impulsive control is a paradigm which uses abrupt state changes to control dynamical systems. The event triggering approach efficiently schedules the control impulses based on the violation of a well designed triggering condition. This talk considers the stabilization of complex dynamical networks via event triggered pinning impulsive control, where only a few nodes receive control impulses to stabilize the overall network. An actuation delay between the violation of the triggering condition and the implementation of the corresponding control impulse is explicitly investigated. Sufficient conditions on the network topology, actuation delay, and control gains are derived to guarantee the asymptotic stability of the overall network. In addition, a positive lower bound on the inter-event time for the pinned nodes is established, thereby excluding Zeno behavior. A numerical example illustrates the effectiveness of the proposed methods.

On asymptotic stability of equations and systems with distributed, unbounded and infinite, delays

L. Berezansky[1], E. Braverman[2]

[1] *Ben-Gurion University of the Negev, Israel, brznsky@bgu.ac.il*
[2] *University of Calgary, Canada, maelena@ucalgary.ca*

Many differential equations of mathematical biology assume delayed production process and instantaneous mortality. Introduction of delay can destabilize the unique positive equilibrium and even lead to chaos. However, for some types of equations and systems, lags in the reproduction term do not change stability properties [2]. Consideration of variable, unbounded and distributed delays emphasizes robustness of this 'absolute stability' property. Influence of an infinite, not just unbounded, delay is also outlined. The influence of small delays in the mortality term is also explored [1].

References

[1] L. Berezansky and E. Braverman, *On stability of equations with an infinite distributed delay*, Nonlinearity **37** (2024), 6, Paper No. 065022, 21 pp.

[2] L. Berezansky and E. Braverman, *Nicholson's blowflies diffeerential equations with a small delay in the mortality term*, Nonlinear Anal. RWA **81** (2025), Paper # 104193, 10 pp.

The VII International AMMCS
Interdisciplinary Conference
Waterloo, Ontario, Canada

Discrete Delay Population Models

C. J. Greyson-Gaito[1], S. Streipert[2], G. S. K. Wolkowicz[1]

[1] *McMaster University, Hamilton, Canada, {christopher@greyson-gaito.com, wolkowic@mcmaster.ca}*
[2] *University of Pittsburgh, Pittsburgh, USA, streipert@pitt.edu*

We present a class of discrete delay models that consider a delay in the reproduction and take, the often neglected, mortality of immature individuals during that maturation delay into account. We discuss the dynamics of such a class of recurrences and specifically explore the dynamics of two survival functions, a Beverton-Holt type and a Ricker type survival. For the general class of such delay models, we find that increasing the delay beyond a critical threshold leads to extinction. Since however maturation delays beyond one breeding cycle are often found in nature, such delayed maturation must also have a benefit leading to a trade-off. We then incorporate such trade-off in these maturation delay models and discuss their effects on the dynamics. For a Beverton–Holt type survival, we find an optimal delay that results in the largest equilibrium level and, for the Ricker type survival, we find that the trade-off can initiate or remove oscillatory behavior.

The VII International AMMCS
Interdisciplinary Conference
Waterloo, Ontario, Canada

Quantifying Statistical Covariance near Limit Cycles of Autonomous Delay Differential Equations

Z. Iklodi[1], H. Dankowicz[1],

[1] *University of Maryland, College Park, USA, {iklodi, danko}@umd.edu*

We present the generalization to systems with delay of a recently published formulation [1] for uncertainty quantification of noisy dynamics near limit cycles of non-linear ODEs. This formulation constructs an adjoint periodic BVP whose solution defines a continuous family of planes transversal to the limit cycle that are invariant under the linearized deterministic flow. Focusing on the intersection of the stochastic trajectories with these planes eliminates the effects of phase dispersion. A second, periodic BVP facilitates the direct analytic and numeric study of statistical covariance of intersections with these planes, without looking at actual realizations of noisy trajectories.

Here, we extend this formulation to the infinite-dimensional case of a stochastic delay-differential equation

$$\mathrm{d}x(t) = f(x(t), x(t-\tau))\,\mathrm{d}t + g(x(t), x(t-\tau))\,\mathrm{d}W_t \tag{1}$$

without first converting this through discretization to a high-dimensional system of stochastic ODEs. Inspired by [2], this is accomplished by the derivation of a triangular system of advection-type PDEs, whose solutions may be used to construct the families of transversal functional hyperplanes and corresponding covariance operators. An example is shown in Figure 1, where panel (a) captures a delay-embedding of an ensemble of stochastic trajectories (red) near an underlying limit cycle (black); panel (b) shows intersections (red) with a subset of transversal planes in the same delay embedding; and panel (c) allows for a comparison between the predicted eigenvalues (solid) of the covariance operators (parameterized by phase) and those obtained through Monte Carlo simulations (circles).

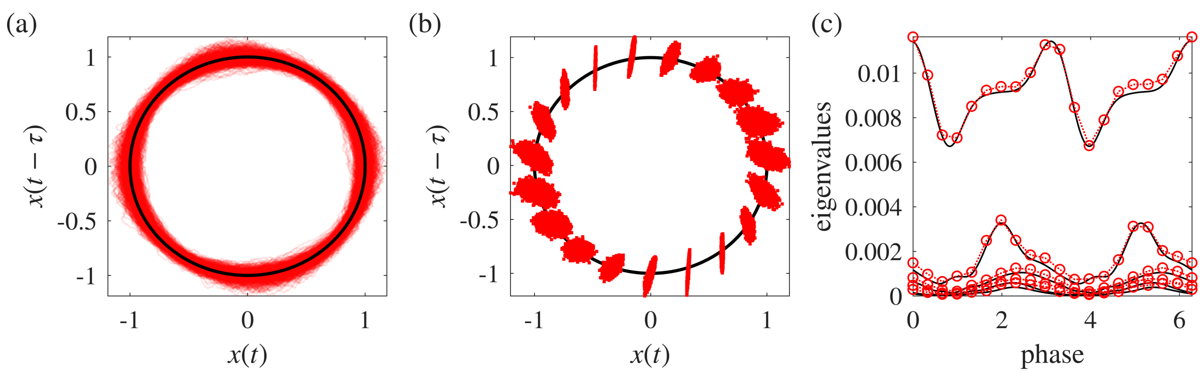

Figure 1: Illustration of uncertainty quantification in the presence of noisy perturbations near a limit cycle of a delay differential equation.

References

[1] Z. Ahsan, H. Dankowicz, and C. Kuehn, *Adjoint-Based Projections for Quantifying Statistical Covariance near Stochastically Perturbed Limit Cycles and Tori*, SIAM Journal on Applied Dynamical Systems **24**, 2, pp. 1455-1493 (2025).

[2] V. Novicenko and K. Pyragas, *Phase reduction of weakly perturbed limit cycle oscillations in time-delay systems*, Physica D: Nonlinear Phenomena, **241** pp. 1090-1098.108 (2012).

Global Asymptotic Stability and Periodicity in Delay Differential Biological Models

A.F. Ivanov[1]

[1] *Pennsylvania State University, Dallas, Pennsylvania, USA, afi1@psu.edu*

We study the problem of global asymptotic stability (GAS) of equilibria and the existence of periodic solutions for simple form delay differential equations, which partial cases include several well-known models from applications such as Mackey-Glass and Nicholson's equations, among others. A special emphasis is placed on the case when the decay term is a nonlinear function. The GAS is derived in terms of underlying interval maps and their property of global attractivity of a unique fixed point. The periodic solutions exist under the assumption of the negative feedback in the system and the instability of the linearized equation about the equilibrium. Numerical and visual demonstrations of a variety of periodic solutions are presented. They confirm the theoretical conclusions as well as show new patterns beyond the theoretical outcomes. This is a joint work with Hideaki Matsunaga of Osaka Metropolitan University.

From Numerics to Rigour: Periodic Orbits in State-Dependent Delay Equations

J.B. van den Berg[1], M. Breden[2], M. Cadiot[3], K. Church[4], J.-P. Lessard[5]

[1] *VU University, Amsterdam, The Netherlands, janbouwe.vanden.berg@vu.nl*
[2] *École Polytechnique, Palaiseau, France, maxime.breden@polytechnique.edu*
[3] *École Polytechnique, Palaiseau, France, matthieu.cadiot@polytechnique.edu*
[4] *Centre de Recherches Mathématiques (CRM), Montreal, Canada, church.kevin@gmail.com*
[5] *McGill University, Montreal, Canada, jp.lessard@mcgill.ca*

State-dependent delay equations (SDDEs) present significant theoretical and computational challenges due to the presence of delays that depend on the evolving state through nonlinear composition terms. In contrast to ordinary differential equations, parabolic partial differential equations, or delay equations with constant delays, SDDEs do not, in general, generate a semiflow. Even in cases where a semiflow can be defined, the dynamics evolve on an infinite-dimensional phase space, and the presence of nonlinear composition operators introduces additional analytical difficulties. Among the most important invariant objects in this setting are periodic solutions, which are central to the understanding of recurrent dynamics, yet are notoriously difficult to establish rigorously.

In this talk, we develop a computer-assisted framework for proving the existence of periodic solutions in genuinely state-dependent delay equations, without relying on reductions to finite-dimensional ODEs or PDE approximations. Our approach combines Fourier expansions with a Newton–Kantorovich scheme formulated in a low-regularity Banach space. A key aspect of the method is the rigorous treatment of nonlinear composition operators, achieved through a combination of discrete Fourier analysis, contour integral representations, and the discrete Poisson summation formula.

The methodology is illustrated through three examples: a periodically forced toy model designed to highlight the main ideas; the autonomous prototypical model studied in [1]; and a recent threshold-type state-dependent delay model arising in [2].

References

[1] R. Calleja, A.R. Humphries and B. Krauskopf, *Resonance phenomena in a scalar delay differential equation with two state-dependent delays*, SIAM J. Appl. Dyn. Syst., 3, 1474–1513, 2018.

[2] T. Gedeon, A.R. Humphries, M.C. Mackey, H.-O. Walther and Z. Wang, *Dynamics of a state-dependent delay-differential equation*, 2025 (https://arxiv.org/abs/2410.13092),

Infection dynamics in the presence of a migratory population

C. McCluskey

Wilfrid Laurier University, Waterloo, Canada, cmccluskey@wlu.ca

We consider compartmental models of disease spread for which there is a single susceptible group S and n post-infection groups $x_1,\ldots,x_n$ (including infectious, quarantined and recovered groups, for example). Healthy individuals (i.e. susceptibles) may travel out of the region being studied, returning later after a fixed duration. This is modelled with a standard linear exit term combined with delayed terms that represents the migrants' return. A fraction σ of the migrants are still susceptible upon return, while the remainder $(1-\sigma)$ join one of the post-infection groups.

We obtain a system of the form

$$\frac{\mathrm{d}S}{\mathrm{d}t} = \nu - (\mu_S + k)S - \Lambda S + \sigma k S(t-\tau) \tag{1}$$

$$\frac{\mathrm{d}\vec{x}}{\mathrm{d}t} = \Lambda S\vec{P} - M\vec{x} + (1-\sigma)k\vec{W}S(t-\tau), \tag{2}$$

where the force of infection is given by

$$\Lambda = \beta_1 x_1 + \ldots + \beta_n x_n, \tag{3}$$

and $\vec{P}$ and $\vec{W}$ are probability vectors, describing how new infections and returning workers, respectively, are distributed into the post-infection groups. The matrix M is an M-matrix that is used to encode movement between the post-infection groups and death.

The movement of returning workers into the post-infection classes means there is no disease-free equilibrium, and hence the usual threshold behaviour (based on a basic reproduction number) does not apply.

We study local and global behaviour of the system, including Lyapunov functions.

The VII International AMMCS
Interdisciplinary Conference
Waterloo, Ontario, Canada

Stability Switches and Multi-Wave Dynamics in a Two-Strain Delay Model Calibrated with Wastewater Data

Bruce Pell[1], Samantha Brozak[2], Tin Phan[3], Fuqing Wu[4], Yang Kuang[2]

[1] *Lawrence Technological University, Southfield, USA, bpell@ltu.edu*
[2] *Arizona State University, Tempe, USA*
[3] *Theoretical Biology and Biophysics, Los Alamos National Laboratory, Los Alamos, USA*
[4] *University of Texas Health Science Center at Houston, Houston, USA*

We present a two-strain compartmental model incorporating temporary cross-immunity via a discrete time delay. We establish biological conditions for strain coexistence based on reproduction numbers (R_i) and identify parameter thresholds that induce stability switches and limit cycles. Calibrated with COVID-19 wastewater surveillance data, the model successfully captures observed multi-wave epidemic patterns and variant competition. Our results demonstrate how mechanistic delay differential equation (DDE) models can enhance the interpretation and forecasting of wastewater-based epidemiological signals.

The VII International AMMCS
Interdisciplinary Conference
Waterloo, Ontario, Canada
May 23, 2026

Gravitational Model with State-Dependent Delay Applied to Galaxy Rotation

E.I. Verriest

Georgia Institute of Technology, Atlanta, GA, USA, erik.verriest@ece.gatech.edu

It was observed that the rotation speed is nearly independent of the distance from the galactic center, which, in a strict Newtonian approach, corresponds with a certain mass distribution in the disk. However, if one assumes luminosity to be proportional to mass density, Newtonian dynamics predicts that the rotation speed should decrease with distance. A remedy for this discrepancy, proposed by Vera Rubin (1928-2026), was to invoke the existence of dark matter, which does not interact with ordinary matter and radiation.

In [2] we proposed an approximation to Einstein's field equations in the case of low velocities and weak gravitational fields. Still assuming a notion of simultaneity, and a flat space, this approximation is based on a finite propagation speed of the (Newtonian) gravitational force, which leads to the modification of Newton's equation by a state-dependent delay. The effect due to a unit point mass in motion, prescribed by a trajectory, $\vec{r}_p(t)$ is described by a three-dimensional Dirac-delta mass density $\rho(\vec{r'},t') = \delta(\vec{r'} - \vec{r}_p(t'))$. The resulting gravitational potential at the fixed point and time, $(\vec{r},t)$, in such a post-Newtonian (pN) theory is then

$$\phi(\vec{r},t) = G\int_{\mathbb{R}^3} \frac{\delta(\vec{r'} - \vec{r}_p(t_b))}{|\vec{r} - \vec{r'}|}\, \mathrm{d}V(\vec{r'}) = \frac{G}{|\vec{r} - \vec{r}_p(t_b)|\left(1 - (\vec{r} - \vec{r}_p(t_b))^\top \dot{\vec{r}}_p(t_b)\right)}. \tag{1}$$

where $t_b = t - \tau(\vec{r'})$ is the *backward or retarded time* satisfying $c\tau(\vec{r'}) = |\vec{r} - \vec{r'}|$. This induced a gravitational entraining effect from moving masses, with repercussions to escape velocities [4] and the motion of binaries [3].

Considering a galactic ring-element at radius r and angle θ, measured from the orbit, with angular velocity ω, we get for an observation point at radius R that $c\tau = \sqrt{R^2 + r^2 + 2Rr\sin\theta_b}$ and

$$\begin{aligned} |\vec{r} - \vec{r}_p(t_b)| &= \sqrt{R^2 + r^2 + 2Rr\sin\theta_b} \\ (\vec{r} - \vec{r}_p(t_b))^\top \dot{\vec{r}}_p(t_b) &= -\omega r R\cos\theta_b. \end{aligned}$$

Integration of (1) over all θ gives the potential at R due to a ring-element. A second integral over r yields then the potential at R due to the entire galaxy. This creates an impasse as the integration is with respect to θ (actual position of a ring element), while the integrand is expressed in terms of the delayed θ_b. Different signal delays on different ring elements render the mass density with respect to the delayed angle, θ_b non-uniform. In this paper, we show how to resolve this seemingly enormously convoluted task, and compare the post-Newonian result to the Newtonian one [1], with potential repercussions for dark matter.

References

[1] G. Bertin, *Dynamics of Galaxies* Cambridge University Press. (2000)

[2] E.I. Verriest, *Post-Newtonian Gravitation*, in *Mathematical and Computational Approaches in Modern Science and Engineering*, Bélair, J., Frigaard, I.A., Kunze, H., Makarov, R., Melnik, R., Spiteri, R.J. (Eds.), pp. 153-164, Springer-Verlag (2016).

[3] E.I. Verriest, *Gravitational Models with State-Dependent Delay: Gravitating Binaries.* In: Kilgour, D.M., Kunze, H., Makarov, R.N., Melnik, R., Wang, X. (eds) *Addressing Modern Challenges in the Mathematical, Statistical, and Computational Sciences*. AMMCS 2023. Springer Proceedings in Mathematics & Statistics, vol 494. Springer-Verlag, pp. 219-229.

[4] E.I. Verriest, *Escape from Gravity: A Post-Newtonian Approach with State-Dependent Delay.* in 2023 *MATRIX Annals*, Vol. 6, David R. Wood, Alison M. Etheridge, Jan de Gier, Nalini Joshi (Eds.), pp. 441-447, Springer-Verlag 2025.

The unusual physics and math of generalized squeezing

S. Ashhab[1]

[1] *Advanced ICT Institute, National Institute of Information and Communications Technology (NICT), 4-2-1, Nukui-Kitamachi, Koganei, Tokyo 184-8795, Japan, ashhab@nict.go.jp*

We analyze the properties and dynamics of generalized squeezed vacuum states, i.e. states obtained by applying a higher-order squeezing operator to the vacuum state. We calculate the squeezing operator numerically by taking the exponential of a truncated Hamiltonian matrix. The simulations suggest that, in stark contrast to displacement and two-photon squeezing, higher-order squeezing leads to oscillatory dynamics [1]. The state is squeezed in the initial stages of the dynamics but the squeezing reverses at later stages, and the state reverts almost completely back to the initial state. The maximum squeezing diminishes with increasing squeezing order, rendering the squeezing mechanism increasingly ineffective. Further investigation reveals that the simulation results depend strongly on whether the state space in the simulation contains an even or odd number of states [2]. This result indicates that the infinite-size limit is not well defined, and it raises questions regarding whether the simulation results are physically meaningful [3, 4]. We show that the squeezing Hamiltonian must be complemented with additional regulating terms to make the results truncation-size independent and physically meaningful. Furthermore, we generalize the squeezing Hamiltonian such that the squeezing order can be a fractional number [5]. This generalization allows us to investigate the gradual evolution of the squeezing dynamics between different (integer) squeezing orders, and it allows us to infer results for certain integer squeezing orders for which the computational simulation of the dynamics is especially challenging.

This work was supported by Japan's Ministry of Education, Culture, Sports, Science and Technology (MEXT) Quantum Leap Flagship Program Grant Number JPMXS0120319794.

References

[1] S. Ashhab and M. Ayyash, *Properties and dynamics of generalized squeezed states*, New J. Phys. **27**, 054104 (2025).

[2] S. Ashhab, F. Fischer, D. Lonigro, D. Braak, and D. Burgarth, *Finite-dimensional approximations of generalized squeezing*, Phys. Rev. A **113**, 013703 (2026).

[3] R. Gordillo-Hachuel and R. Puebla, *Comment on "Properties and dynamics of generalized squeezed states"*, New J. Phys. **28**, 028002 (2026).

[4] S. Ashhab and M. Ayyash, *Reply to Comment on "Properties and dynamics of generalized squeezed states"*, New J. Phys. **28**, 028001 (2026).

[5] S. Ashhab, *Fractional squeezing: spectra and dynamics from generalized squeezing Hamiltonian with fractional orders*, arXiv:2601.15693.

Pulsed Generation of Continuous-Variable Cluster States in Optomechanical Quantum Network: Noise, Scalability, and Optimal Control

A. Govindarajan[1], M. Mazzei[1], D. Guo[1], H. Wang[2], L. Tian[1]

[1] *School of Natural Sciences, University of California, Merced, 5200 North Lake Road, Merced, California 95343, USA {agovindarajan, mmazzei, dingyuguo, ltian}@ucmerced.edu*
[2] *Department of Physics, University of Oregon, Eugene, Oregon 97403, USA {hailin}@uoregon.edu*

Quantum networks are essential for secure quantum communication and scalable quantum technologies [1]. Among various physical platforms, optomechanical quantum networks have emerged as a promising candidate due to their long coherence times [2] and their ability to interface distinct quantum systems, such as superconducting and optical devices. In recent years, multimode optomechanical systems have been intensively explored for generating multipartite entanglement and correlated many-body states [3]. A key resource for quantum networks is cluster states [4]. Continuous-variable (CV) cluster states provide a powerful framework for processing CV quantum information, and large-scale implementations with more than 10^4 modes have been experimentally demonstrated [5, 6, 7]. In mechanical platforms, CV cluster states have primarily been studied using steady-state engineering approaches [8, 9].

Here, we investigate the pulsed generation of CV cluster states in an optomechanical quantum network using quantum control techniques [10]. We consider (i) a three-step protocol based on pulse engineering and (ii) a one-step protocol employing antum optimal control for an optomechanical configuration similar to that of Ref. [2]. The tunability of the system enables the generation of CV cluster states with only linear scaling of resources. We characterize the performance and scalability of these protocols by evaluating the average nullifier of the mechanical modes in the presence of environmental noise and dissipation. Our results reveal that increasing squeezing does not monotonically improve the quality of the cluster states. Furthermore, the quantum optimal control approach can significantly outperform the pulse engineering protocol in robustness against noise. These findings provide new insights into the controlled generation of entangled CV resources in hybrid optomechanical quantum networks and their potential for scalable quantum technologies.

References

[1] J. I. Cirac, P. Zoller, H. J. Kimble, and H. Mabuchi, *Quantum state transfer and entanglement distribution among distant nodes in a quantum network*, Phys. Rev. Lett. **78**, pp. 3221 - 3224 (1997).

[2] M. C. Kuzyk and H. Wang, *Scaling phononic quantum networks of solid-state spins with closed mechanical subsystems*, Phys. Rev. X **8**, 041027 (2018).

[3] M. Aspelmeyer, T. J. Kippenberg and F.Marquardt, *Cavity optomechanics*, Rev. Mod. Phys. **86**, pp. 1391 - 1452 (2014).

[4] H. J. Briegel and R. Raussendorf, *Persistent entanglement in arrays of interacting particles*, Phys. Rev. Lett. **86**, pp. 910 (2001).

[5] C. Weedbrook, S. Pirandola, R. García-Patrón, N. J. Cerf, T. C. Ralph, J. Shapiro and S. Lloyd, *Gaussian quantum information*, Rev. Mod. Phys. **84**, pp. 621 - 669 (2012).

[6] J. Zhang and S. L. Braunstein, *Continuous-variable gaussian analog of cluster states*, Phys. Rev. A **73**, 032318 (2006).

[7] N. C. Menicucci, P. van Loock, M. Gu, C. Weedbrook, T. C. Ralph and M. A. Nielsen, *Universal quantum computation with continuous-variable cluster states*, Phys. Rev. Lett. **97**, 110501 (2006).

[8] O. Houhou, H. Aissaoui and A. Ferraro, *Generation of cluster states in optomechanical quantum systems*, Phys. Rev. A **92**, 063843 (2015).

[9] N. Yazdi, S. Zippilli and D. Vitali, *Generation of stable gaussian cluster states in optomechanical systems with multifrequency drives*, Quantum Sci. Technol. **9**, 035001 (2024).

[10] A. Govindarajan, M. Mazzei, H. Wang and L. Tian, *Pulsed Generation of Continuous-Variable Cluster States in a Phononic Quantum Network*, Preprint ArXiv:2509.12529.

The Chern Theorem and Topological Matter in Fast-Rotating Atomic Nuclei

Mike Guidry[1]

[1] *University of Tennessee, USA, guidry@utk.edu*

The Chern theorem is applied to intrinsically-deformed atomic nuclei, leading to states exhibiting topological quantization of the rotation-aligned component of angular momentum averaged over Hilbert space [Mike Guidry and Yang Sun, PRL 136, 062502 (2026)]. These topologically quantized alignment (TQA) states can emerge when collective rotation breaks intrinsic-frame time reversal symmetry, and differ fundamentally from traditional nuclear states. They exhibit formal analogies with the integer quantum Hall effect, and are a first suggestion that topological matter with novel properties might exist in nuclei. We discuss experimental signatures and speculate that TQA bulk–boundary correspondence could lead to a nuclear Chern insulator, where a rotating nucleus has an insulating bulk and unidirectional charged and uncharged currents at its surface, with detectable consequences for the energy spectrum.

References

[1] Mike Guidry and Yang Sun, PRL 136, 062502 (2026)

Super-Poissonian squeezed light in the deep-strong-coupling regime of the quantum Rabi model

Chon-Fai Kam[1,2], Xuedong Hu[2]

[1] *University of Palermo, Italy, dubussygauss@gmail.com*
[2] *University at Buffalo, The State University of New York, Buffalo, New York, xhu@buffalo.edu*

By analytically solving the quantum Rabi model, we investigate the photonic properties of its ground eigenstate [1]. In particular, we find that in the deep-strong-coupling regime, where the coupling strength g exceeds the mode frequency ω and the photonic state is effectively squeezed in one of its quadratures. The squeezing reaches its maximum at the curve corresponding to the quantum phase transition of the quantum Rabi system and decreases rapidly on both sides of the phase transition. Notably, for $g/\omega \approx 3$, which is experimentally testable in existing trapped-ion platforms, the achievable squeezing parameter can reach approximately $r \approx 0.8$. Intriguingly, the photonic state is squeezed while its number distribution follows a super-Poissonian distribution, with the largest deviation from Poissonian behavior occurring at the phase transition between the normal and superradiant phases. In other words, the ground state of the quantum Rabi model contains super-Poissonian quantum squeezed photons.

We acknowledge support by US ARO and AFOSR.

References

[1] C. Kam and X. Hu, *Super-Poissonian squeezed light in the deep-strong-coupling regime of the quantum Rabi model*, Phys. Rev. A **113**, 033718 (2026).

Testing non-Gaussian entanglement and its applications

Y. Xiang[1]

[1] *Ministry of Education Key Laboratory for Nonequilibrium Synthesis and Modulation of Condensed Matter, Shaanxi Province Key Laboratory of Quantum Information and Quantum Optoelectronic Devices, School of Physics, Xi'an Jiaotong University, Xi'an 710049, China*

Entanglement is seen as a crucial resource for applications ranging from quantum cryptography, quantum metrology, and quantum computation. Recently, significant breakthroughs have recently been achieved in the experimental preparation of non-Gaussian entanglement, which provides strong support for the implementation of universal continuous-variable (CV) quantum computation. However, experimentally detecting entanglement in such complex systems remains a challenging problem, as conventional criteria relying on the density matrix would fail where a full state reconstruction is nearly impossible. In our recent work [1], we propose a neural network to detect CV entanglement, especially for the whole class of experimentally achievable non-Gaussian states, based only on four correlation patterns that can be easily measured via homodyne measurements. Then we extend this framework to classify the entanglement structures of arbitrary multipartite non-Gaussian states [2]. To address the challenge in simulating multipartite CV systems, we propose a quantum data augmentation method that significantly enhances the classification accuracy. Inspired by the resource-preserving free operations in quantum resource theory, a wider range of label-preserving transformations can be designed to be the data augmentation operations and increase the volume and diversity of the training dataset effectively.

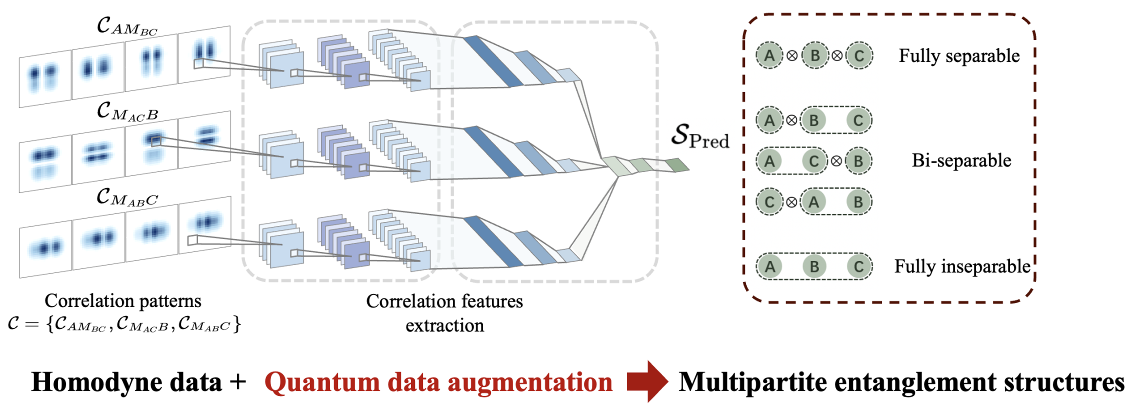

Figure 1: The neural network architecture for the task of testing tripartite non-Gaussian entanglement. Three groups of correlation patterns $C_{AM_{BC}}$, $C_{M_{AC}B}$, and $C_{M_{AB}C}$ provide correlation features of $A-BC$, $B-AC$, and $C-AB$ splitting, respectively. Mode M_{ij} denotes an output mode by mixing modes i and j. The features are extracted by convolutional layers and subsequently classified by fully connected layers into three classes of tripartite entanglement structures.

References

[1] X. Gao, M. Isoard, F. Sun, C. E. Lopetegui, Y. Xiang, V. Parigi, Q. He, and M. Walschaers, *Correlation-pattern-based continuous-variable entanglement detection through neural networks*, Phys. Rev. Lett. **132**, 220202 (2024).

[2] X. Gao, M. Tian, F. Sun, Y. Wu, Y. Xiang, and Q. He, *Use This Template*, in *Classifying Multipartite Continuous Variable Entanglement Structures through Data-augmented Neural Networks*, arXiv: 2409.07909.

Quantum Subspace Expansion Guided by Approximate Symmetries

T. Zeng[1], A.F. Izmaylov[2]

[1] *York University tzeng@yorku.ca*
[2] *University of Toronto artur.izmaylov@utoronto.ca*

Traditional quantum chemistry algorithms on near-term quantum hardware, particularly those utilizing the Variational Quantum Eigensolver (VQE), are severely bottlenecked by deep quantum circuit complexities. Conversely, classical electronic structure algorithms are limited by the exponential scaling of computational costs with basis set size. Quantum Subspace Expansion (QSE) algorithms offer a compelling compromise between these two paradigms. However, QSE approaches frequently suffer from severe numerical instability, giving rise to ill-conditioned matrices when non-orthogonal basis states are generated via quantum circuits.To resolve this bottleneck, we introduce the concept of leveraging approximate symmetries—such as seniority constraints—to systematically structure and optimize the QSE basis. In this talk, we present our recent advances in this direction, detailing the selection of robust approximate symmetry operators. We demonstrate the numerical stability and accuracy of this framework using representative benchmarks on (N_2) and (H_2O) molecular systems. Finally, we discuss prospective generalizations of utilizing approximate symmetries to shield and optimize broader quantum computing architectures.

The VII International AMMCS
Interdisciplinary Conference
Waterloo, Ontario, Canada

Sentiment-Augmented State-Space Models

M. Abdolahi M. S.[1], R. Makarov[2]

[1] *Wilfrid Laurier University, Waterloo, Canada, mabdolahimoghadamsal@wlu.ca*
[2] *Wilfrid Laurier University, Waterloo, Canada, rmakarov@wlu.ca*

Financial markets are shaped by both quantitative signals and qualitative narratives that propagate continuously through financial news. This work develops a unified framework that systematically integrates text-based sentiment into return and volatility forecasting models to better capture asset return distributions, long-memory volatility, and latent market regimes. The empirical analysis is based on over 347,000 firm-specific news headlines and matched financial data for 37 assets spanning equities, cryptocurrencies, and commodities from March 2022 to January 2025. Market sentiment is quantified using two complementary NLP pipelines: a domain-specific FinBERT transformer [1] that produces continuous polarity scores, and a Random Forest classifier trained on TF-IDF bag-of-words features that delivers directional news-impact probabilities at four intraday and interday horizons.

To characterize time-varying market conditions, the framework focuses on sentiment-augmented state-space models [4], specifically three Hidden Markov Model (HMM) architectures: discrete-emission HMMs, Gaussian HMMs, and autoregressive HMMs [3]. Sentiment measures are incorporated as exogenous covariates in the emission dynamics to refine inference of latent regimes associated with bullish, bearish, and high-volatility periods [2]. The proposed methodology jointly targets (i) accurate decoding of hidden state sequences and (ii) economic interpretability of state-dependent distributional and risk characteristics once sentiment information is embedded in the latent structure.

The modelling pipeline culminates in sentiment-augmented Discrete, Gaussian, and Autoregressive HMMs coupled with a novel analogue-based forecasting algorithm that exploits regime-conditional likelihoods for return forecasting. Empirically, enriching state-space models with text-derived sentiment signals substantially sharpens regime detection and improves predictive performance: the integrated framework raises out-of-sample directional forecasting accuracy for 94.4% of the assets, with an average improvement of 20.30% relative to benchmark models without sentiment. Overall, the results provide an interpretable and statistically robust toolkit at the intersection of behavioural finance and machine learning, and demonstrate that qualitative market narratives leave measurable, systematic, and exploitable imprints in asset price dynamics.

References

[1] D. Araci, *FinBERT: Financial Sentiment Analysis with Pre-trained Language Models*, arXiv preprint arXiv:1908.10063 (2019).

[2] J. Wang, *Regime-Switching Factor Investing with Hidden Markov Models*, *Journal of Risk and Financial Management* **13**, 12, p. 311 (2020).

[3] L. Oelschläger, T. Adam and R. Michels, *fHMM: Hidden Markov Models for Financial Time Series in R*, *Journal of Statistical Software* **109**, 9, pp. 1–25 (2024).

[4] R. Bhar and S. Hamori, *Hidden Markov Models: Applications to Financial Economics*, Springer Science & Business Media, New York (2006).

Likelihood inference for discrete stable count models on the Poisson–Tweedie boundary

S. Chen[1], Dr. Z. Wang[1], Dr. D. Soave[1,2]

[1] *Wilfrid Laurier University, Waterloo, Canada*
[2] *Ontario Institute for Cancer Research, Toronto, Canada*

This paper develops likelihood-based inference for discrete stable count models arising as the boundary case of the Poisson–Tweedie family. These models provide a flexible framework for heavy-tailed and overdispersed count data, but induce a nonregular inference problem because the null model lies on the boundary of the parameter space, invalidating standard χ^2 theory for likelihood ratio tests.

We construct a numerically stable maximum likelihood estimation (MLE) framework for both the discrete stable submodel and the full Poisson–Tweedie family. Since the likelihood lacks a closed form, inference is based on recursive evaluation of probabilities and their derivatives. A key theoretical contribution is the establishment of polynomial–logarithmic boundedness for the score and Hessian under a compound Poisson–Sibuya representation. These results ensure integrability of likelihood derivatives and justify stable numerical optimization, with the score growing at most logarithmically in the data and the Hessian controlled by a squared-log envelope.

Using this structure, we implement MLE under nonlinear constraints and study likelihood ratio testing at the boundary. We compare the classical χ^2 calibration with a candidate chi-bar-square (adjusted LRT, aLRT) motivated by nonregular likelihood theory. The aLRT provides a practical boundary correction in the absence of a fully derived asymptotic distribution.

Monte Carlo experiments show that the classical LRT is conservative under the null model, while the aLRT is more aggressive in rejection. Both procedures maintain useful power against negative binomial and near-boundary Poisson–Tweedie alternatives.

An application to National Flood Insurance Program claim counts illustrates the method.

Overall, the results demonstrate how boundedness conditions enable stable MLE in nonregular boundary models and how adjusted likelihood ratio procedures provide a practical—though sensitive—tool for inference in Poisson–Tweedie boundary settings.

The VII International AMMCS
Interdisciplinary Conference
Waterloo, Ontario, Canada

Design-Aware Survival Analysis: Doubly-Robust Estimation under Complex Probability Sampling

Ipseeta Garg[1], David Soave[2], Zilin Wang[3]

[1] *Wilfrid Laurier University, Waterloo, Canada, garg4110@mylaurier.ca*
[2] *Wilfrid Laurier University, Waterloo, Canada, dsoave@wlu.ca*
[3] *Wilfrid Laurier University, Waterloo, Canada, zwang@wlu.ca*

We propose a framework for estimating population-level survival probabilities by integrating information from non-probability cohorts and complex probability surveys. Large health cohorts often contain rich longitudinal time-to-event outcome data but are not representative of the target population, whereas probability surveys provide design-weighted, population-representative covariate information but often lack detailed survival outcomes. The objective of this work is to combine these complementary data sources to obtain valid population-level survival and risk estimates under censoring.

A central challenge in using non-probability cohorts is selection bias arising from unknown inclusion mechanisms. Established inverse probability weighted (IPW) Kaplan-Meier estimators address this issue by reweighting the cohort toward the survey-representative population using estimated inclusion probabilities that are derived from auxiliary covariates observed in both data sources. Similarly, Cox-based outcome regression (OR) estimators use survival models fitted within the cohort to predict population-level survival quantities. However, the validity of these approaches depends on the correct specification of their respective working models: the inclusion model for inverse probability weighting and the survival outcome model for regression-based estimators. Misspecification of either model can lead to substantial bias in the resulting survival estimates.

We extend the doubly robust estimation methodology proposed by [1] to censored survival outcomes by combining inclusion probability-based weighting with outcome regression while incorporating the complex survey design. The proposed estimators remain consistent when either the inclusion model or the survival outcome model is correctly specified. The framework extends the doubly robust inference methodology for continuous outcomes to survival settings, including Kaplan-Meier and Cox proportional hazards models.

Simulation studies evaluate unweighted cohort analyses, inverse probability weighted estimators, regression-standardized estimators, and the proposed doubly robust estimators with respect to bias, efficiency, coverage probability, robustness to model misspecification, and variance estimation. Preliminary findings indicate that the IPW estimators perform well under correct specification of the inclusion model but deteriorate under misspecification. Similarly, the Cox-based OR estimator performs well when the outcome model is correctly specified but fails under misspecification. Whereas the proposed doubly robust estimators maintain improved robustness provided that at least one working model is correctly specified.

The applied component estimates population breast cancer risk by integrating longitudinal outcome data from the Ontario Health Study with design-weighted covariate information from the Canadian Community Health Survey. The analysis produces adjusted estimates of age-specific breast cancer-free survival and corresponding breast cancer risk in the target population.

References

[1] Y. Chen, P. Li and C. Wu, *Doubly robust inference with nonprobability survey samples*, Journal of the American Statistical Association **115**, 532, pp. 2011-2021 (2020).

The VII International AMMCS
Interdisciplinary Conference
Waterloo, Ontario, Canada
August 17-21, 2026

Pricing American Options with Reinforcement Learning

Shamimeh Heydari[1], François-Michel Boire[1], Maia Fraser[1]

[1] *Department of Mathematics and Statistics, University of Ottawa, Ottawa, Canada*
sheydari@uottawa.ca, francois-michel.boire@uottawa.ca, mfrase8@uottawa.ca

We study a martingale-based reinforcement learning framework for pricing European and American-style options. The American problem is formulated as an optimal stopping problem and recast as a penalized stochastic control problem with randomized stop/continue actions, following recent developments in continuous-time reinforcement learning [1].

Our approach uses shared neural networks conditioned on contract characteristics and trained jointly across multiple maturities, strikes, volatilities, and moneyness levels. The learning procedure combines two complementary modes: an offline procedure based on complete simulated paths and an online temporal-difference-type procedure based on one-step martingale orthogonality, both derived from the martingale characterization of value functions [2].

The method first pre-trains a European value approximation from simulated risk-neutral paths and then uses it as a fixed baseline for learning the American early-exercise premium. The final American price is obtained by executing the deterministic stopping rule induced by the learned premium. Under Black–Scholes dynamics, the stopping-based American prices remain accurate across the nine tested contracts, with mean relative errors of 1.33% offline and 1.02% online, and maximum errors of 2.40% and 2.90%, respectively.

We also test the same learned-baseline structure under moderate Merton jump-diffusion dynamics. Although the European value surface is harder to learn in this setting, the American stopping-based prices remain stable, with a mean relative error of 2.08% and a maximum error of 7.03%, the latter occurring in a medium-maturity at-the-money contract with a small early-exercise premium.

Higher-order sensitivities, especially gamma, are more challenging to estimate near payoff kinks and stopping boundaries under the Black–Scholes model, whereas they appear markedly more stable under the Merton model. Overall, these results suggest that martingale-based reinforcement learning provides a flexible framework for learning option values and stopping rules across both diffusion and jump-diffusion dynamics.

References

1. M. Dai, Y. Sun, Z. Q. Xu, and X. Y. Zhou (2025). *Learning to optimally stop diffusion processes, with financial applications*. arXiv:2408.09242.

2. Y. Jia and X. Y. Zhou (2022). *Policy evaluation and temporal-difference learning in continuous time and space: A martingale approach*. Journal of Machine Learning Research, 23.

Positive Returns, Negative Outcomes: Identifying the Dominant Drivers of Retirement Ruin

A. Iu[1]

[1] *Wilfrid Laurier University, Waterloo, Canada, iuxx9590@mylaurier.ca*

The transition from the asset accumulation phase to the decumulation phase marks a fundamental shift in an individual's financial risk landscape. While working years are focused on capital growth, the retirement phase is governed by the precarious objective of sustaining lifelong consumption while mitigating the threat of portfolio depletion. Conventionally, downside market volatility dominates public discourse and shapes the immediate fears surrounding retirement security. This presentation challenges that narrative by examining the joint impact of market returns and inflation regimes on the long-term viability of a wealth portfolio under continuous, inflation-adjusted withdrawals.

By analyzing simulated wealth trajectories and distinguishing between portfolios that achieve long-term survival and those that reach premature depletion, we isolate the specific factors that drive portfolio exhaustion. Our findings reveal a striking paradox: ruined portfolios are rarely characterized by catastrophic equity collapses or severe short-term market shocks. Instead, under elevated inflationary regimes, the minimum return threshold required to ensure portfolio survival shifts significantly upward. Consequently, portfolios frequently face complete exhaustion despite realizing positive asset returns, simply because investment gains fail to generate a sufficient real spread over compounding, inflation-indexed withdrawal demands.

Statistical modelling and robustness checks under simulated market distress further demonstrate that the temporal duration of an inflationary deficit serves as a far more potent and reliable predictor of retirement failure than episodes of extreme market underperformance. Short-term market crashes prove to be largely recoverable, whereas the persistent, long-term erosion of real asset value acts as the dominant structural driver of portfolio ruin. This study highlights the fundamental importance of incorporating inflation sensitivity explicitly into retirement planning, and demonstrate that evaluating decumulation frameworks solely against worst-case return shocks fails to capture the true risks to long-term portfolio sustainability.

Goalscoring Positioning Value: A Metric for Strikers' Off-Ball Positioning in Soccer

J. Jeffreys[1], D. Becker[2], X. Wang[3]

[1] *Wilfrid Laurier University, Waterloo, Canada, jeff8620@mylaurier.ca*
[2] *Wilfrid Laurier University, Waterloo, Canada, dbecker@wlu.ca*
[3] *Wilfrid Laurier University, Waterloo, Canada, xwang@wlu.ca*

Brentford FC owner Matthew Benham, known for his data-driven scouting approach, recently said "For a striker, getting in position is way more informative than finishing". Commonly used metrics, such as expected goals, quantify the quality of shots being taken. A limiting factor of this metric is that it requires a shot to be taken. There are many instances in which a striker gets themselves in a goal scoring position, but a shot is not taken, such as a last-ditch tackle by a defender, or a misplaced pass by a teammate. Other studies have tried to quantify the off-ball positioning of players, such as Off-Ball Scoring Opportunities (OBSO) [1], and have quantified the value of a possession, such as Expected Possession Value (EPV) [2]. Using physics-based models and machine learning models, this research aims to create a new metric, Goalscoring Positioning Value (GPV), that can be applied to individual players to quantify how well they get into reachable goalscoring positions.

To build these models, we use the publicly available Metrica tracking data [3] for initial model development. We hope to also incorporate tracking data from other data sources going forward. We begin by adapting the physics-based pitch control model proposed by Spearman [1] into an individual player pitch control model by considering each player's contribution independently, rather than aggregating within a single team. Using this pitch control model, we then build a pass selection model to estimate where a pass is likely to be played. Following this, we will investigate machine learning methods to find the likelihood of a goal being scored from these high probability locations. Then using our individual player pitch control model, we can see what offensive players occupy these areas. Uncertainty from each component will be propagated and quantified within the GPV framework. This will allow us to determine whether differences between players are statistically meaningful. This model is intended to assist with scouting strikers, potentially uncovering smart recruits for a soccer team that current metrics may undervalue, such as good strikers on poor teams who may be getting into goalscoring positions without receiving the ball.

References

[1] W. Spearman, *Beyond Expected Goals*, in *Proceedings of the 12th MIT sloan sports analytics conference* (pp. 1-17) (2018).

[2] J. Fernández, L. Bornn and D. Cervone, *A framework for the fine-grained evaluation of the instantaneous expected value of soccer possessions*, Machine Learning **110**, 6, pp. 1389-1427 (2021).

[3] https://github.com/metrica-sports/sample-data

The VII International AMMCS
Interdisciplinary Conference
Waterloo, Ontario, Canada
May 28, 2026

Time Series Mediation Analysis with Non-Linear and Machine Learning Methods

T. Marsh[1], D. Becker[2]

[1] *Wilfrid Laurier University, Waterloo, Canada, mars1283@mylaurier.ca*
[2] *Wilfrid Laurier University, Waterloo, Canada, dbecker@wlu.ca*

Non-linearity in mediation analysis has been primarily studied in the context of binary variables which encode a treatment and control, estimating a 'direct' and 'indirect' effect of a covariate (a.k.a. treatment) X on a response Y, with a third variable M (the 'mediator') that is affected by X and in turn affects Y. The focus of mediation analysis in general is to quantify the overall effect of X on Y, including the effect through M. This presentation will focus on one or more continuous treatments and apply non-linear methods, including splines and machine learning models, to mediation analysis in a time series context.

We first explore ARX models modeling X as an AR(p) model, and M, and Y as ARX models (with X and M as exogeneous variables in the definition of Y, and X as an exogenous variable in the definition of M), and find the associated covariances and autocovariances. With this structure, we note that the value of Y at time t depends on the value of X at time $t-1$ as well as M at time $t-1$, which in turn depends on X at time $t-2$; the effect of X on Y requires two time steps in order to go through M.

We then explore splines for each of the models, leveraging the additive basis structure with consistent bases to define a mediation model with as many mediators as there are basis functions. The differentiability of splines allows us to use a derivative definition of the indirect and direct effect to determine how X affects Y. Finally, the derivative definition of the direct and indirect effects can be approximated numerically using the output of a black box model where necessary, allowing our results to apply a broader class of machine learning models. We pay special attention to explainable machine learning methods that produce a differentiable function. Overall, we provide a framework by which mediation analysis can be performed for any time series data. We demonstrate the use and interpretation of this approach using economic indicators that have an assumed causal effect on each other.

The VII International AMMCS
Interdisciplinary Conference
Waterloo, Ontario, Canada

Long-Lasting, Slowly Varying Transient Dynamics from Nonequilibrium Transient Centers

A. Pasion[1,2], F. Magpantay[1]

[1] *Queen's University, Kingston, Ontario, Canada*
[2] *University of the Philippines Baguio, Baguio City, Philippines*

Analysis of mathematical models in ecology and epidemiology often emphasizes asymptotic dynamics, such as stable equilibria and periodic orbits. However, many biologically relevant trajectories exhibit long transient dynamics in which a chosen observable evolves slowly for an extended period before a comparatively rapid transition occurs. On the finite time scales relevant to data collection, management, and intervention, these transients can be more informative than the eventual asymptotic outcome. In this work, we study long-lasting and slowly varying transient dynamics in continuous-time systems through the framework of nonequilibrium transient centers. These special points provide a geometric mechanism for prolonged slow evolution without requiring the trajectory to be near an equilibrium or attractor. We describe how nonequilibrium transient centers give rise to slow regions, how trajectories are drawn into and later escape from these regions in finite time, and how this can generate transients whose duration can be made arbitrarily large. We then illustrate the theory with applications to predator-prey and epidemiological models, focusing on regimes where population densities or disease prevalence remain low for long intervals before an abrupt qualitative shift.

The VII International AMMCS
Interdisciplinary Conference
Waterloo, Ontario, Canada

A Modified Iteration Framework for Pricing American Options

R. Mark Reesor[1], Lars Stentoft[2], Xiaotian Zhu[3]

[1] *Wilfrid Laurier University, Waterloo, Canada, mreesor@wlu.ca*
[2] *University of Western Ontario, London, Canada, lars.stentoft@uwo.ca*
[3] *University of Western Ontario, London, Canada, xzhu444@uwo.ca*

This paper investigates reinforcement learning based algorithms for pricing American options and documents several limitations of standard iterative approaches, including Fitted Q Iteration (FQI) and Least Squares Policy Iteration (LSPI). In particular, we show that both methods tend to overprice American options in many settings due to error amplification in continuation value estimation. Motivated by [1], we develop modified policy iteration algorithms, Modified FQI (MFQI) and Modified LSPI (MLSPI), that restrict policy updates to in the money paths and estimate option values using implied optimal stopping times. Extensive simulations show that the proposed methods deliver substantially lower bias, reduced RMSE, and improved stability relative to standard FQI and LSPI. Compared with a state-of-the-art regression-based benchmark, they provide comparable accuracy in large samples while remaining greater robust in small samples. These results establish the modified policy iteration approach as an efficient and reliable alternative for American option valuation.

References

[1] F. A. Longstaff and E. S. Schwartz, *Valuing American options by simulation: A simple least squares approach*, Rev. Financ. Stud. **14**, 1, pp. 113-147 (2001).

Mitigating Hallucination in Large Language Models through Data Normalization

Y. Shen[1], T. Rathaur[1], R. A. Adeniyi[1], S. Sehra [1], X. Wang [1]

[1] *Wilfrid Laurier University, Waterloo, Canada*

Large language models are widely used in life and across many areas of academic work, such as information query, writing assistance and problem solving, etc. However, their reliability remains a great concern. The literature shows that LLM reliability is compromised by hallucinations, in which model-generated answers sound fluent but are factually incorrect or lack evidence [1, 2]. Although existing studies have discussed hallucination from several perspectives, the role of normalization has not been sufficiently explored. The current work examines the impact of different normalization methods, including input normalization, embedding scaling, activation normalization, and output probability calibration, on hallucination problems.

This work addresses the hallucination problem as a measurable statistical behavior linked to distribution shifts, expression instability, and poor calibration. We adopted different normalization strategies to test factual question answering, summarization, and reasoning tasks using open-source models and finally compared the hallucination rate, calibration error, and robustness of the models under domain shift. We propose breaking down the monofact frequency MFd that causes the hallucination lower bound in the Kalai-Vempala [3] paper into two parts, $\mathrm{MFd}=\mathrm{MFd}_s+\mathrm{MFd}_n$. Here, MFd_s represents the structural factor (true facts that are rare) and MFd_n represents the noise factor. For normalization process N with efficiency of $\eta \in [0,1]$, the bound shifts by $\eta \cdot \mathrm{MFd}_n$. Thus, surface-based normalization is effective for MFd_n-dominated corpora, such as retrieval-augmented generated data, but not for corpora that are dominated by MFd_s (curated misconception benchmarks). The empirical analysis using TruthfulQA ($n = 100$, independent judge) found that the base rate for hallucination is 11% and the theoretical floor is 50% for $\mathrm{MFd} = 0.95$ and $\mathrm{ECE} = 0.10$. The surface normalization and collapse of duplicates yield modest results of 15–17%, matches our expectation for the structurally rare benchmark in the low-MFd_n portion of the plane, where normalization is expected to be weak. This also aligns the empirical findings of Miao *et al.* [4] on the monofact–miscalibration trade-off.

The work presents that the choice of normalization can improve calibration and effectively reduce hallucinations for specific types of hallucinations. It treats normalization as a controlled experimental factor and measures whether changes in input normalization, embedding scaling, activation normalization, and output calibration are associated with changes in factuality hallucination, faithfulness hallucination, and confidence-weighted hallucination risk.

References

[1] Ji, Z., Lee, N., Frieske, R., Yu, T., Su, D., Xu, Y., Ishii, E., Bang, Y. J., Madotto, A., and Fung, P., *Survey of Hallucination in Natural Language Generation*, *ACM Computing Surveys*, 55(12). https://doi.org/10.1145/3571730,(2023).

[2] Huang, L., Yu, W., Ma, W., Zhong, W., Feng, Z., Wang, H., Chen, Q., Peng, W., Feng, X., Qin, B., and Liu, T., *A Survey on Hallucination in Large Language Models: Principles, Taxonomy, Challenges, and Open Questions*, *ACM Transactions on Information Systems*, 43(2)., https://doi.org/10.1145/3703155, (2025).

[3] Kalai, A. T., and Vempala, S. S., *Calibrated Language Models Must Hallucinate*, *arXiv:2311.14648v3*, (2024).

[4] Miao, Y., and Kearns, M., *Hallucination, Monofacts, and Miscalibration: An Empirical Investigation*, *Proceedings of the National Academy of Sciences (PNAS)*, *arXiv:2502.08666*, (2026).

The Summation-by-Parts Framework for Training Neural Networks

Maryam Yalsavar[1], Dongze Li[2], David C. Del Rey Fernández[3]

[1] *University of Waterloo, Waterloo, Canada, myalsava@uwaterloo.ca*
[2] *University of Waterloo, Waterloo, Canada, d336li@uwaterloo.ca*
[3] *University of Waterloo, Waterloo, Canada, ddelreyfernandez@uwaterloo.ca*

Since the seminal work of Raissi, Perdikaris and Karniadakis [1], there has been an explosion in developing physics informed neural network (PINNs) approaches ranging form forward and inverse problems and a variety of linear and nonlinear partial differential equations (PDEs). Current state-of-the-art PINNs approaches are capable of solving parametrized problems and significant headway has been made in solving for weak solutions [3, 5]. Moreover, recently remarkable improvements have been achieved by the addition of physical constraints such as entropy inequalities to PINNs loss functions [4]. Nevertheless, many PINNs approaches remain costly to train and typically do not provide surrogates with industrially relevant error tolerances. This is particularly true in the context of nonlinear PDEs on complex geometries and when weak solutions are of interest (e.g., shocked problems). Alternatively, a number of works have leveraged numerical methods frameworks, such as finite volume [6] and finite-element [2, 7] methods, to train neural networks. The advantage of using numerical methods frameworks is that the training procedure implicitly leverages the mathematical sophistication of such approaches and often leads to less expensive training procedures and surrogates with better error properties. For example, for methods that employ the weak-form of PDEs, the resulting loss function provides a natural scaling for initial and boundary conditions. In this talk, we look to leverage the summation-by-parts (SBP) framework as a means of training machine learning surrogates. The advantage of the SBP approach is that it results in numerical methods that have provable properties. We take advantage of this to construct loss functions that not only appropriately scale initial and boundary conditions but also provides a principled approach to adding physical constraints like conservation and entropy inequalities. We will examine this approach for a variety of linear and nonlinear PDES (e.g., linear advection and compressible Euler equations) on complex geometry using a variety of ML architectures.

References

[1] M. Raissi, P. Perdikaris, and G.E. Karniadakis, *Physics-informed neural networks: A deep learning framework for solving forward and inverse problems involving nonlinear partial differential equations*, J. Comput. Phys. **378**, pp. 686–707 (2019).

[2] M. Abda, M. Hamedi, E. Piollet, C. Blake, and F.P. Gosselin, *The finite element neural network method: One-dimensional study*, Next Research **2**(4), 100885 (2025). DOI: 10.1016/j.nexres.2025.100885.

[3] E. Kharazmi, Z. Zhang, G. E. M. Karniadakis, *hp-VPINNs: Variational physics-informed neural networks with domain decomposition*, Computer Methods in Applied Mechanics and Engineering, 374 (2021), 113547. DOI: 10.1016/j.cma.2020.113547.

[4] T. De Ryck, S. Mishra, R. Molinaro, *wPINNs: Weak Physics Informed Neural Networks for Approximating Entropy Solutions of Hyperbolic Conservation Laws*, SIAM Journal on Numerical Analysis, 62(2) (2024), 811–841. DOI: 10.1137/22M1522504.

[5] C. Liu, H. Wu, *cv-PINN: Efficient learning of variational physics-informed neural network with domain decomposition*, Extreme Mechanics Letters, 63 (2023), 102051. DOI: 10.1016/j.eml.2023.102051.

[6] T. Li, Y. Zou, S. Zou, X. Chang, L. Zhang, X. Deng, *Learning to solve PDEs with finite volume-informed neural networks in a data-free approach*, Journal of Computational Physics, 530 (2025), 113919. DOI: 10.1016/j.jcp.2025.113919.

[7] R. E. Meethal, A. Kodakkal, M. Khalil et al., *Finite element method-enhanced neural network for forward and inverse problems*, Advances in Modeling and Simulation in Engineering Sciences, 10 (2023), 6. DOI: 10.1186/s40323-023-00243-1.

The VII International AMMCS
Interdisciplinary Conference
Waterloo, Ontario, Canada

Improvement of Frontier-Based Exploration Using Carryover-Recovery Prioritization

Y. Miura[1], S. Tarao[2], T. Tomizawa[3]

[1] *National Institute of Technology, Tokyo College, Japan, s26604@tokyo.kosen-ac.jp*
[2] *National Institute of Technology, Tokyo College, Japan, tarao@tokyo-ct.ac.jp*
[3] *National Institute of Technology, Tokyo College, Japan, tomizawa@tokyo-ct.ac.jp*

In unstructured environments such as disaster sites, a mobile robot must autonomously navigate toward target locations while simultaneously estimating its own pose and constructing a map of unknown space. Frontier-based exploration is a widely adopted approach, where an occupancy grid map models sensor uncertainty and the robot iteratively selects frontiers, i.e., boundaries between known and unknown regions, as navigation targets [1, 2]. However, exploration efficiency is highly dependent on frontier selection strategy, and scattered residual frontiers often lead to significant backtracking during the final phase of exploration.

This study aims to improve the efficiency and reliability of frontier-based exploration by reducing such late-stage backtracking. To address this issue, we focus on high-level target selection rather than low-level continuous motion control. The proposed system adopts a hierarchical structure in which reinforcement learning is used for frontier selection, while rule-based methods are employed for path generation and tracking. This design stabilizes the learning process while ensuring feasible robot motion.

We propose a novel prioritization scheme, termed carryover-recovery prioritization, which evaluates each candidate frontier based on its expected contribution to reducing the remaining unobserved or unexplored regions (referred to as "carryover"). Frontiers with higher recovery potential are assigned higher priority and incorporated into the RL-based target-selection policy. The system is implemented in a Unity-based simulation environment using ML-Agents, where occupancy grid mapping and frontier extraction are developed in C#, and the frontier-selection policy is trained using Proximal Policy Optimization (PPO).

We conducted a comparative evaluation on randomized 30 m $\times$ 30 m occupancy grid maps, using the last 50 episodes of each condition. With carryover-recovery prioritization, 45 episodes successfully completed the coverage of the entire map, while 5 episodes timed out during exploration. Without this prioritization, only 39 episodes completed successfully. Furthermore, among the successful episodes, the carryover-aware policy required 14.90% less travel distance than the baseline. The trained policy with the prioritization also showed a preference for nearby, relatively large frontier clusters, which is supposed to help convert each movement into broader coverage gains. From a computational perspective, GPU acceleration increased stable parallel executions from 6 to 11 during a five-day run, while reducing single learning time by 28.9%. Cumulatively, these improvements yielded an approximate 60% reduction in total time required per execution task.

These results demonstrate that explicitly prioritizing frontiers that effectively resolve carryover significantly enhances exploration efficiency without increasing the complexity of low-level control. This study contributes a practical hierarchical framework for improving autonomous exploration and SLAM-based navigation in unknown environments where prior mapping is unavailable.

References

[1] A. Elfes, "Using occupancy grids for mobile robot perception and navigation," *Computer*, vol. 22, no. 6, pp. 46–57, 1989.

[2] B. Yamauchi, "A frontier-based approach for autonomous exploration," in *Proc. IEEE Int. Symp. Computational Intelligence in Robotics and Automation (CIRA)*, pp. 146–151, 1997.

The VII International AMMCS
Interdisciplinary Conference
Waterloo, Ontario, Canada

Glimpses of Fractal Analysis in the Navier-Stokes Regularity Problem

Jaden Saïd

University of Waterloo, Canada, amadmin@uwaterloo.ca

Twenty-six years after the posing of the Millennium Problems by the Clay Mathematics Institute in 2000 and hundreds since the field of fluid mechanics was born, the study of the incompressible Navier-Stokes Equations (NSE) in 3 dimensions remains a highly active field of research. The motion of fluids is wildly interesting in its own right even without considering the myriad of ways we interact with fluids on a daily basis, be it through the all-encompassing weather or the way one's morning coffee pours into a mug.

Much of the work done towards solving the Navier-Stokes Regularity Problem since the 1950s, when a class of weak solutions to the NSE was introduced by Leray and Hopf, has focused on proving regularity results for different classes of weak solutions. More recently, scholars have taken to the tools of fractal geometry to study the smoothness of these weak solutions in a novel way; instead of thinking about the smoothness of the solution directly via Sobolev theory or perturbation methods as in the 2-dimensional case, the structure of the singular set of weak solutions is studied.

This poster is meant to introduce some of the ways tools from fractal geometry, in particular the Hausdorff dimension, have previously been applied to the study of suitable weak solutions with great success. We will come to understand the regularity problem and what a suitable weak solution is, what the Hausdorff measure is, the geometric intuition of the Hausdorff dimension, and then study the famous result by Caffareli, Kohn and Nirenberg that the set of singular times (those times t for which a suitable weak solution blows up at a point in space) must have Hausdorff dimension less than 1. This fractal-based analysis tells us a great deal about the singular sets of these solutions, and represents a milestone which modern research continues to build off.

References

[1] James C. Robinson; The Navier Stokes regularity problem. *Philos Trans A Math Phys Eng Sci* 26 June 2020; 378 (2174): 20190526.

[2] Caffarelli, L., Kohn, R. and Nirenberg, L. (1982), Partial regularity of suitable weak solutions of the navier-stokes equations. *Comm. Pure Appl. Math.*, 35: 771-831.

[3] Terrence Tao; 245C, Notes 5: Hausdorff dimension. https://terrytao.wordpress.com/2009/05/19/245c-notes-5-hausdorff-dimension-optional/

[4] Scheffer, V; Hausdorff measure and the Navier-Stokes equations. *Commun.Math. Phys.* 55, 97?112 (1977).

The VII International AMMCS
Interdisciplinary Conference
Waterloo, Ontario, Canada

Prototyping of an Omnidirectional Mobile Ball-Throwing Robot for Simulating a Tennis Opponent

N. Sawada[1], S. Tarao[2], T. Tomizawa[3]

[1] *National Institute of Technology, Tokyo College, Japan, s26606@tokyo.kosen-ac.jp*
[2] *National Institute of Technology, Tokyo College, Japan, tarao@tokyo-ct.ac.jp*
[3] *National Institute of Technology, Tokyo College, Japan, tomizawa@tokyo-ct.ac.jp*

In recent years, the development of AI-equipped tennis ball machines has been actively pursued[1][2]. However, many commercially available devices exhibit limitations in both mobility and ball-delivery capabilities, requiring further improvements to realistically emulate a human opponent. This study aims to develop a ball machine system based on a cyber-physical system (CPS), enabling realistic movement and the ability to generate both vertical and horizontal spin.

The system operation is divided into two phases: the return-receiving phase and the launch phase. The return-receiving phase involves tracking and analyzing the balls returned by the player. To achieve this, a simulation environment approximating a real tennis court is constructed using Unity. Within this environment, ball trajectories are learned using a Transformer model[3], enabling estimation of landing position, velocity, and spin rate. Based on these estimations, robot motion is simulated to generate control commands for the physical machine. In contrast, the launch phase determines the robot's actions based on the opponent's return and executes ball delivery. In this phase, models are trained in a simulation environment to determine the type and speed of the return shot based on the incoming ball characteristics and to predict the landing position under given conditions. For locomotion, an omnidirectional mechanism developed in previous research is adopted. This mechanism is designed as a four-wheel-drive system with steering motors on each wheel and is expected to provide improved omnidirectional grip on the contact surface compared to omni-wheels and Mecanum wheels. To date, the basic operation of this omnidirectional mechanism has been preliminarily verified.

This paper reports ball detection using a stereo camera and trajectory learning in the return-receiving phase. Evaluation results in the simulation environment indicate that ball detection is accurate from the robot's baseline to the opponent's baseline under cloudy daytime conditions. However, under sunny daytime or artificially lit nighttime conditions, detection becomes unstable around and beyond the net depending on the ball speed. This instability is attributed to insufficient contrast caused by harsh lighting or longer required exposure times. Regarding trajectory learning, while spin rate estimation showed limited correlation with the ground truth due to visual tracking constraints, other parameters demonstrated robust performance; specifically, position estimation accuracy improved with stronger topspin, while velocity estimation accuracy improved with stronger backspin.

References

[1] Acemate Tennis, *Acemate Tennis Robot | The World's First AI Tennis Rally Robot*, 2026, `https://www.acematetennis.com/`.

[2] pongbot, *Pace S Pro AI Tennis Ball Machine*, `https://store.pongbotsports.com/products/pace-s-pro`

[3] A. Vaswani, N. Shazeer, N. Parmar, J. Uszkoreit, L. Jones, A.N. Gomez, Ł. Kaiser, and I. Polosukhin, *Attention Is All You Need*, in I. Guyon et al. (eds.), Advances in Neural Information Processing Systems 30 (NeurIPS 2017), Curran Associates, Inc., pp. 5998–6008 (2017).

Physics-Informed Neural Networks for Identifying Tumor Metabolic Dynamics

Shadi Vandvajdi [1,2], Mahla Poudineh[1], Mohammad Kohandel[2]
[1] *Department of Electrical and Computer Engineering, University of Waterloo, Waterloo, ON, Canada*
[2] *Department of Applied Mathematics, University of Waterloo, Waterloo, ON, Canada*

Cancer metabolism is characterized by dynamic changes in glucose consumption and lactate production that drive tumor growth and adaptation. We present an integrated experimental–computational framework that combines multiplexed glucose–lactate sensing with Physics-Informed Neural Networks (PINNs) to identify tumor metabolic dynamics from sparse measurements. Experimental glucose and lactate data were integrated with a mechanistic model describing oxidative and glycolytic cell populations and metabolic state transitions. The governing dynamics were represented as a nonlinear system of ordinary differential equations and incorporated into a PINN framework through a composite loss function combining data fidelity and physics-based constraints [1]. This approach enables simultaneous reconstruction of metabolic trajectories and estimation of biologically meaningful parameters. The framework was applied to prostate cancer (DU145) and glioblastoma (GBM) models exhibiting distinct metabolic phenotypes. Results demonstrate accurate reconstruction of glucose and lactate dynamics and robust parameter inference under limited and noisy data conditions. The inferred parameters revealed distinct metabolic phenotypes and transition dynamics, providing quantitative insight into tumor metabolic plasticity. These findings extend previous PINN-based studies of tumor glucose–lactate metabolism [2] and highlight the potential of physics-informed machine learning for characterizing tumor metabolism from limited experimental observations [3].

Tumor metabolic dynamics were modeled using coupled ordinary differential equations describing oxidative and glycolytic cell populations, glucose consumption, and lactate production [4]. The governing equations were incorporated into a Physics-Informed Neural Network framework through a loss function combining data-fitting and physics-based residual terms:

$$\frac{dp_o}{dt} = \frac{1}{\tau_o}(1-p_o-p_g)p_o + \frac{1}{\tau_{go}}\chi_L(L)p_g - \frac{1}{\tau_{og}}\chi_L^*(L)\chi_G(G)p_o, \quad (1)$$

$$\frac{dp_g}{dt} = \frac{1}{\tau_g}(1-p_o-p_g)p_g - \frac{1}{\tau_{go}}\chi_L(L)p_g + \frac{1}{\tau_{og}}\chi_L^*(L)\chi_G(G)p_o, \quad (2)$$

$$\frac{dG}{dt} = -\kappa_o\frac{G}{G+\lambda L+n_*}p_o - \kappa_G\frac{G}{G+G_*}p_g, \quad (3)$$

$$\frac{dL}{dt} = -\kappa_L\frac{L}{G/\lambda+L+m_*}p_o + 2\kappa_G\frac{G}{G+G_*}p_g. \quad (4)$$

$$\mathcal{L} = \lambda_d\,\mathcal{L}_{\mathrm{data}} + \lambda_p\,\mathcal{L}_{\mathrm{physics}}. \quad (6)$$

$$\frac{d\vec{u}(t)}{dt} = \mathcal{N}\vec{u}(t), \quad t\in[0,T]. \quad (5)$$

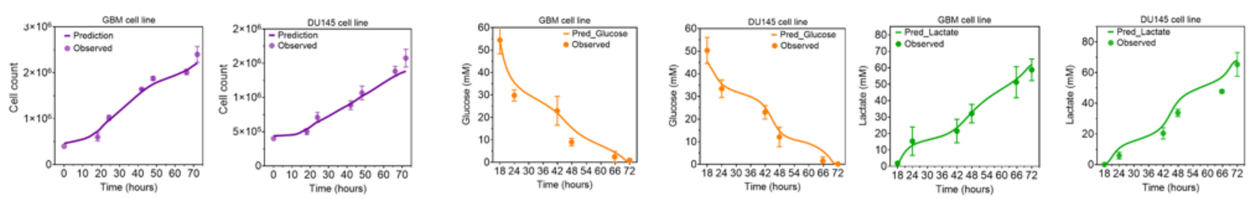

Figure 1. PINN reconstruction of glucose and lactate dynamics for DU145 and GBM cell models. Solid lines represent model predictions, while markers indicate experimental measurements.

References

[1] Raissi, M., Perdikaris, P., Karniadakis, G.E. Physics-informed neural networks: A deep learning framework for solving forward and inverse problems involving nonlinear PDEs.J. Comput. Phys., 378 (2019), 686–707.

[2] Vandvajdi, S., Mao, Y., Poudineh, M., & Kohandel, M. (2025). Investigating glucose–lactate metabolism in glioblastoma multiforme via universal physics-informed neural networks. Mathematical Biosciences and Engineering, 22(9), 2486–2505.doi:10.3934/mbe.2025091.

[3] Vandvajdi, S., Mao, Y., Abouali, H., Shokouhian, B., Daubon, T., Kohandel, M.,& Poudineh, M. (2026). Multiplexed detection and quantification of glucose and lactate during cancer proliferation: an integration of experimental and computational approaches. ACS Sensors, 11, 3190–3203. doi:10.1021/acssensors.5c04493

[4] Mendoza-Juez, B., Martínez-González, A., Calvo, G. F., and Pérez-García, V. M. (2012). A mathematical model for the glucose–lactate metabolism of in vitro cancer cells. Bulletin of Mathematical Biology, 74(5), 1125–1142.

The VII International AMMCS Interdisciplinary Conference Waterloo, Ontario, Canada

Applications of Modeling and Simulation in Wargaming

M. Abdelazez[1], A. Ghanmi[1]

[1] *Defence Research and Development Canada, {mohamed.abdelazez,ahmed.ghanmi}@forces.gc.ca*

The Canadian Joint Warfare Center (CJWC) is modernizing their wargaming capabilities to support future complex multi-domain operations. The CJWC has already explored the applications of Large Language Models (LLMs) to accelerate the development of wargames. Currently, the CJWC is interested in exploring the applications of Modeling and Simulation in Wargaming. This paper presents a literature review of the applications of M&S across the different phases (design, execution, and analysis) of a wargame and recommendations for military organizations on the adoption of M&S for wargaming.

There is no one agreed upon definition of wargaming; the North Atlantic Treaty Organization (NATO) defines wargaming as 'a simulation of a military operation, by whatever means, using specific rules, data, methods and procedures.' [1] Wargaming in defence is applied to develop human decision-making through education and training, to rigorously analyse and test plans across all levels of warfare, and inform real-world executive decisions by exploring future scenarios, assessing risks, and generating insights into how forces, concepts, and technologies may need to adapt [1]. Within the defence community, wargaming is also essential for Professional Military Education (PME), capability development, technology road mapping, and the analytical comparison of courses of action (COAs), making it a foundational tool for shaping both present and future military effectiveness [2]. However, traditional manual methodologies face significant challenges, including inherent qualitative subjectivity, high cognitive load, and lengthy time requirements that limit the number of scenarios explored [3]. Furthermore, manual adjudication is often constrained by the "curse of dimensionality," where the exponential growth of potential combat interactions becomes challenging to monitor [2].

Modeling and Simulation (M&S) mitigates key limitations of traditional wargaming by enabling automated adjudication, reducing human bias, and supporting faster-than-real-time exploration of expanded decision spaces [4]. When integrated with validated combat models, M&S converts qualitative roleplay into quantitative metrics such as lethality, survivability, and mission success probability, strengthening analytical rigor across strategic, operational, and tactical contexts. Advanced methods, including Hierarchical Reinforcement Learning, address problem complexity by decomposing large-scale scenarios into hierarchical sub-tasks [2]. Practical applications span technology assessment through agent-based simulation, tactical support via automated terrain and route analysis, crewed-uncrewed teaming concepts, and theater-level evaluation using Bayesian and network-based models throughout wargame design, execution, and analysis [3-5].

References

[1] M. o. Defence, *Wargaming Handbook*. United Kingdom Minitsry of Defence, 2017.

[2] S. Black, "Mastering the Digital Art of War: Developing Intelligent Combat Simulation Agents for Wargaming Using Hierarchical Reinforcement Learning," *arXiv preprint arXiv:2408.13333,* 2024.

[3] K. Brathen, R. A. Seehuus, and O. M. Mevassvik, "Simulation support to wargaming for tactical operations planning," *Simulation and Wargaming,* pp. 223-247, 2021.

[4] V. Mittal and A. Davidson, "Combining wargaming with modeling and simulation to project future military technology requirements," *IEEE Transactions on Engineering Management,* vol. 68, no. 4, pp. 1195-1207, 2020.

[5] A. Najgebauer, S. Wojciechowski, R. Antkiewicz, and D. Pierzchała, "Simulation and Artificial Intelligence Methods for Wargames: Case Study–"European Thread"," *Simulation and Wargaming,* pp. 157-182, 2021.

Prediction of Lassa Fever Outbreak in Nigeria using Statistical and Machine Learning Algorithms: An Outlook of the Model Performance

M. O. Adenomon[1], F. Apiyanteide[2], S. E. Chaku[3]

1. Nasarawa State University, Keffi, Nigeria, adenomonmo@nsuk.edu.ng
2. Nasarawa State University, Keffi, Nigeria, afranco@datascienceandtech.com
3. Nasarawa State University, Keffi, Nigeria, chakushammah@nsuk.edu.ng

Since the first cases of Lassa fever were diagnosed in Northeastern Nigeria in 1969 [1], the disease has been one of the neglected tropical diseases with no definitive cure, no approved vaccines and poor public health measures to mitigate the burden of the disease. This study sought to compare statistical [2] and machine learning algorithm [3] in the forecasting of Lassa fever in Nigeria and thereafter make a 5-year forecast of the infection using the best performing algorithm. Data for the study was obtained from the Nigerian Centre for Disease Control and Prevention (NCDC) weekly epidemiological report website from 2018 – 2025 using an excel template that collected relevant information of the disease (year, epidemiological week, number of confirmed cases, and number of confirmed deaths). Data collected was uploaded into Google Collaboratory environment with Python 3. This was cleaned and processed using a train-test split of 80:20% with a seeding of the codes to ensure reproducibility and then the development of code pipelines for identified statistical and machine learning algorithms. Model performance evaluation was conducted using R^2, MAE, RMSE and MPD. The best performing models were identified using R^2 and thereafter a 5-years forecast of Lassa fever confirmed cases and deaths in Nigeria was done. Result showed that on the overall, AdaBoost was superior among the competing Machine Learning Algorithms with performance evaluation metric values of 0.7796, 89, 24.11902, 36.63752 and 13.01384 for R2, MAE, RMSE and MPD respectively in predicting confirmed cases of Lassa fever while SARIMA was superior among the competing Statistical Algorithms with performance evaluation metric values of 0.664822, 5.962272, 8.594706 and 11.799430 for R^2, MAE, RMSE and MPD respectively in predicting Lassa fever deaths in Nigeria using historical data from 2018 to 2025. Based on the overall best algorithm for Lassa fever forecast in Nigeria, an estimated 2845 (95% Confidence Interval of 8 to 15518) confirmed cases of Lassa fever are projected to occur in Nigeria from January 2026 – December 2030 while an estimated 781 confirmed deaths (95% Confidence Interval 243 to 1990) are projected to occur in Nigeria from January 2026 to December 2030. This study clearly demonstrates that there is ‘no one size fits all’ algorithm for modelling infectious diseases outbreaks such as Lassa fever. An in-depth understanding of the most suitable algorithm which could be statistical or machine learning model is critical for effective infectious disease modelling.

References

[1]. T.P .Monath, A short history of Lassa fever: the first 10-15 years after discovery. Curr Opin Virol. **37**, pp. 77-83(2019). doi: 10.1016/j.coviro.2019.06.005.

[2]. G.E.P. Box, G.M. Jenkins, G.C. Reinsel, G.M. Ljung, Time series analysis: forecasting and control. 5th ed. Hoboken: John Wiley & Sons; 2015.

[3]. A. Mohamed, M. Abdelrehim, R. Al-Barazie, Context matters in machine learning based disease prediction with insights from diverse clinical and symptom data. Scientific Reports. 28;15(1):42669 (2025).

Analysis of Lassa Fever Cases and Climate in Nigeria using Predictive Supervised Learning

M. O. Adenomon[1], M. J. Davis[2], O.S. Ogungbemi[3], C. A. Adenomon[4], T. J. Babalola[5]

1. Nasarawa State University, Keffi, Nigeria, adenomonmo@nsuk.edu.ng
2. University of Waterloo, Canada, mj2davis@uwaterloo.ca
3. Oregon State University, USA, ogungbeo@oregonstate.edu
4. Federal Medical Centre, Keffi, Nigeria, bukkynet82@gmail.com
5. Federal Polytechnic, Nasarawa, Nasarawa State, babalolajoy643@gmail.com

Lassa fever is an acute viral hemorrhagic fever and a zoonotic disease caused by the Lassa virus, which is endemic in most countries of West Africa [1-2]. The disease is a neglected tropical disease with no definitive cure, no approved vaccines, and poor public health measures to mitigate the burden of the disease. This study employed machine learning algorithms [3] to analyze Lassa fever and climate data to identify the climatic conditions that trigger Lassa fever in Nigeria and the best-performing machine learning algorithm. Data for Lassa fever were obtained from the Nigerian Centre for Disease Control and Prevention (NCDC) weekly epidemiological report website from 2018 to 2025, and climate data were obtained from the climate in Africa website (www.climateinafrica.com). Lagos was used as a proxy for national environmental trends, and to account for ecological delays in vector dynamics, we apply temporal lagging (1-2 months) to climatic predictors (Precipitation and Temperature). We evaluated and compared the predictive performance of four algorithms: Support Vector Regression (SVR), Decision Tree (DT), Random Forest (RF), and Artificial Neural Networks (ANN). To achieve this, the data was cleaned and processed using an 80-20% train-test split with fixed random seeds to ensure reproducibility. Model performance evaluation was conducted using R^2, MAE (mean absolute error), and RMSE (root mean square error). Finally, we used feature importance analysis to provide empirical evidence for the most significant climatic determinants of Lassa fever outbreaks. The result revealed SVR dominated in predicting Lassa fever in Nigeria [3] with R^2=0.5494, MAE=11.902, and RMSE=19.1236, while precipitation was the most significant determinant of the number of Lassa fever cases in Nigeria. This study clearly demonstrates that Lassa fever is transmitted during the wet season. Therefore, personal hygiene and environmental sanitation should be encouraged in both rural and urban communities in Nigeria to curb the spread of Lassa fever during the wet season.

References

[1]. Bond N, Schieffelin JS, Moses LM, Bennett AJ, Bausch DG. A historical look at the first reported cases of Lassa fever: IgG antibodies 40 years after acute infection. The American journal of tropical medicine and hygiene. 2013 Feb 6;88(2):241.

[2]. A. S. Oluwole, T. Nkonyana, Forecasting Lassa Fever Outbreaks progression with Machine Learning. International Conference on Electtrical, Computer, Communications and Machatronics Engineering (ICECCME), 2022, 1-5.

[3]. T. K. Samson, O. Aromolaran, T. Akingbade, Lassa Fever Cases and Mortality in Nigeria: Quantile Regression Vs machine Learning Models. Journal of Public Health in Africa, 2024, 14(12), 2712.

The VII International AMMCS
Interdisciplinary Conference
Waterloo, Ontario, Canada

Time-Symmetric and Symplectic Parallel-in-Time Gauss–Legendre and Hermite Methods for Hamiltonian Systems

Axi Aguilera[1,2], Xiangmin Jiao[1,2], Charalampos Markakis[1]

[1] Department of Applied Mathematics and Statistics, Stony Brook University, Stony Brook, NY, USA, {axi.aguilera, xiangmin.jiao, charalampos.markakis}@stonybrook.edu
[2] Institute for Advanced Computational Science, Stony Brook University, Stony Brook, NY, USA

Long-time energy-preserving simulations in relativistic astrophysics, numerical relativity, celestial mechanics, and related PDE applications demand robust structure-preserving integration. While symplectic and time-symmetric schemes (e.g., Gauss–Legendre and Hermite formulas) effectively preserve phase-space geometry and bound energy drift [1], their sequential time-marching remains constrained by temporal dependency.

To mitigate this bottleneck, this work investigates how existing parallel-in-time (PinT) all-at-once (AAO) paradigms [2, 3] can be adapted for high-order geometric discretizations of Hamiltonian systems. We develop and analyze two novel AAO algorithmic formulations that reorganize the implicit algebraic equations across time slabs. This breaks sequential dependency while strictly preserving the symplectic and time-symmetric properties of the base integrators.

The first algorithm, an AAO self-consistent iteration (AAO-SCI), achieves efficiency through fundamental algorithmic restructuring. By grouping local stage computations across multiple time slabs into batched evaluations of the Hamiltonian vector field, it improves contiguous data access and vectorization. The global trajectory is then reconstructed via a prefix scan. For a discrete state matrix $\mathbf{Y}^{(k)}$, the update is

$$\mathbf{Y}^{(k+1)} = \mathbf{1} \quad \mathbf{y}_0 + h\mathscr{L}\mathscr{F}(\mathbf{Y}^{(k)}), \tag{1}$$

where $\mathscr{L}$ is a lower-triangular accumulation operator. The second algorithm applies an AAO Newton method to the global nonlinear residual. This yields a block lower-bidiagonal Jacobian and an affine recurrence for stage corrections $\delta\mathbf{z}_n$:

$$\delta\mathbf{z}_n = \mathbf{A}_n\delta\mathbf{z}_{n-1} + \mathbf{c}_n. \tag{2}$$

Because affine map composition is associative, Eq. (2) admits a parallel scan-based algebraic solve well-suited for multithreading in addition to vectorization.

To demonstrate practical utility for ODEs and PDEs, we benchmark nonseparable post-Newtonian (1PN–4PN) gravity approximations to the two-body problem in general relativity. By amortizing local iterative overhead, the batched AAO-SCI algorithm yields about an order of magnitude single-core speedup over standard serial implementations. These findings demonstrate how reorganizing existing AAO concepts delivers critical algorithmic acceleration, enabling more efficient, long-time structure-preserving simulations for demanding ODE and PDE applications.

References

[1] J.M. Sanz-Serna, Runge-Kutta schemes for Hamiltonian systems, BIT Numer. Math. 28, 4, pp. 877-883 (1988).

[2] J.L. Lions, Y. Maday, and G. Turinici, A “parareal” in time discretization of PDEs, C. R. Acad. Sci. Paris Ser. I Math. 332, 7, pp. 661-668 (2001).

[3] B.-B. Zhu and Y.-L. Zhao, Symplectic all-at-once method for Hamiltonian systems, Symmetry 13, 10, pp. 1930 (2021).

The VII International AMMCS
Interdisciplinary Conference
Waterloo, Ontario, Canada

Evolutionary Gaslighting: The Emergence of Skepticism in Deceptive Environments

Enamul Haque[1]

[1] *University of Waterloo, Waterloo, Canada,*
enamul.haque@uwaterloo.ca

Every adaptive system relies on environmental signals to guide behaviour, but when signals are systematically corrupted, trust can become a liability. We introduce *Evolutionary Gaslighting*: a condition where environmental signals are inverted at a fixed deception rate δ, and agents evolve a heritable skepticism trait $\sigma \in [0,1]$ – the probability of ignoring the signal and adopting a baseline waiting strategy. Using a payoff matrix that rewards correct action ($+2$), penalises gaslit action (-3), and grants a survival baseline for inaction ($+0.5$), we derive the expected fitness

$$\mathbb{E}[F] = (1-\sigma)(2-5\delta)+0.5\sigma.$$

The evolutionary gradient $\partial\mathbb{E}[F]/\partial\sigma = 5\delta - 1.5$ vanishes at $\delta^* = 0.3$: for $\delta < 0.3$ selection favours trust ($\sigma = 0$); for $\delta > 0.3$ it favours full skepticism ($\sigma = 1$).

We test this prediction with a genetic algorithm simulation ($N = 200$, 250 generations, 30 independent trials per δ). Figure 1 shows the mean evolved $\bar{\sigma}$ across deception rates. The curve is sharply sigmoidal, with the steepest jump ($\Delta\bar{\sigma} = 0.350$) at $\delta = 0.5$, confirming the analytical tipping point. At the transition boundary ($\delta = 0.4$–0.5) we observe *strategy fracturing*: a spike in phenotypic variance (std. dev. $= 0.165$) where trusting and skeptical subpopulations coexist – a computational analogue of biological bet-hedging. At $\delta = 1.0$, the population converges on $\bar{\sigma} = 0.991$ and achieves a fitness floor of 50.0, avoiding the catastrophic -300.0 that a naive trusting strategy would incur.

These results establish skepticism as a mathematically predictable, threshold-triggered evolutionarily stable strategy. The broader implication is that persistent deception can force adaptive systems into epistemic withdrawal – a survival mechanism that, while fitness-preserving, disables learning, coordination, and responsiveness to change. Future work will extend the model to social networks, non-stationary environments, and multi-gene architectures for selective skepticism.

Keywords: Evolutionary game theory, deception, skepticism, misinformation, bet-hedging, artificial life.

References

[1] J. Maynard Smith, *Evolution and the Theory of Games*, Cambridge University Press (1982).
[2] R. Dawkins and J.R. Krebs, *Animal Behaviour* **27**, pp. 1130–1138 (1979).
[3] J. Seger and H.J. Brockmann, *Oxford Surveys in Evolutionary Biology* **4**, pp. 182–211 (1987).
[4] C. Wardle and H. Derakhshan, *Council of Europe report* (2017).

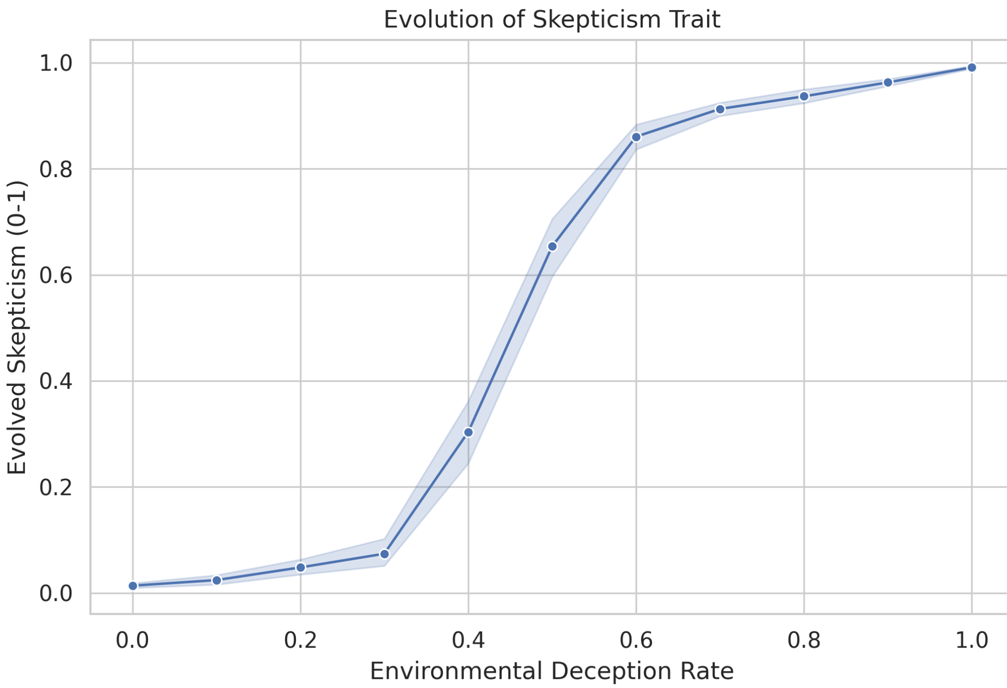

Figure 1: Mean evolved skepticism $\bar{\sigma}$ versus deception rate δ. The sigmoidal transition confirms the predicted tipping point $\delta^* = 0.3$. Error bands show 95% CIs.

The VII International AMMCS Interdisciplinary Conference
Waterloo, Ontario, Canada

Edge-Cloud Runtime Validation of Neural Stimulation Devices Using Timed Colored Petri Nets and Hierarchical Reinforcement Learning

N. Majma[1], S. M. Sharifi[2]

[1] *Naghshejahan Higher Education Institute, Iran, majma@naghshejahan.ac.ir*
[2] *Islamic Azad University, Isfahan Branch, Iran, sharifi@iau.ir*

Brain neural stimulation devices, particularly responsive neural stimulation systems for epilepsy management, require continuous and dependable validation because incorrect decisions during runtime may directly affect patient safety. This study presents an adaptive runtime validation framework for a brain neural stimulation device operating within a Body Area Network and an edge-cloud architecture. Extending our previous work on fuzzy-rule-based WBAN modeling using multi-level fuzzy colored Petri nets and reinforcement learning [1], the proposed framework integrates Timed Colored Petri Nets, fuzzy logic, and hierarchical reinforcement learning to model device behavior, handle uncertainty in physiological and brain signals, and adapt decision-making based on feedback from the patient's body.

In the proposed architecture, real-time sensing and stimulation are performed at the Internet-of-Body device level, while the main validation and decision-making modules are deployed on the edge node to satisfy latency and safety requirements. The edge node executes preprocessing, fuzzy risk assessment, Petri-net-based behavioral modeling, and the hierarchical reinforcement learning agent. The high-level manager selects among monitoring, stimulation delegation, and inhibition actions, whereas the low-level worker generates the stimulation pattern when activated. This manager-worker decomposition follows the principle of hierarchical decision-making and temporal abstraction in hierarchical reinforcement learning [2].

A cloud layer is incorporated as a centralized knowledge and policy-management repository. It stores versioned Policy/RuleSet artifacts, model weights, and performance metadata generated after training or retraining on the edge. This cloud-based layer enables secondary analysis, cross-device knowledge consolidation, comparison of policy versions, and future redeployment of improved policies to other edge nodes without placing the real-time control loop in the cloud. Therefore, the proposed model preserves low-latency runtime validation at the edge while enabling long-term evolutionary learning through cloud-based policy management.

The framework was evaluated using ten expert-defined reference scenarios and an augmented dataset of 1530 scenarios generated through noisy and interpolated physiological profiles. Before learning, the system missed all seizure cases, achieving only 30% accuracy. After hierarchical reinforcement learning, the system achieved 100% sensitivity, 80% accuracy, 83.33% F1-score, 100% correction coverage, and 70% intervention rate. These results indicate that combining formal Petri-net modeling, fuzzy uncertainty handling, hierarchical learning, and cloud-based policy versioning can support safer and more adaptive runtime validation of intelligent neural stimulation devices.

References

[1] N. Majma and S. M. Babamir, Modeling and simulation of fuzzy-rule based WBAN using multi-level fuzzy colored Petri-nets and reinforcement learning, Journal of Computational Science, 83, 102455, 2024. DOI: 10.1016/j.jocs.2024.102455.
[2] S. Pateria, B. Subagdja, A. H. Tan, and C. Quek, Hierarchical Reinforcement Learning: A Comprehensive Survey, ACM Computing Surveys, 54(5), pp. 1–35, 2021. DOI: 10.1145/3453160.

The VII International AMMCS
Interdisciplinary Conference
Waterloo, Ontario, Canada

A Mathematical Investigation of the Role of Intracranial Pressure in the Functional-Structural Interactions of Synchronized Neurons

A. H. Moore[1], C. S. Drapaca[2]

[1] *Pennsylvania State University, University Park, PA, USA ahm5470@psu.edu*
[2] *Pennsylvania State University, University Park, PA, USA csd12@psu.edu*

Elevated intracranial pressure (ICP) and seizures (due to aberrant neuronal synchronization) have been reported in brain diseases like hydrocephalus and traumatic brain injuries [1]. Mechanotransduction processes linking ICP and neuronal functions and synchronization are still poorly understood. This work investigates the functional-structural responses of two nearby (not connected through synapses) synchronized neurons to increased ICP using mathematical modeling and corresponding numerical simulations in MATLAB. A coupled Hodgkin-Huxley-Lotka-Volterra model is proposed that has the following features. Neuronal synchronization is modeled using a given synchronization time and a time-dependent Lagrange multiplier in the Hodgkin-Huxley equations. The ion gates of neuronal membranes are assumed to behave mechanically like fractional Maxwell linear viscoelastic materials [2]. The reversal potentials of the ion species are replaced by extended Nernst potentials that depend not only on the osmotic difference but also on the hydrostatic pressure difference between the intra- and extracellular spaces [3]. Also, an ICP-activated current is added to the synchronized Hodgkin-Huxley equations. The interactions among the volumes of the two neurons and the extracellular cerebrospinal fluid surrounding them are described by Lotka-Volterra equations. These equations contain rates dependent on the action potentials predicted by the synchronized Hodgkin-Huxley equations and Michaelis-Menten-like terms modeling volumetric regulatory mechanisms. An ICP-dependent term of the Starling's equation is lastly added to the equations describing the volumetric dynamics of the neurons. Under the assumption of osmotic equilibrium, the effects of elevated ICP taken from literature [4, 5] on the patterns of action potentials are studied using numerical simulations. Preliminary results show that both delayed and seizure-like action potentials can be obtained from variations in the hydrostatic pressure difference across neuronal membrane.

References

[1] Epilepsy Foundation, *Traumatic Brain Injury and Epilepsy*, `https://www.epilepsy.com/causes/structural/traumatic-brain-injury-epilepsy` (Accessed: Feb. 16, 2026).

[2] C.S. Drapaca, *Fractional Calculus in Neuronal Electro-Mechanics*, Journal of Mechanics and Materials and Structures, Coupled Field Problems and Non-Local Continua: CFPNC-2015, **12**, 1, pp.35-55 (2017). `https://doi.org/10.2140/jomms.2017.12.35`

[3] R. Schlögl, *Membrane Permeation in Systems far from Equilibrium*, Berichte der Bunsengesellschaft für physikalische Chemie, **70**, pp. 400-414 (1966). `https://doi.org/10.1002/bbpc.19660700403`

[4] H.-Y. Lai, C.-Y. Lee, H.-H. Hsu, S.-T. Lee, *The Intracranial Volume Pressure Response in Increased Intracranial Pressure Patients: Part 1. Calculation of the Volume Pressure Indicator*, Acta Neurochir. **154**, pp. 2271-2275 (2012). `https://doi.org/10.1007/s00701-010-0765-8`

[5] M. Kasprowicz, M. Czosnyka, Z. Czosnyka, S. Momjian, P. Smielewski, H. Juniewicz, J.D. Pickard, *Hysteresis of the Cerebrospinal Pressure-Volume Curve in Hydrocephalus*, in Kuroiwa, T., et al. Brain Edema XII. Acta Neurochirurgica Supplements, **86**, pp. 529-532 (2003). `https://doi.org/10.1007/978-3-7091-0651-8_108`

Synchronization properties in *C. elegans*: Relating behavioral circuits to structural and functional neuronal connectivity

G. K. Sar[1], A. Patton[1], E. Towlson[1,2,3,4], J. Davidsen[1,2]

[1] *Complexity Science Group, Department of Physics and Astronomy, University of Calgary, Calgary, AB, Canada, {gourabkumar.sar,andrew.patton,emma.towlson,joern.davidsen}@ucalgary.ca*
[2] *Hotchkiss Brain Institute, University of Calgary, Calgary, AB, Canada*
[3] *Department of Computer Science, University of Calgary, Calgary, AB, Canada*
[4] *Alberta Children's Hospital Research Institute, University of Calgary, Calgary, AB, Canada*

A central question in neuroscience is how neural processing generates or encodes behavior. *Caenorhabditis elegans* is well suited to addressing this question, given its compact nervous system and near-complete structural connectome. Despite this, findings from previous studies remain inconclusive. While some have shown that the connectome can robustly encode specific behaviors such as locomotion, others report that functional connectivity can be reconfigured across behaviors. We aim to understand the relationship between structural connectivity, functional connectivity and biological behavior *in silico* by using an experimentally motivated computational model [1] leveraging the structural connectome [2]. Stimulation of specific neurons in the model induces oscillatory neural responses, enabling us to infer neuronal functional connectivity. Functional connectivity is found to be stronger among some neurons, allowing us to identify functional communities. We find that electrical synapses play a critical role in determining functional communities, and the resulting mesoscale functional architecture is predominantly gap junctionally assortative. Furthermore, comparison with behavioral circuits shows that locomotion circuits are largely segregated into distinct functional communities while other circuits are more distributed across multiple functional communities. We also observe that stimulation of neurons belonging to these distributed circuits elicits a more synchronized neuronal response compared to stimulation of neurons within the more segregated circuits. This is consistent with the presence of behavioral patterns that originate in one circuit and terminate in another (e.g., chemosensation leading to locomotion), such that stimulation of one circuit can activate the other and eventually result in a synchronized response. We also find a large repertoire of chimera-like synchronization patterns upon stimulation of certain behavioral circuits (chemosensation, mechanosensation) indicating high dynamical flexibility. Overall, our results demonstrate that while certain behaviors are governed by functionally segregated circuits, others emerge from the synchronization of multiple functional communities, which are, to begin with, influenced by the underlying structural connectivity.

References

[1] J. Kunert, E. Shlizerman and J. N. Kutz, *Low-dimensional functionality of complex network dynamics: Neurosensory integration in the Caenorhabditis elegans connectome*, Physical Review E **89**, 5, pp. 052805 (2014).

[2] L. R. Varshney, B. L. Chen, E. Paniagua, D. H. Hall and D. B. Chklovskii, *Structural properties of the Caenorhabditis elegans neuronal network*, PLoS Computational Biology **7**, 2, pp. e1001066 (2011).

The VII International AMMCS
Interdisciplinary Conference
Waterloo, Ontario, Canada

Augmented Sample Size Calculation With Truncated Data

Jiayi Zhang[1], Mateen Shaikh[2]

[1] *Thompson Rivers University,Canada, zhangj2311@mytru.ca*
[2] *Thompson Rivers University,Canada, mshaikh@tru.ca*

Incomplete data, including truncated and censored observations, can lead to information loss and effect statistical inference. My work develops an effective sample size framework (ESS) to quantify information loss in incomplete data. An Expectation–Maximization (EM) algorithm is used to estimate the ESS, which is then incorporated into inference procedures by replacing the nominal sample size.

The effective sample size is defined as combining fully observed, truncated, and censored observations, the effective sample size can be written as

$$m_{\text{eff}} = \sum_{i \in O} 1 + \sum_{j \in T} w_j^{(T)} + \sum_{k \in C} w_k^{(C)}, \tag{1}$$

where O, T, and C denote the sets of fully observed, truncated, and censored observations, respectively.The weights $w_j^{(T)}$ and $w_k^{(C)}$ take values in $(0,1]$ and quantify the relative information contribution of truncated and censored observations. They are computed from the corresponding truncation or censoring probabilities under the assumed distribution, with smaller weights assigned to observations containing greater information loss.

Simulation studies compare the proposed method with conventional approaches using confidence interval coverage, Type I error, power, bias, and mean squared error. Real-data applications are also considered.The results show that the proposed ESS effectively reflects information loss and generally provides better type I error and confidence coverage but poorer power than methods based only on the observed sample size.

References

[1] Munasinghe, Minoli R. *Robust Regression Models with Missing and Censored Data via the EM Algorithm*. Diss. Thompson Rivers University, 2024.

[2] Liu, T., Fan, J., Luo, Y., Tang, N., Li, G., and Du, X. *Adaptive Data Augmentation for Supervised Learning over Missing Data*. Proceedings of the VLDB Endowment, 14(7), 1202–1214, 2021.

[3] Bian, Y., Yi, G. Y., and He, W. *Boosting Prediction with Data Missing Not at Random*. Journal of Computational and Graphical Statistics, 35(1), 406–417, 2026.

[4] X. Chen, Y. Liu, and T. Sun, *Constrained Optimization Methods in Modern Statistical Learning*, Journal of Machine Learning Research **22**, pp. 1–45 (2021).

[5] Shin, T., Long, J. D., and Davison, M. L. *An Evaluation of Methods to Handle Missing Data in the Context of Latent Variable Interaction Analysis: Multiple Imputation, Maximum Likelihood, and Random Forest Algorithm*. Japanese Journal of Statistics and Data Science, 5(2), 629–659, 2022.

Index of Authors

The AMMCS 2026 Conference
Book of Abstracts